FORAMINIFERAL PALEONTOLOGY, BIOSTRATIGRAPHY AND SEQUENCE STRATIGRAPHY OF THE PERMIAN-TRIASSIC BOUNDARY BEDS OF THE BOLKAR DAĞI UNIT (CENTRAL TAURIDES, TURKEY)

A THESIS SUBMITTED TO
THE GRADUATE SCHOOL OF NATURAL AND APPLIED SCIENCES
OF
MIDDLE EAST TECHNICAL UNIVERSITY

BY

AYSEL HANDE ESATOĞLU

IN PARTIAL FULFILLMENT OF THE REQUIREMENTS
FOR
THE DEGREE OF MASTER OF SCIENCE
IN
GEOLOGICAL ENGINEERING

MAY 2011

Approval of the thesis:

FORAMINIFERAL PALEONTOLOGY, BIOSTRATIGRAPHY AND SEQUENCE STRATIGRAPHY OF THE PERMIAN-TRIASSIC BOUNDARY BEDS OF THE BOLKAR DAĞI UNIT
(CENTRAL TAURIDES, TURKEY)

submitted by **AYSEL HANDE ESATOĞLU** in partial fulfillment of the requirements for the degree of **Master of Science in Geological Engineering Department, Middle East Technical University** by,

Prof. Dr. Canan Özgen _______________________
Dean, Graduate School of **Natural and Applied Sciences**

Prof. Dr. M. Zeki Çamur _______________________
Head of Department, **Geological Engineering**

Prof. Dr. Demir Altıner _______________________
Supervisor, **Geological Engineering Dept., METU**

Examining Committee Members:

Prof. Dr. Asuman Günal Türkmenoğlu
Geological Engineering Dept. METU _______________________

Prof. Dr. Demir Altıner
Geological Engineering Dept. METU _______________________

Assoc. Prof. Dr. Bora Rojay
Geological Engineering Dept. METU _______________________

Assoc. Prof. Dr. İsmail Ömer Yılmaz
Geological Engineering Dept. METU _______________________

Dr. Zühtü Batı
Exploration Dept., TPAO _______________________

Date: 16.05.2011

I hereby declare that all information in this document has been obtained and presented in accordance with academic rules and ethical conduct. I also declare that, as required by these rules and conduct, I have fully cited and referenced all material and results that are not original to this work.

Name, Last Name: Aysel Hande, Esatoğlu

Signature:

ABSTRACT

FORAMINIFERAL PALEONTOLOGY, BIOSTRATIGRAPHY AND SEQUENCE STRATIGRAPHY OF THE PERMIAN-TRIASSIC BOUNDARY BEDS OF THE BOLKAR DAĞI UNIT (CENTRAL TAURIDES, TURKEY)

Esatoğlu, Aysel Hande

M.Sc., Department of Geological Engineering

Supervisor: Prof. Dr. Demir Altıner

May 2011, 184 pages

The aim of this study is to designate paleontologic, biostratigraphic and sequence stratigraphic characteristics of the Permian-Triassic Boundary beds of the Bolkar Dağı Unit in the Hadim region (Central Taurides).

For this purpose a 48,06m thick stratigraphic section, composed of limestone, siltstone and sandstone, was measured and 116 samples were analyzed through the Permian Taşkent Formation and the Triassic Ekinlik Formation which belong to allochthonous Bolkar Dağı Unit in Central Taurides.

By the detailed examination of thin section samples, 37 species and 29 genera of foraminifera were identified. Based on these determinations two foraminiferal assemblage zones have been defined including the Permian-Triassic boundary. These assemblage zones are the Changhsingian "*Nodosaria*" *elabugae-Nestellorella dorashamensis* - *Reichelina changhsingensis* Assemblage Zone and the Greisbachian *Spirorbis phlyctaena-Rectocornuspira kalhori* Assemblage Zone.

In order to establish the sequence stratigraphic framework of the study area detailed microfacies analysis carried out and according to these, 12 microfacies types were defined. Basing on interpretations of the vertical configuration of these microfacies types 6 main and 10 sub-type cycles were designated. Throughout the measured section 24 shallowing-upward meter-scale cycles and two sequence boundaries were determined. These sequence boundaries coincide well with the

global sea level changes across the Permian-Triassic boundary and the Changhsingian-Greisbachian boundary falls within the transgressive systems tract of a third-order depositional squence spanning from latest Changhsingian to Greishbachian.

Keywords: Permian-Triassic boundary, Benthic foraminifera, Meter-scale cycles, Central Taurides.

ÖZ

BOLKAR DAĞI BİRLİĞİ'NİN (ORTA TOROSLAR, TÜRKİYE) PERMİYEN-TRİYAS SINIR TABAKALARINDA FORAMİNİFER PALEONTOLOJİSİ, BİYOSTRATİGRAFİ VE SEKANS STRATİGRAFİSİ

Esatoğlu, Aysel Hande
Yüksel Lisans, Jeoloji Mühendisliği Bölümü
Tez Yöneticisi: Prof. Dr. Demir Altıner
Mayıs 2011, 184 sayfa

Bu çalışmanın amacı Hadim bölgesinde (Orta Toroslar) Bolkar Dağı Birliği'nin Permiyen-Triyas sınır tabakalarındaki paleontolojik, biyostratigrafik ve sekans stratigrafik özellikleri belirlemektir.

Bu amaçla kireçtaşı, silttaşı ve kumtaşlarından oluşan 48,06m kalınlığında bir stratigrafik kesit ölçülmüştür. Allokton Bolkar Dağı Birliği'nde yer alan Permiyen yaşlı Taşkent Formasyonu ve Triyas yaşlı Ekinlik Formasyonu'na ait toplam 116 örnek incelenmiştir.

İnce kesitlerin detaylı incelenmesi sonucunda foraminifer topluluklarına ait 37 tür ve 29 cins tanımlanmıştır. Bu tanımlamalar temel alınarak Permiyen-Triyas sınırını da içeren iki topluluk zonu belirlenmiştir. Bu biyozonasyon "*Nodosaria*" *elabugae-Nestellorella dorashamensis* - *Reichelina changhsingensis* Topluluk Zonu (Çangsingiyen) ve *Spirorbis phlyctaena-Rectocornuspira kalhori* Topluluk Zonu'ndan (Griesbakiyen) oluşmaktadır .

Çalışma alanının sekans stratigrafik çatısını tesbit etmek amacıyla detaylı mikrofasiyes analizleri yapılmış ve 12 mikrofasiyes tipi belirlenmiştir. Bu mikrofasiyes tiplerinin dikey sıralanmaları temel alınarak 6 temel 10 alt devir tanımlanmıştır. Ölçülen stratigrafik kesit boyunca 24 metre ölçekli üste doğru sığlaşan devir ve iki sekans sınırı tesbit edilmiştir. Bu sekans sınırları global deniz düzeyi değişimleri ile uyumluluk göstermektedir. Çangsingiyen-Griesbakiyen sınırı

en geç Çangsingiyen-Griesbakiyen yaş aralığına karşılık gelen üçüncü derece bir sekansın transgresif sistemler dizisine karşılık gelmektedir.

Anahtar Kelimeler: Permiyen-Triyas sınırı, Bentik foraminifer, Metre-ölçekli devirsellik, Orta Toroslar.

To my parents…

ACKNOWLEDGEMENTS

I am greatly indepted to my supervisor Prof. Dr. Demir ALTINER for his valuable advice, guidance, constructive recommendation, motivating encouragements and endless support in all stages of this thesis.

I express my gratitude to Prof. Dr. Asuman Günal TÜRKMENOĞLU, Assoc. Prof. Dr. İsmail Ömer YILMAZ, Assoc. Prof. Dr. Bora ROJAY and Dr. Zühtü BATI for their valuable recommendations for the thesis.

I would like to thank to the General Directorate of Mineral Research and Exploration for their support during my field and laboratory studies.

I would like to thank Mr. İsmet ALAN for his help during my field studies.

I would like to thank Mrs. Ayşe Atakul ÖZDEMİR for her valuable advices and encouragaments.

I am also indebted to all my friends especially Dr. Ayhan ILGAR, Mr. Mehmet VEKLİ, Mrs. Serap KAYA, and Mrs. Gönül CULHA for their help and support.

Finally, I am grateful to my mother, father and brother for their endless encouragements, support and understanding during my study.

TABLE OF CONTENTS

LIST OF FIGURES

CHAPTER 1

INTRODUCTION

1.1.Purpose and Scope

The main objective of this thesis is to delineate the Permian-Triassic (P-Tr) boundary through the carbonate deposits of the allochthonous Bolkar Dağı Unit widely exposed in Central Taurides by using calcareous benthic foraminifera and to study the sedimentary cyclicity whether the eustatic sea level changes had an impact on the Permian-Triassic boundary beds. For this purpose, a 48,06m thick stratigraphic section has been measured through the Taşkent Formation and the Ekinlik Formation of the Bolkar Dağı Unit.

The most severe disaster event in the Phanerozoic history of earth’s life happened in the Permian-Triassic transition, and it eliminated more than 90 % of all marine species (Erwin, 1994). Multiple scenarios suggesting the causes of the P-Tr event have been proposed by many researchers but there is growing evidence that the following four major triggers are the most likely causes for this crisis: bolide impact, flood basalt eruption of the Siberian Traps, shallow water anoxia and catastrophic release of seafloor methane (Knoll et al., 2007). Unlike other fossil groups, foraminifers are one of the most common fossil groups through the P-Tr transition and are distributed in a variety of facies settings (Song et al. 2009b). In this study, a detailed taxonomic analysis is presented in order to document their diversity and the biotic turnover across the Permian-Triassic boundary. The foraminiferal inventory from the P-Tr boundary beds of the Bolkar Dağı Unit is being given in such a detail for the first time in Turkey in this thesis.

To determine the sedimentary cyclicity and the sequence stratigraphic evolution of the study area detailed microfacies anaysis has been carried out. In addition to observations in the field, by using standard microfacies zones and microfacies models of Flügel (2004), sedimentary cyclicity and stacking patterns of cycles have been determined in order to understand the controls on cyclicity. Bed-scale sequence stratigraphic studies are rare in Turkey, particularly on upper Paleozoic rocks. From this point of view this thesis can also be considered as one of the pioneering studies in Turkey.

1.2. Geopraphic Setting

The study area is located at 3 km southwest of the Gaziler Village that belongs to the town of Hadim (Figure 1). The town of Hadim can be reached by the Konya-Hadim highway and the section is measured to the north of the Hadim-Gaziler road. It is situated on the topographic map of Konya-N29-d4 of 1:25.000 scale. The coordinates of the measured section start at 36461216 E - 4098240 N and finish at 36461150 E - 4098186 N.

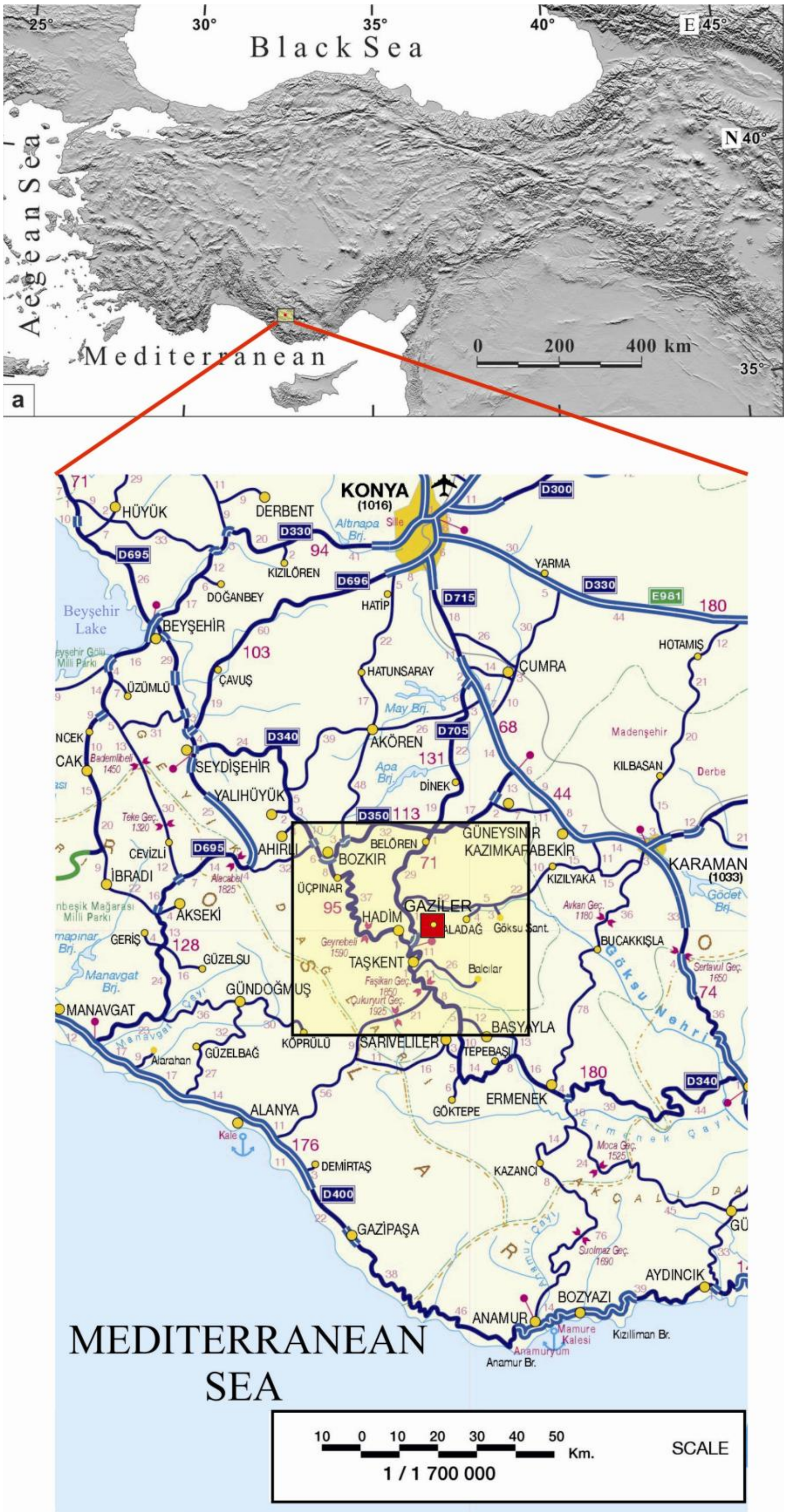

Figure 1. Geographic setting of the study area and the location of the measured section.

1.3. Medhods of Study

This study is built up on the field and laboratory studies successively. A 48,06m thick stratigraphic section was measured mainly composed of carbonates and 116 samples were collected on bed-scale basis (Figure 2). More than one sample were collected from thicker beds by sampling them in equal intervals. Samples were oriented by indicating the top of each bed. Beds were examined carefully by using a hand-lense in order to locate the fossiliferous zones and microfacies changes. Stacking patterns of probable meter-scale cycles were observed, interpreted and photographed during the field study.

For micropaleontological and microfacies analysis thin sections were prepared from each sample. To build up a biostratigraphical framework and delineate P-Tr boundary, benthic foraminifera have been used because important changes occur in the density and diversity of benthic foraminifera across the boundary. Thin sections were investigated carefully under the microscope and a large number of photopraphs were taken in order to detect the variations in the populations.

For the microfacies analysis, thin sections were investigated under the microscope. Each level sampled was photographed and samples were classified according to their biological content and lithological components. The classification and changing patterns of microfacies, combined with field observations, have yielded us the architecture of meter-scale cycles. The sequence stratigraphic framework of the study area has been constructed by the stacking patterns of meter-scale cycles.

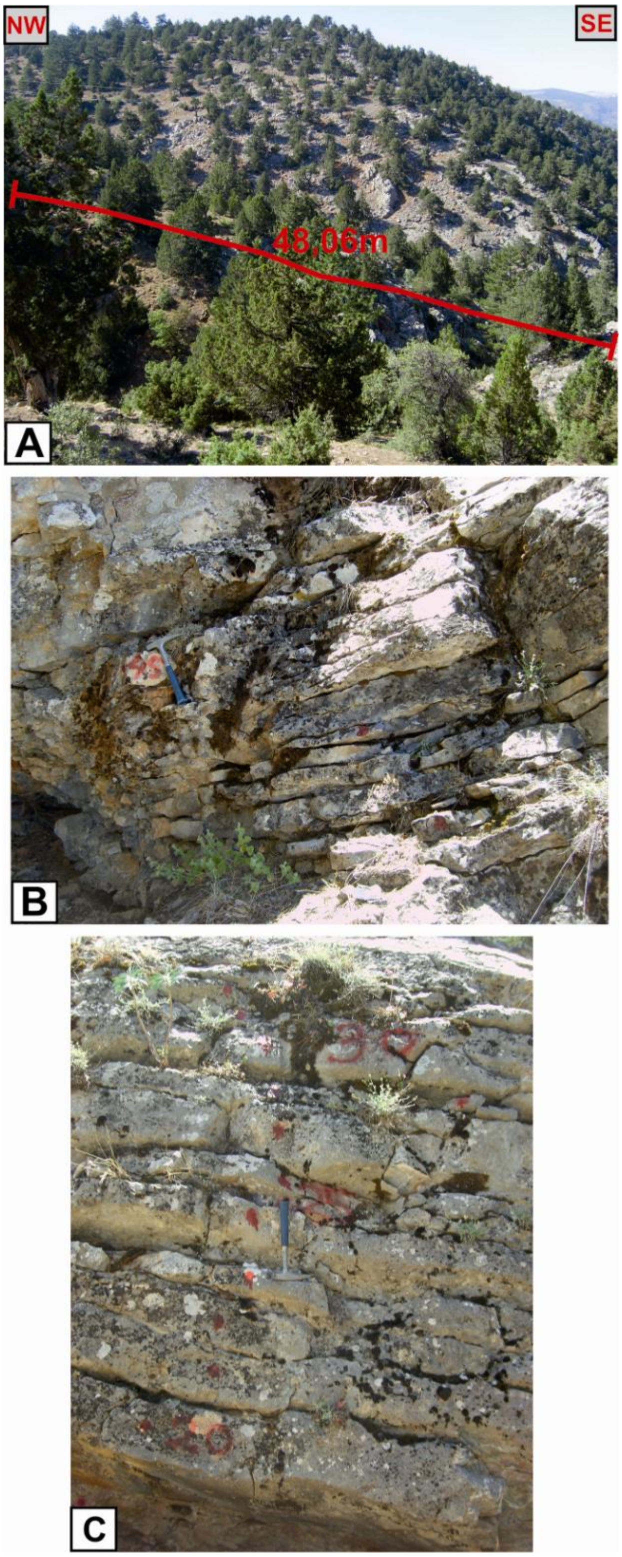

Figure 2. A. Location of the measured section. B. and C. close-up view of measured section showing sampling points.

1.4. Previous Works

Taurides have been studied by many researchers since the second half of nineteenth century. Blumenthal (1944, 1947, 1951 and 1956) was the first researcher to discover the basic structures and features of the Tauride Belt. Blumenthal studied the geologic, geomorphologic and tectonic structure of Seydişehir-Beyşehir region, which is located at northwest of the Bolkar Dağı Unit. He also studied the geographic, stratigraphic and tectonic features of the Aladağ Unit and the Upper Paleozic, Mesozoic and Cenozoic and tectonic features of the Bolkardağı region. Most of the previous works carried out in the following years did not include the Bolkar Dağı Unit. For example, Monod (1977), described the autochthon from Cambro-Ordovician to Cretaceous and examined allochthonous units in two different rock assemblages as Beyşehir-Hoyran Nappes and Antalya Nappes. Dumont (1976) studied the geology and stratigraphy of Dipoyraz Dağı to the of Seydişehir-Beyşehir region. Poisson (1977) carried out detailed stratigraphic studies in Beydağları and Susuz Dağ. In Gutnic et al. (1979), Gutnic, Monod, Poisson and Dumont presented detailed stratigraphic sections, their correlations and maps illustrating tectonic structure of Tauride Belt.

It was Özgül (1971, 1976, 1984 and 1997) who documented the important geologic, stratigraphic and tectonic features and the geodynamic evolution of the Taurides. He defined the Geyikdağı Unit as autochthon while South Central Anatolia and Central Taurus Units as the allochthonous units. According to Özgül (1971), our study area is situated in the allochthonous South Central Anatolia Unit. Özgül and Gedik (1973) studied the Lower-Middle Cambrian Çaltepe Limestones and the Upper Cambrian-Lower Ordovician Seydişehir Formation in the Seydişehir and Hadim regions located to the northwest of our study area. Finally Özgül (1976) distinguished different tectonostratigraphic units in southern Turkey and named them as Bolkar Dağı Unit, Aladağ Unit, Geyik dağı Unit, Alanya Unit, Bozkır Unit and Antalya Unit. He realised that these units were extending laterally hundreds of kilometers with tectonic contacts between them and commonly forming allochthonous covers on each other. He described the Bolkar Dağı Unit comprising

Middle Upper Devonian-Lower Tertiary shelf type carbonates and detrital rocks. He had mentioned the same unit as the South Central Anatolia Unit in Özgül (1971). In Özgül (1984) he stated that the Bolkar Dağı Unit is distinguished from the Aladağ Unit by its regional greenschist metamorphism, the presence of frequent discordances and the absence of the characteristic biozones and lithozones of the Aladağ Unit. Demirtaşlı (1984) studied the Bolkar Mountains and differentiated two tectono-stratigraphic units (Bolkar Dağı Unit at the north and the Aladağ unit at the south) showing considerable stratigraphic differences. Özgül (1997), defined the stratigraphic features of tectono-stratigraphic units of the Bozkır-Hadim-Taşkent region and divided the Bolkar Dağı Unit into nine lithostratigraphic units as Hocalar Formation (Devonian), Kongul Formation (Lower-Middle Carboniferous), Taşkent Formation (Upper Permian), Ekinlik Formation (Triassic), Morbayır Formation (Lias), Sinat Dağı Limestone (Jurassic-Lower Cretaceous), Pusula Group (Lias-Upper Cretaceous), Topyatak Limestone (Cenomanian) and Söğüt Formation (Senonian). The Taşkent Formation and the Ekinlik Formation are important lithostratigraphic units for this study because, the studied stratigraphic section has been measured across these formations. Şenel (1999) proposed new definitions for the autochthonous, parautochthonous and allochthonous rock units of Taurus Belt. He named the autochthonous rock units, west to east, as Beydağları autochthon, Anamas - Akseki autochthon, and the Southeast Anatolian autochthon; the allochthonous rock units in turn are called the Lycian nappes, Antalya nappes, Alanya nappe, Beyşehir-Hoyran-Hadim-Bolkar nappes, Yahyalı-Munzur nappes and Bitlis-Pötürge-Malatya nappes. According to Şenel (1999), the Bolkar Dağı Unit defined by Özgül (1976) takes place in the allochthonous Beyşehir-Hoyran-Hadim-Bolkar nappes.

In Turkey, sequence stratigraphic studies on the Taurides carbonates began by the studies of Marine Micropaleontology Research Unit, directed by Prof. Dr. Demir Altıner. Important sequence stratigraphic and cyclostratigraphic studies were carried out by researchers in carbonate platform deposits of Tauride Belt which could be reference to the present study. The MSc. study of Yılmaz (1997) was the first sequence stratigraphic study for this region, in which, he studied the sequence stratigraphy, cyclostratigraphy and dasyclad algal taxonomy in the Upper Jurassic (Kimmeridgian)-Upper Cretaceous (Cenomanien) peritidal carbonates of the Fele area. After this study several MSc. thesis were carried out by Akçar (1998), Bayazıtoğlu (1998), Gaziulusoy (1999) which decribed the meter-scale cyclic deposits and sequence stratigraphy in the Cretaceous carbonate successions of the Western Taurides. Altıner et al. (1999) made the first high-resolution sequence stratigraphic correlation within Geyikdağı Unit and described the types of meter-scale shallowing upward cyclic deposits, four second order cycles, 26 third order cycles and compared with the global sea level fluctuations within the Upper Jurassic-Upper Cretaceous platform carbonates of Western Taurides. Also Yılmaz and Altıner (2001) and Yılmaz (2002) are important studies, in which they discussed the cyclicity and sequence stratigraphy of Jurassic and Cretaceous peritidal carbonates of the Tauride platform. In addition to these studies, Pütürgeli (2002), Şen (2002), Ünal (2002), Ünal et al. (2003), Atakul (2006) and Dinç (2009) studied and defined meter-scale shallowing upward cycles in the carbonates of the allochthonous Aladağ Unit. Studies of Ünal (2002) and Ünal et al. (2003) became important references for the present study in which cyclic stratigraphy across the Permian-Triassic boundary in the Aladağ Unit was defined and global correlation of Permian-Triassic boundary beds in comparison with selected sections in the world was presented.

Paleontological and biostratigraphical studies are very important to determine the evolution of the Tauride Belt. Sellier de Civrieux and Dessauvagie (1965) carried out a detailed study of microfaunas from Upper Permian successions of Tauride Belt and submited a reclassification of some Nodosariidae. Later, Çatal and Dağer (1974) reported the presence of genus *Colaniella* in the Upper Permian limestones of the Konya-Bozkır region. Permian –Triassic transition in the Aladağ region is studied by Işık (1983) who defined concurrent range zones based on foraminifers. Important biostratigraphical and paleontological studies about the Permian and the Triassic faunas of the Taurides have been carried out by Lys and Marcoux (1978), Altıner and Zaninetti (1977, 1981), Altıner (1981, 1984, 1988, 1999), Altıner and Brönnimann (1980), Altıner et al. (1980, 1992, 2000, 2003, 2007), Altıner and Özgül (2001), Altıner and Özkan-Altıner (2001, 2010), Groves et al. (2005), Kobayashi and Altıner

(2008a, 2008b). Altıner (1984) studied the Upper Permian deposits of the Tauride-Anatolide platform and the Arabian platform by examining seven stratigraphic sections measured from these platforms. He recognized one hundred and four foraminiferal species and distinguished four informal biostratigraphic units (Assemblages) of Foraminifera from these deposits. Middle-Upper Permian marine carbonates are distinguished in two contrasting biofacies belts (Northern Biofacies Belt and Southern Biofacies Belt) in Turkey (Altıner et al. 2000). In this study the Bolkar Dağı Unit, including our study area, is established as part of the Northern Biofacies Belt. Groves et al. (2005) studied the extinction, survival and recovery of lagenide foraminifers in the Permian-Triassic boundary interval in the Central Taurides and stated that lagenide foraminifers experienced a catastrophic reduction in diversity at or near the Permian-Triassic boundary.

Important paleontologic and biostratigraphic studies were carried out about Permian and Triassic faunas by many researchers outside the world. Kobayashi (1999) studied the Tethyan uppermost Permian foraminiferal faunas and proposed a reconstructed oceanic plate stratigraphy for Japanese terranes using presence and distribution of *Palaeofusulina.* Pronina-Nestell and Nestell (2001) studied the small foraminifers and fusulinaceans of the Upper Changhsingian deposits of the Northwestern Caucasus and correlated to deposits of the South Primorye. Another important study was carried out by Groves et al. (2003) in which they determined the evolutionary radiation and paleobiogeographic distribution of the Order Lagenida. Kobayshi (2004) studied the biostratigraphic and sedimentologic features of Lopingian Mitai Formation and disconformably overlying Triassic Kamura Formation in Japan. Eiland and Gudmundsson (2004) carried out a study about the taxonomy of some Nodosariinae collected in the North Atlantic. One of the most important studies about the end Permian mass extinction was Groves and Altıner (2005) in which they summarized the record of foraminiferal extinction, survival and recovery across the Permian-Triassic boundary. Marquez (2005) carried out a study about the recovery of foraminiferal faunas after the Late Permian extinction in the western Tethys. Vachard et al. (2008) studied the Permian succession of the island of Hydra (Greece) and described *Glomomidiella* gen. n. a (genus of Foraminifera).

Karavaeva and Nestell (2007) carried out a study about Permian foraminifers of the Omolon Massif (Russia) and described 47 new species of Nodosariid small foraminifers. Songzhu et al. (2007) studied the small foraminiferal fauna discovered from the upper Changhsingian Dalong Formation (South China). Song et al. (2007) studied the foraminifers from Permian-Triassic boundary strata and reported foraminifers in the Meishan section (South China) for the first time. Groves et al. (2007) carried out an important study about the lagenide foraminifers of the Permian-Triassic boundary sections in the Southern Alps and designated that the only survivors were ‘’*Nodosaria*’’ *elabugae* and unidentified species in *Geinitzina* and *Nodosinelloides*.

In recent years Song et al. (2009) carried out quantitative analysis to determine the foraminiferal extinction patterns near the P-Tr boundary and emphasized that the Miliolida, Fusulinida and Lagenida had been affected from the crisis with an extinction rate of 100%, 96%, and 92%, respectively. Gaillot et al. (2009) dealed with the microfacies and microfossil content of the latest Permian calsisponges-bearing reef limestones of the Wujiaping Formation (South China) and compared the biotic content with the Khuff Formation (time equivalents in the Middle East). Krainer and Vachard (2009) performed a study in the Lower Triassic Werfen Formation of the Karawanken Mountains (Southern Austria) and presented the determination of disaster forms of the earliest Triassic. One of the recent studies dealing with Changhsingian foraminiferal fauna is performed by Wang et al. (2010) in southern Tibet (China). They proposed the *Reichelina pulchra-Colaniella parva-Dilatofusulina orthogonios* Zone to represent the last assemblage biozone of Permian foraminifers and correlated to the *Palaeofusulina sinensis* Zone.

The most severe and greatest in magnitude disaster event in the Phanerozoic history of Earth’s life, happened in the Permian-Triassic transition, and it eliminated more than 90% of all marine species (Erwin 1994). The end-Permian mass extinction has long been regarded as a single event but the extinction actually occured in two distinct phases; first at the Middle-Late Permian boundary (Guadalupian-Lopingian boundary) and second at the Permian-Triassic boundary as first pointed out by Stanley and Yang (1994) and Jin et al. (1994).

The Permian-Triassic Boundary Working Group (PTBWG) was established by the International Commission on Stratigraphy (ICS) in 1981. The ammonoid *Otoceras* was considered as the index fossil of the P-Tr boundary until 1984. In 1986 *Hindeodeus parvus* was proposed to substitute as the boundary marker (Yin et al., 1986), which later obtained the majority approval of PTBWG. In 1994 Yin et al. published a paper in which they recommended to set the P-Tr boundary at the first appearance of *Hindeodus parvus* Bed 27c of Meishan. This paper later served as the draft in polling for the formal acceptance of PTBWG. After several votings, finally the proposal was approved in March 2001 by the IUGS Executive Committee. As a result, the GSSP of the P-Tr boundary is defined at the base of Bed 27c, Meishan Section D, Changxing Country, Zhejiang Provinve, China, at the horizon where the conodont *Hindeodus parvus* first appeared (Yin *et al.* 2001).

1.5. Regional Geological Setting

As emphasized in Özgül (1984), because it shows most of the characteristic features of the Tauride Belt, Central Taurides was intensely studied by many reaserchers. These studies have shown that the Central Taurides region is composed of a number of tectono-stratigraphic rock units which are distinguished by their stratigraphical, structural and metamorphic features (Blumenthal 1944, 1947, 1951; Özgül, 1971, 1976; Monod, 1977; Gutnic et al., 1979). These rock units are defined and named as Bolkar Dağı Unit, Aladağ Unit, Geyik Dağı Unit, Alanya Unit, Bozkır Unit and Antalya Unit by Özgül (1976) (Figure 3, Figure 4, Figure 5). Among these nappes, Alanya and Antalya units are the tectonic units of southern origin and will be out of the scope of the regional geological setting section of this thesis.

Among these tectonic units, the Geyik Dağı Unit is placed at the base of all other units including the tectonic units of northern and southern origin and considered as the autochthon with respect to the rock units tectonically overlying it

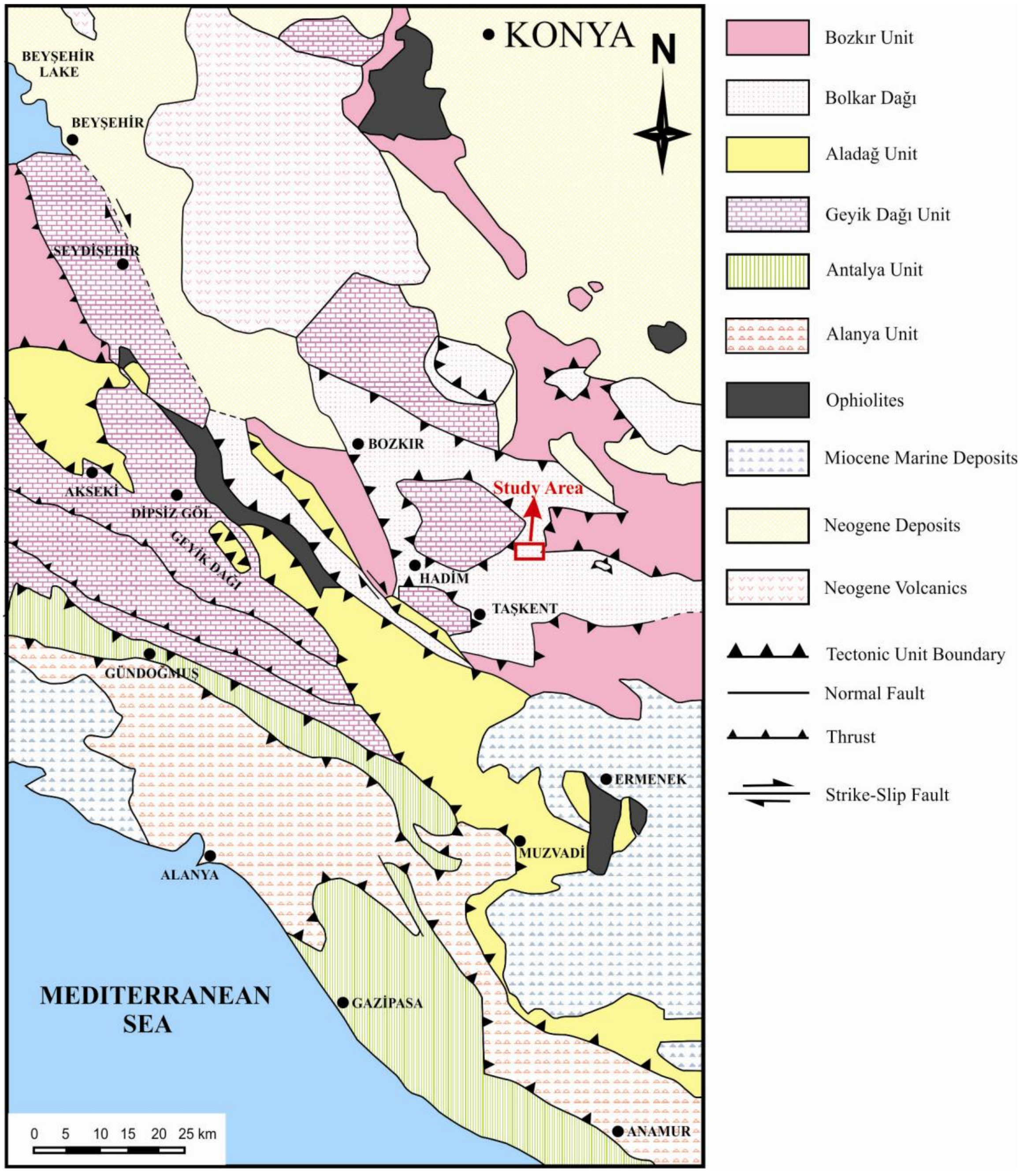

Figure 3. Tectonic map of the study area redrawn from Özgül (1984).

(Özgül 1976, 1984, 1997) (Figure 3, Figure 4). Geyik Dağı Unit occupies large areas in the western part of the central Taurides and disappears under the allochthonous units in the southward direction. This unit is composed of platform type sediments starting with Cambrian and Ordovician rocks and transgressive Mesozoic-Lower Tertiary carbonate rocks consisting largely of carbonates (Özgül 1984). The Lower Paleozoic of the Geyik Dağı Unit comprises the Çaltepe Formation composed of dolomites, neritic limestones and nodular limestones, the Hamzalar Formation mainly composed of dark coloured shales and the Seydişehir Formation which consists of micaceous turbiditic clastics (Özgül and Gedik 1973; Özgül 1984, 1997). The Mesozoic sequence of the Geyik Dağı Unit, which lies with an unconformity over the Lower Paleozoic basement, consists mostly of platform type carbonates (Özgül 1984) (Figure 4).

The Aladağ Unit, which is composed of shelf type clastics and carbonates of Upper Devonian-Upper Cretaceous age was named as the "Hadim Nappe" in Blumenthal (1944) and 'Bademli-Çamlık Unit' in Monod (1977). Aladağ Unit consists Gölboğazı Formation (Devonian), Yarıcak Formation (Carboniferous), Çekiç Dağı Formation (Permian), Gevne Formation (Triassic), Çambaşı Formation (Jurassic-Cretaceous) and Zekeriya Formation (Maastrichtian) (Figure 4). The Gölboğazı Formation is mainly composed of quartzite and shale intercalations, reefal limestones and dolomite layers. The Yarıcak Formation, mainly includes shelf type limestones with quartzite intercalations and comprises a dark coloured shale level at the lower part of the formation. The Çekiç Dağı Formation of Permian age, composed mainly of foraminiferal and algal limestones compries quartzites at the lower part of the unit. The Trissic Gevne Formation, mainly contains shallow marine carbonates and clastics. The Liassic-Upper Cretaceous Çambaşı Formation is made up of a thick carbonate succesion comprising dolomite and shallow marine limestones. Lastly, the Maastrichtian Zekeriya Formation of the Aladağ Unit is composed of clastics including olistoliths and olistrostroms (Özgül 1984, 1997) (Figure 3).

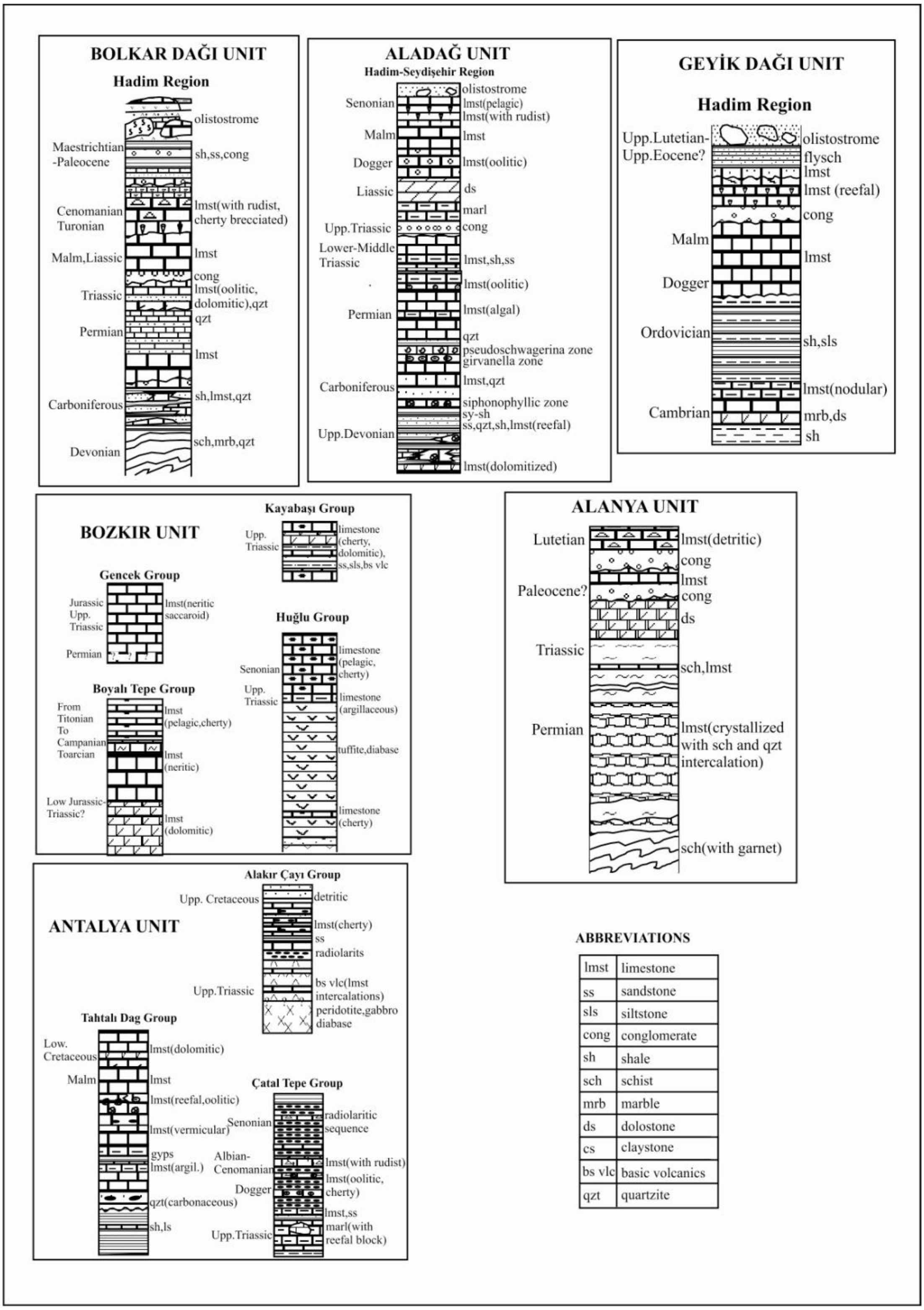

Figure 4. Stratigraphic sections of Bolkar Dağı, Aladağ, Geyik Dağı, Bozkır, Alanya and Antalya units (simplified from Özgül,1976).

The Bolkar Dağı Unit locates in the North of Central Taurides between the Central Anatolian metamorphic massifs and the Tauride Belt (Figure 3). The Unit comprises shelf type clastics and carbonates of Devonian to Upper Cretaceous age and, unlike Aladağ and Geyik Dağı units, shows regional metamorphism in greenschist facies (Figure 3). The grade of metamorphism increases towards the north and stratigraphically deeper levels of the sequence. The Bolkar Dağı Unit is composed of Hocalar Formation, Kongul Formation, Taşkent Formation, Ekinlik Formation, Morbayır Formation, Sinat Dağı Limesone, Pusula Group, Topyatak Limestone and Söğüt Formation (Figure 4). The Hocalar Formation of Devonian age is the oldest rock unit of the region and comprises low grade metamorphics with recrystallized limestone and quartzite intercalations. The Lower-Middle Carboniferous Kongul Formation, is composed of dark coloured and fine grained clastics with reefal limestone intercalations. The Upper Permian Taşkent Formation is mainly composed of algal and foraminiferal limestones and also includes quartzite intercalations in the upper levels. Ekinlik Formation of Triassic age consists of neritic carbonates and clastics. The overlying Morbayır Formation of Liassic age is mainly made up of conglomerate and sandstone. The Sinat Dağı Limestone of Jurassic and Lower Cretaceous is absolutely made up of neritic limestone whereas Liassic-Upper Cretaceous Pusula Group includes neritic and pelagic limestones. The Topyatak Limestone of Cenomanian age is mainly composed of limestones with rudists. Söğüt Formation of Senonian includes pelagic limestones and flischoidal clastics (Özgül 1997) (Figure 3).

Bozkır Unit has an appearence of a melange containing pelagic and neritic limestones deposited in Triassic-Cretaceous time span, radiolarite, submarine volcanic rocks, tuff, diabase, serpentinite and ultramafic blocks of various sizes and ages (Figure 3). Bozkır Unit is composed of Korualan Group that consists Kayabaşı and Başkışla Formations, Huğlu Group, comprising Dedemli, Mahmut Tepesi and Kovanlık Formations, Boyalı Tepe Group comprising Kuztepe and Asar Tepe Formations and Soğucak Limestone (Figure 4). The Korualan Group consists pelagic and shallow marine carbonates, radiolarite, clastics and submarine volcanics. The Huğlu Group is made up of green coloured volcanics with shale and pelagic limestone alternations, cherty pelagic limestone and clastics with blocks. The Boyalı Tepe Group comprises thick neritic carbonate succesion and pelagic limestone with chert intercalations. The Soğucak Limestone is absolutely composed of neritic limestone (Özgül 1997) (Figure 3).

Within the regional geological frame our study area is located in the Bolkar Dağı Unit. The stratigraphic section measured across the Permian-Triassic boundary comprises the upper part of the Taşkent Formation and the lowermost part of the Ekinlik Formation of this tectonic unit which is one of the main tectonic entities of the Tauride Belt.

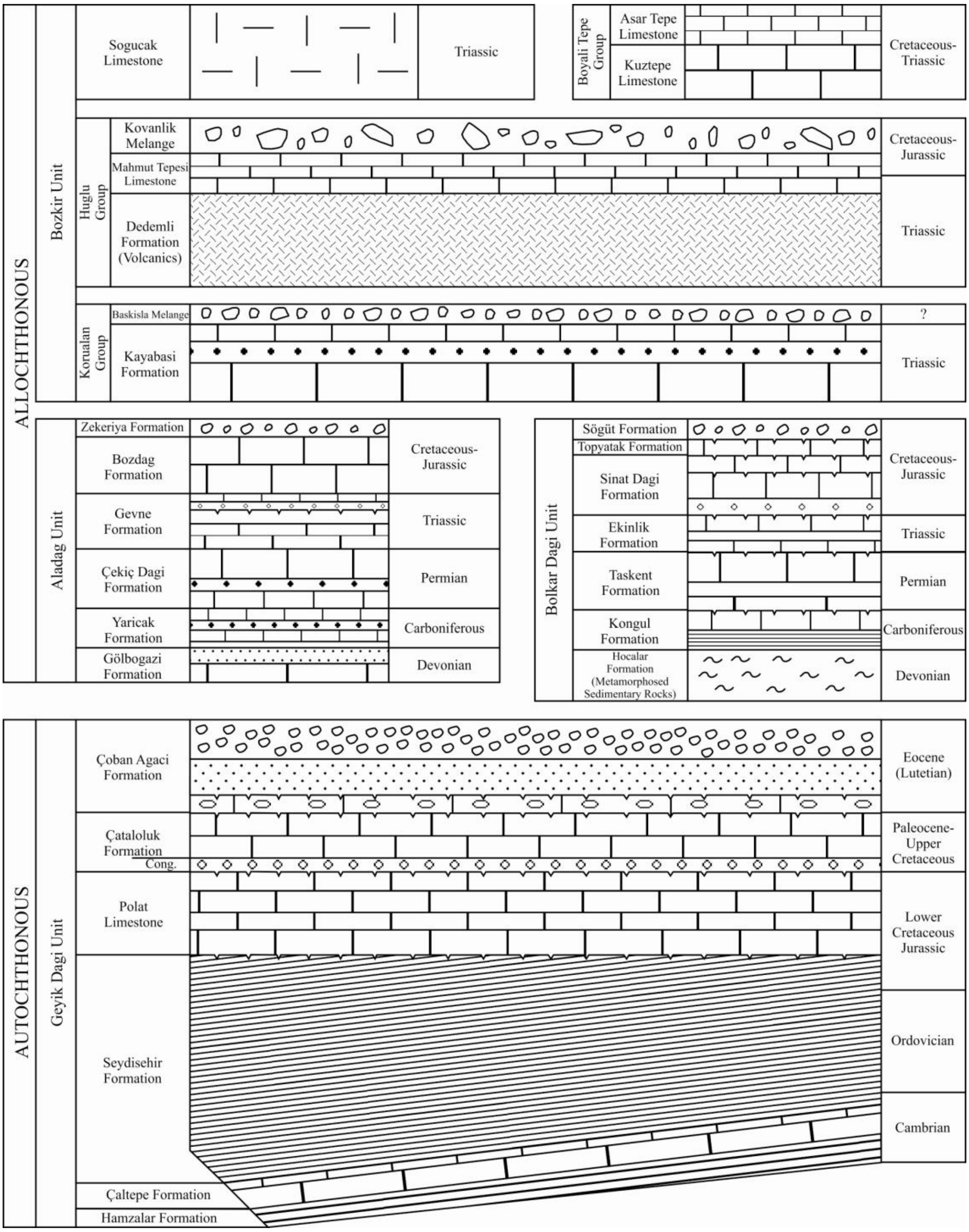

Figure 5. Autochthonous and allochthonous units in the Hadim-Taşkent area. (Altıner and Özgül, 2001)

CHAPTER 2

LITHOSTRATIGRAPHY AND BIOSTRATIGRAPHY

2.1. Lithostratigraphy

In the study area, carbonate succesions of Permian-Senonian age belonging to Bolkar Dağı Unit are widely exposed (Figure 6). The Unit begins with the Devonian Hocalar Formation, which is composed of dominantly green coloured low grade metamorphised slate, dolomite and quartzite levels (Figure 7). Hocalar Formation is followed by Carboniferous Kongul Formation, which includes dark coloured shale and quartzite with limestone alternations at the base and oolitic limestone at the upper parts (Figure 7). The succesion passes to the Permian Taşkent Formation following an unconformity surface. The Taşkent Formation is composed of foraminiferal and algal limestone including shale and clayey limestone intercalations in the upper parts (Figure 7, Figure 8). The Taşkent Formation is unconformably overlain by the Triassic Ekinlik Formation (Figure 7). The Ekinlik Formation is composed of dolomites at its base, shale and quartzite with limestone intercalations in the middle part and benthic foraminiferal and algal limestone in the upper parts (Figure 7, Figure 9). The Ekinlik Formation is overlain by the Jurassic-Lower Cretaceous Sinat Dağı Formation by an unconformity surface. The Sinat Dağı Formation is composed of algal and benthic foraminiferal limestone in the lower part, oolitic limestone in the middle and stromatolitic and algal oncolitic limestone in the upper part. The Sinat Dağı Formation is overlain unconformably by the Topyatak Limestone of Cenomanian age which is mainly composed of limestone with rudist. The succesion passes to the Senonian Söğüt Formation with an unconformity surface and continues upward with pelagic limestone and sandstone-shale intercalations with olistoliths and olistrostroms (Özgül 1997) (Figure 7).

The measured section is situated across the boundary between the Upper Permian Taşkent Formation and the Triassic Ekinlik Formation (Figure 7).

2.1.1. Taşkent Formation

The type locality of the Upper Permian Taşkent Formation is located in 1,5 km west of Dereiçi Village of the Bozkır Town. The Formation is mainly composed of abundant foraminiferal and algal limestone, and it begins with limestone with shale intercalations and clayey limestone and includes quartzite and shale intercalations in the upper parts (Figure 8).

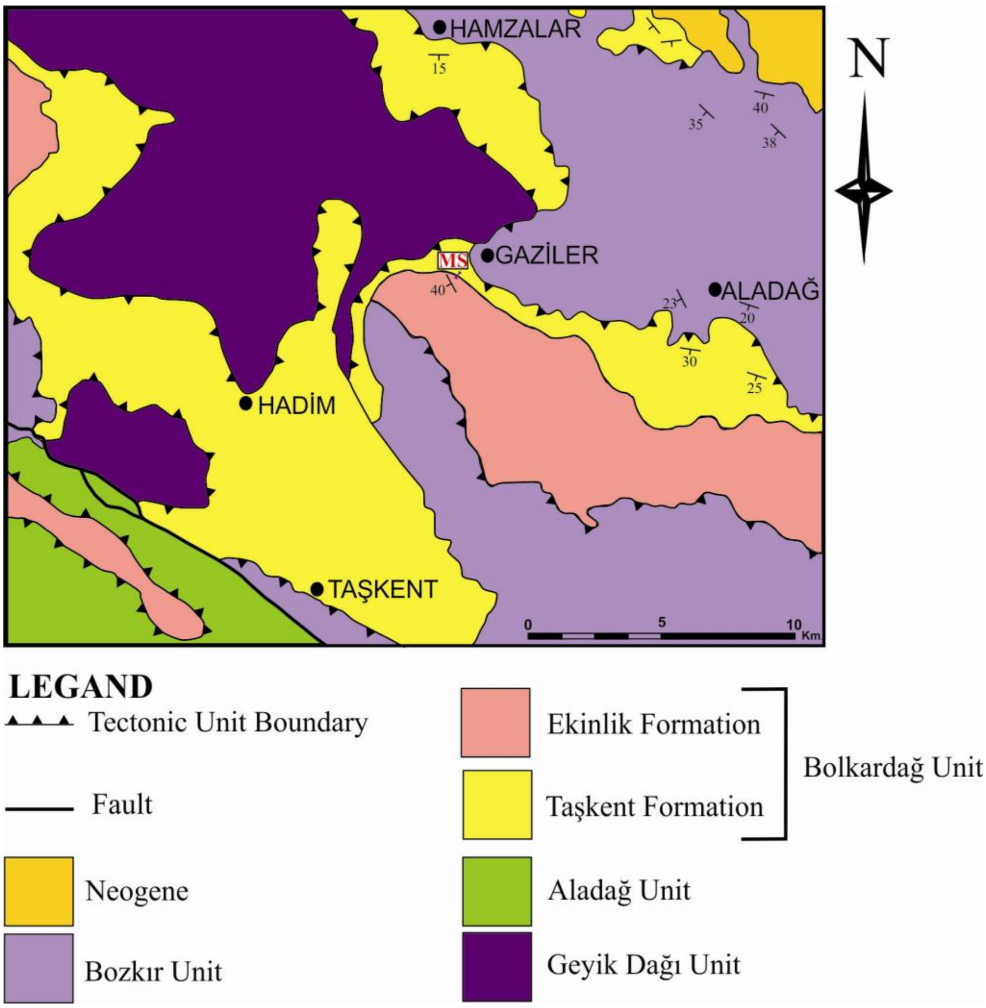

Figure 6. Geologic map of the study area (simplified and redrawn from 1/500.000 scale geologic map of MTA).

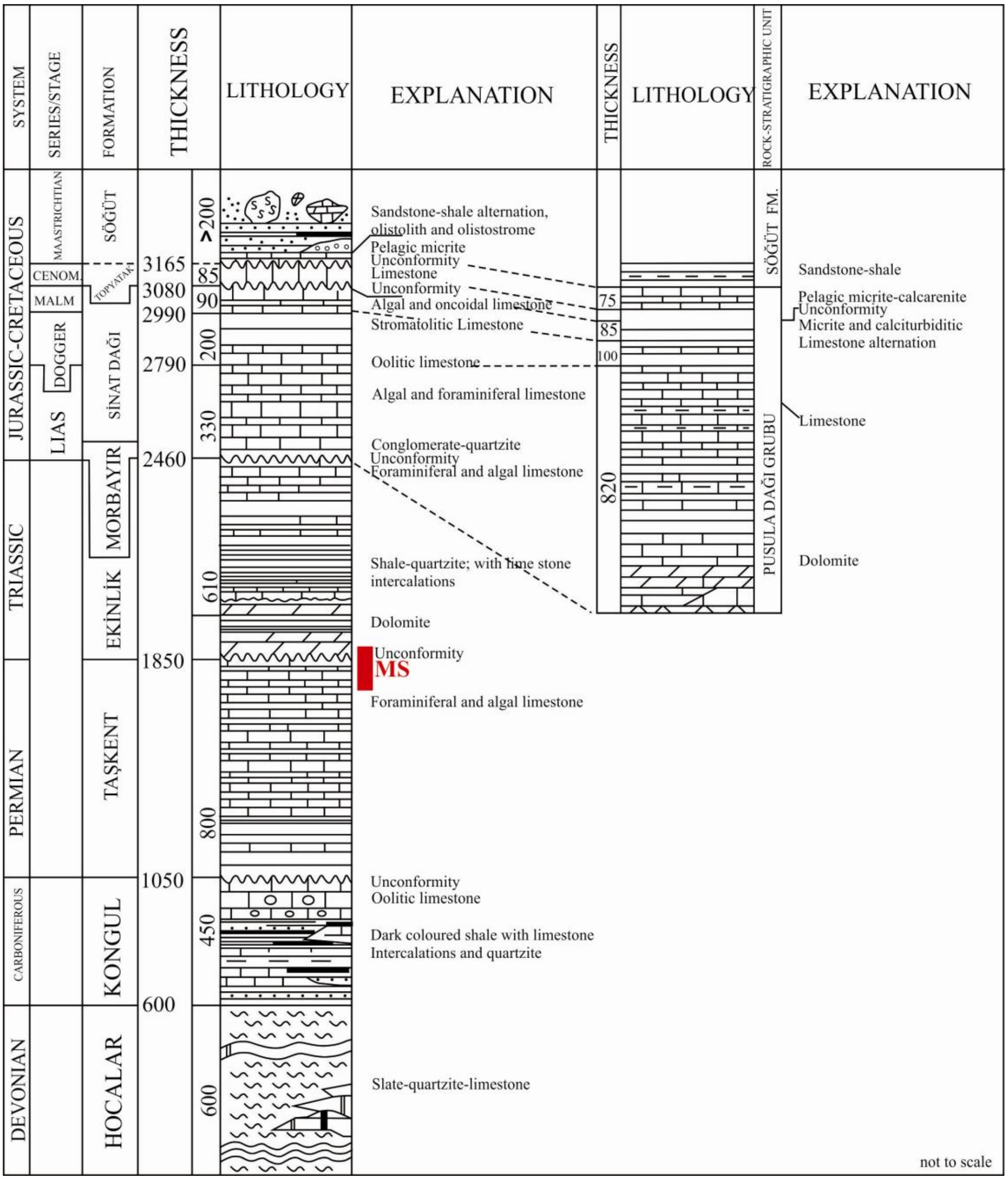

Figure 7. Generalized columnar section of the Bolkar Dağı Unit in the Hadim-Taşkent area (simplified from Özgül, 1997). The solid red line shows the stratigraphic position of the measured section.

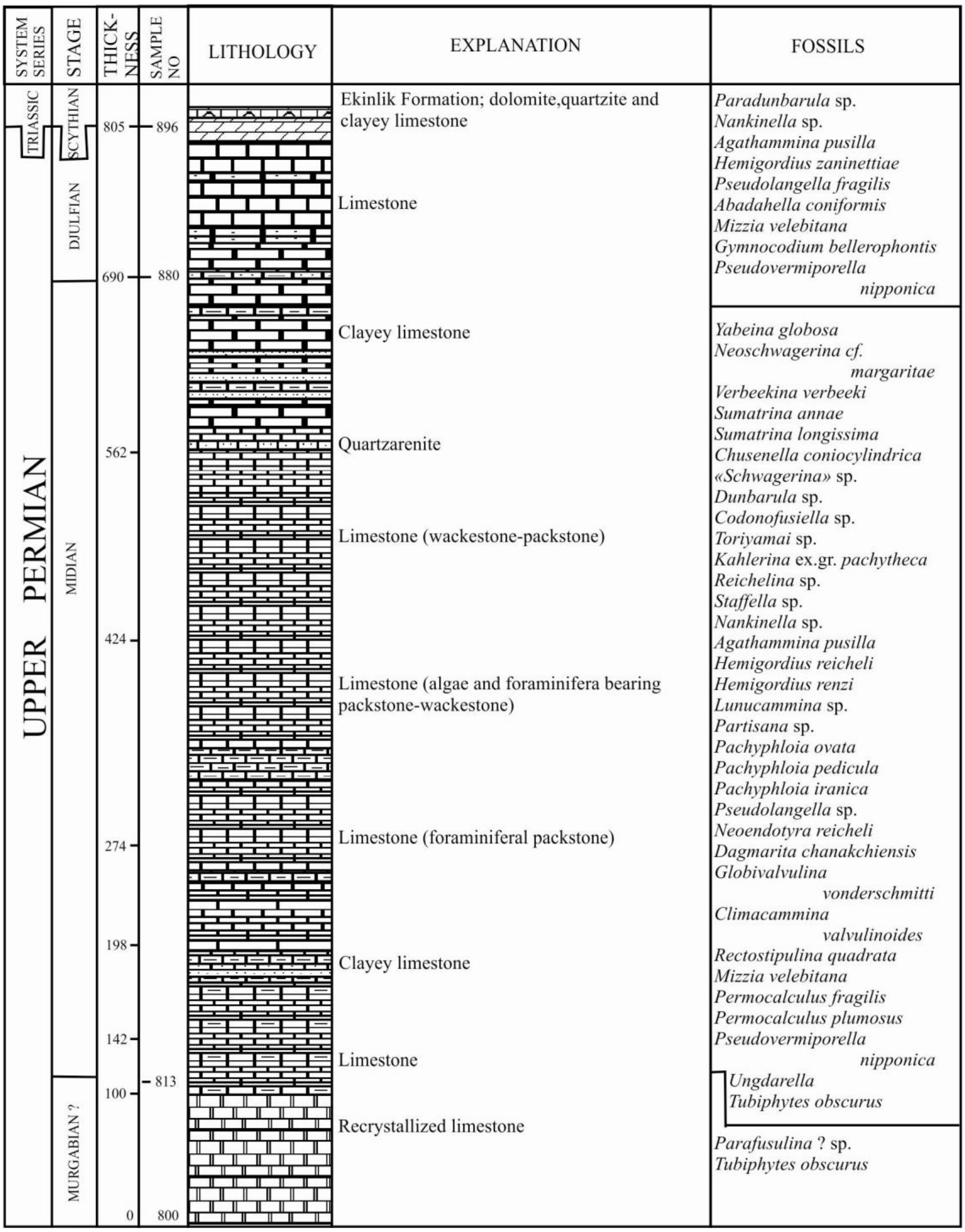

Figure 8. Generalized columnar section of the Taşkent Formation (simplified from Özgül, 1997).

The formation unconformably overlies various levels of the Kongul and Hocalar Formations and is overlain unconformably by the Ekinlik (Triassic) and Söğüt (Senonian) Formations. The thickness of the formation at the type locality is 805m (Özgül 1997) (Figure 8). Beside the rich foraminiferal and algal fossil content, the Taşkent Formation also contains brachiopods, gastropods, corals, bryzoa and crinoids (Figure 8). According to the lithologic features and fossil content, the Taşkent Formation represents a shallow shelf environment begining with a trangression and ending with a regression (Özgül 1997).

2.1.2. Ekinlik Formation

The Triassic part of the studied measured section is situated in the Ekinlik Formation. The type section of the formation is located at 6 km southwest of the Hadim Town. The formation consists intercalations of silt and sand sized clastics and shallow marine limestones (Figure 9). The Ekinlik Formation unconformably overlies mostly the Taşkent Formation of Permian and the Kongul Formation of the Carboniferous age in some localities. The formation is overlain unconformably by the Sinat Dağı Formation of Jurassic age (Özgül, 1997). The thickness of the formation is generally 610m in the type locality (Figure 9). The fossil content of the formation is poor, however, from the samples collected from the type locality the foraminiferal assemblages of Late Scythian-Anisian-Ladinian ages have been identified (Figure 9). The Ekinlik Formation is deposited in supratidal, intertidal and subtidal environmental conditions (Özgül 1997).

Within this generalized stratigraphic framework the studied section is measured across the Upper Permian Taşkent Formation and the Triassic Ekinlik Formation in order to document foraminiferal paleontology, biostratigraphy and sequence stratigraphy of the Permian-Triassic boundary beds of the Bolkar Dağı Unit.

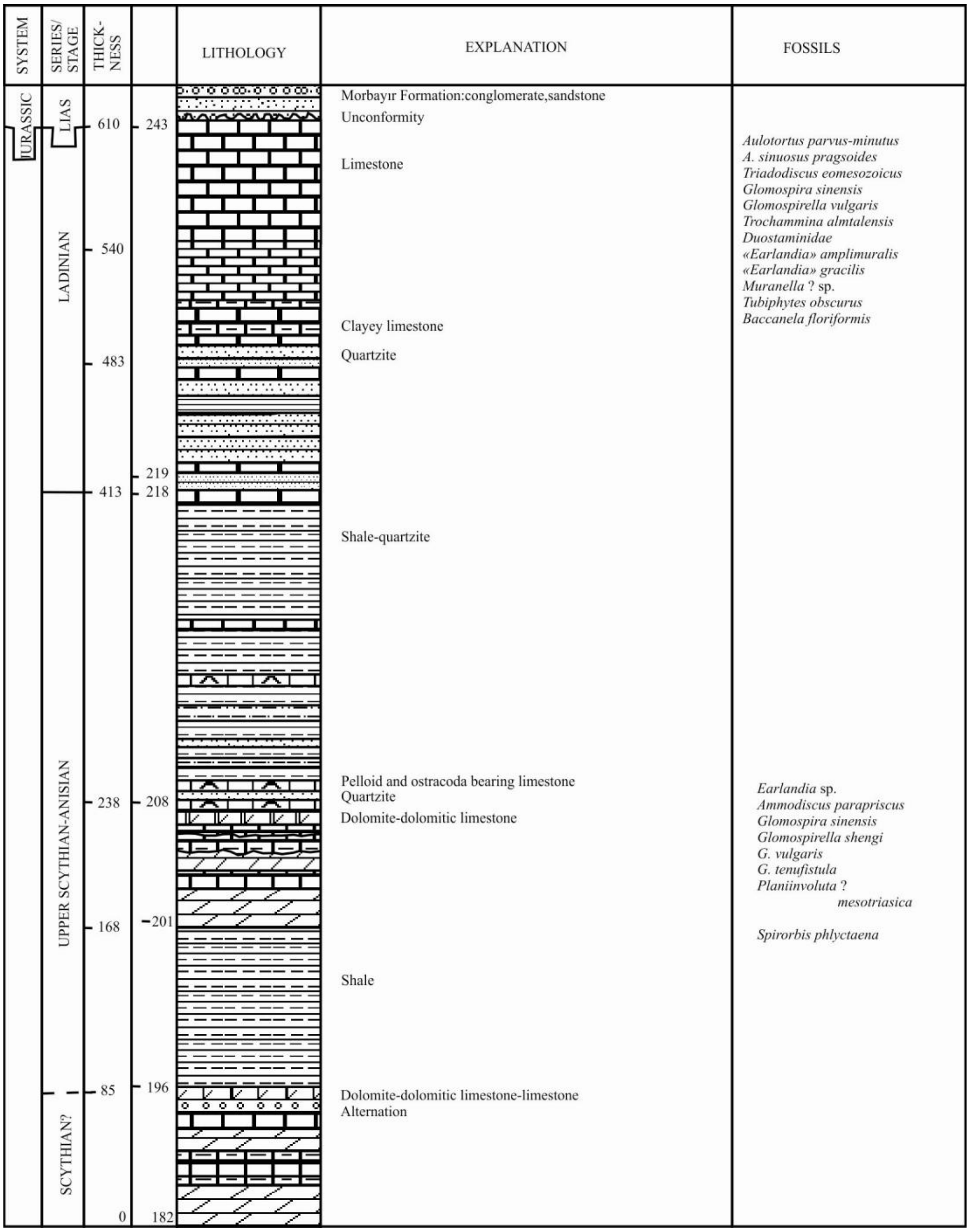

Figure 9. Generalized columnar section of the Ekinlik Formation (simplified from Özgül, 1997).

2.1.3. The Measured Section

The measured section in this study is placed through the Taşkent Formation and the Ekinlik Formation and represents the Permian-Triassic boundary beds (Figure 10). Throughout the 48,06 m thick stratigraphic section, 116 samples have been collected. At the base, the measured section begins with dark grey coloured wackestone-packstone rich in calcareous benthic foraminifera. Than a wackestone facies rich in calcareous algae and also foraminifera is observed between the samples AH-11 and AH-16. By the sample AH-17 the diversification of the calcareous foraminifera decreases and a dark gray coloured micrite is observed. From the base of the section the thickness of the layers vary between 3-82cm. Than a thick (220cm) siltstone layer overlies these limestones. After this siltstone layer, regularly positioned dark grey coloured wackestone-packstone with high diversification of foraminifera and wackestone rich in calcareous algea are deposited. Above this well diversified layers the fossil content decreases between the sample AH-37 and AH-41 and a mudstone facies with lagenoid foraminifers is deposited. After this mudstone facies the diversification begins to increase again and a wackestone-packstone facies is observed. Than a peloidal packstone to grainstone and an oolitic grainstone facies representing high energy environmental conditions is observed by the sample AH-64 and AH-65 respectively. From this level to the sample AH-90 we observe the alternation of diversified wackestone-packstone facies, peloidal packstone to grainstone facies and oolitic grainstone facies. By the sample AH-90 a 100cm thick siltstone layer overlies these limestones. Between the samples AH-91 and AH-95 the section continues with quartz arenitic sandstone and siltstone alternation with limestone intercalation. Again a thick (200cm) siltstone layer is observed by the sample AH-96. In this part of the section each layer was sampled carefully to observe the boundary. The Changhsingian foraminifers are observed for the last time in the sample AH-97 and the section passes to Greisbachian layers by the sample AH-98. Towards the upper part of the section, between the samples AH-97 and AH-102 the section continues with *Spirorbis phlyctaena*-rich wackestone and sandy or silty lime mudstone alternation. By the sample AH-104, a 73cm thick pseudoolitic or recrystallized coated grain packstone representing higher energy conditions is observed. Between the sample AH-105 and AH-108 the deposition continues regularly with Greishbachian wackestone rich in *Spirorbis phlyctaena and Rectocornuspira kalhori* and thin layers of sandy or silty lime mudstone alternation. By the sample AH-109 again a pseudoolitic or recrystallized coated grain packstone facies is observed. Throughout the top of the measured section the succession continues with *Spirorbis phlyctaena*-rich wackestone and sandy or silty lime mudstone alternations. The top of the measured section is represented by the sample AH-116 which is composed of *Spirorbis phlyctaena*-rich wackestone.

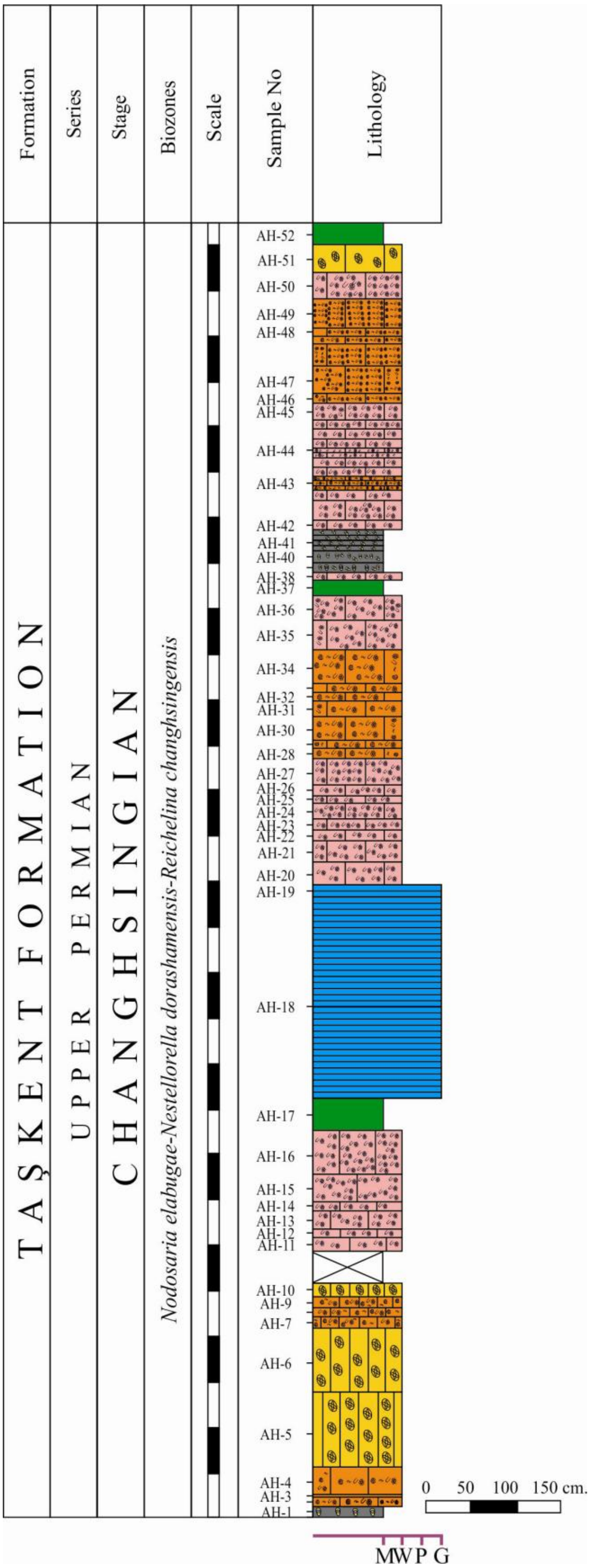

Figure 10. Lithostratigraphy of the measured section with calcareous foraminifer biozones.

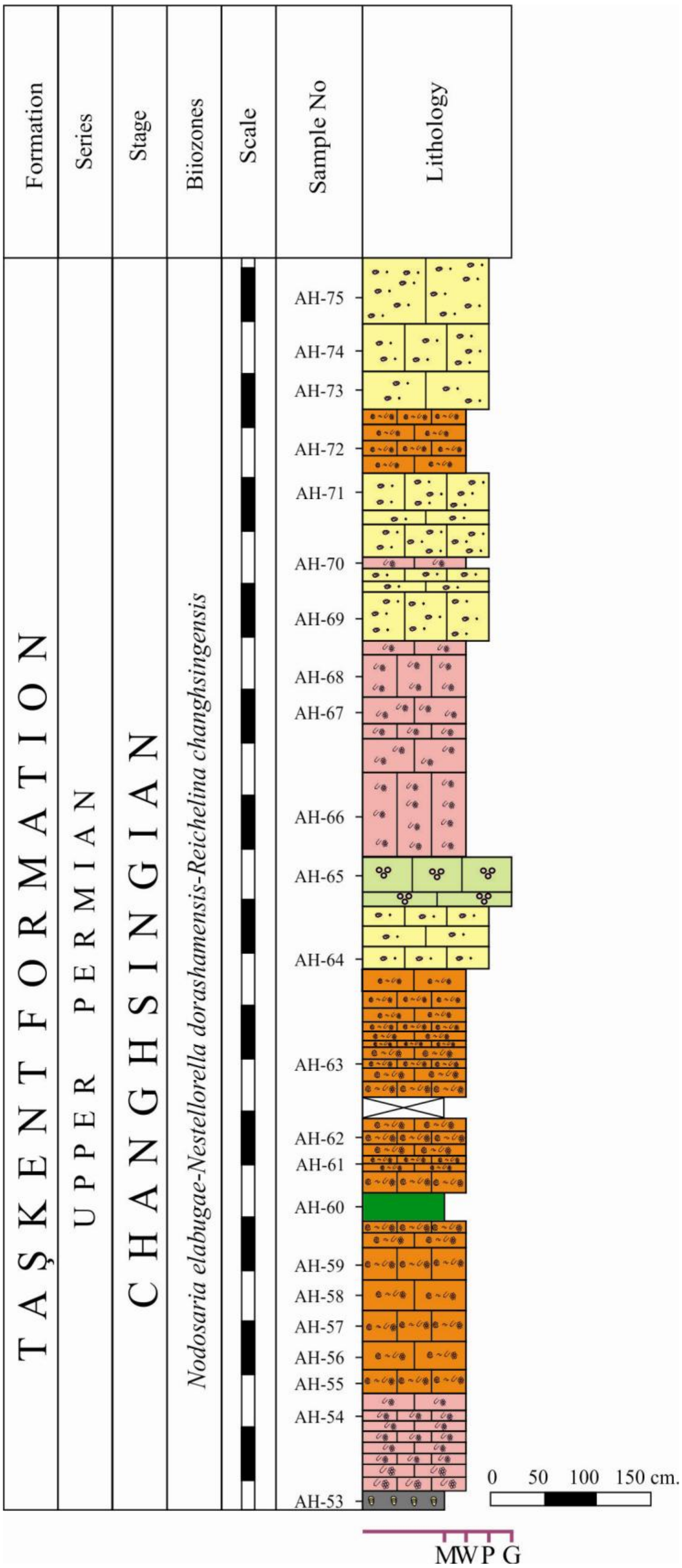

Figure 10. Continued.

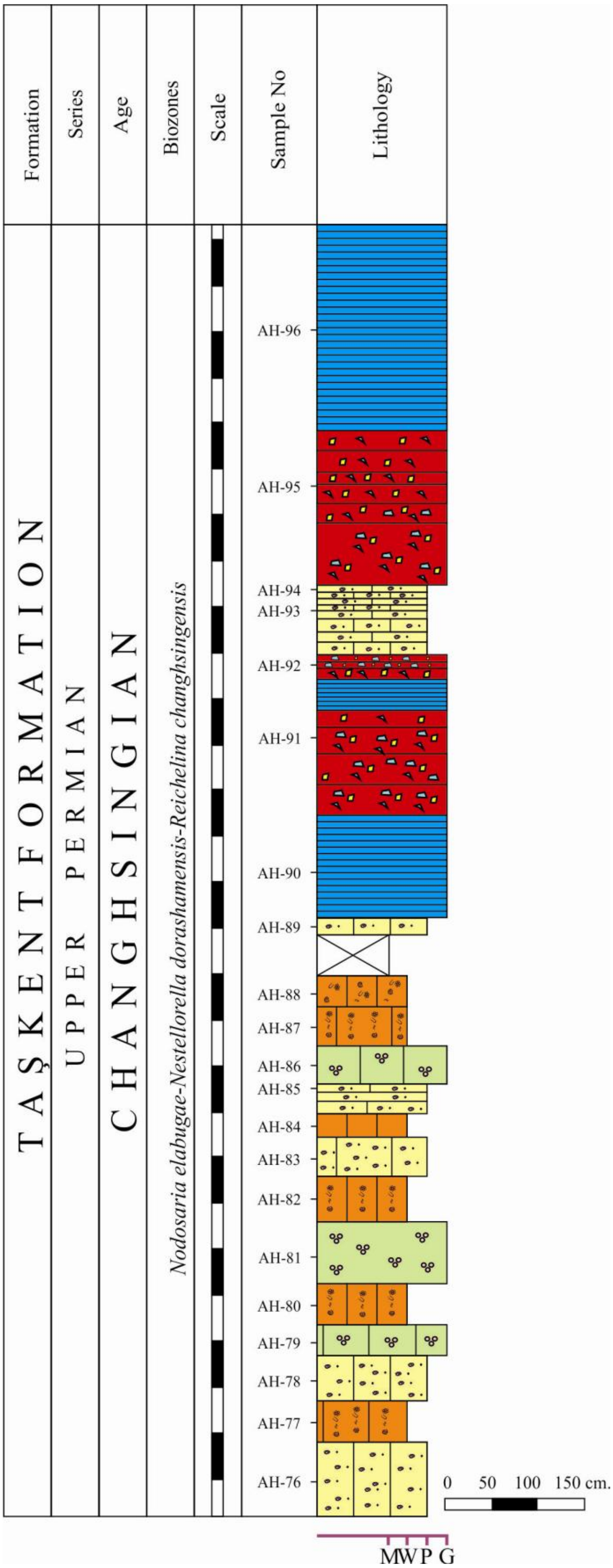

Figure 10. Continued.

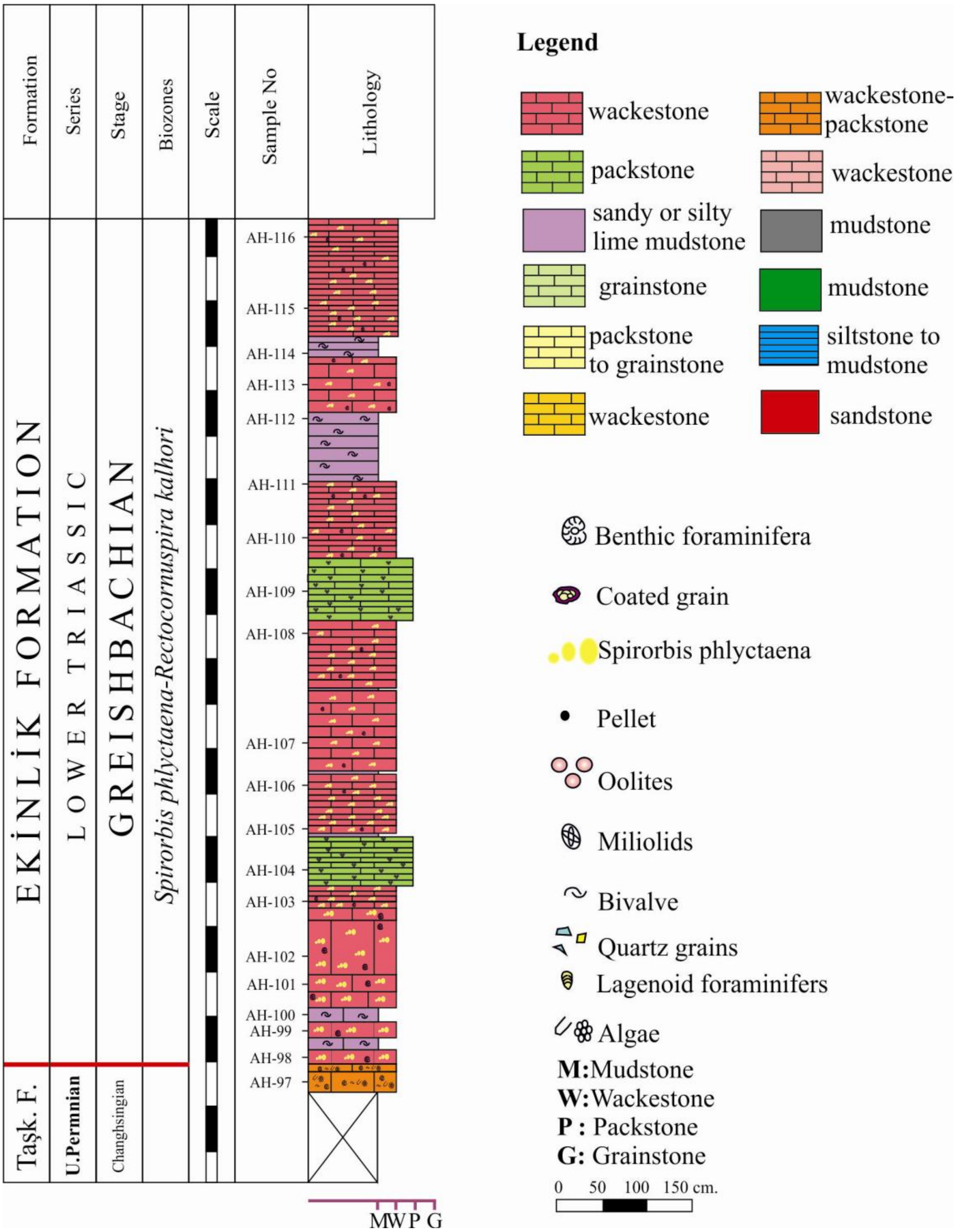

Figure 10. Continued.

2.2. Biostratigraphy

The foraminiferal inventory of Upper Permian deposits of Tauride-Anatolide platform dominated mainly by carbonates can be characterized by the general absence of neoschwagerinid-verbeekinid fusulines, rare occurences of *Paleofusulina* and the aberrant fusulines (*Codonofusiella*, *Reichelina*) in spite of the abundance of smaller Foraminifera (Altıner, 1984). Within The Upper Permian deposits of Tauride-Anatolide platform, four assemblages (Assemblage I, II, III, IV) of Foraminifera is distinguished and named by Altıner (1984). In this study the Assemblage III is characterized by *Nankinella* sp., *Reichelina tenuissima* M.-Maklay, *Hemigordius bronnimanni* Altıner, *H. zaninettiae* Altıner, *H. guvenci* Altıner, *H. padangensis* (Lange), *Paraglobivalvulina gracilis* Zaninetti and Altıner, *Lousettita elegantissima* Altıner and Brönnimann, *Lunucammina ichnousa* Sellier de Civrieux and Dessauvagie, *Pachyphloia iranica* Bozorgnia, *Frondina* n. sp. , *Pseudotristix solida* Reitlinger and Assemblage IV is characterized by *Codonofusiella schubertelloides* Sheng, *Palaefusulina* cf. laxa Sheng, other undetermined species of *Palaefusulina*, *"Hemigordiopsis'' renzi evolutus* Lys, *Kamurana bronnimanni* Altıner and Zaninetti, *Paradagmarita monodi* Lys, *Paradagmarita flabelliformis* Zaninetti, Altıner and Çatal, *''Ichthyolaria'' latilimbata* Sellier de Civrieux and Dessauvagie, *Nodosaria armeniensis* Efimova, *Robuloides gibbus* Reichel and *Robuloides gourisiensis* Reichel. At the upper boundary of this assemblage most of these Permian species disappeared and new Mesozoic assemblages began to replace the Paleozoic ones (Altıner, 1984).

In Altıner and Özgül 2001, the Middle-Upper Permian of the Bolkar Dağı Unit and Aladağ Unit was studied and the succession of the Aladağ unit in the Hadim area was divided as Midian –Md1 *Dunbarula* Zone, Djulfian Dj1 *Septoglobivalvulina gracilis* Zone and Uppermost Djulfian-Dorashamian Do1 *Paradagmarita* Zone. *Septoglobivalvulina gracilis* Zone has been defined as an interval from the last occurence of *Dunbarula* to the first occurence *Paradagmarita* in this study. Lastly, *Paradagmarita* Zone has been characterized by the total range of *Paradagmarita* and the other species of foraminifera recorded in the zone are,

Table 1: Foraminiferal distribution chart.

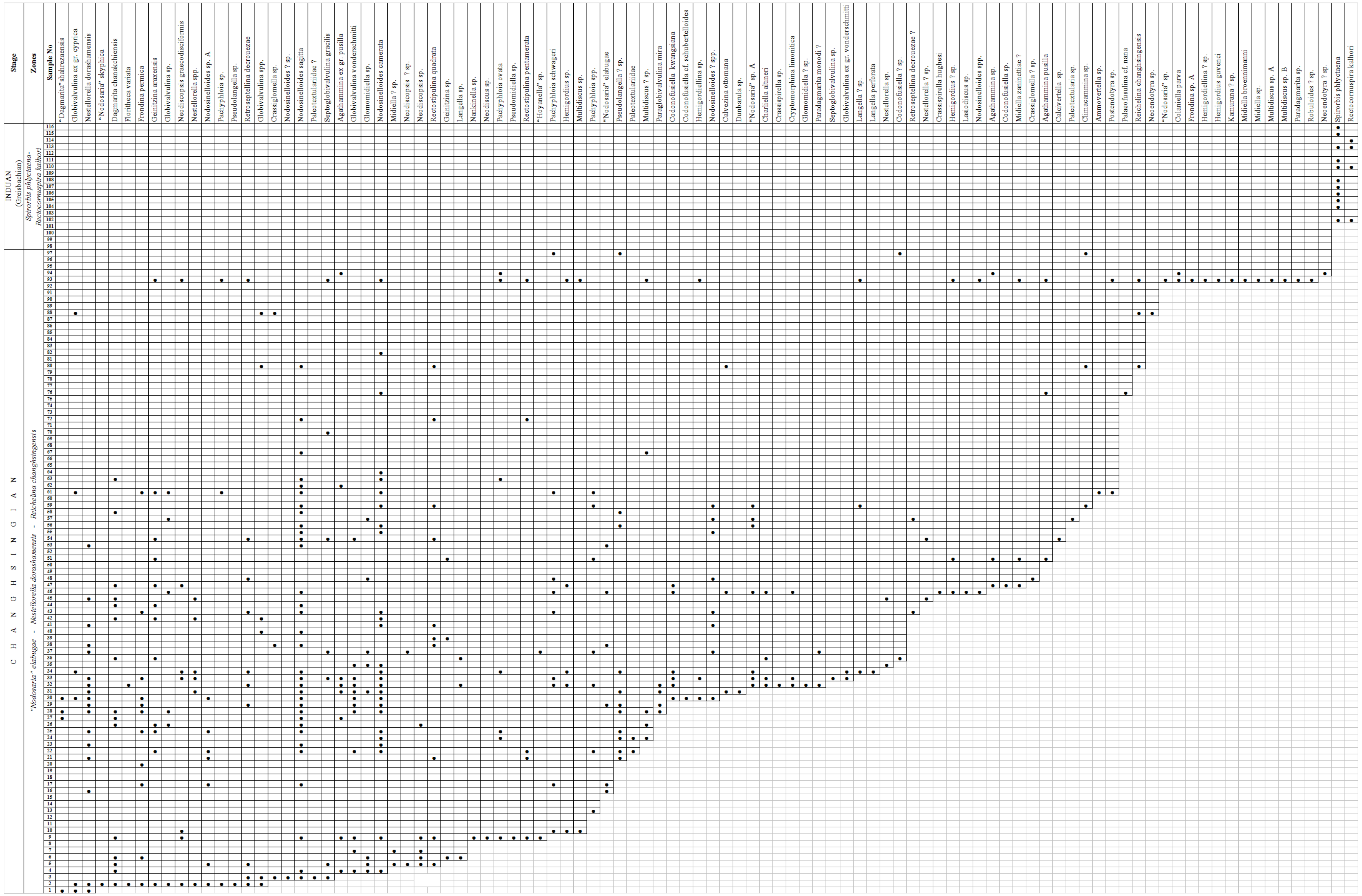

Staffella sp., *Dagmarita chanakchiensis*, *Paradagmarita monodi*, *Lousettita elegantissima*, *Globivalvulina vonderschmitti*, *Septoglobivalvulina gracilis*, *Pachyphloia ovata*, *P. schwageri*, *Geinitzina postcarbonica*, *Geinitzina* sp. *Hemigordius* spp., *Cornuspira* sp., *Rectostipulina quadrata* (Altıner and Özgül 2001).

According to the detailed analysis of thin sections of samples the measured section across the Permian-Triassic boundary is divided into two biozones. The lower assemblage zone "*Nodosaria*" *elabugae-Nestellorella dorashamensis-Reichelina changhsingensis* represents the Changsingian part of the measured section and the upper zone (*Spirorbis phlyctaena-Rectocurnuspira kalhori* Zone) represents the Greisbachian part of the measured section.

2.2.1. "*Nodosaria*" *elabugae* - *Nestellorella dorashamensis* - *Reichelina changhsingensis* Assemblage Zone

This assemblage zone is composed of an alternation of various types of facies including bioclastic wackestone with diversified foraminifera, wackestone with miliolid foraminifera, coated packstone and oolitic grainstone. The zone begins at the bottom of the measured section and terminates by the sample AH-97. The base of the assemblage zone is quite diversified in foraminifers and contains "*Dagmarita*" *shahrezaensis*, *Globivalvulina* ex gr. *cyprica* and *Nestellorella dorashamensis* (Table 1). Upwards in the section the fossil content gets richer by the presence of *Floritheca variata*, *Globivalvulina* sp., *Pachyphloia* sp., *Retroseptellina decrouezae* and *Rectostipulina pentamerata*. Between samples AH-11 and AH-15 a certain decrease observed in the diversification (Table 1). By the sample AH-20 foraminifers become abundant and a richer diversity period begins and continues until the sample AH-66. In this part of the section various lagenid foraminifers such as *Nestellorella dorashamensis*, "*Nodosaria*" *elabugae*, *Nodosinelloides sagitta*, *Nodosinelloides camerata*, *Frondina permica* and *Geinitzina araxensis* are recorded in high number of individuals. Apart from these species *Charliella altineri*, *Dagmarita chanakchiensis*, *Nestellorella* spp., *Rectostipulina quadrata*, *Agathammina* ex. gr. *pusilla*, *Globivalvulina vonderschmitti*, *Glomomidiella* sp., *Paraglobivalvulina mira*, *Codonofusiella kwangsiana* are frequently recored in the samples (Table 1). Between samples AH-60 and AH-92 the abundance and diversity in foraminifers decrease again. This part of the assemblage zone contains *Palaeofusulina nana*, *Reichelina changhsingensis*, *Nodosinelloides sagitta*, *Globivalvulina* spp., *Septoglobivalvulina gracilis*, *Nodosinelloides camerata*, *Rectostipulina quadrata*, *Calvezina ottomana*, *Neoendotyra* sp. and *Agathammina pusilla*. By the sample no AH-93 again an enrichment is observed in the foraminiferal content. *Pachyphloia ovata*, *Rectostipulina pentamerata*, *Hemigordius* sp., *Multidiscus* sp., *Hemigordiellina* sp., *Postendotyra* sp., *Colaniella parva*, *Midiella broennimanni* and *Paradagmarita* sp. represent a part of foraminifers recorded in this part of the assemblage zone. The upper boundary of the assemblage zone is defined by the presence of some biostratigraphically undiagnostic Permian foraminifers including *Pachyphloia schwageri*, *Pseudolangella* ? sp. and *Climacammina* sp. recored in the sample AH-97.

The other species recorded in “*Nodosaria*” *elabugae* - *Nestellorella dorashamensis* - *Reichelina changhsingensis* Assemblage zone are: “*Nodosaria*” *skyphica*, *Neodiscopsis* sp., *Nodosinelloides* sp. A, *Pseudolangella* sp., *Crassiglomella* sp., Paleotextulariidae ?, *Midiella* ? sp., *Geinitzina* sp., *Langella* sp., *Nankinella* sp., *Neodiscus* sp., *Pseudomidiella* sp., “*Hoyanella*” sp., *Pachyphloia* spp., *Multidiscus* ? sp., *Dunbarula* sp., *“Nodosaria”* sp. A, *Crassispirella* sp., *Cryptomorphina limonitica*, *Paradagmarita monodi* ?, *Septoglobivalvulina* sp., *Globivalvulina* ex gr. *vonderschmitti*, *Langella perforata*, *Nestellorella* sp., *Crassispirella hughesi*, *Hemigordius* ? sp., *Lasiodiscus* sp., *Nodosinelloides* spp., *Agathammina* sp., *Codonofusiella* sp., *Midiella zaninettiae* ?, *Crassiglomella* ? sp., *Calcivertella* sp., *Paleotextularia* sp., *Ammovertella* sp., *Frondina* sp. A, *Hemigordiellina* ? sp., *Hemigordius guvenci*, *Kamurana* ? sp., *Midiella* sp., *Multidiscus* sp. A, *Multidiscus* sp. B, *Robuloides* ? sp. and *Neoendotyra* ? sp.

2.2.2. *Spirorbis phlyctaena-Rectocornuspira kalhori* Assemblage Zone

This zone is composed of *Spirorbis phlyctaena*-rich wackestone, pseuduoolitic or recrystallized coated grain packstone and sandy or silty lime mudstone alternations. It is defined as the interval between the level where the last occurence of Permian foraminifers is observed and the last bed at the top of the section (Table 1). The zone is characterized by the frequent occurrences of *Spirorbis phlyctaena* and *Rectocornuspira kalhori*, typical taxa for most of the Greisbachian strata in the world. Brönnimann et al. (1972a) studied the Triassic smaller foraminiferal fauna in the Elika Formation (Northern Iran) and the Siusi Formation (Northern Italy) and described *Earlandia* spp. *Cornuspira mahajeri* and *Rectocornuspira kalhori* in the lowermost Triassic strata. Altıner et al. (1980) have studied the Pınarbaşı (Taurides), Julfa (NW-Iran) and Gheshlagh and Gheselgaleh (eastern Elburz, Iran) and stated that the first abundant occurrence of the *Spirorbis* appeared everywhere in these localities above the lowermost Triassic beds. Also Altıner et al.(1980) recorded the occurence of *Rectocornuspira kalhori* and *Earlandia* sp. at the lowermost Triassic of these sections. Işık (1983) studied the foraminiferal population of the Permian-Triassic boundary beds in the Aladağ Unit (Taurides, Turkey), and defined *Cyclogyra* ? *mahajeri*, *Rectocornuspira kalhori* and *Earlandinita* sp. Assamblage Zone representing the lowermost Triassic interval of the measured section. Broglio-Loriga et al. (1986) studied in the lower Triassic sequences of the Dolomites (Italy) and recorded the existence of "*Cyclogyra-Rectocornuspira*" in these sequences. Another study carried out about the foraminiferal stratigraphy of the Triassic beds was Oravecz-Scheffer (1987) in which the presence of *Rectocornuspira kalhori* was reported in the earliest Triassic strata of the Transdanubian Mid Mountains (Hungary).

Ramovs (1986) reported the presence of the *Cornuspira kahleri* in the lowermost Triassic beds in the Slovenian part of the Karawanken Mountains. Köylüoğlu and Altıner (1989) recorded *Rectocornuspira kalhori* in the earliest Triassic strata of the Hakkari region (southeast Turkey). Jenny Deshusses (1991) was another study which documented *Cornuspira mahajeri* and *Rectocornuspira kalhori* in the lowermost Triassic beds of the Carnic Alps, Austria. Rettori (1995) studied the Julian Alps and Northern Calcareous Alps (northern Italy) and reported *Rectocornuspira kalhori* in the lowermost Triassic beds. Ünal et al. (2003) and Groves et al. (2005) studied in the Central Taurides (Turkey) and described and illustrated *Rectocornuspira kalhori* in the lower Triassic (Greisbachian) beds. Wignall and Hallam (1996) and Ezaki (2003) studied the end-Permian mass extinction and the lowermost Triassic beds respectively in Sichuan Province (South China) and described the presence *Rectocornuspira kalhori* at the basal Triassic strata. Groves et al. (2007) also recorded *Earlandia* spp. and *Rectocornuspira kalhori* near and above the Permian-Triassic boundary extinction level. Gaillot (2006), in his study in the Khuff Formation, determined the presence of *Rectocornuspira kalhori* in the lowermost Triassic strata. Recently, Krainer and Vachard (2009) studied the lower Triassic Werfen Formation of the Karawanken Mountains (Southern Austria) and reported a relatively numerous assemblage of *Postcladella* a new genus replacing the name *Rectocornuspira*, *Earlandia dunningtoni*, *Spirorbis phlyctaena* and *Meandrospira pusilla* in the lower Traissic interval.

2.2.3. Permian-Triassic Boundary

Until 1984, the ammonoid Otoceras was considered as the index fossil of the Permian-Triassic boundary. Later in March 2001 the GSSP of the Permian-Triassic boundary is defined at the base of the Bed 27c, Meishan Section D. Changxing Country, Zhejiang Province, China, at the horizon where the conodont *Hindeodus parvus* appeared (Yin et al., 2001).

Calcareous foraminifera is also used to define the Permian-Triassic boundary. The disappearence of Permian foraminifers and the appearence of *Rectocornuspira kalhori* is used to determine the Permian-Triassic boundary. In southern Turkey Altıner and Zaninetti (1981), Köylüoğlu and Altıner (1989), Altıner et al. (2005), Groves et al. (2005), Payne et al. (2007), in Italy Broglio-Loriga et al. (1986), Groves et al. (2007), in Carnic Alps (Austria) Jenny Deshusses (1991) and Krainer and Vachard (2009), in South China, Wignal and Hallam (1996) and Ezaki (2003) have used the presence of *Rectocornuspira kalhori* as the Greisbachian marker.

The Permian-Triassic boundary beds in the measured section is composed of bioclastic wackestone-packstone with diversified foraminifera and *Spirorbis phlyctaena*-rich wackestone and sandy silty mudstone alternation. The Permian-

Triassic boundary was determined as at the base of the level AH-98 overlying the level AH-97 containing the Permian foraminifers. A diversified foraminiferal fauna is observed in the sample AH-97 associated with several algae and gastropods. The sample AH-98 does not contain any Permian foraminifera and the earliest *Spirorbis phlycateana* and *Rectocornuspira kalhori* of Triassic are recorded in the sample AH-102 (Table 1).

Along the measured section the Permian-Triassic boundary is delineated between, as previously defined, the Changhsingian "*Nodosaria*" *elabugae* - *Nestellorella dorashamensis* - *Reichelina changhsingensis* Assemblage Zone and the Greisbachian *Spirorbis phlyctaena-Rectocornuspira kalhori* Assemblage Zone (Table 1).

CHAPTER 3

SEQUENCE STRATIGRAPHY

Sloss (1963) considered sequences to be major rock stratigraphic units traceable over major areas of a continent and bounded by unconformities of interregional scope for the first time. Also he recognized that such sequences had chronostratigraphic significance. On the other hand with the work of Vail (1975) and Vail et al. (1977) seismic stratigraphy evolved in the 1970’s. This new metod for analyzing seismic-reflection data stimulated a revolution in stratigraphy. The concepts of seismic stratigraphy were published together with a global sea-level cycle chart (Vail et al. 1977), based on the underlying assumption that eustasy is the main driving force behind sequence formation at all levels of stratigraphic cyclicity. In these studies the concepts are defined based on the depositional sequences. The depositional sequence concept has been redefined by Mitchum et al.(1977) as a stratigraphic unit composed of a relatively conformable succession of genetically related strata and bounded at its top and base by unconformities and their correlative conformities. All these progresses with the combination outcrop and well data led to the evolution of sequence stratigraphy concept.

Sequence stratigraphy is the study of rock relationships within a chronostratigraphic framework of repetitive, genetically related strata bounded by surfaces of erosion or nondeposition, or their correlative conformities (Van Woganer et al., 1988).

The fundamental unit of sequence stratigraphy is the sequence, which is bounded by unconformities and their correlative conformities. A sequence can be subdivided into systems tracts**,** which are defined by their position within the sequence and by the stacking pattems of parasequence sets and parasequences bounded by marine-flooding surfaces. Sequences, parasequence sets, and parasequences are defined and identified by the physical relationships of strata; including the lateral continuity and geometry of the surfaces bounding the units, vertical and lateral stacking patterns, and the lateral geometry of the strata within these units (Van Woganer et al. 1988).

Following these studies about the siliciclastic rocks**,** for the first time Sarg (1988) described the application of sequence stratigraphy to the interpretation of carbonate rocks, documenting with outcrop, well-log, and seismic examples most aspects of the conceptual models. Carbonate sequence stratigraphy plays a major role in reservoir characterization and simulation. Intensive analyses of outcrop data, detailed facies studies of carbonate cycles have led to the development of 3-D models describing depositional and diagenetic patterns of carbonate rocks and predicting carbonate reservoirs.

A cycle is a group of rock units that occur in a certain order with one unit being frequently repeated throughout the succession (Flügel, 2004). The stratigraphic record is a composite of several orders of superimposed sedimentary cycles, depending on their casual mechanisms. They range from the high-frequency Milankovitch-scale climatic cycles (often 1m to a few meters in thickness) to third-order (mostly 1 to 2 My in duration) and fourth-order (<0,5My in duration) eustatic cycles, and larger (several million years in duration) tectonic cycles (Haq and Schutter, 2008).

The stratification of the carbonate platforms is caused by stacking of meter-scale depositional sequence displaying a shallowing upward trend. The shallowing upward sequences consist of repetitions of subdital facies bounded by peritidal facies, subaerial exposure surfaces and/or marine flooding surfaces (Flügel, 2004).

In this study shallowing-upward meter-scale cycles are determined across the Permian-Triasssic boundary beds of Bolkar Dağı Unit. The cycles are determined according to vertical arrangement of microfacies types. In order to determine the microfacies types representing distint environmental and depositional conditions, detailed microfacies analysis is carried out. According to the features of shallowing-upward cycles system tracts are determined and the sequence stratigraphic model of the measured section is presented (Figure 30).

3.1. Microfacies Types

The increasing importance of limestones and dolomites as reservoir rocks and the use of thin section fossils in subdividing carbonate platforms gave substantial impetus to the progress of microfacies research. The microfacies term is originally defined by Brown (1943) as petrographic and paleontologic criteria studied in thin sections. Today, microfacies is regarded as the total of all sedimentological and paleontological data which can be described and classified from thin sections, peels, polished slabs or rock samples (Flügel, 2004). All the limestone classifications commonly used in facies analyses are based on textural and compositional criteria. The most widely used classifications are those of Dunham (1962) and Folk (1959, 1962). Microfacies based on thin section studies subdivides facies into units of similar compositional aspects that reflect specific depositional environments and controls.

A facies model is a generalized summary of a given depositional system (Walker 1992). Wilson (1975) used the succession of major facies belts on rimmed tropical carbonate platforms to establish a Standard Facies Model. In his model Wilson defined 10 Standard Facies Zones describing idealized facies belts along an abstract transect from open marine deep basins across a slope, a pronounced marginal rim and an iner platform to the coast (Flügel, 2004). Standard microfacies types are virtual categories that summarize microfacies with identical criteria. Most SMF types are based on dominant characteristics comprising grain types, biota or depositional textures (Flügel, 2004). Wilson (1975) distinguished 24 SMF Types and used these types as additional criteria in differentiating the major facies belts of an idealized rimmed carbonate shelf. After him, Flügel (2004) determined 26 SMF Types for rimmed carbonate platforms (Figure 11). Also he studied about carbonate

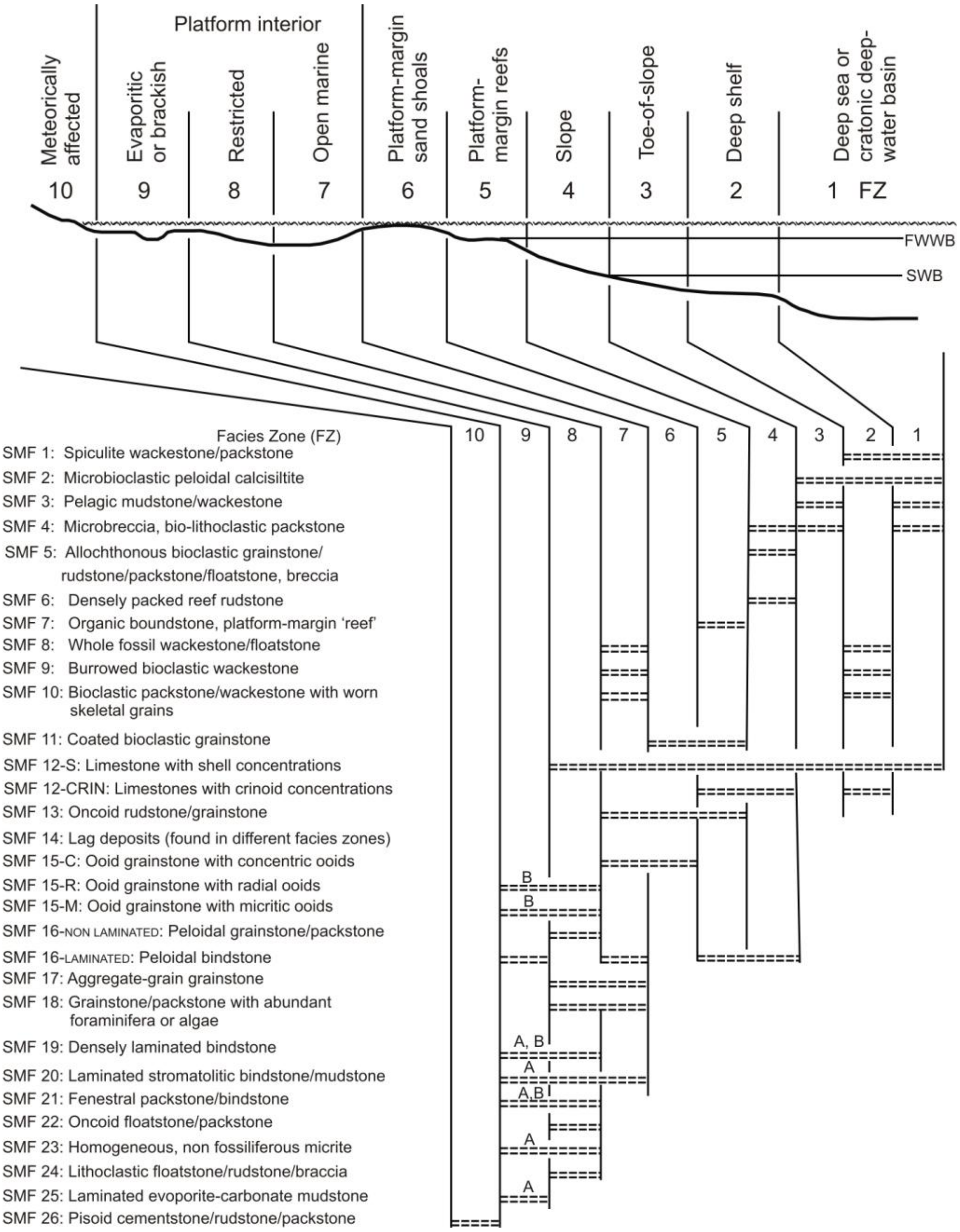

Figure 11. Distribution of SMF Types in the Facies Zones (FZ) of Wilson (1975) of the rimmed carbonate platform model (A:Evaporatic, B:Brackish), (Flügel, 2004).

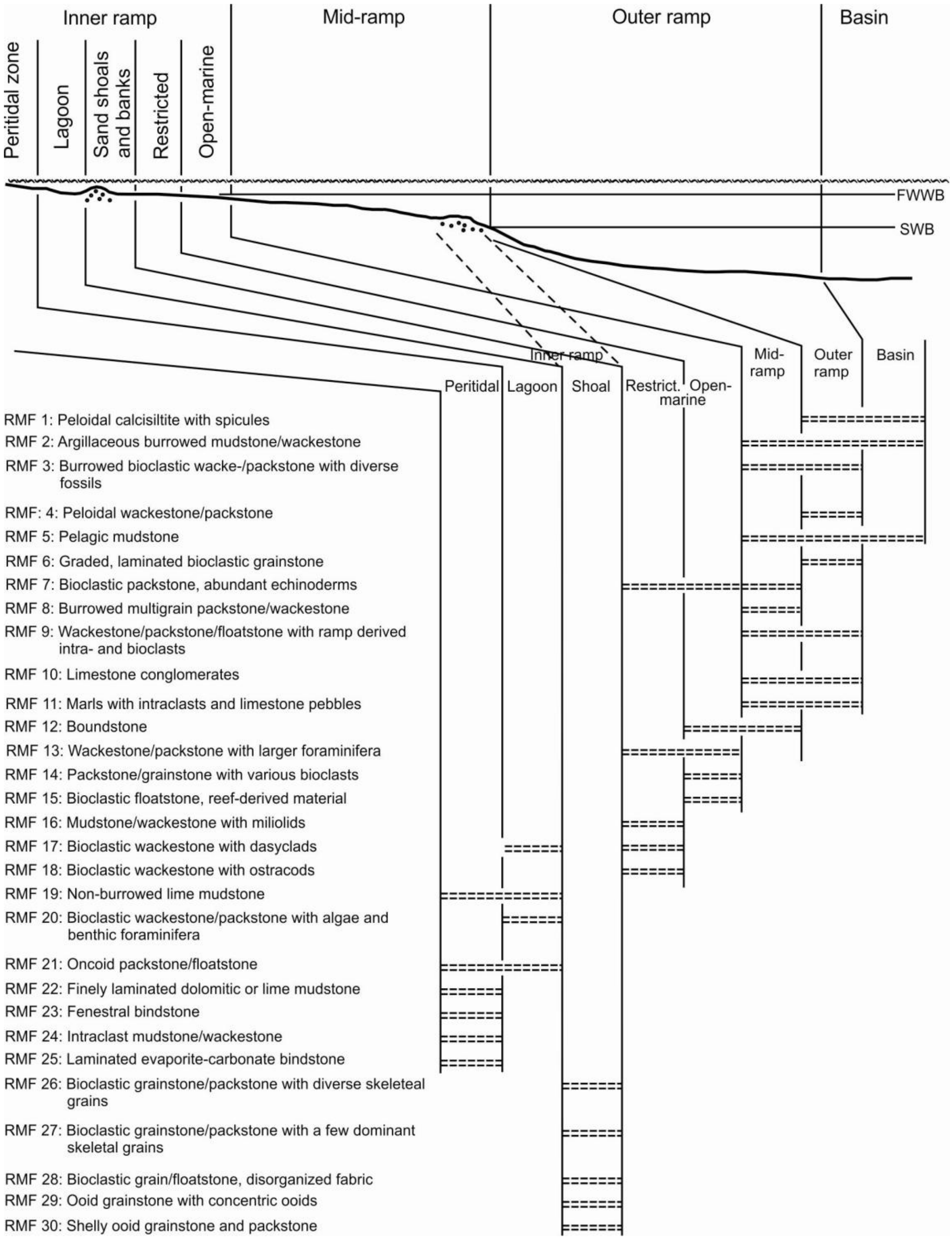

Figure 12. Distribution of microfacies types in different parts of a homoclinical carbonate ramp (Flügel, 2004).

ramps and idendified 30 Ramp Microfacies Types (RMT) distributed througout the deeper outer ramp zones, mid ramps and shallow inner ramp zones (Figure 12).

Under the light of this information the carbonates have been classified according to the Dunham (1962) and 12 microfacies types were distinguished. The determined microfacies types in this study are; mudstone with lagenoid foraminifera, bioclastic wackestone with calcareous algae and benthic foraminifera, bioclastic wackestone-packstone with diversified foraminifera, wackestone with miliolid foraminifera, unfossiliferous mudstone, peloidal packstone to grainstone, oolitic grainstone, siltstone to mudstone and quartz arenitic sandstone, *Spirorbis phlyctaena*-rich wackestone, pseudoolitic or recrystallized coated grain packstone, sandy or silty lime mudstone.

3.1.1. MF 1 Mudstone with Lagenoid Foraminifera

This facies type is composed of micrite and includes lagenoid benthic foraminifers such as *Nodosinelloides camerata*, “*Nodosaria*” *elabugae, Langella* sp. and *Nodosaria* sp. (Figure 13). This facies type represents possibly the deposits laid down below the wave base in the platform interior observed in the samples AH-1, AH-37, AH-39, AH-40 and AH-41. It is probably the equivalent of SMF 9 corresponding to the open marine zone (FZ 7) of the platform interior (Flügel, 2004).

3.1.2. MF 2 Bioclastic Wackestone with Calcareous Algae and Benthic Foraminifera

This microfacies is rich in calcareous algae and contains also benthic foraminifera and gastropods. The common texture of the facies is wackestone (Figure 14) and is placed landward side of the MF 1. It is observed in the intervals between AH-11 and AH-16, between AH-20 and AH-27, between AH-44 and AH-45 and in the upper part of the section between samples AH-66 and AH-68 (Figure 30).

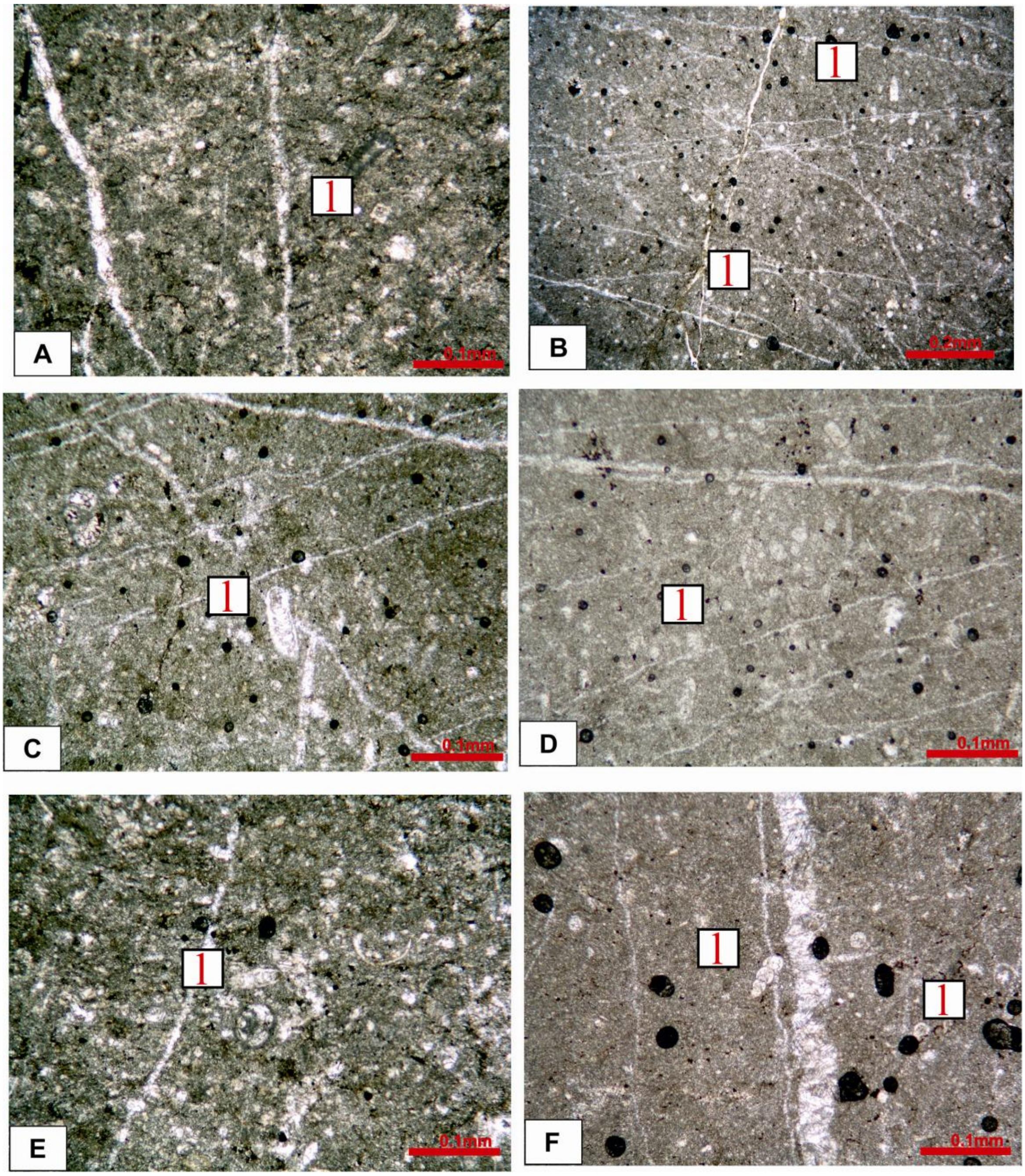

Figure 13. Photomicrographs of the MF 1 mudstone with lagenoid foraminifera microfacies, (l: lagenoid foraminifera), (A:AH-39, B-C-D:AH-40, E:AH-41, F:AH-53).

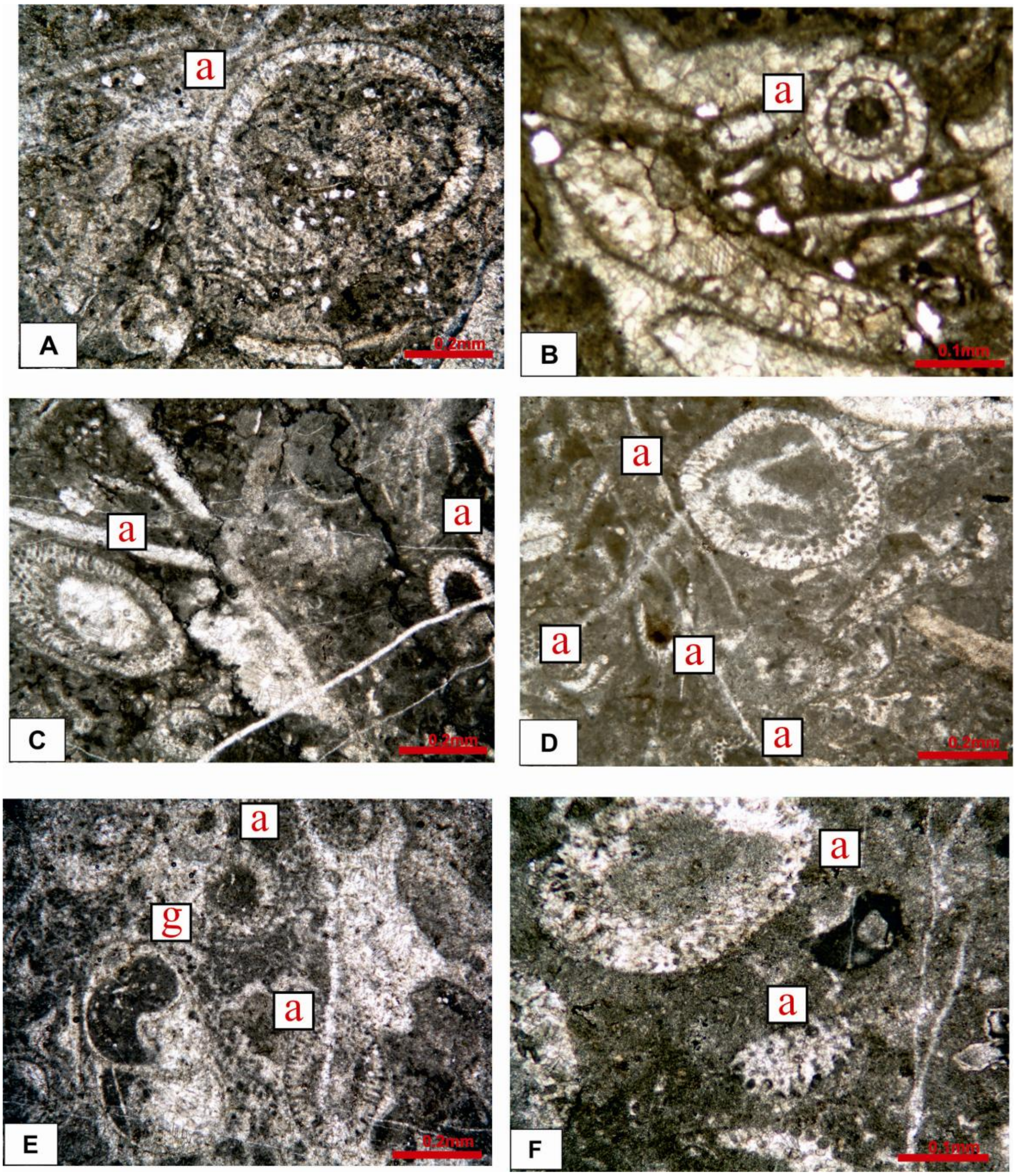

Figure 14. Photomicrographs of the MF 2 bioclastic wackestone with calcareous algae and benthic foraminifera microfacies (a: algae), (A:AH-11, B:AH-12, C:AH-24, D:AH-26, E:AH-35, F:AH-44).

This type of facies corresponds to RMF17 (Bioclastic wackestone with dasyclads) of Flügel (2004) deposited in the restricted part of the inner ramp.

3.1.3. MF 3 Bioclastic Wackestone-Packstone With Diversified Foraminifera

This microfacies type is characterized by the highly diversified benthic foraminiferal assemblages. *Nodosinelloides* spp., *Globivalvulina* sp., *Codonofusiella* sp., *Frondina permica*, *Dagmarita chanakchiensis* and *Rectostipulina quadrata* are the most frequently encountered taxa. Apart from these foraminifera, algae, gastropoda and echinodermata fragments are also present in the microfacies (Figure 15).

MF 3 is probably the equivalent of SMF 18 (Grainstone/Packstone with abundant foraminifera or algae) of Flügel (2004) and corresponds to FZ8 (restricted environment of platform interior) of Wilson (1975).

3.1.4. MF 4 Wackestone with Miliolid Foraminifera

This microfacies is generally observed in the lower part of the measured section. In this type, the foraminifers decrease in diversity but the abundance of miliolids increases (Figure 16).

This microfacies type is similar to RMF 16 (Mudstone, wackestone or packstone with abundant miliolid foraminifera) defined by Flügel (2004). According to the RMF model of Flügel (2004) wackestone with abundant miliolid foraminifera is deposited in the restricted environment of the inner ramp.

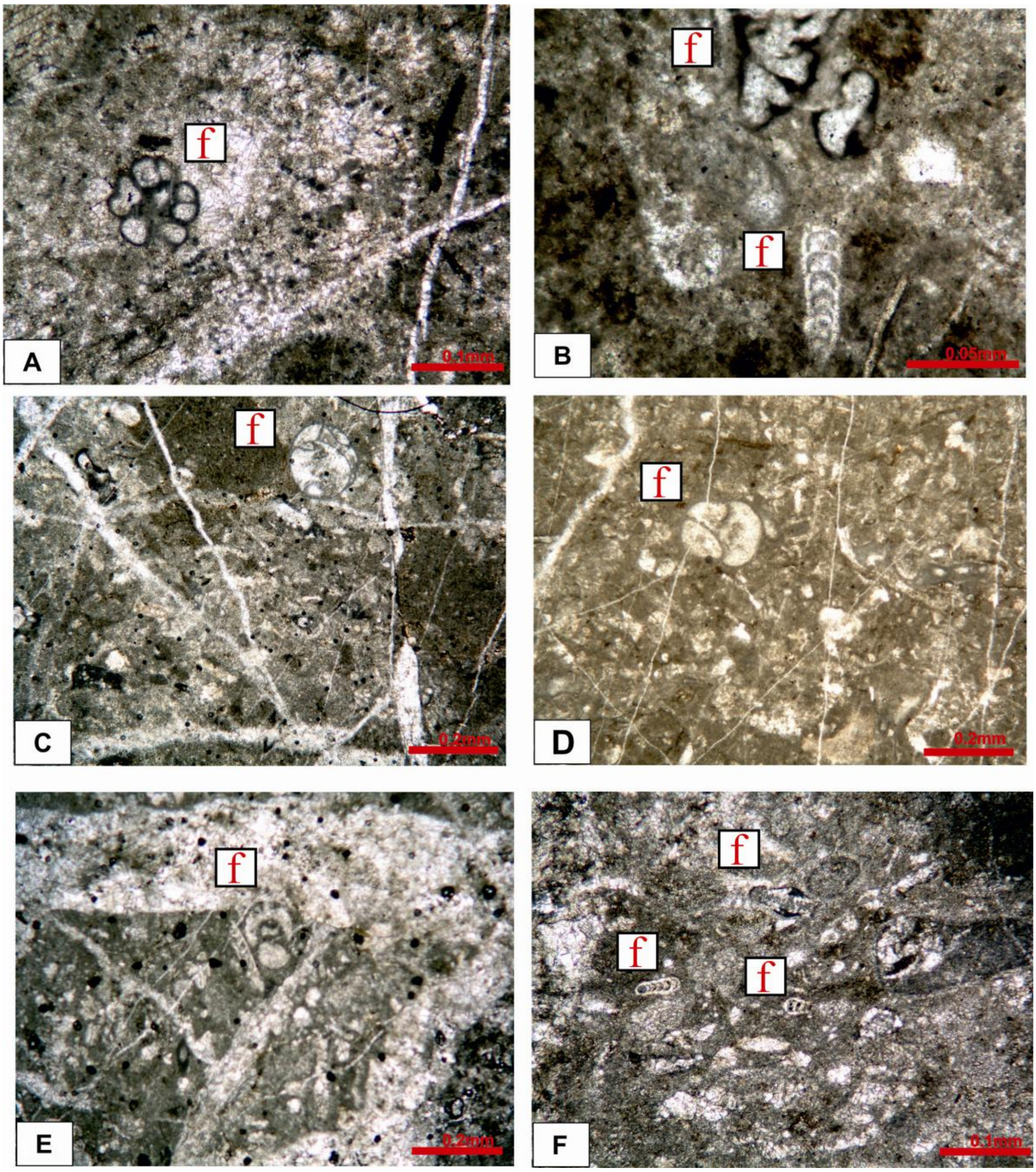

Figure 15. Photomicrographs of the MF 3 bioclastic wackestone-packstone with diversified foraminifera microfacies (f: foraminifers), (A:AH-2, B:AH-3, C:AH-28, D:AH-32, E:AH-59, F:AH-62)**.**

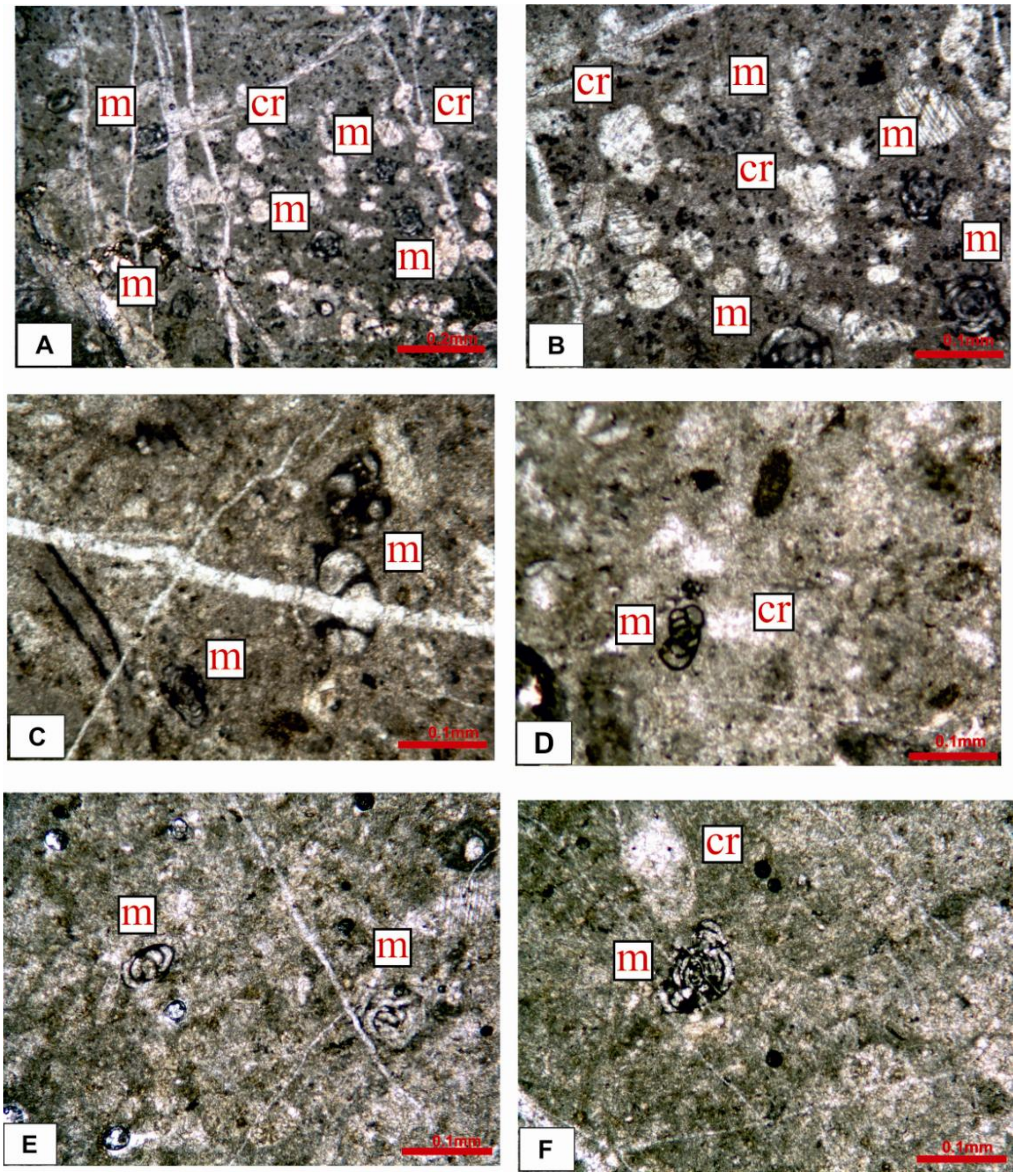

Figure 16. Photomicrographs of the MF 4 wackestone with miliolid foraminifera microfacies (m: miliolid foraminifer, cr: crinoid), (A-B:AH-5, C-D:AH-10, E-F:AH-37).

3.1.5. MF 5 Unfossiliferous Mudstone

This microfacies is mainly composed of unfossiliferous lime mudstone and deposited in the low energy conditions of lagoonal environment of inner ramp settings (Figure 17). This microfacies type is similar to the SMF 23 (Non-laminated homogeneous micrite and microsparite without fossils) of Flügel (2004). Throughout the measured section generally this microfacies type takes place at the top of shallowing up-ward cycles (Figure 30). According to the SMF model of Flügel (2004) this microfacies type is deposited in the tidal flats (FZ 8) and around the arid evaporitic coasts (FZ 9A).

3.1.6. MF 6 Peloidal Packstone to Grainstone

This facies type includes grains most of which are coated bioclasts, exhibit micrite envelopes and additional grain types may be rounded intraclasts, peloids, foraminifers and algae (Figure 18). This facies type resembles to SMF 16 of Flügel (2004) and corresponds to FZ 8 of the Standard Facies Zones of Flügel (2004).

3.1.7. MF 7 Oolitic Grainstone

In this microfacies type, the laminae of the ooid cortices are radially structured and the grains are poorly sorted (Figure 19). This microfacies type is similar to the SMF 15 (Oolite commonly oolitic grainstones but also oolitic wackestones) of Flügel (2004) and corresponds to high energy marine settings on oolitic shoals, tidal bars and beaches (FZ 8 or FZ 9).

3.1.8. MF 8 Siltstone to Mudstone

This microfacies represents the siliciclastic influx into the depositional area. In the measured section it is observed as thick layers corresponding to samples AH-18, AH-19, AH-90 and AH-96 (Figure 20, Figure 30).

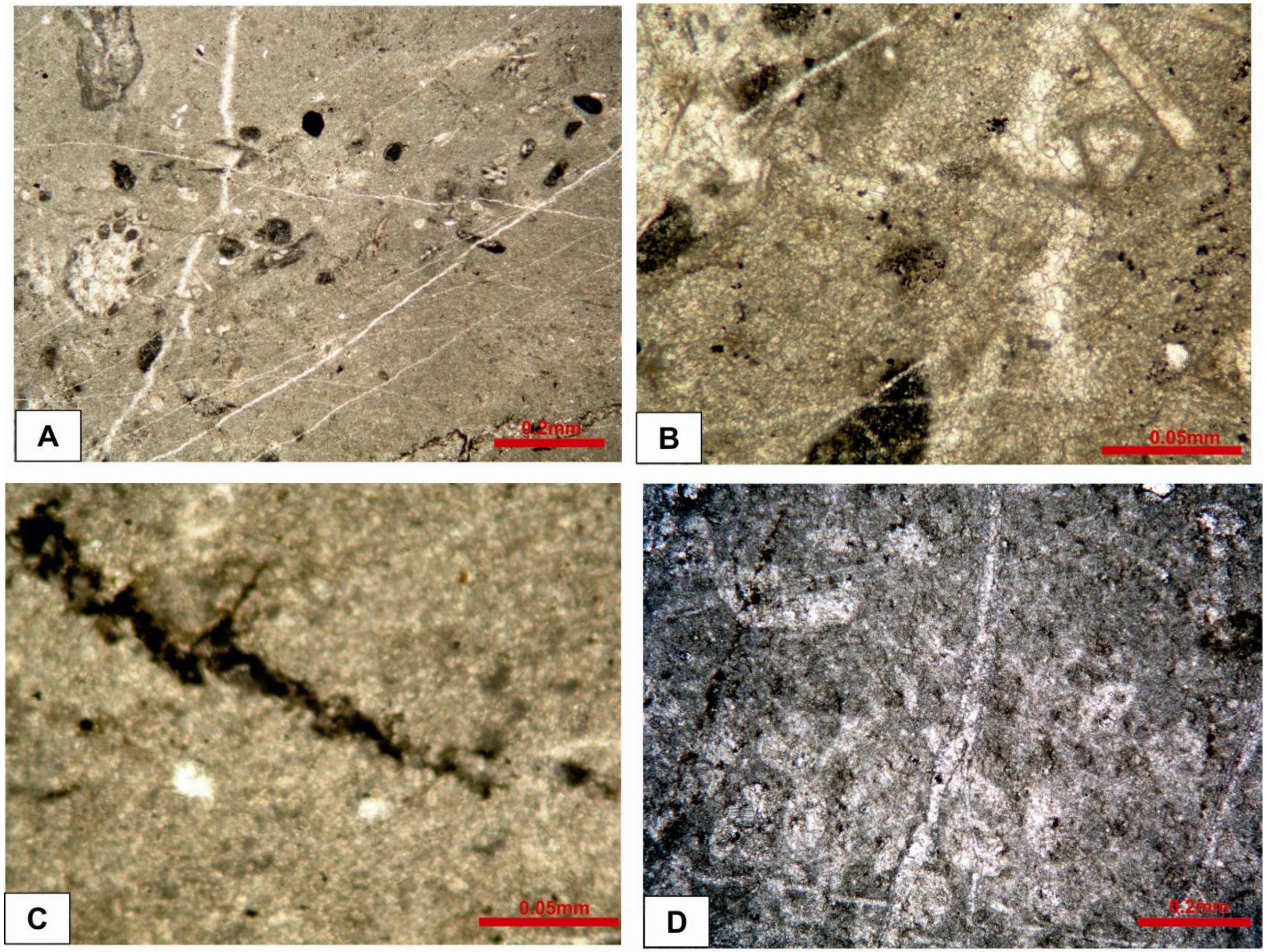

Figure 17. Photomicrographs of the MF 5 Unfossiliferous mudstone microfacies (A-B-C: AH-17, D: AH-60).

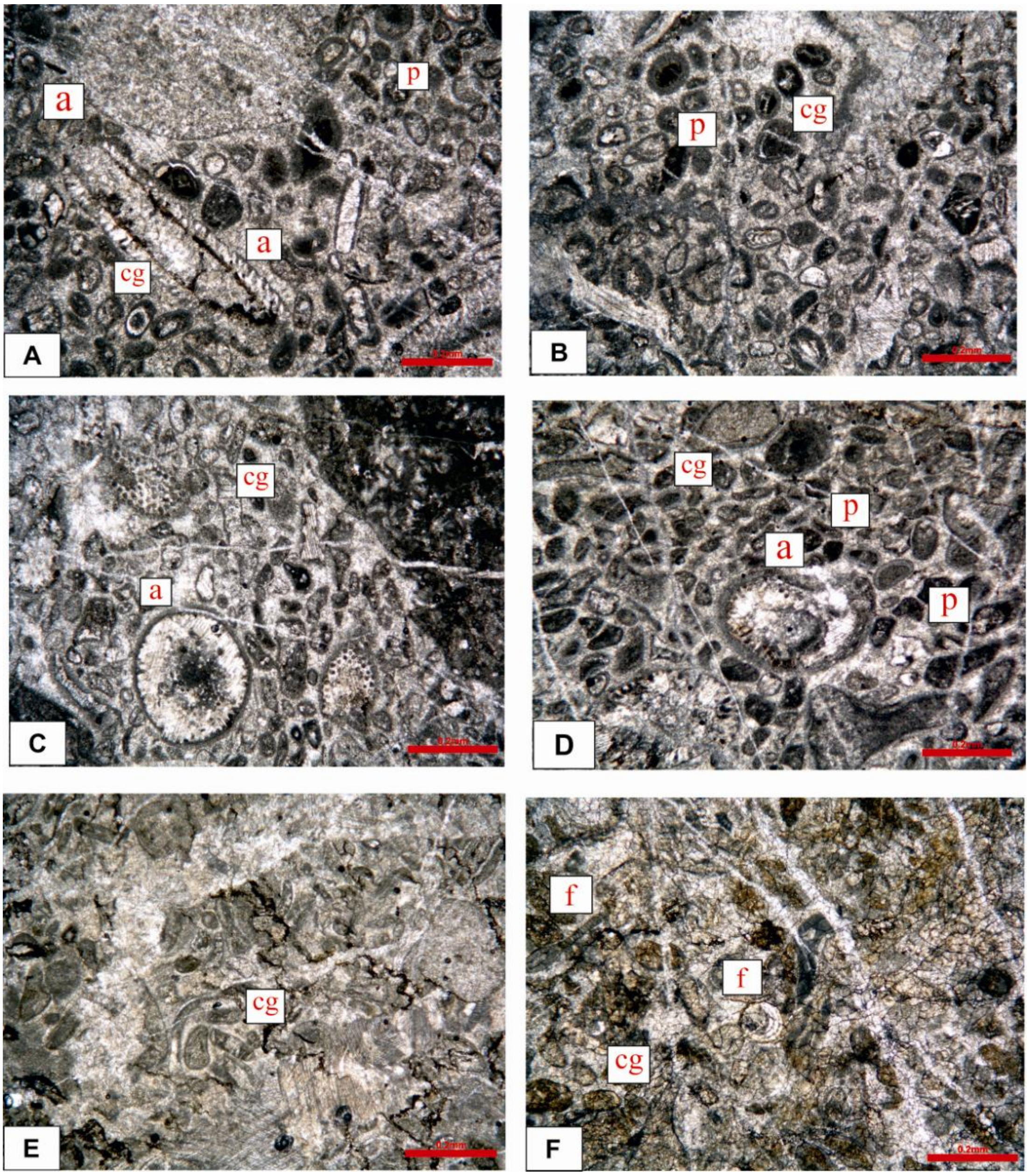

Figure 18. Photomicrographs of the MF 6 Peloidal packstone to grainstone microfacies (a: algae, f: foraminifera, cg: coated grain, p: peloid), (A-B:AH-64, C:AH-69, D:AH-71, E:AH-89, F:AH-93).

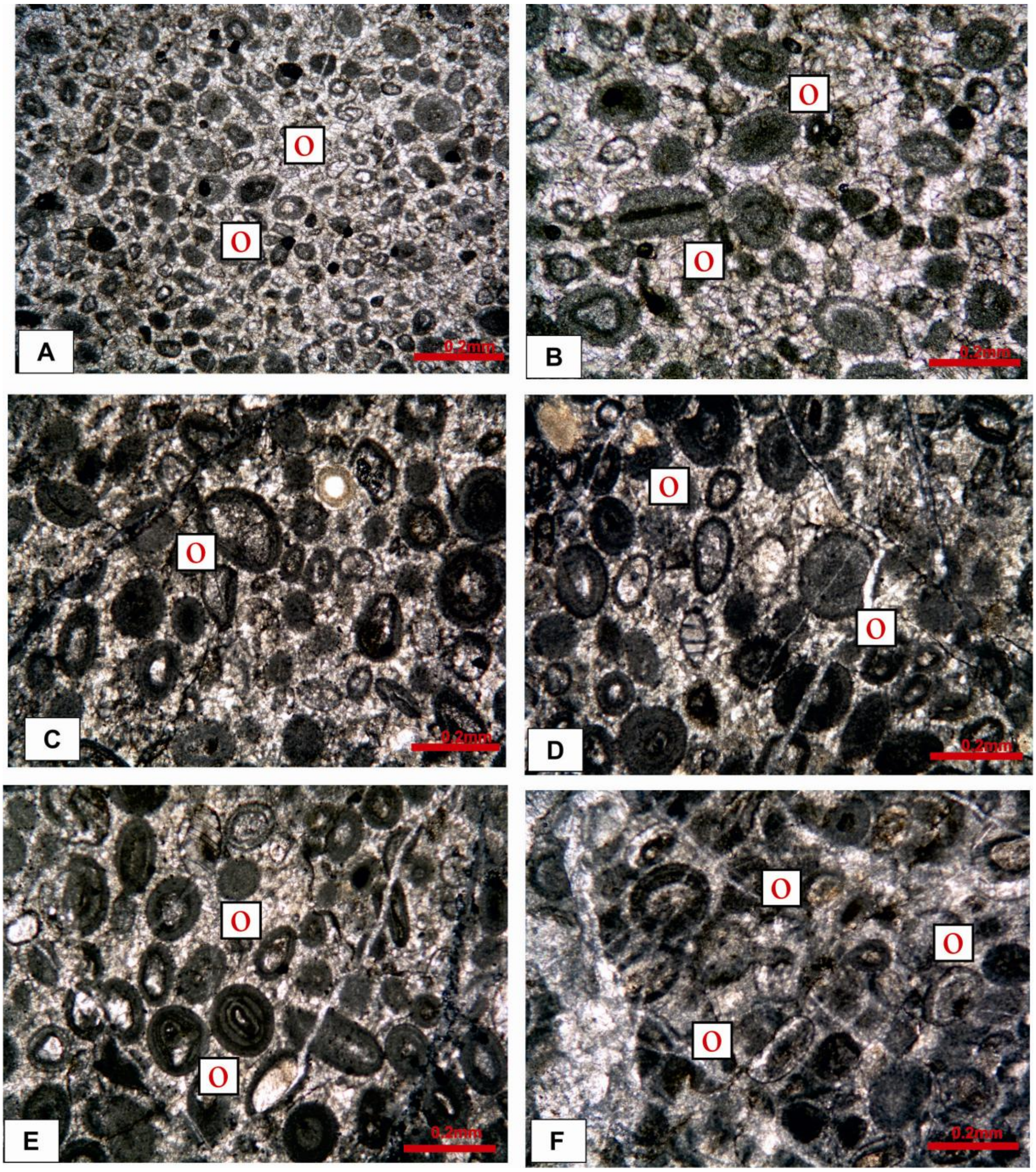

Figure 19. Photomicrographs of the MF 7 oolitic grainstone microfacies (A-B:AH-65, C-D-E:AH-79, F:AH-86).

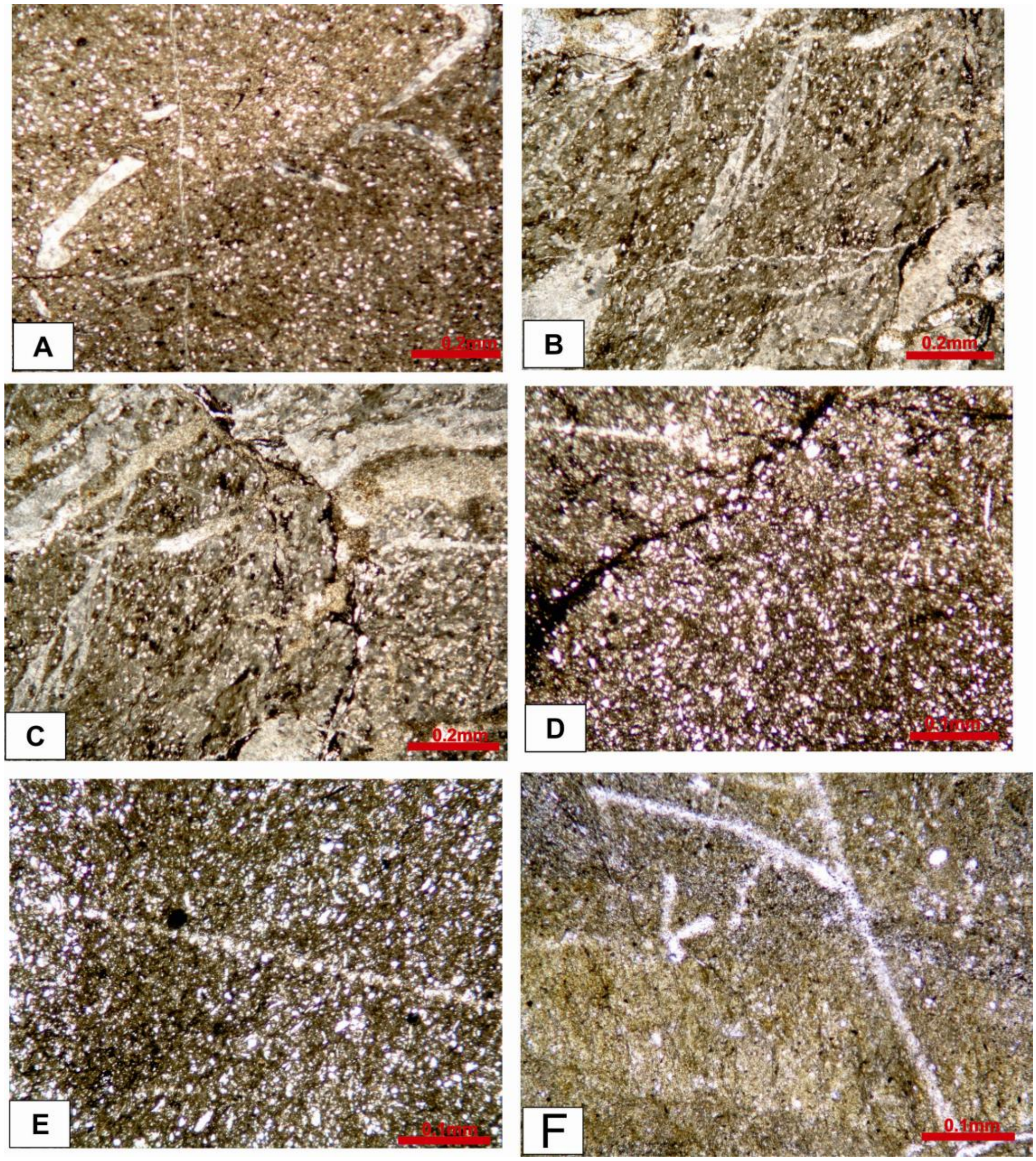

Figure 20. Photomicrographs of the MF 8 siltstone to mudstone microfacies (A:AH-18, B-C:AH-19, D-E:AH-90, F:AH-96).

3.1.9. MF 9 Quartz Arenitic Sandstone

This facies is mostly composed of sand size quartz fragments and does not include any fossils, pellets or intraclasts (Figure 21). This facies takes place in the regressive part of cycles due to the increasing siliciclastic input brought in the basin.

3.1.10 MF 10 *Spirorbis phlyctaena*-rich Wackestone

This facies takes place in the Triassic part of the measured section. The facies includes *Spirorbis phlyctaena* and the foraminifer *Rectocornuspira kalhori* (Figure 22). Thin lamellibranch shells are also rarely observed. This facies type is intensely dolomitized. It is similar to the facies described from the Lower Triassic Werfen Formation of the Karawanken Mountains (Southern Austria) which include *Spirorbis phlyctaena* and *Postcladella* sp. (= *Rectocornuspira),* (Krainer and Vachard, 2009).

3.1.11. MF 11 Pseudoolitic or Recrystallized Coated Grain Packstone

This type represents the higher energy conditions of the Triassic part of the measured section. The nuclei of the oolites are composed of intraclasts, *Spirorbis phlyctaena* fragments and pellets (Figure 23). This microfacies type also resembles to the SMF 22 (oncoid floatstone/packstone) of Flügel (2004) and corresponds to restricted or evaporitic or brackish zone of the platform interior(FZ 8 or FZ9).

3.1.12. MF 12 Sandy or Silty Lime Mudstone

This microfacies type is unfossiliferous and also dolomitized (Figure 24). It is similar to the RMF 22 (Finely-laminated dolomitic or lime mudstone) of Flügel (2004). According to the model of Flügel (2004), the depositional area of this facies is a lagoonal environment at the back of sand shoals and banks.

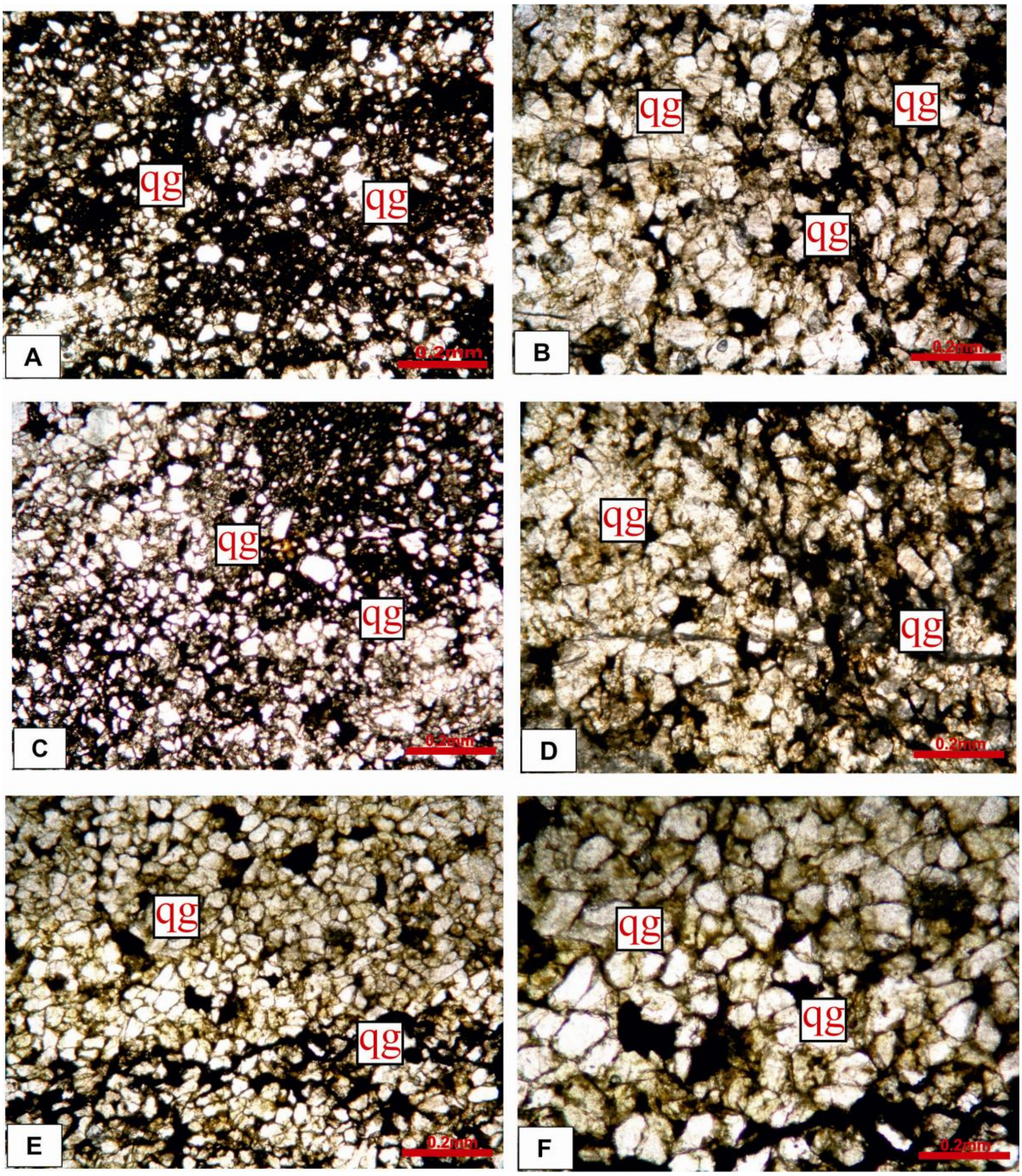

Figure 21. Photomicrographs of the MF 9 quartz arenitic sandstone microfacies (qg: quartz grain), (A-B:AH-91, C-D:AH-92, E-F:AH-95).

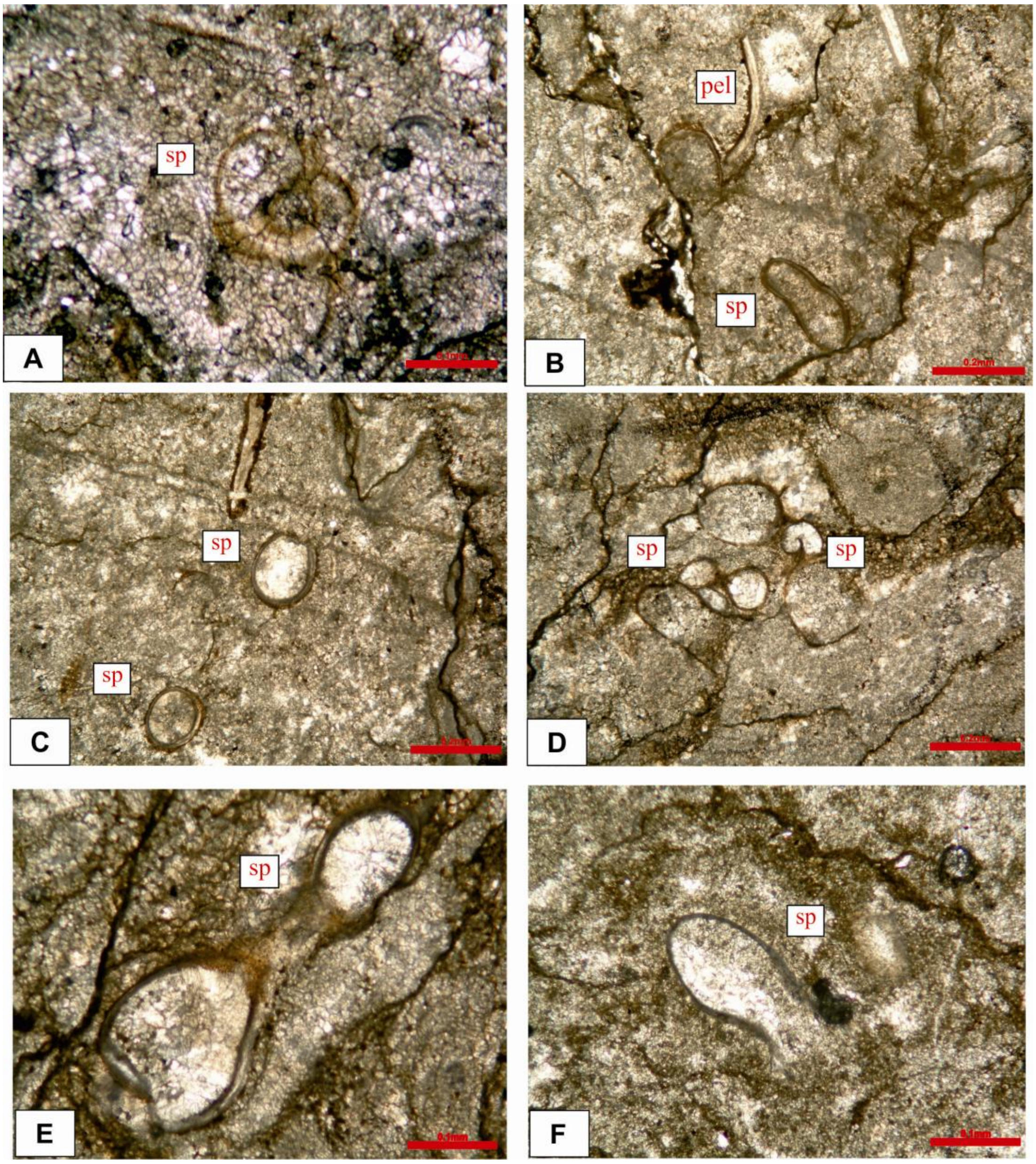

Figure 22. Photomicrographs of the MF 10 *Spirorbis phlyctaena*-rich wackestone microfacies (sp: *Spirorbis phlyctaena*, pel: pelecypod), (A:AH-102, B-C:AH-105, D-E:AH-107, F:AH-115).

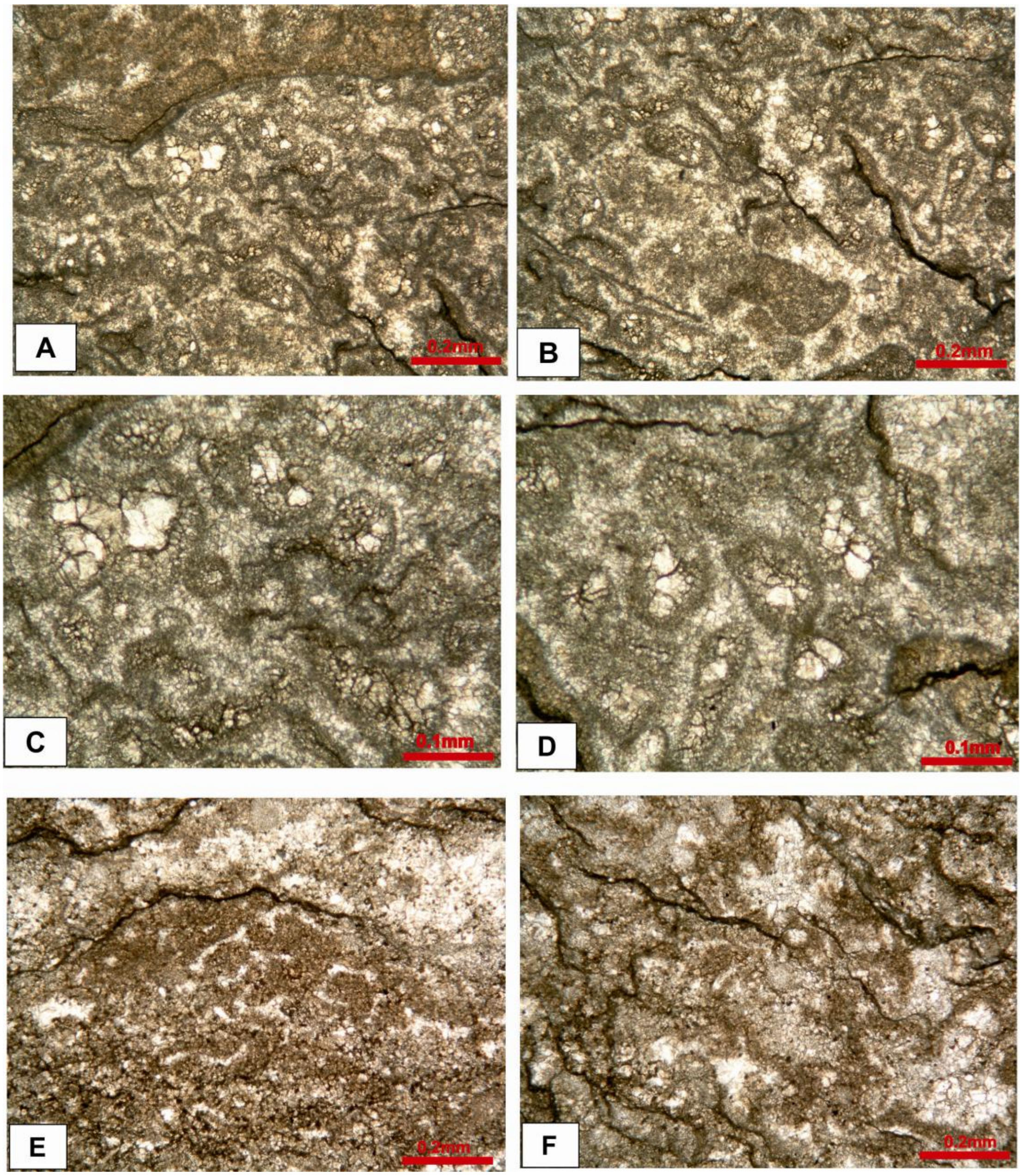

Figure 23. Photomicrographs of the MF 11, pseudoolitic or recrystallized coated-grain packstone microfacies (A-B-C-D:AH-104, E-F:AH-109).

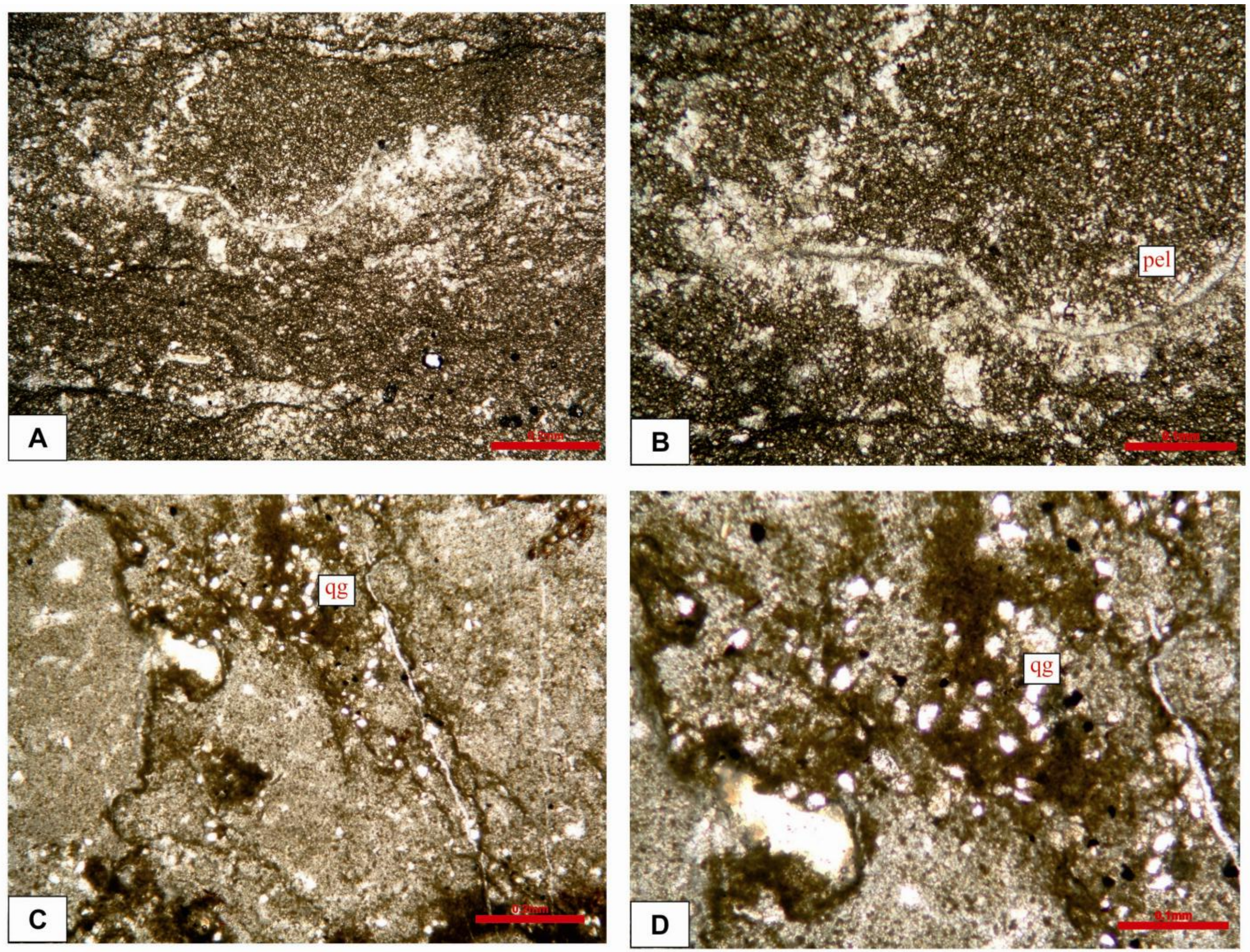

Figure 24: Photomicrographs of the MF 12, sandy silty mudstone microfacies (pel: pelecypod, qg: quartz grains), (A-B: AH-112, C-D: AH-114).

3.2. Meter-Scale Shallowing Upward Cycles (Parasequences)

The fundamental building blocks of sequences are parasequences and parasequence sets. A parasequence is a relatively conformable succession of genetically related beds or bedsets bounded by marine flooding surfaces and their correlative surfaces (Wagoner, 1985). Siliciclastic parasequences are progradational and therefore shoal upward. Carbonate parasequences are commonly aggradational and also shoal upward (Van Wagoner, 1988). The other denomination of parasequence is meter-scale shallowing upward cycles. Meter scales cycles dominated many shallow water successions throughout the history of carbonate rocks. These high frequency depositional cycles are fundamental sequence stratigraphic units of carbonate platforms (Flügel, 2004).

The depositional sequence was subdivided into lowstand, transgressive, and high stand and falling stage system tracts on the basis of internal surfaces that correspond to changes in the direction of shoreline shift from regression to transgression and vice versa (Catuneanu, 2006).

The highstand system tract is bounded by the maximum flooding surface at the base, and by a composite surface at the top that includes a portion of the subaerial unconformity, the basal surface of forced regression, and the oldest portion of the regressive surface of marina erosion (Catuneanu, 2006). The falling-stage system tract corresponds to the “lowstand fan” of Posamentier et al. (1988) and includes all strata that accumulate in a sedimentary basin during the forced regression of the shoreline. The lowstand system tract is defined as all sedimentary deposits accumulated during the stage of early-rise normal regression which is bounded by the subaerial unconformity and its marine correlative conformity at the base, and by the maximum regressive surface at the top. The transgressive system tract is bounded by the maximum regressive surface at the base, and by the maximum flooding surface at the top (Catuneanu, 2006).

Facies evolution and stacking pattern allow to define elementary, small-scale, medium-scale, and large scale sequences. Some depositional sequences display well marked sequence boundaries, others are limited by transgressive or maximum flooding surfaces. The hierarchical organisation of such sequence-stratigraphic elements implies that sea-level fluctuations were an important factor in their formation, and that these fluctuations had different frequencies (Strasser et al., 1999).

In this study a 48,06 m thick stratigraphic section was measured across the Permian-Triasssic boundary beds of Bolkar Dağı Unit. As a result of microfacies analysis carried out by the investigation of thin sections under microscope 12 microfacies types were determined and according to the vertical arrengement of these microfacies types throughout the section 24 shallowing upward cycles were distinguished. The thickness of the cycles range from 382 cm to 30 cm in thickness. The average thickness of the cycles is 179,92 cm.

3.2.1. Types of Shallowing Upward Cycles

Based on the stacking pattern of microfacies types 6 types main and 10 sub-types of cycles were designated throughout the measured section. These cycles were mainly deposited under shallow marine subtidal environmental conditions. Shallowing character of the cycles are determined according to the presence of lagoonal mudstone, oolitic packstone and siliciclastic deposits at the top of the cycles.

3.2.1.1. A Type Cycles

This type of cycle begins with mudstone with lagenoid foraminifera at the base and continues with bioclastic wackestone-packstone with diversified foraminifera. A type cycles are capped by wackestone with miliolid foraminifera at the top (Figure 25). This type of cycle is observed at the bottom of the measured section (Figure 30).

3.2.1.2. B Type Cycles

This type of cycles is characterized by bioclastic wackestone with calcareous algae and benthic foraminifera at the base and unfossiliferous mudstone capping the top of the cycle. (Figure 25). B type cycles take place near the base of the measured section (Figure 30).

3.2.1.3. C Type Cycles

C type cycles include two subtypes (C1 and C2). This microfacies type represents a gradual shallowing upward trend. In C1 sub-type the cycle begins with bioclastic wackestone with calcareous algae and benthic foraminifera at the base. Moving upwards bioclastic wackestone-packstone with diversified foraminifera overlies this microfacies (Figure 26). The top of the cycle is constituted by unfossiliferous mudstone. The presence of this lagoonal unfossiliferous mudstone at the top of the cycles indicate a shallowing trend throughout the cycles. C2 sub-type is differentiated from C2 by having mudstone with lagenoid foraminifera at the base of the cycle (Figure 27).

3.2.1.4. D Type Cycles

D type cycles are composed of two different sub-types (D1 and D2). These cycles both begin by bioclastic wackestone-packstone with diversified foraminifera at the base and culminate with oolitic grainstone facies which represents higher energy depositional conditions. D1 sub-type cycles differentiate from D2 in having a transitional packstone-grainstone facies in the cycle (Figure 27).

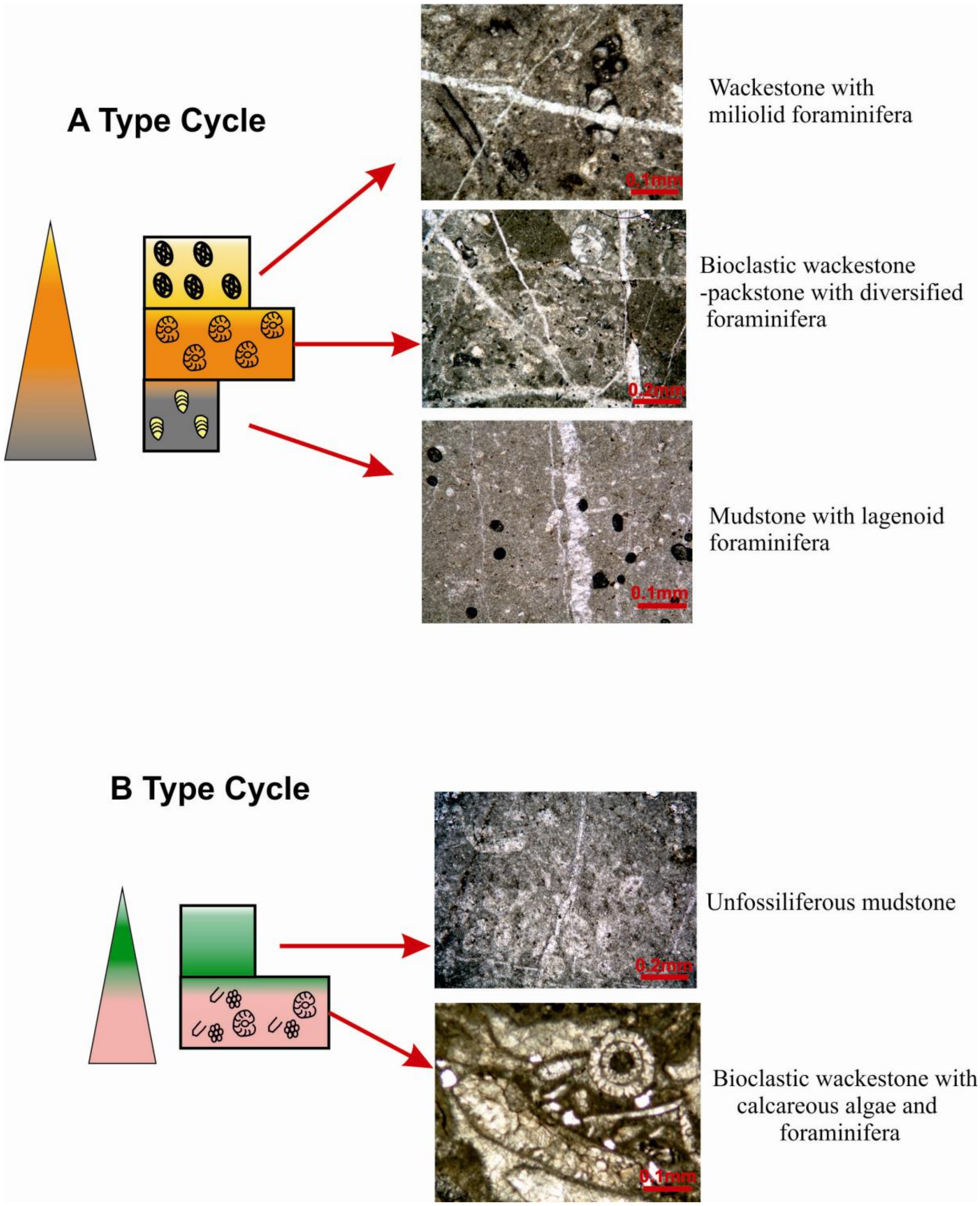

Figure 25: A type cycle and B type cycle with the representing photomicrographs of the microfacies types deposited within these cycles.

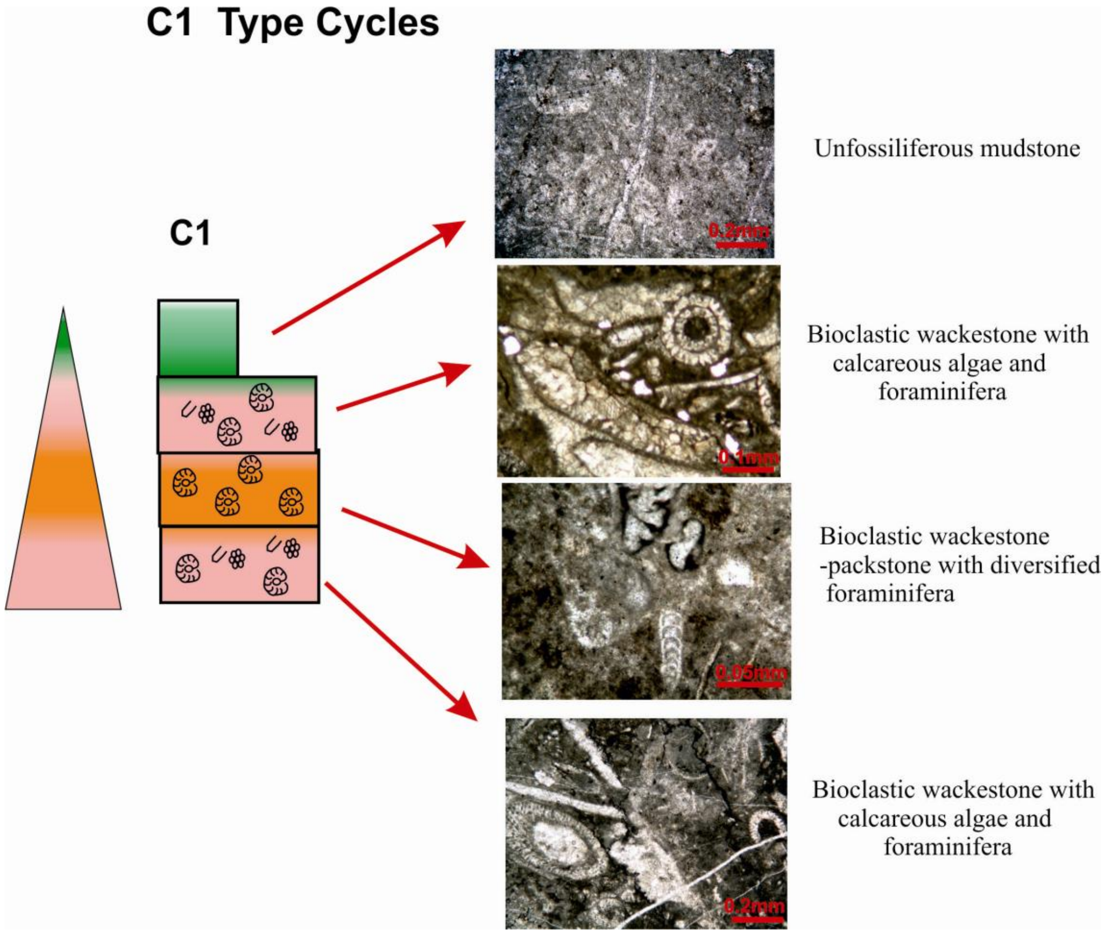

Figure 26: C1 type cycle with the representing photomicrographs of the microfacies types deposited within this cycle.

3.2.1.5. E Type Cycles

Under this cycle two sub-types are defined and named as E1 and E2. Both sub-types which are composed of peloidal packstone to grainstone at the top of cycles. They differ from each other by microfacies types that they have at the bottom of the cycles. E1 sub-type begins with bioclastic wackestone-packstone with diversified foraminifera on the other hand E2 sub-type begins by bioclastic wackestone with calcareous algae and benthic foraminifera at the base of the cycle (Figure 28).

3.2.1.6. F Type Cycles

F type cycles comprise the cycles in the Triassic part of the measured section. This type is composed of *Spirorbis phlyctaena*-rich wackestone, pseudoolitic or recrystallized coated grain packstone and sandy or silty lime mudstone. According to the vertical configuration of these microfacies types three sub-types were determined. All these three cycles (F1, F2 and F3) begin with *Spirorbis phlyctaena*-rich wackestone at the base (Figure 28, Figure 29) . In F1 sub-type cycles *Spirorbis-phlyctaene* rich wackestone is overlain by pseudoolitic packstone and sandy or silty lime mudstone represents the top of the cycle. In F2 sub-type cycle pseodoolitic packstone facies is absent. F2 is capped by sandy or silty lime mudstone. On the other hand F3 sub-type cycle is characterized by pseudoolitic packstone at the top (Figure 29).

3.3. Duration Of Cycles

Cycles are hierarchically clasasified by the duration of sea-level changes whereby rates of eustatic changes and amplitudes reflect the generating processes. Typical high frequency, meter scale cycles including fifth- and fourth- order cycles with durations of a few ten thousand years (for fifth order), a few hundred thousand years (for fourth order) and grouped into third order cycles formed on a scale of about 1 to 10 million years. Second order cycles have durations of ranging from 10 to 100

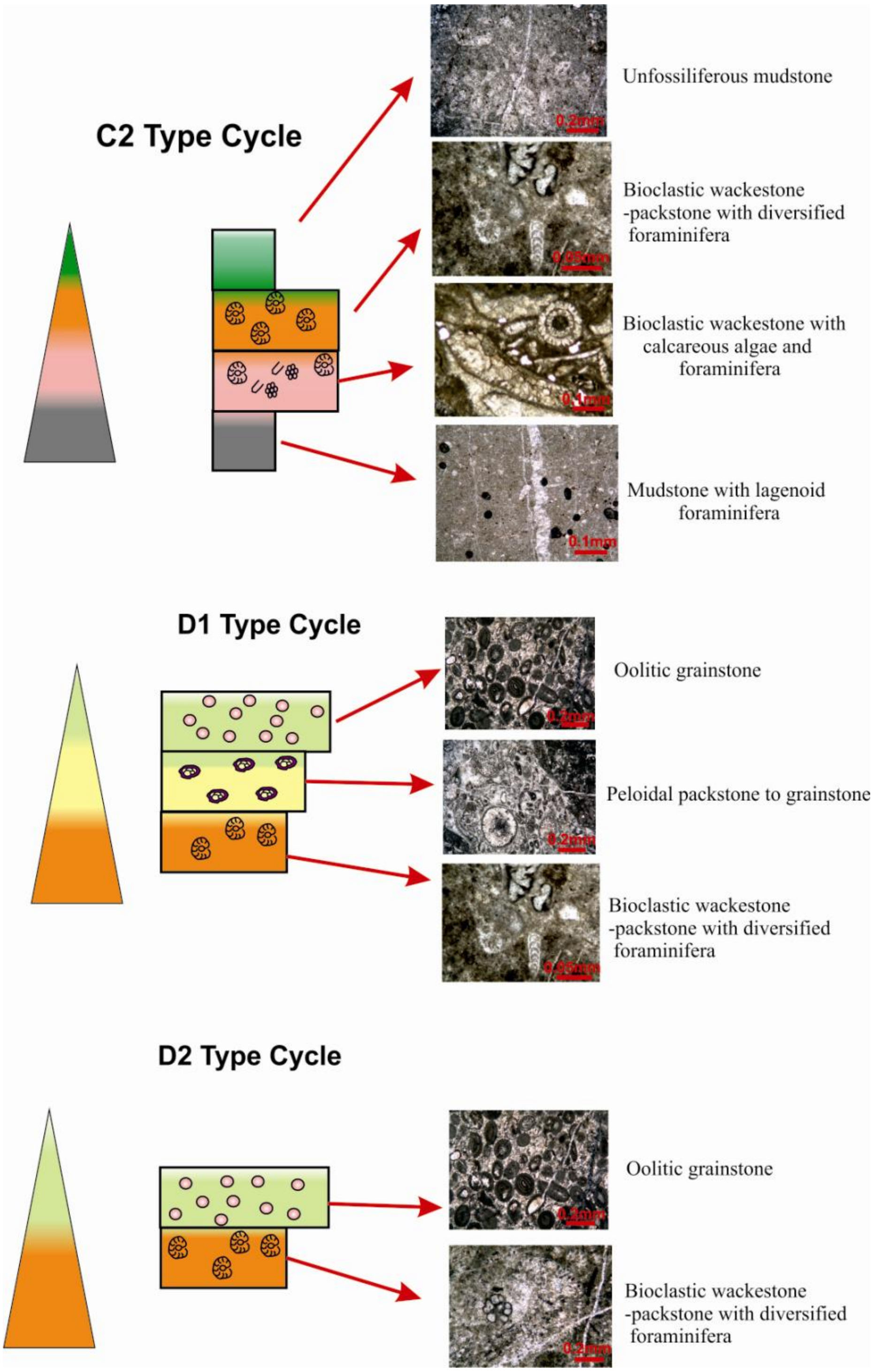

Figure 27: C2, D1 and D2 type cycles and with the representing photomicrographs of the microfacies types deposited within these cycles.

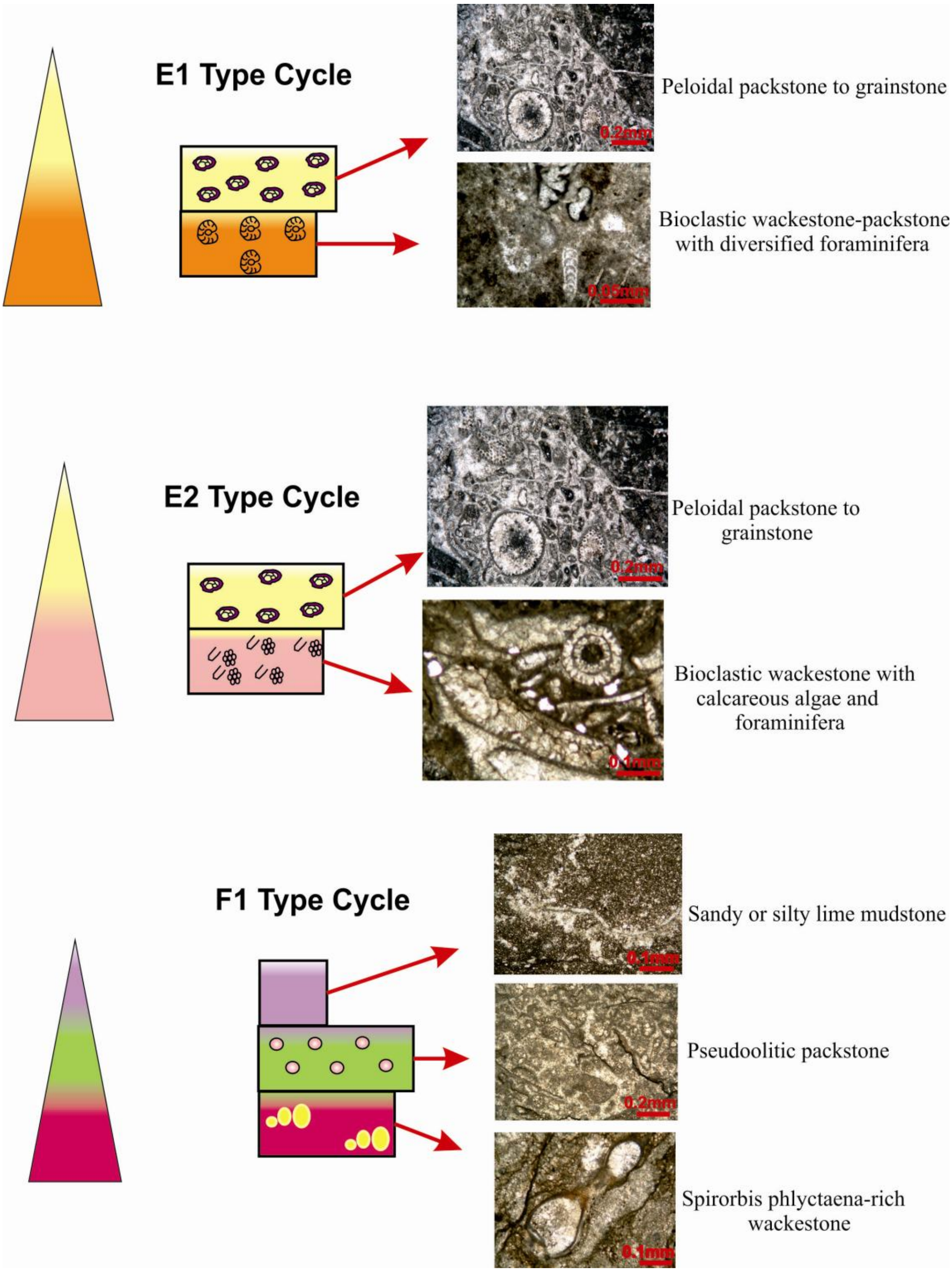

Figure 28: E1, E2 and F1 type cycles with the representing photomicrographs of the microfacies types deposited within these cycles.

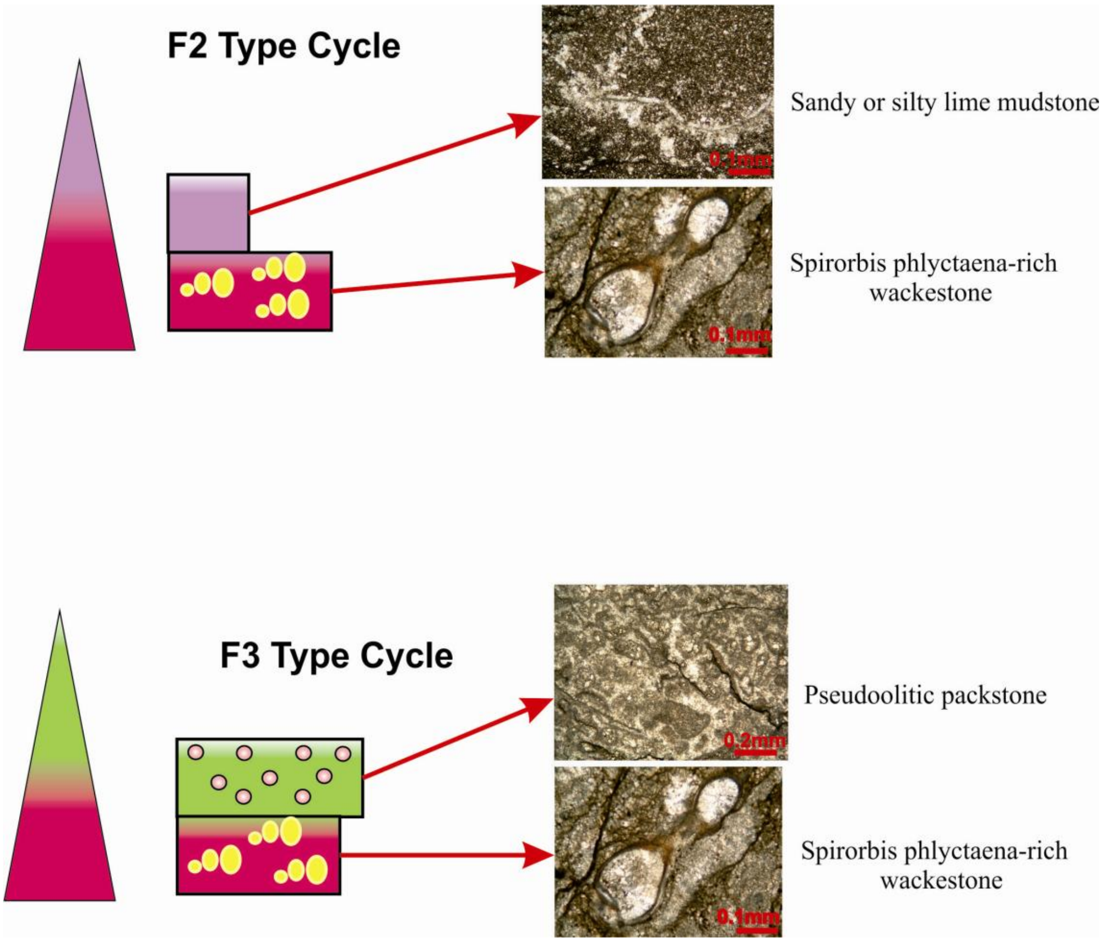

Figure 29: F2 and F3 type cycles with the representing photomicrographs of the microfacies types deposited within these cycles.

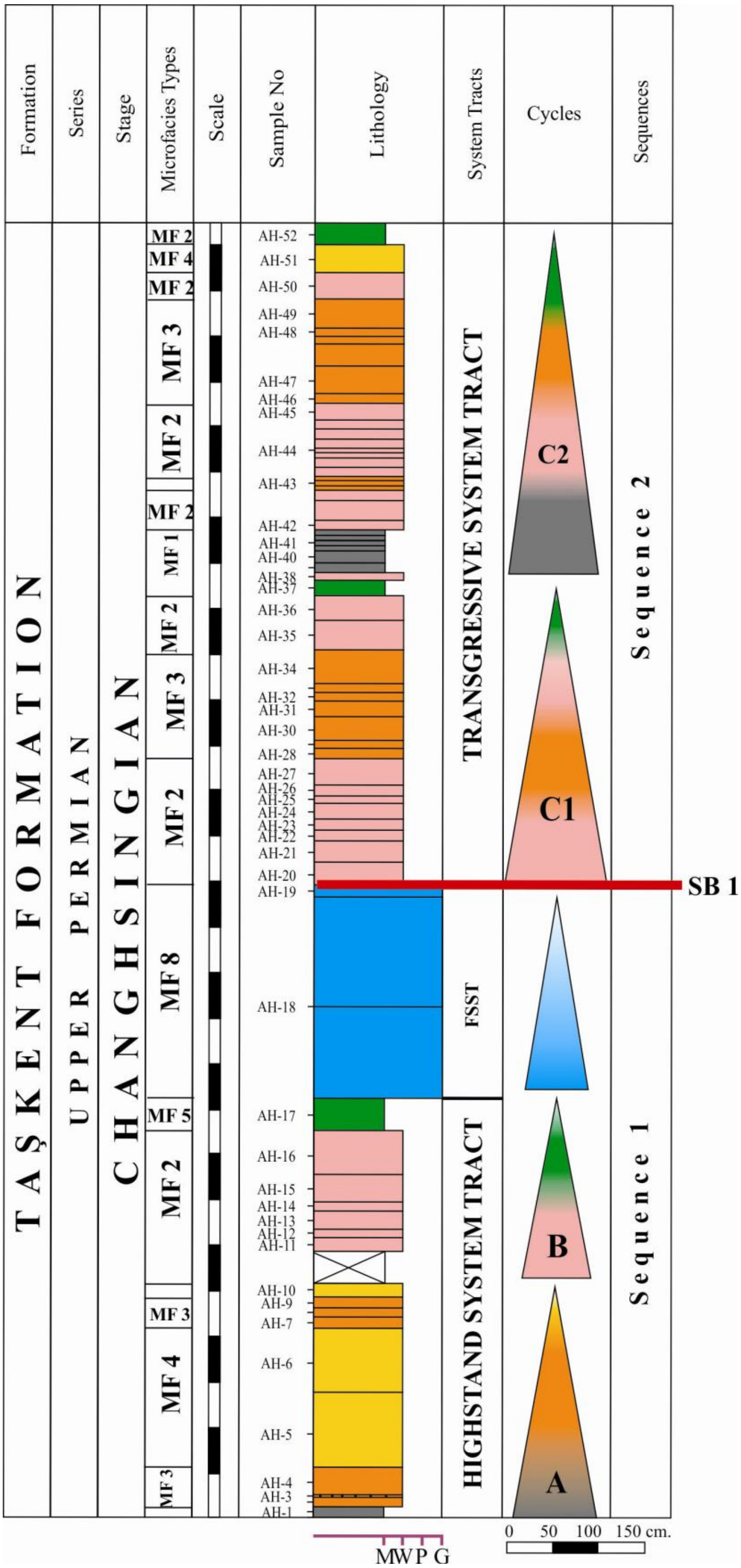

Figure 30. Sequence stratigraphical construction of the measured section showing stacking pattern of shallowing upward cycles, system tracts and sequences.

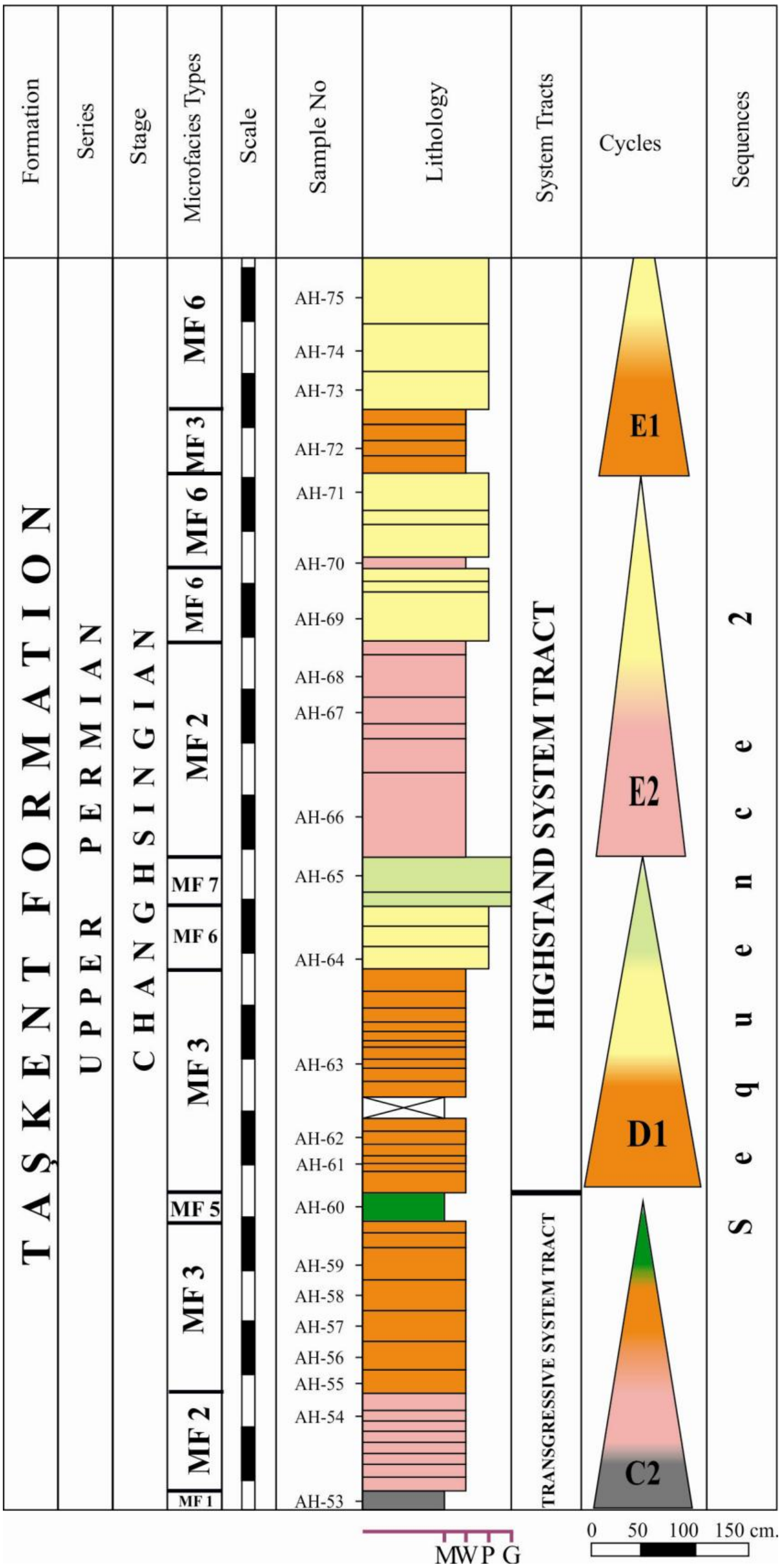

Figure 30. Continued.

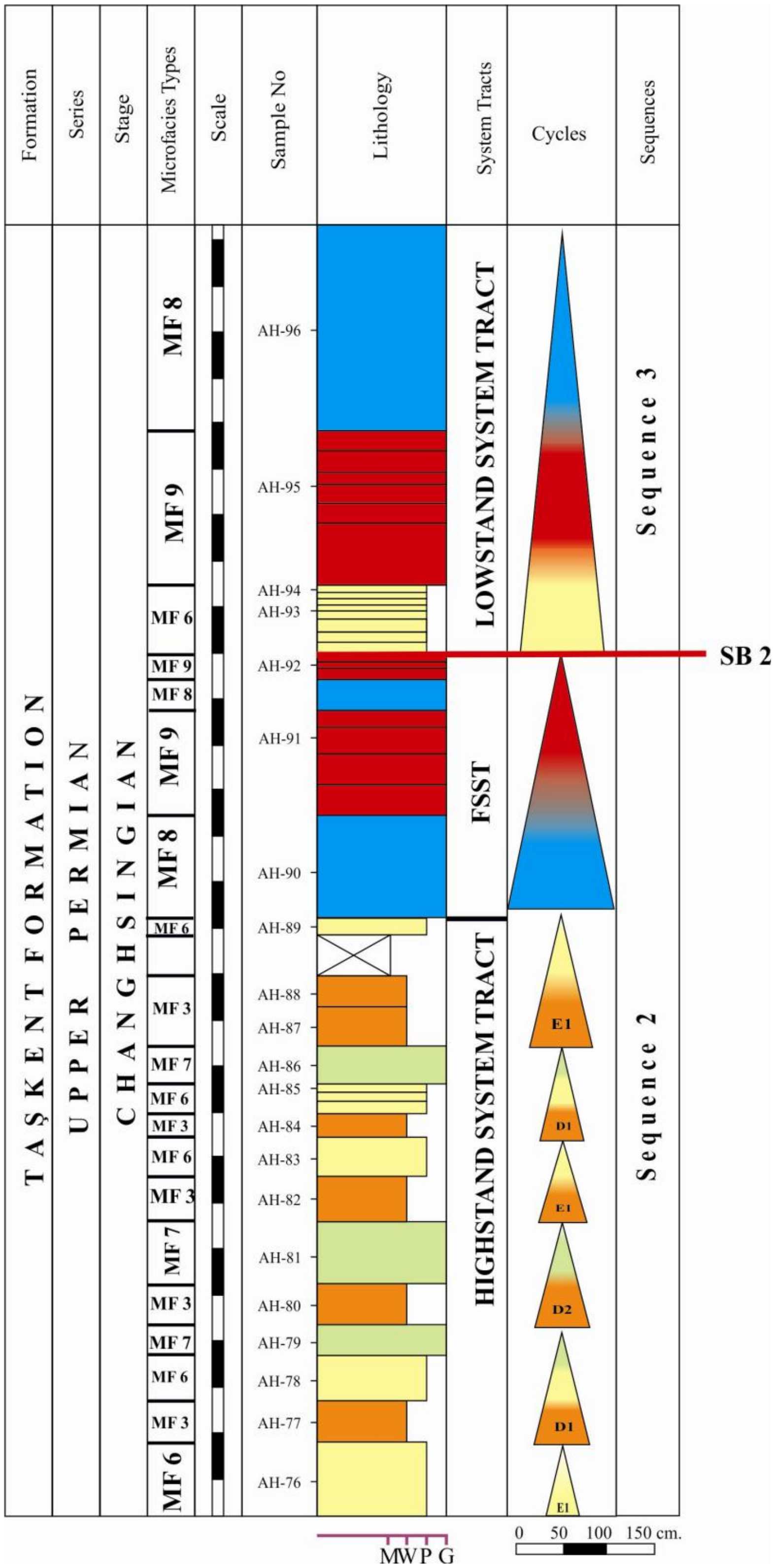

Figure 30. Continued.

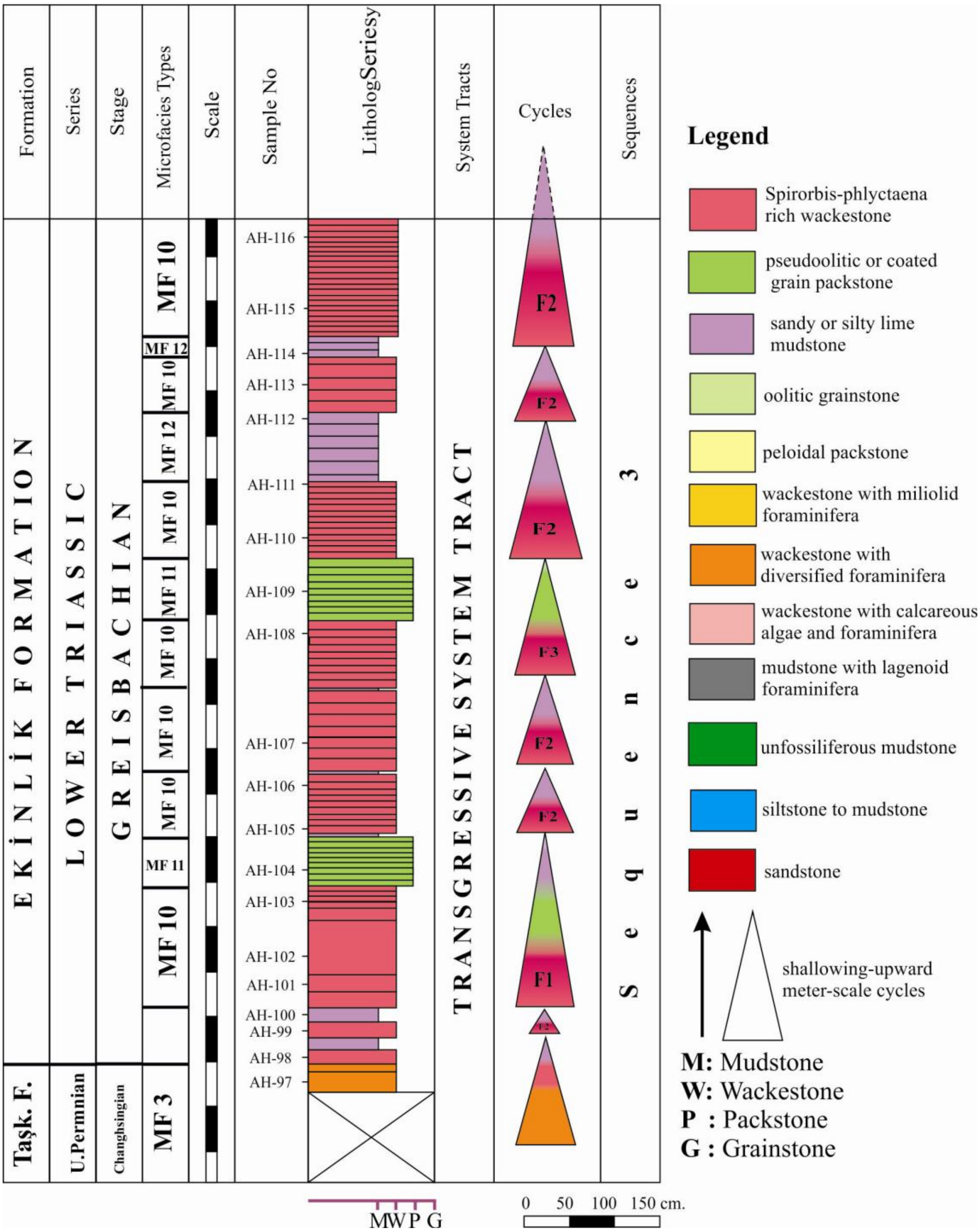

Figure 30. Continued.

Ma and first order cycles last several hundreds of million years. First and second order cycles attributed to long term sea-level changes and tectonics will not control the internal architecture of carbonate sequences because the rates of amplitudes of sea level fluctuation (1-2cm/1000years) are two orders of magnitude less than carbonate sedimentation rates (10-1000cm/1000years). The formation of sedimentary cycles in the third, fourth and fifth order bands have been explained by Milankovitch cycles but also by autocyclic factors and tectonic controls. Causes of third order cycles are waxing and waning of polar ice caps (glacio-eustasy) and changes in the volume of ocean basins (tectono-eustasy) (Flügel, 2004)

The alternation between the glacial and interglacial ages is explained best by the Milankovitch cycles, named after a Yugoslavian geophysicist who first calculated them in 1920's and 1930's. These cycles cause periodic variations in the amount of heat Earth receives from the Sun. The shape of Earth's orbit around the Sun changes cyclically, being more circular at some times and more elliptical at others. The degree of ellipticity of Earh's orbit is known as eccentricity. A nearly circular orbit has low eccentricity, and a more elliptical orbit has high eccentricity (Einsele, 1991). The time interval of one cycle of variation from low to high eccentricity is about 100.000 years. Small-scale shallow lagoonal to peritidal sequences related to cyclic sea level fluctuations have been documented from many geologic epochs and by many authors (Fisher 1964, Goldhammer et al. 1987, Strasser 1988). In many sections, the 100.000 eccentricity cycle seems to be particularly well developed (Einsele, 1991).

Haq and Schutter (2008) have reconstructed a history of sea-level fluctuations for the entire Paleozoic by using stratigraphic sections from pericratonic and cratonic basins. They documented one hundred and seventy two eustatic events for the Paleozoic, varying in magnitude from a few tens of meters to 125 meters. Throughout the measured section two sequence boundaries determined (SB1 and SB2). These sequence boundaries coincide well with sequence boundaries determined in Changhsingian by Haq and Schutter (2008). According to their chart a sequence boundary exist at the middle part of Changhsingian by 252.5 Ma and and a younger sequence boundary (251.5 Ma) exist at the upper part just below the Permian-Triassic

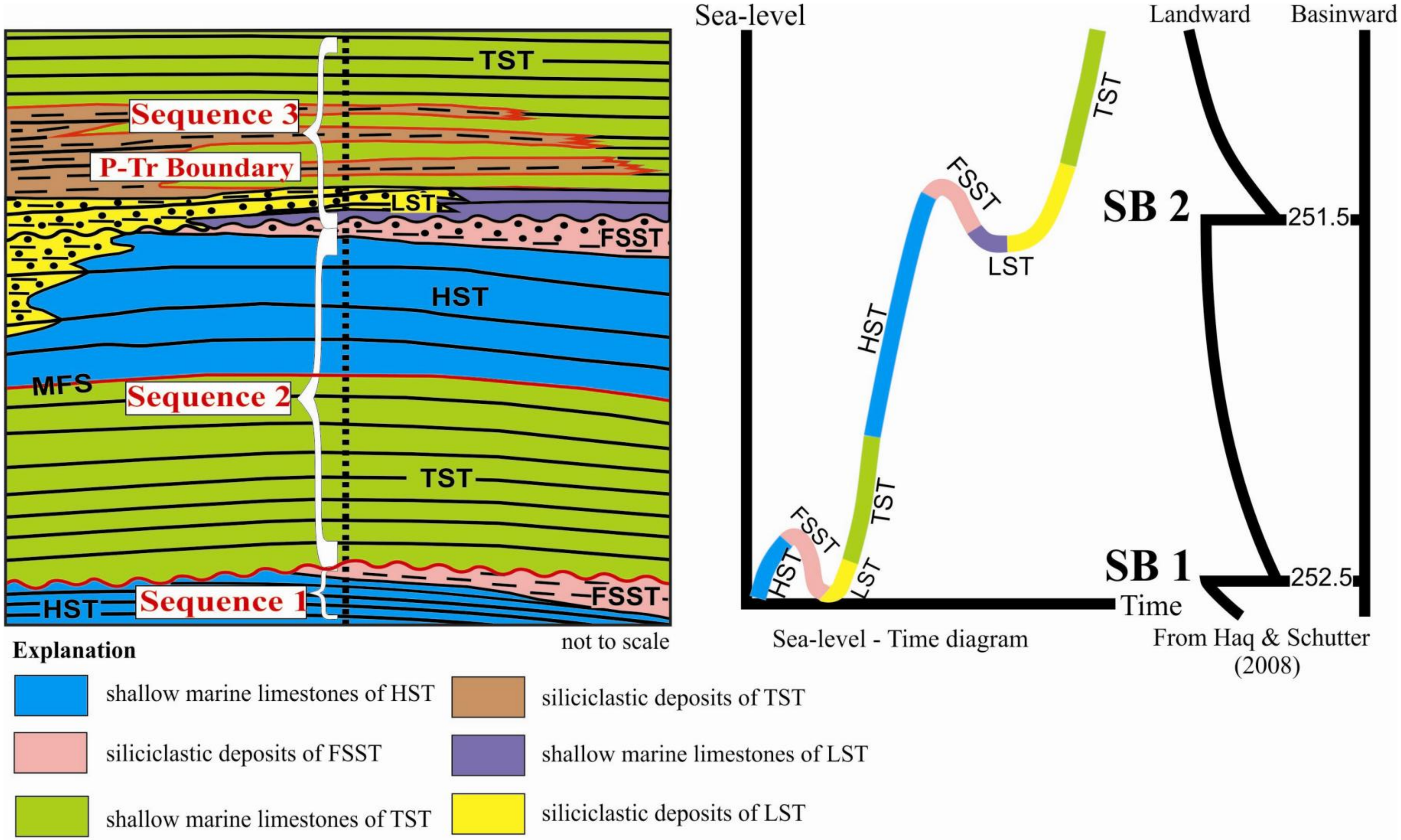

Figure 31: A hypothetical model showing the sequence stratigraphical interpretation and the position of the measured section.

boundary. Throughout the measured section 11 meter-scale cycles have been determined between SB1 and SB2. The duration of the cycles are approximately 90.900 and can be interpreted as Milankovitch eccentricity cycle. (Figure 31).

3.4. Sequence Stratigraphic Interpretation

Basing on microfacies analysis and field observations, sequence stratigraphic interpretation of the study area is presented. According to the characteristics and the vertical configuration of the shallowing upward cycles, system tracts have been delineated throughout the measured section. Three sequences and two sequence boundaries were determined. In sequence 1 only highstand system tract and falling stage system tract deposits can be observed along our measured section. The highstand system tract deposits are composed of mudstone with lagenoid foraminifera, bioclastic wackestone-packstone with diversified foraminifera, wackestone with miliolid foraminifera, bioclastic wackestone with calcareous algae and benthic foraminifera and unfossiliferous mudstone facies which are represented as A type and B type cycles in the lowermost part of the stratigraphic section. These deposits display a transition from carbonate-dominated highstand system tract deposits to silicilastic-dominated falling stage system tract deposits until sample AH-19. Between samples AH-19 and AH-20 the thick siltstone layer is overlain by bioclastic wackestone with calcareous algae and benthic foraminifera. This abrupt change in the deposition is interpreted as the first sequence boundary which assigns the top of sequence 1 and the base of sequence 2. C1 and C2 sub-type cycles contains bioclastic wackestone with calcareous algae and benthic foraminifera, bioclastic wackestone-packstone with diversified foraminifera mudstone with lagenoid foraminifera and unfossiliferous mudstone, which exhibit a clear gradual shallowing upward trend and backstepping stacking pattern of these cycles record a deepening from siltstone to open marine limestone and mudstone. The increasing marine influence and retrogradational character of the deposits are interpretted to represent a progressive incresase in sediment accommodation space and these deposits are interpreted as transgressive system tract deposits of sequence 2. The average thickness of the C type cycles is 353,5 cm within this interval. D and E type cycles, mainly composed of peloidal packstone to grainstone and oolitic grainstone record a progressive shallowing and decreasing sediment accommodation space in our study area. These sediments are interpreted as highstand system tract deposits of sequence 2. The thickness of the D type cycles varies between 88cm to 300cm and the thickness of E type cycles varies between 82 cm to 272 cm. The second sequence boundary is located between the samples AH-92 and AH-93. Between samples AH-94 and AH-96 the deposition of sandstone and siltstone is observed associated with a reduction in sediment accommodation space and these siliciclastic deposits are interprested as lowstand system tract deposits of sequence 3. From the sample AH-97 to the top of the measured section the transgressive system tract deposits of the sequence 3 are observed which are represented by F type cycles. Permian-Triassic boundary is located in the trangressive system tract deposits of the sequence 3. Altıner et al. (1980) recorded a transgressive phase in the uppermost Permian at Julfa and north of the Eastern Elbruz. Angiolini et al. (2010) has also reported the Permian-Triassic boundary in the trangressive system tract deposits of the Elihah River section in the Alborz Mountains (North/Iran).

CHAPTER 4

SYSTEMATIC PALEONTOLOGY

Family Syzraniidae VACHARD in VACHARD and MONTENAT, 1981

Genus *Rectostipulina* JENNY-DESHUSSES, 1985

Type species: *Rectostipulina quadrata* JENNY-DESHUSSES, 1985

Rectostipulina quadrata JENNY-DESHUSSES, 1985

Pl. VIII, figs. 1, 2

1978. *Stipulina* n. gen. ? Lys and Marcoux, pl. 1, fig. 14

1980. *Stipulina* Lys and Marcoux; Lys et al., p. 86-87, pl. 3, fig. 14, 15

1984. *Stipulina* sp. Altıner, pl. 2, fig. 14.

1985. *Rectostipulina quadrata* Jenny-Deshusses, p.153-155, pl. 1, fig. 1-7.

1981. "*Stipulina*" Lys in Lys and Marcoux; Zaninetti, Altıner and Çatal, pl. 12, figs. 3, 8, 9, 14, 18, 19, 21.

1989. *Rectostipulina quadrata* Jenny-Deshusses; Köylüoğlu and Altıner, pl. 11, fig. 24, 26, 27

1991. *Rectostipulina quadrata* Jenny-Deshusses; Vachard and Ferriére, pl. 4, fig. 16.

1996. *Rectostipulina quadrata* Jenny-Deshusses; Leven and Okay, pl. 8, fig. 22

1997. *Rectostipulina* sp. Nestell and Pronina, pl. 1, fig. 29, 30.

1998. *Rectostipulina quadrata* Jenny-Deshusses; Cirilli, Pirini Radrizzani, Ponton and Radrizzani, pl. 2, fig. 8.

2005. *Rectostipulina quadrata* Jenny-Deshusses; Groves et al., figs. 23.5-23.12

2007. *Rectostipulina quadrata* Jenny-Deshusses; Groves et al., figs.6.9, 7.1-7.3

2007. *Rectostipulina quadrata* Jenny-Deshusses; Song et al., figs. 2.CC-2.EE, 2.JJ, 5.O, 6.J, 7.Q.

2009. *Rectostipulina quadrata* Jenny-Deshusses; Song et al., figs. 11.4, 11.5.

2010. *Rectostipulina quadrata* Jenny-Deshusses; Angiolini et al., figs. 4.30, 4.31.

Description:

Test is tubular and no septation is observed. The chambers appear square-shaped in the transverse section. The wall is two layered; inner one is dark microgranular layer and the outer one is thick hyaline layer. In addition the outer layer becomes thicker at the corners of the square.

Dimensions(mm):

Diameter of the tubular chamber:0,037

Thickness of the wall:0,006

Stratigraphic Distribution:

Rectostipulina quadrata is recovered from most of the samples from base to middle part of the Changhsingian stage of the measured section.

Rectostipulina pentamerata Groves, Altıner and Rettori, 2005

Pl. VIII, figs. 3-5

1981. "*Stipulina*" Lys in Lys and Marcoux; Zaninetti, Altıner and Çatal, pl. 12, figs. 11, 12, 16.

1989. *Rectostipulina quadrata* Jenny-Deshusses; Köylüoğlu and Altıner, pl. 11, fig. 25.

1998. *Rectostipulina* sp. pentagonal form. Cirilli, Pirini Radrizzani, Ponton, and Radrizzani, pl. 2, fig. 9.

2005. *Rectostipulina pentamerata* Groves, Altıner and Rettori; Groves et al., figs. 23.1-23.4

2007. *Rectostipulina pentamerata* Groves, Altıner and Rettori; Groves et al., figs. 7.4-7.6

2009. *Rectostipulina pentamerata* Groves, Altıner and Rettori; Song et al., figs. 11.6-11.8.

2010. *Rectostipulina pentamerata* Groves, Altıner and Rettori; fig 4.29.

Description:

Test is tubular. The tubular chamber is pentagonal in transverse section, and rectangular in oblique section. Wall thickness increases at the corners of the pantagonal.

Dimensions (mm):

Diameter of the tubular chamber:0,033

Thickness of the wall:0,006

Remarks:

The difference between *Rectostipulina quadrata* and *Rectostipulina pentamerata* is the number of chamber sides. *Rectostipulina quadrata* has four-sided chambers and appears square in transverse sections, *Rectostipulina pentamerata* has five-sided chambers and appears pentagonal in tranverse sections. The oblique section of both species may appear rectangular so transverse section must be observed to decide on the species.

Stratigraphic Distribution:

Rectostipulina pentamerata is recovered from Changhsingian stage of the measured section.

Family Protonodosariidae MAMET and PINARD, 1992

Genus *Nodosinelloides* MAMET and PINARD, 1992

Type species: *Nodosinelloides potievskayae* MAMET and PINARD, 1996

Nodosinelloides sagitta MIKLUKHO-MAKLAY, 1954

Pl. I, figs. 1-6, Pl. II, figs. 1-14

1954. *Nodosaria sagitta* Miklukho-Maklay, p. 27-28, pl. 2, fig. 14.

1981. *Nodosaria sagitta* Miklukho-Maklay; Altıner, pl. 42, fig. 3-5

1996. *Nodosaria sagitta* Miklukho-Maklay; Leven and Okay, pl. 10, fig. 27-28.

1989. *Protonodosaria sagitta* (Miklukho-Maklay); Köylüoğlu and Altıner, pl. 9, fig. 17.

1997. ? *Protonodosaria* sp. B Kobayashi, pl. 5, fig.19.

2001. *Polarisella sagitta* (Miklukho-Maklay); Pronina-Nestell and Nestell, pl.2, fig.12.

2003. *Nodosinelloides* spp. Ünal, Altıner, Yılmaz, and Özkan-Altıner, pl. 1, fig. 25.

2005. *Nodosinelloides sagitta* (Miklukho-Maklay), Groves et al., figs. 18.14-18.21, 18.23-18.30.

2009. *Nodosinelloides sagitta* (Miklukho-Maklay), Song, Tong, Chen, Yang and Wang, figs. 11.17-11.21.

Description:

Test is elongate. The number of the postproloculus chambers is 6-10. Early chambers are more compressed and hemispherical. Height of later chambers increase and they have a subcylindrical form.

Dimensions (mm):

Height of the test:0,1525

Diameter of the last formed chamber:0,03

Height of the last formed chamber:0,0275

Thickness of the wall:0,005

Remarks: This form differs from *Nodosinelloides camerata* by having taller chambers and a longer and thinner appearence.

Stratigraphic Distribution:

This species is one of the most commonly occuring foraminifers in our thin sections. It is found in most of the samples in the Changhsingian Stage of measured section.

Nodosinelloides camerata MIKLUKHO-MAKLAY, 1954

Pl. III, figs. 1-12

1954. *Nodosaria longissima* Suliemanov subsp. *Camerata* Miklukho-Maklay, p. 22-23, pl. 2, fig, 3, 4.

1988. *Nodosaria longissima* Suliemanov subsp. *Camerata* Miklukho-Maklay; Pronina, pl.2, fig. 15, 16.

2001. *Nodosaria longissima* Suliemanov subsp. *Camerata* Miklukho-Maklay; Pronina-Nestell and Nestell, pl.2, fig. 9, 10.

2001. *Protonosaria* sp. Kobayashi, 2001, fig. 3.26.

2003. *Nodosinelloides* spp. Ünal, Altıner, Yılmaz, and Özkan-Altıner, pl. 1, fig. 24, 27-29.

2005. *Nodosinelloides camerata* (Miklukho-Maklay, 1954); Groves et al., figs. 19.18-19.26

2007. *Nodosinelloides camerata* (Miklukho-Maklay, 1954); Song, Tong, Zhang, Wang and Chen, figs. 3.D, 3.J and 3.K.

2009. *Nodosinelloides camerata* (Miklukho-Maklay, 1954); Song, Tong, Chen, Yang and Wang, figs. 11.22-11.23.

Description:

Test is elongate and chambers are uniserially arrenged. The number of the chambers after proloculus is 4-6. Chambers are compressed and hemispherical. The width of the chambers slowly increases in the later chambers.

Dimensions (mm):

Height of the test:0,045

Diameter of the last formed chamber:0,022

Height of the last formed chamber:0,012

Thickness of the wall:0,005

Remarks:

Nodosinelloides camerata differs from *Nodosinelloides sagitta* from having more hemispherical chambers and a more compressed appearence.

Stratigraphic Distribution:

This species is also one of the abundant foraminifers in Changhsingian stage of the Taşkent Formation.

Nodosinelloides sp. A

Pl. VI, figs. 12, 13

Decription:

The test is elongate. The chambers are arranged uniserially. The shape of the chambers is subrectangular. Throughout the growth of the test the width of the chambers increases gradually but on the other hand the height of the chambers increases abruptly. The wall is thin. The apperture appears as a simple opening at the top of the test.

Dimensions (mm):

Height of the test:0,13

Diameter of the last formed chamber:0,034

Height of the last formed chamber:0,028

Thickness of the wall:0,004

Remarks:

Nodosinelloides sp. A differs from others by the shape chambers, abruptly increasing chamber height and the having a thin wall.

Stratigraphic Distribution:

Nodosinelloides sp. A is recovered from Changhsingian stage of the measured section.

Nodosinelloides spp.

Pl. VI, fig. 14

Description:

Under *Nodosinelloides* spp. we group several forms having a large number of uniserially arranged chambers. The number of postprolocular chambers varies between 7-12. The shape of the chambers is subrectangular. The height and the width of the chambers increase gradually and regularly throughout the growth.

Dimensions (mm):

Height of the test:0,115

Diameter of the last formed chamber:0,027

Height of the last formed chamber:0,017

Thickness of the wall:0,001

Stratigraphic Distribution:

Nodosinelloides spp. is recovered from Changhsingian stage of the measured section.

Nestellorella dorashamensis PRONINA, 1989

Pl. VII, figs. 1-16

1988. *Pseudolangella doraschamensis* Pronina; Pronina, pl. 2, fig. 51-53.

1989. *Pseudolangella doraschamensis* sp. nov; Pronina, p. 33-34, pl. 2, fig. 32-35

2007. *Pseudolangella doraschamensis* Pronina; Groves et al., fig. 10.6-8.

Description:

A spherical proloculus is followed by uniserially arrenged 4-6 chambers. Test is small.

Dimension (mm):

Height of the test:0,08

Diameter of the last formed chamber:0,048

Height of the last formed chamber:0,024

Thickness of the wall:0,008

Stratigraphic Distribution:

Nestellorella dorashamensis is recorded from the Changhsingian stage of the measured section.

Genus *Langella* SELLIER DE CIVRIEUX and DESSAUVAGIE, 1965

Type species: *Padangia perforata* LANGE, 1925

Langella sp.

Description:

Test is elongate and uniserially arranged. Chambers increase rapidly in size in the early stage, later a slight increase of size is observed. Chambers are subglobular in shape and slightly arched towards the preceeeding chamber.

Dimensions (mm):

Height of the test:0,085

Diameter of the last formed chamber:0,042

Height of the last formed chamber:0,03

Thickness of the wall:0,008

Remarks: The most diagnostic feature of the *Langella* sp. is having a very thick hyaline wall.

Stratigraphic Distribution:

Langella sp. is recovered from Changhsingian stage of the measured section.

Langella perforata LANGE, 1925

Pl. V, fig. 13

1925. *Padangia perforata* sp. nov., Lange, p. 228-229, pl. 1, fig. 21.

1983. *Langella perforata* Lange; Jenny-Deshusses, p. 101, pl. 2, fig. 2-3.

1984. *Padangia perforata* Lange; Lin, p. 117, pl. 1, fig. 44, 45a, 45b

2003. *Langella perforata* Lange; Ünal et al., pl. 1, fig. 42.

Description:

The test consists two postprolocular chambers which are uniserially arranged. The chambers are hemispherical. *Langella perforata* has a thick hyaline wall.

Dimension (mm):

Height of the test:0,28

Diameter of the last formed chamber:0,16

Height of the last formed chamber:0,116

Thickness of the wall:0,076

Stratigraphic Distribution:

Langella perforata is recovered from Changhsingian stage of the measured section.

Genus *Pseudolangella* SELLIER DE CIVRIEUX and DESSAUVAGIE, 1965

Type species: *Pseudolangella fragilis* SELLIER DE CIVRIEUX and DESSAUVAGIE, 1965

Pseudolangella sp.

Pl. V, fig. 11

Description:

Test is elongate and hemispherical chambers are uniserially arranged. The number of postproloculus chambers is 4. The chambers are arched towards to sides of the previous chamber. A thick hyaline wall is observed.

Dimension (mm):

Height of the test:0,075

Diameter of the last formed chamber:0,03

Height of the last formed chamber:0,019

Thickness of the wall:0,0035

Remarks:

Pseudolangella sp. distinguished from *Langella* sp. by having thinner wall.

Stratigraphic Distribution:

Pseudolangella sp. is recovered from the Changhsingian stage of the measured section.

Family Geinitzinidae BOZORGNIA, 1973

Geinitzina araxensis PRONINA, 1989

Pl. IV, fig. 11, Pl. V, figs. 1-4

1981. *Lunucammina postcarbonica* (Spandel, 1901); Altıner, pl. 41, fig. 13, 15-18.

1989. *Lunucammina postcarbonica* (Spandel, 1901); Köylüoğlu and Altıner, pl. 8, fig. 20-21.

1989. *Geinitzina araxensis* Pronina, p. 34-35, pl. 2 fig. 1, 2.

2003. *Geinitzina postcarbonica* Spandel, 1901; Ünal, Altıner, Yılmaz, and Özkan-Altıner, pl. 1, fig. 21, 22.

2005. *Geinitzina araxensis* Pronina; figs. 20.7-20.14.

2007. *Geinitzina araxensis* Pronina; Song, Tong, Zhang, Wang and Chen, figs. 2.V, 5.K, 5.L, 5.R, 6.E, 6.F.,7.I., 7.T, 7.Y,7.Z, 7.GG, 7.JJ.

Description:

The number of postproloculus chambers is 6-8. Chambers are uniserially arranged, slightly arched and rounded at their lateral margins. Throughout the growth the chamber heights do not change so much but widths of the chambers increase gradually.

Dimensions (mm):

Height of the test:0,026

Diameter of the last formed chamber:0,23

Height of the last formed chamber:0,005

Thickness of the wall:0,001

Remarks:

Geinitzina araxensis differs from other *Geinitzina* species by flat and wide chambers.

Stratigraphic Distribution:

Specimens were recovered from the Changhsingian stage of the measured section.

Family Robuloadidae REISS, 1963 nomen translat LOEBLICH and TAPPAN, 1984

Genus *Calvezina* SELLIER DE CIVRIEUX and DESSAUVAGIE, 1965

Type Species: *Calvezina ottomana* Sellier de Civrieux and Dessauvagie, 1965

Calvezina ottomana SELLIER DE CIVRIEUX and DESSAUVAGIE, 1965

Pl. V, fig. 16, Pl. VI, fig. 1

1965. *Calvezina ottomana* Sellier de Civrieux and Dessauvagie, p. 53-54, pl. 11, fig. 3; pl. 14, fig. 9

1973. *Calvezina* cf. *ottomana* Sellier de Civrieux and Dessauvagie; Bozorgnia, pl.35, fig. 10.

1978. *Calvezina ottomana* Sellier de Civrieux and Dessauvagie; Lys and Marcoux, pl. 1, fig. 19.

1980. *Calvezina ottomana* Sellier de Civrieux and Dessauvagie; Lys, Colchen, Bassoullet, Marcoux and Mascle, pl. 4, fig. 1.

1981. *Calvezina* sp. Vachard and Montenat, pl.14, fig. 12

1989. *Calvezina ottomana* Sellier de Civrieux and Dessauvagie; Köylüoğlu and Altıner, pl. 9, fig. 12.

1989. *Calvezina* sp. Köylüoğlu and Altıner, pl. 9, fig. 13

1996. *Calvezina* ? sp. Leven and Okay, pl. 10, fig.20

2003. *Calvezina* sp. Ünal, Altıner, Yılmaz and Özkan-Altıner, pl. 1, fig. 41.

2005.*Calvezina ottomana* Sellier de Civrieux and Dessauvagie; Groves et al., figs. 23.23-23.25, 23.27, 23.30, 24.1, 24.2, 24.8, 24.9

2007. *Calvezina ottomana* Sellier de Civrieux and Dessauvagie; Groves et al.; figs. 6.19-6.23.

2009. *Calvezina ottomana* Sellier de Civrieux and Dessauvagie; Song, Tong, Chen, Yang and Wang, figs. 10.23-10.25.

2010. *Calvezina ottomana* Sellier de Civrieux and Dessauvagie; Angiolini et al., fig. 4.15

Description:

The spherical proloculus is followed by 4-5 uniserially arranged chambers. The second and third chamber may be slightly curved. *Calvezina ottomana* has a thin hyaline wall structure.

Dimensions (mm):

Height of the test:0,059

Diameter of the last formed chamber:0,026

Height of the last formed chamber:0,01

Thickness of the wall:0,002

Remarks:

Calvezina ottomana is differentiated from other lagenide foraminifers by relatively thinner hyaline wall and irregular chamber shapes in especially second and third chambers.

Stratigraphic Distribution:

Calvezina ottomana is not very abundant in our measured section and represented by three specimens recorded from lower and middle part of the Changhsingian stage.

Genus *Cryptomorphina* SELLIER DE CIVRIEUX AND DESSAUVAGIE, 1965

Type Species: *Cryptopmorphina limonitica* SELLIER DE CIVRIEUX AND DESSAUVAGIE, 1965

Cryptopmorphina limonitica SELLIER DE CIVRIEUX AND DESSAUVAGIE, 1965

Pl. V, figs. 14, 15

1965. *Cryptopmorphina limonitica* Sellier de Civrieux and Dessauvagie, p. 51-52, pl. 11, fig. 6; pl. 23, fig. 24.

2005. *Cryptopmorphina limonitica* Sellier de Civrieux and Dessauvagie; Groves et al., figs. 22.15?, 22.16?, 22.17

2007. *Cryptopmorphina limonitica* Sellier de Civrieux and Dessauvagie; Groves et al., figs. 6.5-6.8, 6.10, 6.12.

Description:

The globular proloculus is followed by 2-3 postprolocular subglobular chambers by a uniserial arrangament. The earlier chambers increase gradually but the last chambers increase abruptly and arced strongly towards the proloculus. The top of the last chamber is slightly flattened. Also the last chamber has a thicker outer hyaline layer that envelopes the previous chambers.

Dimension (mm):

Height of the test:0,15

Diameter of the last formed chamber:0,0875

Height of the last formed chamber:0,0375

Thickness of the wall:0,001

Stratigraphic Distribution:

Cryptomorphina limonitica is recorded from lower and middle part of Changhsingian stage of measured section.

Genus *Robuloides* REICHEL, 1946

Type species: *Robuloides lens* Reichel, 1946

Robuloides ? sp.

1946. *Robuloides lens* Reichel, p. 536, text-fig. 21-26, pl. 19, fig. 6, 7

1946. *Robuloides acutus*, Reichel, p. 537, text-fig. 27-29, pl.19, fig. 8, 9

1954. *Robuloides lens* Reichel; Miklukho-Maklay, p. 64, pl. 10, fig. 8-11

1981. *Robuloides lens* Reichel; Altıner, pl. 42, fig. 8-14

1988. *Robuloides acutus,* Reichel; Pronina, pl. 2, fig. 65-66

1989. *Robuloides lens* Reichel; Köylüoğlu and Altıner, pl. 10, fig. 16, 17

1991. *Robuloides acutus*, Reichel; Vachard and Ferriére, pl. 4, fig. 10, 11

1996. *Robuloides lens* Reichel; Leven and Okay, pl. 9, fig. 29, 30

1997. *Robuloides lens* Reichel; Kobayashi, pl. 5, figs. 7-10.

1999. *Robuloides lens* Reichel; Kobayashi, fig. 1.12

2003. *Robuloides lens* Reichel; Ünal, Altıner, Yılmaz, and Özkan-Altıner, pl. 1, fig. 45.

2005. *Robuloides lens* Reichel; Groves et al., figs. 24.3-24.7, 24.10-24.13

2006. *Robuloides lens* Reichel; Kobayashi, pl. 2, figs. 25, 26.

2007. *Robuloides lens* Reichel; Groves et al., figs. 7.22, 7.25-7.27

2007. *Robuloides lens* Reichel; Song, Tong, Zhang, Wang and Chen, fig. 5.G, 6.H, 6.I, 7.E, 7.H, 8.I.

2009. *Robuloides lens* Reichel; Song, Tong, Chen, Yang and Wang, figs. 10.33-10.35.

2010. *Robuloides lens* Reichel; Angiolini et al., fig. 4.32.

Description:

Test is lenticular to nautiloid. Planispiral involute coiling is observed with two or three whorls. The wall is calcareous hyaline.

Dimension (mm):

Diameter of the test:0,035

Thickness of the wall:0,002

Stratigraphic Distribution:

Our single specimen occurs in the sample AH-93 belonging to the uppermost part of the Changhsingian stage of our measured section.

Genus *Frondina* SELLIER DE CIVRIEUX and DESSAUVAGIE, 1965

Type species: *Frondina permica* SELLIER DE CIVRIEUX and DESSAUVAGIE, 1965

Frondina permica SELLIER DE CIVRIEUX and DESSAUVAGIE, 1965

Pl. V, figs. 5-10

1965. *Frondina permica* Sellier de Civrieux and Dessauvagie, p. 59-60, pl.5, fig. 17, 18, 21-23, 26-28, 32, 33; pl. 16, fig. 5, 8, 12; pl. 17, fig. 1, 3, 5, 6

1978. *Frondina permica* Sellier de Civrieux and Dessauvagie; Lys and Marcoux, pl. 1, fig. 18

1978. ? *Frondina permica* Sellier de Civrieux and Dessauvagie; Zaninetti, Brönnimann, Hubber and Moshtaghian, pl.86, fig.28

1979. *Frondina permica* Sellier de Civrieux and Dessauvagie; Whittaker, Zaninetti and Altıner, pl. 2, figs. 15, 16.

1980. *Frondina permica* Sellier de Civrieux and Dessauvagie; Lys, Colchen, Bassoullet, Marcoux and Mascle, p. 87, pl. 4, fig. 2, 3

1981. *Frondina permica* Sellier de Civrieux and Dessauvagie; Altıner, pl. 39, fig. 10-14

1987. *Frondina permica* Sellier de Civrieux and Dessauvagie; Noé, pl. 32, fig. 9

1989. *Frondina permica* Sellier de Civrieux and Dessauvagie; Köylüoğlu and Altıner, pl. 9, fig. 4-8

1996. *Frondina* cf. *permica* Sellier de Civrieux and Dessauvagie; Leven and Okay, pl. 8, fig. 27.

2003. *Frondina permica* Sellier de Civrieux and Dessauvagie; Ünal, Altıner, Yılmaz, and Özkan-Altıner, pl. 1, fig. 32-34, 38.

2004. ? *Lunucammina* sp. A Kobayashi, fig. 6.38, 6.39.

2005. *Frondina permica* Sellier de Civrieux and Dessauvagie; Groves et al., figs. 21.12-21.20, 22.6-22.14.

2007. *Frondina permica* Sellier de Civrieux and Dessauvagie; Groves et al., figs.7.9, 7.10, 7.15-7.17, 7.20.

2007. *Frondina permica* Sellier de Civrieux and Dessauvagie; Song, Tong, Zhang, Wang and Chen, fig. 7.S.

2009. *Frondina permica* Sellier de Civrieux and Dessauvagie; Song, Tong, Chen, Yang and Wang, figs. 11.37-11.39.

Description:

Test is elongate. The number of uniserially arranged chambers is 4-6. Chambers are strongly arched towards the proloculus. The chambers envelop the preceeding chambers so the chambers are seen as crescent-shape in the frontal longitudinal section.

Dimension (mm):

Height of the test:0,06

Diameter of the last formed chamber:0,026

Height of the last formed chamber:0,013

Thickness of the wall:0,002

Remarks:

Frondina permica differs from *Ichthyofrondina palmata* by less arched and less enveloped chambers.

Stratigraphic Distribution:

Frondina permica is recovered from the Changhsingian stage of the measured section.

SUPERFAMILY COLANIELLOIDEA FURSENKO, 1959

Family Colaniellidae Fursenko, 1959

Genus *Colaniella* Likharev, 1939

Colaniella parva (Colani, 1924)

Pl. XI, figs. 3, 4

1924. *Pyramis parva* Colani, p. 181, pl. 29, fig. 2, 4-14, 15a-15f, 16, 17, 19, 21, 24.

1975. *Colaniella parva* (Colani); Ishii et al., pl. 1, fig. 1-3, pl. 4, fig. 4.

1980. *Colaniella parva* (Colani); Lys, Colchen, Bassoullet, Marcoux and Mascle, pl. 5 figs. 12-17.

1981. *Colaniella cylindrica* K. V. Miklukho-Maklay; Hase et al., fig. 4.

1981. *Colaniella inflata* (K. L. Wang); Hase et al., fig. 4-6.

1981. *Colaniella* sp., Hase et al., fig. 4-7.

1981. *Colaniella minima* K.L. Wang; Hase et al., fig. 4-8, 4-13.

1981. *Pseudocolaniella* sp., Hase et al., fig. 4-10.

1997. *Colaniella parva* (Colani); Kobayashi, pl. 2, figs. 1-27.

1999. *Colaniella parva* (Colani); Kobayashi, figs. 1.14, 1.15.

2001. *Colaniella parva* (Colani); Pronina-Nestell and Nestell, pl. 3, fig. 16.

2004. *Colaniella parva* (Colani); Groves, Rettori and Altıner, figs 7.4-7.6.

2006. *Colaniella parva* (Colani); Kobayashi, pl. 1, figs. 1-20, 22-24.

2009. *Colaniella parva* (Colani); Song, Tong, Chen, Yang and Wang, figs. 10.14-10.18.

2010. *Colaniella parva* (Colani), Wang et al., Figs.4.9-4.13.

Description:

Test is elongate, subfusiform. Spherical proloculus is followed by strongly overlapped uniserially arranged chambers increasing their height and width gradually throughout the growth. Chambers are devided into chamberlets by radially arranged primary and secondary plate like partitions. The wall is perforate with fibrous or radial structure and may have a very thin opaque layer. The form appears circular in the transverse section.

Dimensions (mm):

Diameter of the test: 0,093

Thickness of the wall:0,006

Stratigraphic Distribution:

Our single specimen was recorded from sample AH-93 in the Changhsingian part of the measured section.

SUPERFAMILY Nodosarioidea EHRENBERG, 1838

Family Nodosariidae EHRENBERG, 1838

Genus *Nodosaria* LAMARCK, 1812

Type species: *Nautilus radicula* LİNNÉ, 1758

‘‘Nodosaria’’ elabugae CHERDYNTSEV, 1914

Pl. VI, figs. 2-6

1914. *Nodosaria elabugae* Cherdyntsev, p. 34-35, pl. 2 fig. 1, 2.

1939. *Nodosaria elabugae* Cherdyntsev; Likharev, p. 30, pl. 1, fig. 2, 3.

1965. *Nodosaria armeniensis* Efimova; Reitlinger, pl. 2, fig. 6, 7.

1978. *Nodosaria armeniensis* Efimova; Lys and Marcoux, pl. 1, fig. 15.

1981. *Nodosaria armeniensis* Efimova; Altıner, pl. 42, fig. 1, 2.

1985. ? *Nodosaria nechajevi* Tcherdintsev; Epshtein, Terekhova and Solov'eva, pl.

1986. *Nodosaria angjieshanensis* Wang, p. 120, pl. 2, fig. 4.

1994. *Nodosaria* cf. *armeniensis* Efimova; Vachard and Colin, pl. 2, fig. 3, 4, 13, 14, 16, 17.

1996. *Cryptoseptida* ? sp. Kobayashi, fig. 5.25.

2005. "*Nodosaria" elabugae* Cherdyntsev; Groves et al., figs.19.11-19.17.

2007. "*Nodosaria" elabugae* Cherdyntsev; Groves et al.,figs. 8.18, 8.22-8.30.

Description:

Test is small and elongate. The number of postprolocular chambers is 4-5. Chambers are subspherical. Upper face of the chambers has an oscillating appearence.

Dimensions (mm):

Height of the test:0,053

Diameter of the last formed chamber:0,02

Height of the last formed chamber:0,017

Thickness of the wall:0,005

Remarks:

"Nodosaria" elabugae is differtiated from other species by having a thicker chamber wall and subspherical chamber shape.

Stratigraphic Distribution:

The occurence of this species is relatively rare. *"Nodosaria" elabugae* is recorded only four samples (AH-17, AH-29, AH-38 and AH-53) of the Changhsingian stage of the measured section.

"*Nodosaria*" *skyphica* EFIMOVA, 1974

Pl. VI, fig. 7

1959. *Nodosaria* sp. Ho, p. 417, pl. 8, fig. 22-25

1974. *Nososaria hoi skyphica* Efimova, p. 71-72, pl. 5, fig. 5,6.

1974. *Nodosaria piricamerata* Efimova, p. 73-74, pl. 5, fig.12

1978. *Nodosaria piricamerata* Efimova, pl. 1, fig. 11

1988. *Dentalina* sp. He, p.90, pl. 2, fig. 21.

1992. *Nodosaria* cf. *piricamerata* Efimova; Scourtsis-Coroneou, Trifonova, and Tselepides, pl. 1, fig. 2.
1992. *Nodosaria skyphica* Efimova; Scourtsis-Coroneou, Trifonova, and Tselepides, pl. 1, fig. 6.
1994. *Nodosaria skyphica* Efimova; Trifonova, p. 45, pl. 5, fig. 23-26, pl. 6, fig.1.
1994. *Nodosaria piricamerata* Efimova; Trifonova, p. 43, pl. 6, fig. 15, 16.
2005. *"Nodosaria" skyphica* Efimova; Groves et al., figs. 19.2-19.8.
2007. *"Nodosaria" skyphica* Efimova; Song, Tong, Zhang, Wang and Chen, fig. 5.A.
2007. *"Nodosaria" skyphica* Efimova; Groves et al., figs. 7.28, 7.29.

Description:

Test is elongate and chambers are uniserially arranged. The number of chambers is 6-8. The chambers are egg-shaped and the thicker part is at the top of each chamber. About one-fifth of each chamber projects into the following chamber.

Dimension (mm):

Height of the test:0,12

Diameter of the last formed chamber:0,03

Height of the last formed chamber:0,024

Thickness of the wall:0,006

Remarks:

This species differs from other "*Nodosaria*" by in having egg-shaped chambers and arrangement of the chambers one another.

Stratigraphic Distribution:

"*Nodosaria*" *skyphica* is one of the rare fossil groups in the studied section. This species recorded only at sample AH-2 in the lowermost part of the Changsingian stage of the studied section.

"*Nodosaria*" sp. A

Pl. VI, figs. 8-11

Description:

The test is composed of uniserially arranged spherical chambers. The number of the postprolocular chambers is 4-5. Every chamber attached to another from the uppermost part of the chamber so the frontal view of the test appears like chain-shaped. The apperture appears as a simple opening at the top of the test.

Dimensions (mm):

Height of the test:0,19

Diameter of the last formed chamber:0,036

Height of the last formed chamber:0,044

Thickness of the wall:0,008

Remarks:

"*Nodosaria*" sp. A differs from other "*Nodosaria*" by the shape of chambers and arrangament of the chambers.

Stratigraphic Distribution:

"*Nodosaria*" sp. A is recorded from the Changhsingian stage of measured section.

Genus *Pachyphloia*, LANGE, 1925

Type species: *Pachyphloia ovata* LANGE, 1925

Pachyphloia ovata LANGE, 1925

Pl. IV, figs. 3-7, 9

1925. *Pachyphloia ovata* Lange, p. 231, pl. 1. Fig. 24a, 24b.

1954. *Pachyphloia ovata* Lange; Miklukho-Maklay, p. 44-45, pl. 5, fig. 1.

1954. *Pachyphloia angulata* Miklukho-Maklay, p. 51-52, pl. 5, fig. 10.

1965. *Pachyphloia cukurkoyi* Sellier de Civrieux and Dessauvagie, p. 37-38, pl. 4, fig. 1-3; pl. 5, fig. 2, 8, 9; pl. 6, fig. 3, 4, 6-8, 12; pl. 7, fig. 1, 4; pl. 13, fig. 4

1974. *Pachyphloia ovata* Lange; Wang, p. 287, pl. 149, fig. 13.

1978. *Pachyphloia* sp. Zaninetti, Brönnimann, Huber and Moshtaghian, pl. 86, fig. 24.

1981. *Pachyphloia ovata* Lange; Altıner, pl. 40, fig. 6-15.

1986. *Pachyphloia ovata* Lange; Kobayashi, pl. 2, figs. 14-18, 24, 25, 27-30, 32.

1989. *Pachyphloia ovata* Lange; Köylüoğlu and Altıner, pl. 8, fig. 1-7.

1991. *Pachyphloia ovata* Lange; Vachard and Ferriére, pl. 4, fig. 13.

2001. *Pachyphloia ovata* Lange; Kobayashi, pl. 1, fig. 27-29, 31-34.

2001. *Pachyphloia angulata* Miklukho-Maklay; Pronina Nestell and Nestell, pl. 3, fig. 1, 2.

2003. *Pachyphloia* ex gr. *ovata* Lange; Ünal, Altıner, Yılmaz, and Özkan-Altıner, pl.1 fig. 15-16.

2003. *Pachyphloia* ex gr. *ovata* Lange; Groves, Altıner and Rettori, fig. 1.24, 1.27, 1.28.

2004. *Pachyphloia ovata* Lange; Groves, Rettori and Altıner, fig. 7.1-7.3

2005. *Pachyphloia ovata* Lange; Kobayashi, figs. 3.7-3.11.

2005. *Pachyphloia ovata* Lange; Groves et al., figs. 20.15-20-27.

2006. *Pachyphloia ovata* Lange; Kobayashi, pl. 2, figs. 15-17, 20.

2007. *Pachyphloia ovata* Lange; Gaillot and Vachard, pl. 72, figs. 5, 23, pl. 73, figs. 4, 8

2009. *Pachyphloia ovata* Lange; Song, Tong, Chen, Yang and Wang, figs. 10.28-10.30.

Description:

Test is elongate and compressed. The number of chambers is 6-7. Uniserially arranged chambers are strongly arched. A well developed lamellar thickening can be observed in the lateral longitudinal sections.

Dimensions (mm):

Height of the test:0,1

Diameter of the last formed chamber:0,021

Height of the last formed chamber:0,02

Thickness of the wall:0,009

Stratigraphic Distribution:

Pachyphloia ovata is recovered from Changhsingian stage of the measured section.

Pachyphloia schwageri SELLIER DE CIVRIEUX and DESSAUVAGIE, 1965

Pl. IV, fig. 1

1965. *Pachyphloia schwageri* Sellier de Civrieux and Dessauvagie, p.38-39, pl. 4, fig. 4-16; pl. 5, fig. 1, 3-7, 10-16, 19; pl.6, fig. 1, 2, 5, 11, 13; pl. 7, fig, 2, 3; pl. 8, fig. 1, 3, 4; pl. 9, fig. 3; pl. 14, fig. 2; pl. 16, fig. 2.

1979. *Pachyphloia schwageri* Sellier de Civrieux and Dessauvagie; pl. 3, figs. 7, 17.

1981. *Pachyphloia schwageri* Sellier de Civrieux and Dessauvagie; Altıner, pl. 40, fig. 16-18.

1989. *Pachyphloia schwageri* Sellier de Civrieux and Dessauvagie; Köylüoğlu and Altıner, pl. 8, fig. 8-12.

1986. *Pachyphloia ovata* Lange; Kobayashi, pl. 2, fig. 27-29, 30, 32

1996. *Pachyphloia* sp. Leven and Okay, pl.10, fig. 5.

2005. *Pachyphloia schwageri* Sellier de Civrieux and Dessauvagie; Groves et al., figs. 21.1-21.11.

2007. *Pachyphloia schwageri* Sellier de Civrieux and Dessauvagie; Groves et al., figs. 8.7-8.9, 8.11-8.14, 8.20, 8.21.

2009. *Pachyphloia schwageri* Sellier de Civrieux and Dessauvagie; Song, Tong, Chen, Yang and Wang, figs. 10.26, 10.27.

Description:

Test is elongate, chambers are uniserially arrenged and strongly arched towards the proloculus. Secondary lamellarity is developed at the sides of the test.

Dimensions (mm):

Height of the test:0,158

Diameter of the last formed chamber:0,03

Height of the last formed chamber:0,02

Thickness of the wall:0,01

Remarks:

Pachyphloia schwageri differes from *Pachyphloia ovata* by its thinner secondary lamellae and less arched chambers.

Stratigraphic Distribution:

Pachyphloia schwageri is recovered from the Changhsingian stage of the measured section.

SUPERFAMILY BISERIAMMINOIDEA CHERNYSHEVA, 1941

Family Biseriamminidae, CHERNYSHEVA, 1941

Genus *Globivalvulina* SCHUBERT, 1921

Type species: *Valvulina bulloides* BRADY, 1876

Globivalvulina sp.

Description:

Globular chambers are biserially arrenged, with axis of biseriality enrolled in a planispiral to slightly trochoid configuration. Wall is microgranular and may have an inner fibrous or radial layer that is well developed along the septa.

Dimension (mm):

Diameter of the test:0,11

Width of the test:0,06

Width of the wall:0,005

Stratigraphic Distribution:

Globivalvulina sp. is recovered from lower and middle part of Changhsingian stage of the measured section.

Genus *Charliella* ALTINER and ÖZKAN-ALTINER, 2001

Type species: *Charliella rossae* ALTINER and ÖZKAN-ALTINER, 2001

Charliella altıneri Gaillot and Vachard, 2006

Pl. X, figs. 2-4

2006. *Charliella* sp. Insalaco et al., pl. 2, fig. 8

2006. *Charliella altıneri* sp. nov. Gaillot and Vachard in Gaillot, p. 65, pl. I.6, fig. 5-8, 12-14, pl. I.7, fig. 5, pl. I.8, fig.8, pl. II.10, fig. 1-16, pl. II.11, fig. 1-15, pl. II.31, fig. 2-3, pl. II.33, fig. 7, 17, pl. III.15, fig. 1, 5, pl. III.22, fig. 5, pl. IV.5, fig. 3

2006. *Charliella altıneri* Gaillot Vachard et al., fig. 9(4)

Description:

Biserially enrolled chambers are globular in early volutions than get angular throughout the last whorls. Size of chambers increases gradually and increases rapidly throughout the last chambers. *Charliella altıneri* is characterized by four layered wall structure. The outer layer is translucent, the second layer is microgranular, the third layer is translucent fibrous and the inner fourth layer is again microgranular.

Dimension (mm):

Diameter of the test:0,14

Width of the test:0,078

Width of the wall:0,004

Remarks:

Charliella altıneri differs from other *Globivalvulina* by having relatively angular chambers and four-layered wall structure.

Genus *Retroseptellina* KÖYLÜOĞLU and ALTINER, 1989

Type species: *Globivalvulina decrouezae*, (KÖYLÜOĞLU and ALTINER, 1989)

Retroseptellina decrouezae, (KÖYLÜOĞLU and ALTINER, 1989)

Pl. VIII, figs. 11-13

1970. *Globivalvulina graeca* Reichel; Canuti et al. Fig.

1989. *Globivalvulina decrouezae* sp. nov. Köylüoğlu and Altıner, p. 479-481, text-fig. 8A-H, J-K, pl. 7, fig. 13-16

1998. *Globivalvulina decrouezae* Köylüoğlu and Altıner; Altıner and Özkan-Altıner, pl. 3, fig. 23.

2001. *Paraglobivalvulina globosa* Wang; Pronina-Nestell and Nestell, pl. 5, fig. 2-3.

2005. *Septoglobivalvulina decrouezae* Köylüoğlu and Altıner; Mohtat-Aghai and Vachard, pl. 2, fig. 17.

2006. *Retroseptellina decrouezae* Köylüoğlu and Altıner; Vachard et al., fig. 9.5.

2009. *Retroseptellina decrouezae* Köylüoğlu and Altıner; Gaillot, Vachard, Galfetti and Martini, fig. 6.5.

Description:

Chambers are biserially coiled with few whorls. They are semirectangular and the increasing rate of chamber width is higher than increasing rate of chamber height. *Retroseptellina decrouezae* has a single layered microgranular wall structure. This species is characterized by the hook shaped appearance of the backward curvatured septa.

Dimension (mm):

Diameter of the test:0,104

Width of the test:0,08

Width of the wall:0,02

Remarks:

Retroseptellina decrouezae is differentiated from *Globivalvulina* species by the shape of chambers, hook shaped backward curved septa and single layered wall structure.

Genus *Septoglobivalvulina* LIN, 1978

Type Species: *Septoglobivalvulina guangxiensis* LIN, 1978

Septoglobivalvulina sp.

Description:

Test is biserially coiled. Chambers are subglobular. The last chamber larger than former chambers and covers almost all previous chambers so the test has an involute or seminvolute appearence. *Septoglobivalvulina* has a dark single layered wall structure.

Dimension (mm):

Diameter of the test:0,073

Width of the test:0,06

Width of the wall:0,0026

Remarks:

Septoglobivalvulina sp. differs from *Globivalvulina* sp. by the abrupt enlargement of the covering last chamber. Also *Septoglobivalvulina* sp. differs from *Paraglobivalvulina* sp. in having a subglobular test shape and single layered wall structure. However *Septoglobivalvulina* sp. differs from *Retroseptellina* by not having a hook shaped backward curved septa.

Stratigraphic Distribution:

Septoglobivalvulina sp. is recovered from only one sample at the Changhsingian part of measured section.

Genus *Paraglobivalvulina* REITLINGER, 1965

Type species: *Paraglobivalvulina mira* REITLINGER, 1965

Paraglobivalvulina mira REITLINGER, 1965

Pl. IX, figs. 7, 8

1965. *Paraglobivalvulina mira* gen. nov. sp. nov. Reitlinger; Bozorgnia, p. 145, pl. 39, fig. 13-14.

1978. *Paraglobivalvulina mira* Reitlinger; Lys and Marcoux, pl. 1, fig. 7-8.

1979. *Paraglobivalvulina mira* Reitlinger; Whittaker, Zaninetti and Altıner, pl. 1, figs. 12, 15.

1980. *Paraglobivalvulina mira* Reitlinger; Lys, Colchen, Bassoullet, Marcoux and Mascle, pl. 3, figs. 7-10

1981. *Paraglobivalvulina mira* Reitlinger; Zhao et al. pl. 2, fig.11.

1981. *Paraglobivalvulina mira* Reitlinger; Zaninetti and Altıner, pl. figs. 1-7, 9, 11.

1981. *Paraglobivalvulina mira* Reitlinger; Zaninetti, Altıner and Çatal, pl. 10, figs. 1-13.

1984. *Paraglobivalvulina mira* Reitlinger; Altıner, pl. 1, fig. 16-18.

1986. *Paraglobivalvulina mira* Reitlinger; Haas et al., pl.1, fig. 1-2.

1989. *Paraglobivalvulina mira* Reitlinger; Köylüoğlu and Altıner, pl. 7, fig. 1-2.

1996. *Paraglobivalvulina mira* Reitlinger; Rauzer Chernousova et al., pl. 18, fig. 9.

2004. *Paraglobivalvulina mira* Reitlinger; Kobayashi, figs. 7.1-7.4.

2006. *Paraglobivalvulina mira* Reitlinger; Kobayashi, pl. 2, fig. 14.

Describtion:

Chambers are biserially arranged planispirally to slightly trochospirally enrolled. Later chambers envelope the previous chambers so the test has an involute appearence. Short interseptal partitions produce small chamberlets. Chamber by a strongly recurved apertural tongue appears hooklike in thin section.

Dimension:

Diameter of the test:0,175

Width of the test:0,15

Width of the wall:0,0075

Remarks:

Paraglobivalvulina mira differes from other species of *Globivalvulina* in having a thick microgranular wall and an enveloped, involute and globular test appearence.

Stratigraphic Distribution:

Paraglobivalvulina mira is recovered from lower parts of the Changhsingian stage of our measured section.

Genus Dagmarita REYTLINGER, 1965

Type species: *Dagmarita chanakchiensis* Reytlinger, 1965

Dagmarita chanakchiensis REITLINGER, 1965

Pl. IX, figs. 9, 10

1965. *Dagmarita chanakchiensis* sp. nov., Reitlinger, p. 63, pl. 1, fig. 10-12.

1973. *Dagmarita chanakchiensis* Reitlinger; Bozorgnia, p. 144-145, pl.39, fig.6-8.

1978. *Dagmarita chanakchiensis* Reitlinger; Lys and Marcoux, pl. 1, fig. 1.

1980. *Dagmarita chanakchiensis* Reitlinger; Altıner and Brönnimann, pl. 1, fig. 11, 13-18.

1981. *Dagmarita chanakchiensis* Reitlinger; Altıner, p. 290-291, pl. 37, fig. 11-13, 18.

1984. *Dagmarita chanakchiensis* Reitlinger; Altıner, pl. 1, fig. 6-7.

1988. *Dagmarita chanakchiensis* Reitlinger; Okimura, fig. 3.1, 3.2.

1989. *Dagmarita chanakchiensis* Reitlinger; Köylüoğlu and Altıner, pl. 6, fig. 10, 11, 13.

1996. *Dagmarita chanakchiensis* Reitlinger; Leven and Okay, pl. 8, fig. 20, pl. 9, fig. 31.

1999. *Dagmarita chanakchiensis* Reitlinger; Kobayashi, fig. 1.13.

2003. *Dagmarita chanakchiensis* Reitlinger; Ünal et al., pl. 1, fig. 3-4.

2004. *Dagmarita chanakchiensis* Reitlinger; Kobayashi, figs. 7.10-7.12.

2007. *Dagmarita chanakchiensis* Reitlinger; Gaillot and Vachard, pl. 45, fig. 4, pl. 46, figs. 1-7

2010. *Dagmarita chanakchiensis* Reitlinger; Angiolini et al., figs 4.5, 4.6.

2010. *Dagmarita chanakchiensis* Reitlinger; Wang, Ueno, Zhang and Cao, figs. 5.20-5.22.

Description:

Test is biserial and rectilinear. *Dagmarita chanakchiensis* has a dark thin microgranular wall structure. Chambers are angular subspherical and have thornlike projections at the outer margins.

Dimensions (mm):

Height of the test:0,09

Width of the test:0,025

Thickness of the wall:0,003

Stratigraphic Distribution:

Dagmarita chanakchiensis is recorded in most of the samples of the Changhsingian stage of the measured section.

“*Dagmarita*” *shahrezaensis* Mohtat-Aghai and Vachard, 2003

Pl. IX, figs. 11, 12

? 1980. *Dagmarita chanakchiensis* Reitlinger; Lys in Lys et al., pl.3, fig. 11-12.

? 1994. *Dagmarita chanakchiensis* Reitlinger; Fontaine et al., pl. 3, fig. 6.

Description:

Test is biserially arrenged and rectilinear in shape. Chambers are globular and gradually enlarge throughout the later chambers. “*Dagmarita*” *shahrezaensis* has a microgranular single-layered wall structure.

Dimension (mm):

Height of the test:0,091

Width of the test:0,043

Thickness of the wall:0,003

Remarks:

“*Dagmarita*” *shahrezaensis* differ from *Dagmarita chanakchiensis* by the shape of chambers and by lacking thornlike projections at the outer margins of the chambers.

Stratigraphic Distribution:

“*Dagmarita*” *shahrezaensis* is recored from the lower and middle parts of the Changhsingian stage of the measured section.

Genus *Paradagmarita* Lys in Lys and Marcoux, 1978

Type Species: *Paradagmarita monodi* Lys in Lys and Marcoux, 1978

Paradagmarita sp.

Plate X, fig. 1

Description:

Subglobular chambers are biserially arranged, slightly trochospiral involute at the initial stage, later stage is relatively long and uncoiled. Wall is dark, microgranular to granular.

Dimension (mm):

Height of the test:0,107

Width of the test:0,068

Thickness of the wall:0,002

Stratigraphic Distribution:

Paradagmarita sp. is recorded from the Changhsingian stage of the measured section.

Paradagmarita monodi ? Lys in Lys and Marcoux, 1978

Plate IX, fig. 13

1978. *Paradagmarita monodi* sp. nov. Lys in Lys and Marcoux, p. 1419-1420, pl.1, fig. 2.

1981. *Paradagmarita monodi* Lys in Lys and Marcoux; Zaninetti, Altıner and Çatal, pl. 2, fig. 6, pl. 3, fig. 9-23.

1984. *Paradagmarita monodi* Lys in Lys and Marcoux; Altıner, pl. 1, fig. 1-2.

1989. *Paradagmarita monodi* Lys in Lys and Marcoux; Köylüoğlu and Altıner, pl. 6, fig. 1-8

1996. *Paradagmarita monodi* Lys in Lys and Marcoux; Rauzer-Chernousova et al., p. 72, pl. 18, fig. 14.

2003. *Paradagmarita monodi* Lys in Lys and Marcoux; Ünal et al., pl. 1, fig. 1-2.

Description:

The test has a lozenge shape external appearance. *Paradagmarita monodi* has a two stage of growth. In the initial stage biserial chambers are sligthly trochospirally enrolled and throughout the later growth stage biserial chambers are uncoiled. Coiled part is relatively long. Chambers are subglobular. Wall is dark microgranular.

Dimensions (mm):

Height of the test:0,1625

Width of the test:0,0975

Thickness of the wall:0,01

Remarks:

The specimen in our section resembles to *Paradagmarita monodi* but the section is not clear enough so we used ? .

Stratigtraphic Distribution:

Paradagmarita monodi is recorded from middle parts of the Changhsingian part of the measured section.

SUPERFAMILY NOBECULARIDEA JONES in GRIFFTH and HENFREY, 1875

Family Calcivertellidae LOEBLICH and TAPPAN, 1964

Genus *Calcivertella* CUSHMAN and WATERS, 1928

Calcivertella sp.

Description:

Globular proloculus encircled by gradually enlarging tubular undivided second chamber. The second chamber gradually enlarges, irregularly coiles at the initial stage, later appears in zig-zag series, finally uncoils and appears rectilinear. The wall is calcareous, porcelaneous.

Dimension (mm):

Length of the test:0,048

Thickness of the wall:0,003

Stratigraphic Distribution:

Calcivertella sp. is recorded in the Changhsingian stage of the measured section.

Genus *Ammovertella* CUSHMAN, 1928

Type Species: *Ammodiscus (Psammophis) inversus* Schellwien, 1898

Ammovertella sp.

Pl. XIV, fig. 11, 12

Description:

Proloculus is followed by undivided elonged tubular second chamber that grows in zig-zag series. Wall is finely agglutinated.

Dimensions (mm):

Chamber length: 0.069

Diameter:0,0022

Stratigraphic Distribution:

Ammovertella sp. is recorded from the Changhsingian stage of the measured section.

Genus *Hemigordiellina* MARIE, 1960

Type Species: *Hemigordiellina diversa* CUSHMAN and WATERS, 1930

Description:

Proloculus followed by streptospirally coiled tubular second chamber. Wall is porcelaneous.

Dimensions (mm):

Diameter of the test:0.089

Thickness of the wall:0.0017

Remarks:

Hemigordiellina sp. differes from *Glomospira* sp. by the wall structure. *Glomospira* has a finely agglutinated wall structure however *Hemigordiellina* sp. has a porcelaneous wall.

Stratigraphic Distribution:

Hemigordiellina sp. is recorded from the Changhsingian stage of the measured section.

Genus *Hoyanella* RETTORI, 1994

Type Species: Glomospira sinensis HO, 1959

"*Hoyanella*" sp.

Pl. XIII, figs. 9, 10

Description:

Test is small and discoidal. The coiling is glomospiral at the initial stage than planispiral evolute. The wall is porcelaneous.

Dimensions (mm):

Diameter of the test:0,047

Thickness of the wall:0,004

Stratigraphic Distribution:

"*Hoyanella*" sp. is recorded from Changhsingian stage of the measureed section.

Genus *Agathammina* NEUMAYR, 1887

Type Species: *Serpula pusilla* GEINITZ in GEINITZ and GUTBIER

Agathammina sp.

Description:

Test is ovate, globular proloculus followed by an semi-sigmoidally enrolled undivided tubular second chamber. Wall is calcareous, imperforate, porcelaneous.

Dimensions (mm):

Length of the test:0,055

Thickness of the wall:0,001

Remarks:

It is generally indicated that the second chambers are enrolled in five planes as in *Quinqueloculina* but in our specimens a semi-sigmoidally coiling is observed.

Stratigraphic Distribution:

Stratigraphic Distribution:

Agathammina sp. is recorded from the Changhsingian stage of the measured section.

Agathammina pusilla GEINITZ EM. WOLANSKA, 1959

Pl. XI, figs. 7, 8

1848. *Serpulla pusilla* Geinitz, p. 6, pl. 3, fig. 3-6.

1876. *Trochammina pusilla* (Geinitz); Brady, p.78, pl. 3 fig. 4, 5

1978. *Hemigordius parvulus* sp. nov., Lin, p. 39, pl. 5, fig. 18-19.

1979. *Agathammina pusilla* (Geinitz); Whittaker, Zaninetti and Altıner, pl. 2, figs. 5, 9.

1981. *Agathammina pusilla* (Geinitz); Zaninetti, Altıner and Çatal, pl. 10, figs. 16-20.

1984. *Agathammina pusilla* (Geinitz); Altıner, pl. 2, fig. 5

1986. *Agathammina* ex gr. *pusilla* (Geinitz); Vuks and Chediya, pl. 9, fig. 18.

1988. *Agathammina elongata* sp. nov., Pronina, p. 60, fig. 3.10.

1989. *Agathammina pusilla* (Geinitz); Köylüoğlu and Altıner, pl. 11, fig. 10.

1990. *Agathammina pusilla* (Geinitz); Lin et al. p. 81, p.218, pl. 26, fig. 20-23.

2003. *Agathammina pusilla* (Geinitz); Ünal, Altıner, Yılmaz and Özkan-Altıner, pl. 2, figs. 1-3.

2005. *Agathammina pusilla* (Geinitz); Kobayashi, fig. 3.41.

2006. *Agathammina pusilla* Geinitz; Nestell and Nestell, p. 10, pl. 3, fig. 1-5.

2009. *Agathammina pusilla* (Geinitz); Song, Tong, Chen, Yang and Wang, figs. 8.30-8.32.

2009. *Agathammina pusilla* Geinitz; Krainer and Vachard, pl. 2, figs. 7, 10.

Description:

Test is large and elongate. Proloculus is followed by semi-sigmoidally enrolled undivided tubular second chamber.

Dimensions (mm):

Length of the test:0,273

Thickness of the wall:0,0038

Remarks:

Agathammina pusilla is differed from other *Agathammina* sp. by having a larger test.

Stratigraphic Distribution:

Agathammina pusilla is recorded from middle and upper part of Changhsingian stage of the measured section.

Genus *Hemigordius* SCHUBERT, 1908

Type Species: *Cornuspira schlumbergeri* HOWCHIN, 1895

Hemigordius sp.

Pl. XI, figs. 12-18, Pl. XII, fig. 1

Description:

Test discoidal, spherical proloculus is followed by enrolled undivided tubular second chamber, early whorls are streptospiral, later whorls are planispiral and evolute. The wall is calcareous, porcelaneous.

Dimensions (mm):

Diameter of the test:0,083

Thickness of the wall:0,002

Stratigraphic Distribution:

Hemigordius sp. is recorded from the Changhsingian stage of the measured section.

Genus *Midiella* PRONINA, 1988

Type Species: *Hemigordius broennimanni* ALTINER, 1978

Midiella sp.

Pl. XII, fig. 5

Description:

Test is inflated disciodal, spherical proloculus is followed by undivided tubular second chamber early whorls are streptospiral, later whorls are oscillating or sigmoidal and involute.

Dimension:

Diameter of the test:0,072

Thickness of the wall:0,001

Remarks:

Midiella sp. differs from *Hemigordius* sp. by later whorls. *Midiella* sp. has involute sigmoidal whorls, but *Hemigordius* sp. has planispiral evolute later whorls.

Stratigraphic Distribution:

Midiella sp. is recorded in the upper part of Changhsingian stage of the measured section.

Midiella broennimanni ALTINER, 1978

Pl. XII, fig. 4

1978. *Hemigordius bronnimanni* n. sp., Altıner, pl. 1, fig. 1-6.

1981. *Hemigordius bronnimanni* Altıner; Altıner, pl. 43, fig. 1-6.

1984. *Hemigordius bronnimanni* Altıner; Altıner, pl. 2, fig. 2.

1989. *Hemigordius bronnimanni* Altıner; Kotlyar et al., pl. 3, fig. 5.

2001. *Midiella bronnimanni* Altıner; Pronina-Nestell and Nestell, pl. 1, fig. 12-13.

2003. *Hemigordius bronnimanni* Altıner; Altıner et al., text-fig 6.

Description:

Test is ovoid, inflated. Globular proloculus is followed by a tubular second chamber which is coiled streptospirally at the initial stage of growth and sigmoidally at the later stage of the growth.

Dimensions (mm):

Diameter of the test:0,0472

Thickness of the wall:0,0018

Stratigraphic Distribution:

Midiella bronnimanni is recovered from the upper part of the Changsingian stage of the measured section.

Midiella zaninettiae ? ALTINER, 1978

Pl. XII, fig. 3

1978. *Hemigordius zaninettiae* n. sp. Altıner, pl. 1, fig. 7-14.

1981. *Hemigordius changxingensis* sp. nov. Wang in Zhao et al., p. 47, 73, pl. 1, fig. 16.

1981. *Hemigordius zaninettiae* Altıner; Altıner, pl. 43, fig. 7-14.

1989. *Hemigordius (Midiella) zaninettiae* Altıner; Pronina, fig. 2.19, 2.20.

1989. *Hemigordius zaninettiae* Altıner; Köylüoğlu and Altıner, pl. 11, fig. 3-5.

1990. *Hemigordius changxingensis* Wang; Lin et al., pl. 24, fig. 36.

1996. *Hemigordius zaninettiae* Altıner; Leven and Okay, pl. 9, fig. 22, 23.

1998. *Hemigordius zaninettiae* Altıner; Altıner and Özkan Altıner, pl. 4, fig. 17.

2001. *Midiella zaninettiae* Altıner; Pronina-Nestell and Nestell, pl. 1, fig. 17.

2003. *Hemigordius zaninettiae* Altıner; Altıner et al., text-fig. 6.

2003. *Hemigordius zaninettiae* Altıner; Ünal et al., pl. 1, fig. 47.

Description:

Test is ovoid, inflated, initially streptospiral coiling, later oscillating coiling.

Dimensions (mm):

Diameter of the test:0,08

Thickness of the wall:0,002

Stratigraphic Distribution:

Midiella zaninettiae is recorded from the middle and upper part of the Changhsingian stage of measured section.

SUPERFAMILY CORNUSPIROIDAE SCHULZE, 1854

FAMILY NEODISCIDAE LIN, 1984

Glomomidiella sp. Vachard , Rettori and Angiolini, 2008

Type species: *Glomomidiella nestellorum* Vachard, Rettori and Angiolini, 2008

Glomomidiella sp.

Pl. XIII, figs. 11-17, Pl. XIV, figs. 1-4

Description:

Test is spherical to ovoid. Spherical proloculus is followed by a tubular streptospiral involute coiled second chamber. In the last whorls faint pseudoseptation is present. The wall is porcelaneous. Aperture is a simple terminal opening.

Dimensions (mm):

Diameter of the test:0,076

Thickness of the wall:0,004

Remarks:

Glomomidiella sp. differs from *Glomospira* sp. by the type of wall as *Glomospira* sp. has agglutinated wall structure and by having pseudoseptation in the last whorls.

Stratigraphic Distribution:

Glomomidiella sp. is recorded from the Changhsingian stage of the measured section.

Family Neodiscidae LIN, 1984

Genus *Neodiscus* MIKLUKHO-MAKLAY, 1953

Type Species: *Neodiscus milliloides* MIKLUKHO-MAKLAY, 1953.

Neodiscus sp.

Description:

Spherical proloculus is followed by an undivided tubular second chamber which is coiled glomospirally at the initial stage and planispirally involute at the later stage. The wall is thick and buttresses are developed.

Dimensions (mm):

Diameter of the test:0,072

Thickness of the wall:0,002

Stratigraphic Distribution:

Neodiscus sp. is recorded from the Changhsingian stage of the measured section.

Genus *Crassiglomella* sp.

Type Species: *Glomospira guangxiensis* LIN, 1978

Pl. XIV, figs. 5-10

Description:

Spherical proloculus is followed by an undivided tubular chamber which is entirely glomospirally coiled, has buttresses at the contact with the preceeding whorl.

Dimensions (mm):

Diameter of the test:0,11

Thickness of the wall:0,002

Stratigraphic Distribution:

Crassiglomella sp. is recorded from Changhsingian stage of measured section.

Genus *Multidiscus* MIKLUKHO-MAKLAY, 1953

Type Species: *Nummulostegina padangensis,* LANGE, 1925

.

Multidiscus sp. A

Pl. XII, fig. 7

Description:

The spherical proloculus is followed by planispirally coiled undevided tubular second chamber. The coiling is involute but the last whorl coils evolutely.

Dimensions:

Diameter of the test:0,185

Thickness of the wall:0,005

Stratigraphic Distribution:

Multidiscus sp. A is recorded from the Changhsingian part of the measured section.

Multidiscus sp. B

Pl. XII, fig. 8, 9

Description:

The spherical proloculus is followed by planispirally coiled undivided tubular second chamber. The coiling is involute. *Multidiscus* sp. B has a noteworthy large proloculus.

Dimensions (mm):

Diameter of the test:0,16

Diameter of the proloculus: 0,0178

Thickness of the wall:0,005

Stratigraphic Distribution:

Multidiscus sp. B is recorded from the Changhsingian part of the measured section.

Genus *Crassispirella* sp.

Type Species: *Crassispirella hughesi* (Gaillot and Vachard, 2007)

Pl. XI, fig. 11

Description:

The proloculus is followed by an undivided tubular second chamber. Initially glomospiral, later planispiral evolute coiling is observed in the second chamber. The test is composed of a porcelaneous thick wall.

Dimensions (mm):

Diameter of the test:0,163

Thickness of the wall:0,0038

Stratigraphic Distribution:

Crassispirella sp. is observed in the lower part of Changhsingian stage of the measured section.

Crassispirella hughesi (Gaillot and Vachard, 2007)

Pl. XI, fig. 10

2005. *Hemigordius* sp., Hughes, pl. 2, fig. 11.

2005. *Brunsiella concava* Spandel; Hughes, pl. 2, fig. 12.

2006. *Crassispirella hughesi* sp. nov., Gaillot and Vachard,pl. 55, fig. 3, pl. 56., fig 10, pl. 58, fig. 17-19, pl. 59, fig. 7-10, 12, pl. 66, fig. 17-18

Description:

Test is large and discoidal biconcave. Coiling is glomospiral at the initial stage than followed by aligned whorls and a last evolute whorl. Wall is porcelaneous and also has buttresses.

Dimensions (mm):

Diameter of the test:0,138

Thickness of the wall:0,004

Stratigraphic Distribution:

Crassispiralla hughesi is recorded from the Changsingian stage of the measured section.

Genus *Neodiscopsis* (Gaillot and Vachard, 2007)

Type Species: *Hemigordius specialis* LIN LI and SUN, 1990

Neodiscopsis sp.

Pl. XII,fig. 11, Pl. XII, figs. 13-17, Pl. XIII, figs. 1-4

Description:

Test is large discoidal to lenticular, aligned or sigmoidal coiling at the initial stage oscillating at the later stage.

Dimensions (mm):

Diameter of the test:0,09

Thickness of the wall:0,006

Stratigraphic Distribution:

Neodiscopsis sp. is recorded from the Changhsingian stage of the measured section.

SUPERFAMILY CALIGELLOIDEA REITLINGER,1959

Genus *Floritheca* (Gaillot and Vachard, 2007)

Type Species: *Floritheca variata* gen. nov. sp. nov.

Floritheca variata (Gaillot and Vachard, 2007)

Pl. XI, figs. 1, 2

2004. *Globivalvulina* sp. Kobayashi, fig. 6.41

2006. *Insolentitheca* (?) sp. Insalaco et al. pl. 1, fig. 21

2007. *Floritheca variata* sp. nov., Gaillot and Vachard, pl. 5, fig. 4, pl. 13, fig. 2, pl. 15, fig. 1-3, pl. 16, fig. 1-22, pl. 17, fig. 10, pl. 18, fig. 12, 14.

Description:

Globular, subglobular, egg-shaped or sometimes ellipsoidal chambers are arranged around a globular to subglobular chamber so the test has a flower-like appearance. Wall of the chambers is microgranular.

Dimension (mm):

Diameter of the test:0,0875

Thickness of the wall:0,00375

Remarks:

In our thin sections one of eight chambered and one of six chambered specimens are recorded. In other studies more chambered specimens have also been recorded by other authours.

Stratigraphic Distribution

Floritheca variata (Gaillot and Vachard,2007) is recorded from lower and middle part of the Changsingian stage of our measured section.

Superfamily SQUAMULINACEA REUSS and FRITSCH, 1861

FAMILY SQUAMULINIDAE REUSS and FRITSCH, 1861

Genus *Rectocornuspira* WARTHIN, 1930

Type Species: *Rectocornuspira lituiformis* WARTHIN, 1930.

Rectocornuspira kalhori BRÖNNIMANN, ZANINETTI and BOZORGNIA, 1972

Pl. XVII, figs. 1-7

1972. *Rectocornuspira kalhori* sp. nov. Brönnimann, Zaninetti and Bozorgnia, pl. 1, fig. 1-20, pl. 2, fig. 1-23, pl. 4, fig. 1, 3, 5-7, 12-15

1981. *Rectocornuspira kalhori* Brönnimann, Zaninetti and Bozorgnia; Altıner and Zaninetti, pl. 78, fig. 1-18.

1983. *Rectocornuspira kalhori* Brönnimann, Zaninetti and Bozorgnia; Işık, pl. 1, fig. 11.

1989. *Rectocornuspira kalhori* Brönnimann, Zaninetti and Bozorgnia; Köylüoğlu and Altıner, pl. 1, fig. 1-8.

1993. *Rectocornuspira* cf. *kalhori* (Brönnimann, Zaninetti and Bozorgnia); Trifonova, p. 38, pl.5, fig. 6, pl. 9.

1995. *Rectocornuspira kalhori* Brönnimann, Zaninetti and Bozorgnia; Rettori, p. 104-106, pl. 19, fig. 7-14.

1995. *Cornuspira mahajeri* (Brönnimann, Zaninetti and Bozorgnia); Rettori, pl. 19, fig. 1-5

2003. *Rectocornuspira kalhori* Brönnimann, Zaninetti and Bozorgnia; Ünal, Altıner, Yılmaz and Özkan-Altıner, pl. 2, fig. 10-12.

2005. *Rectocornuspira kalhori* Brönnimann, Zaninetti and Bozorgnia; Groves, Altıner and Rettori, text-figs. 9.2., 9.3.

2007. *Rectocornuspira kalhori* Brönnimann, Zaninetti and Bozorgnia; Groves et al., fig. 12.1.

2007. "*Cornuspira*" *mahajeri* Brönnimann, Zaninetti and Bozorgnia; Angiolini et al., fig. 6.8-6.11.

2007. *Rectocornuspira kalhori* Brönnimann, Zaninetti and Bozorgnia; Groves et al. fig. 12.

2009. *Rectocornuspira kalhori* Brönnimann, Zaninetti and Bozorgnia; Song, Tong, Chen, Yang and Wang, figs. 7.7-7.10.

2010. "*Cornuspira*" *mahajeri* Brönnimann, Zaninetti and Bozorgnia; Angiolini et al., fig. 4.35.

Description:

The globular proloculus is followed by tubular second chamber which is planispirally enrolled in the early stage and uncoiled rectilinear in the adult stage. The wall is calcareous, porcelaneous.

Dimensions (mm):

Diameter of the test:0,041

Thickness of the wall:0,001

Remarks:

Rectocornuspira kalhori is important for being the lowermost Triassic (Greisbachian) marker.

Stratigraphic Distribution:

Rectocornuspira kalhori is recored in the Greisbachian stage of the measured section and observed in the sample AH-102 for the first time.

Family OZAWAINELLIDAE THOMPSON and FOSTER, 1937

Genus *Reichelina* ERK, 1941; emend. MIKLUKHO-MAKLAY, 1951

Reichelina changhsingensis, SHENG in SHENG and CHANG, 1958

Pl. X, figs. 5, 6

1986. *Reichelina changhsingensis* Sheng et Chang; Kobayashi, pl. 3, figs. 20-25, 28

2004. *Reichelina changhsingensis* Sheng et Chang; Orlov-Labkovsky, pl. 1 fig. 8

2004. *Reichelina changhsingensis* Sheng and Chang; Kobayashi, fig. 6.17-6.26.

2006. *Reichelina changhsingensis* Sheng and Chang; Kobayashi, pl. 2, figs. 4-8.

2010. *Reichelina changhsingensis* Sheng and Chang; Wang, Ueno, Zhang and Cao, fig. 3.1.

Description:

Test is lenticular, early stage is planispirally involute enrolled inflated along the axis of coiling. Final whorl increases rapidly in height uncoiled and straight. The wall is with tectum and diaphanotecha.

Dimensions(mm):

Diameter of the test:1,25

Width of the test:0,5

W/D:0,4

Length of the last part: 1,175

The thickness of the wall:0, 025

Stratigraphic Distribution.

Reichelina changhsingensis is recorded from upper part of Changhsingian stage of measured section.

ORDER SEDENTARIDA LAMARCK, 1818

FAMILY SERPULIDAE JOHNSTON, 1865

Genus *Spirorbis* DAUDIN, 1800

Type Species: *Serpula spirorbis* Linné, 1758

Spirorbis phlyctaena

Pl. XVII, figs. 8-11; Pl. XVIII, figs. 1-19

1972. *Spirorbis phlyctaena* sp. n., Brönnimann and Zaninetti, text-fig. 1-4, pl. 10, fig. 1-9, pl. 11, fig. 1-15, pl. 12, fig. 2, 4-6, 8-13

1972. *Spirorbis phlyctaena* Brönnimann and Zaninetti, pl. 2, fig. 5, pl. 6, fig. 1-4, 7.

2009. *Spirorbis phlyctaena* Brönnimann and Zaninetti; Krainer and Vachard, pl. 2, fig. 5, pl. 6, figs. 1-4, 7.

Description:

The test is coiled tubiculous.

Dimensions (mm):

Diameter of the test:0,32

Width of the test:0,116

Remarks:

Spirorbis phlyctaena survives just above the Permian-Triassic boundary and very important in biostratigraphic studies for the determination of the boundary. *Spirorbis phlyctaena* is observed in the lowermost Triassic successions of most important Permian-Triassic boundary sections. Some of these sections are Elika Fm. Central Alborz (Brönnimann and Zaninetti, 1972), Tabas area (Brönnimann et al., 1973), Julfa area (Baud et al., 1974), Zagros-South Fars (Insalaco et al., 2006) , Siusi Formation, Dolomites, Italy (Brönnimann and Zaninetti, 1972), Pınarbaşı, Eastern Taurus, Turkey (Altıner, 1981; Altıner and Zaninetti, 1981).

Stratigraphic Distribution:

Spirorbis plycateana is recorded from Greishbachian stage of the measured section.

CHAPTER 5

DISCUSSIONS AND CONCLUSIONS

In the Hadim region of the Central Taurides a 48,06m thick stratigraphic section was measured through the Permian Taşkent Formation and the Triassic Ekinlik Formation of the Bolkar Dağı Unit. The purpose of this study was to designate the foraminiferal paleontological, biostratigraphical and sequence stratigraphical features of the Permian-Triassic boundary beds of the Bolkar Dağı Unit which is one of the most important tectonic units within the structure of the central Taurides.

In this study a detailed taxonomic examination was carried out and the calcareous benthic foraminifera was taxonomically classified according to the wall structure, chamber number, coiling type, apertural features and dimensions of the test. According to these discriminational features 37 species and 29 genera of benthic foraminifera were identified. The lagenoids, miliolids and the fusulinids are the main foraminifer groups that have been identified. The measured section was devided into two biostratigraphic zones. These assemblage zones are the Changhsingian "*Nodosaria*" *elabugae - Nestellorella dorashamensis - Reichelina changhsingensis* Assemblage Zone and the Greisbachian *Spirorbis phlyctaena-Rectocornuspira kalhori* Assemblage Zone. In the measured section the Permian-Triassic boundary is delineated between the Changhsingian "*Nodosaria*" *elabugae-Nestellorella dorashamensis-Reichelina changhsingensis* Assemblage Zone and the Greisbachian *Spirorbis phlyctaena-Rectocornuspira kalhori* Assemblage Zone. By the transition from the Permian beds to the Triassic beds all previously recorded lagenoid, miliolid and the fusulinid foraminifers became extinct and the newcomers *Spirorbis phlyctaena* and *Rectocornuspira kalhori* appeared for the first time at the base of Lower Triassic beds. However, Groves et al.(2005) recorded the "*Nodosaria*" *elabugae* in the basal Triassic strata of the Gevne Formation (Central Taurides) as a survivor which escaped from the end-Permian extinction event.

The studied carbonate succesions in the Hadim region were deposited in a shallow marine environment during the Changhsingian and the Greisbachian. Sea level fluctiations are important allocyclic mechanisms controlling the configuration of the deposition in this kind of environments. In order to understand the meter-scale cyclicity a detailed microfacies analysis was carried by investigation of samples and field observations. According to the microfacies analysis 12 types were distinguished comprising mudstone with lagenoid foraminifera, bioclastic wackestone with calcareous algae and benthic foraminifera, bioclastic wackestone-packstone with diversified foraminifera, wackestone with miliolid foraminifera, unfossiliferous mudstone, peloidal packstone to grainstone, oolitic grainstone, siltstone to mudstone, quartz arenitic sandstone, *Spirorbis phlyctaena*-rich wackestone, pseudoolitic or recrystallized coated grain packstone and sandy or silty lime mudstone. According to the vertical configuration of these microfacies types 6 main types and 10 sub-types of shallowing upward cycles were designated. Shallowing character of cycles were determined according to the presence of lagoonal mudstone, oolitic packstone and siliciclastic deposits at the top of the cycles. A-type cycles are mainly composed of wackestone-packstone facies with diversified foraminifera overlain by wackestone with miliolids. B-type cycles begin with bioclastic wackestone with calcareous algae and are capped by unfossiliferous mudstone. C-type cycles are characterized by the presence of wackestone-packstone with diversified foraminifera and bioclastic wackestone with calcareous algae at the base and are capped by unfossiliferous mudstone at the top. D-type cycles begin with wackestone-packstone with diversified foraminifera at the base and are overlain by oolitic grainstone. E-type cycles are characterized by the peloidal packstone to grainstone facies at the top. F-type cycles comprise the cycles in the Triassic part of the measured section. This type is composed of *Spirorbis phlyctaena*-rich wackestone, pseudoolitic packstone and sandy or silty lime mudstone.

Meter-scale shallowing-upward cycles are correspond to parasequences which are the fundamental building blocks of system tracts and sequences. Throughout the measured section two sequence boundaries were determined according to the stacking pattern of the shallowing-upward cycles (SB1 and SB2). These sequence boundaries coincide well with the sequence boundaries defined in the Changhsingian by Haq and Schutter (2008). According to the correlation with their chart, one of the sequence boundaries is located at the middle of the Changhsingian (252.5 Ma) and a younger sequence boundary (251.5 Ma) corresponds to the upper part of the Changhsingian just below the Permian-Triassic boundary. Throughout the measured section 11 meter-scale cycles have been determined between SB1 and SB2. The duration of the cycles are approximately 90.900 and can be interpreted as Milankovitch eccentricity cycle.

Haq and Schutter (2008) illustrated the Permian-Triassic boundary in the transgressive system tract deposits of their onlap curve of Permian-Triassic sea level changes. In the present study, the Permian-Triassic boundary is also recorded in the transgressive system tract deposits of the Sequence 3 in the measured section. It can be concluded that the shallow marine carbonate successions of the the Bolkar Dağı Unit (Central Taurides) recorded a similar stacking pattern with the other Permian-Triassic boundary sections of the world.

The present thesis is one of the pioneering studies on the paleontology, biostratigraphy and sequence stratigraphy of the Bolkar Dağı Unit. In the future studies, the Permian-Triassic boundary beds of the Bolkar Dağı Unit should be documented with more studies similar to the present one in order to increase the resolution in foraminiferal biostratigraphy and sequence stratigraphy.

REFERENCES

Adachi, S. 1985. Smaller foraminifers of the Ichinotani formation (Carboniferous-Permian), Hida Massif, central Japan. Sci. Rep., Inst. Geosci., Univ. Tsukuba., 6, pp. 59-139.

Akçar, N., 1998. Meter-scale cyclic deposits in the Lower Cretaceous peritidal Carbonates of the Üzümlü Area (Western Taurides, Turkey). M.Sc. Thesis, Middle East Technical University, Ankara, Turkey, 109 p. (unpublished).

Ali, J. R., Wignall, P. B. 2007. Comment on "Fusiline biotic turnover across the Guadalupian-Lopingian (Middle-upper Permian) boundary in mid-oceanic carbonate build-ups: Biostratigraphy of accreted limestone in Japan" by Ayano Ota and Yukio Isozaki. Journal of Asian Earth Sciences, 30, pp. 199-200.

Altıner D. 1981. Recherches stratigraphiques et micropaleontologiques dans le Taurus Oriental au NW'de Pınarbaşı (Turquie). These Universite de Geneve, No. 2005, Geneve, 450 p.

Altıner D. 1988. Pseudovidalinidae n. fam. and *Angelina* n. gen. from the Upper Permian of South and Southeast Turkey. Revue de Paléobiologie, vol. spéc. 2, 25-36.

Altıner D. 1999 - *Sengoerina argandi,* n. gen., n. sp., and its position in the evolution of Late Permian biseriamminid foraminifers. Micropaleontology, 45/2, 215-220.

Altıner D. and Özkan Altıner S., 1998. *Baudiella stampflii* n.gen., n.sp., and its position in the evolution of Late Permian ozawainellid fusulines. Revue de Paléobiologie, 17, 163-175.

Altıner D., Baud A., Guex J., Stampfli G. 1980. - La limite Permien-Trias dans quelques localités du Moyen-Orient: recherches stratigraphiques et micropaléontologiques. Riv. Ital. Paleont., 85 (1979), 3-4, 683-714.

Altıner D., Brönnimann P. 1980. - *Louisettita elegantissima* n.gen., n.sp., un nouveau foraminifère du Permien supérieur du Taurus oriental (Turquie). Notes Lab. Paléont. Univ. Genève, 6/3, 39-43.

Altıner D., Groves J. R., Özkan-Altiner S., Yılmaz İ. Ö., Atakul A. 2007. *Necdetina*, a new fusulinoidean foraminifera with recrystallized or replaced wall from the Middle Permian of the Central Tauride Belt, Turkey. Journal of Foraminiferal Research, 37, 360-371.

Altıner D., Savini R., Özkan-Altiner S. 2003. – Morphological variation in *Hemigordius harltoni* Cushman & Waters, 1928: remarks on the taxonomy of Carboniferous and Permian hemigordiopsids. Rivista Italiana di Paleontologia e Stratigrafia, 109, 2, 195-211.

Altıner D., Zaninetti L. (1981) - Le Trias dans la région de Pınarbaşı, Taurus oriental, Turquie: unités lithologiques, micropaléontologie, milieux de dépot. Riv. Ital. Paleont., 86/4, 705-760.

Altıner D., Zaninetti L. 1977. *Kamurana brönnimanni*, n.gen., n.sp., un nouveau foraminifère porcelané du Permien supérieur du Taurus oriental, Turquie. Notes Lab. Paléont. Univ. Genève, 1/6, 1-5.

Altıner D., Zaninetti L., Martini R., Alkan H. 1992. – *Siculocosta floriformis*, n.sp., (Siculocostidae, Milioliporacea), un nouveau foraminifère de Trias supérieur (Norien-Rhetien) récifal du Taurus occidental (Nappes Lyciennes), Turquie. Revue de Paléobiologie, 11/2, 313-322.

Altıner, D. 1978. Trois nouvelles espéces de genre *Hemigordius* (Foraminifére) du Permien supérieur de Turquie (Taurus oriental). Notes du Laboratoire de Paleontologie de L'Universite de Geneve, 5, 27-31.

Altıner, D. 1984. Upper Permian foraminiferal biostratigraphy in some localities of the Taurus Belt. In: Tekeli O. and Göncüoğlu M.C. (ed.), Geology of the Taurus Belt, Mineral Research and Exploration Institude of Turkey Publication, 255-268.

Altıner, D. 1984. Upper Permian foraminiferal biostratigraphy in some localities of the Taurus Belt. International Symposium on the Geology of the Taurus Belt (Ankara, 1983), Maden Tetkik ve Arama Enstitüsü Yayınlarından (MTA), 255–266.

Altıner, D. and Özgül, N. 2001. Paleoforams 2001; International Conference on Paleozoic Benthic Foraminifera; Carboniferous and Permian of the allochthonous terranes of the Central Tauride Belt, Southern Turkey. Guide Book. 35 p.

Altıner, D. and Özkan-Altıner S. 2010. *Danielita gailloti* n.gen., n. sp., within the evolutionary framework of Middle-Late Permian dagmaritins. Turkish Journal of Earth Sciences (Turkish J. Earth Sci.), 19, 497-512.

Altıner, D. and Özkan-Altıner, S. 2001. *Charliella rossae* n. gen., n. sp., from the tethyan realm: remarks on the evolution of Late Permian biseriamminids. Journal of Foraminiferal Research, 31(4), 309-314.

Altıner, D. and Savini, R. 1995. Pennsylvanian foraminifera and biostratigraphy of the Amazonas and Solimoes Basin (North Brazil). Revue de Paleobiologie, 14(2), pp. 417-453.

Altıner, D., Özkan-Altıner, S. and Koçyiğit, A. 2000. Late Permian foraminiferal biofacies in Turkey. In: E. Bozkurt, J.A., Winchester and J.D.A., Piper (eds.), Tectonics and magmatism in Turkey and the surrounding area, Geological Society, London, Special publication, 173, 83-96.

Altıner, D., Yılmaz, İ.Ö., Özgül, N., Bayazıtoğlu, M. and Gaziulusoy, Z. E. 1999. High resolution sequence stratigraphic correlation in the Upper Jurassic (Kimmeridgian)–Upper Cretaceous (Cenomanian) peritidal carbonate deposits, Western Taurides, Turkey. Geological Journal, 34, 139-150.

Angiolini, L., Checconi, A., Gaetani, M., and Rettori, R. 2010. The latest Permian mass extinction in the Alborz Mountains (North Iran). Geological Journal, 45, pp. 216-229.

Atakul, A. 2006. Lower-Middle Carboniferous boundary in Central Taurides, Turkey (Hadim area): paleontological and sequence stratigraphic approach. M.Sc. Thesis, Middle East Technical University, Ankara, Turkey, 201 p. (unpublished).

Bayazıtoğlu, M. 1998. Short distance sequence stratigraphic correlation in a carbonate succession of Fele area (North of Beyşehir Lake), Western Taurides, Turkey. M.Sc. Thesis, M.E.T.U., Ankara, Turkey, 125 p. (unpublished).

Blumenthal, M. M. 1944. Bozkır güneyinde Toros sıradağlarının serisi ve yapısı. İstanbul Üniversitesi Fen Fakültesi Mecmuası, V. B. 9, 95-125.

Blumenthal, M. M. 1947. Beyşehir-Seydişehir hinterlandındaki Toros dağlarının jeolojisi. Maden Tetkik Arama Enst. Ankara, seri D, 2, 242 p.

Blumenthal, M.M. 1951. Recherches geologiques dans le Taurus occidental dans l'arriere-pays d'Alanya. Veröffentlichungen des Institutes für Lagerstattenforschung der Turkei, Seri D, no. 5.

Blumenthal, M.M. 1952. Das taurische Hochgebirge des Aladağ, neuere forschungen zu seiner geographie, stratigraphie und tektonik. Veröffentlichungen des Institutes für Lagerstattenforschung der Turkei, Seri D, no. 6.

Blumenthal, M.M. 1956. Karaman Konya Havzası Güney batısında Toros Kenar Silsileleri ve Şist Radyolarit Formasyonu Stratigrafi Meselesi. Maden Tetkik Arama Enst. Derg., 48, 1-36.

Bozorgnia, F. 1973. Paleozoic foraminiferal biostratigraphy of central and east Alborz Mountains, Iran. National Iranian Oil Company, Geological Laboratories, Publication, 4, 1-185.

Bozorgnia, F., 1965. Qum Formation stratigraphy of the Central Basin of Iran and its intercontinental position. Bulletin of the Iranian Petroleum Institute, 24, 69-75.

Brady, H.B. 1873. On *Archaediscus karreri* a new type of Carboniferous Foraminifera. Annals and Magazine of Natural History, 4 (12): 286-290.

Brady, H.B. 1876. A monograph of Carboniferous and Permian Foraminifera (the genus Fusulina excepted). Palaeontographical Society, 30: 1-166.

Broglio-Loriga, C., Neri, C., Pasini, M., and Posenato, R. 1986. Marine Fossil Assemblages from Upper Permian to Lowermost Triassic in the Western Dolomites (Italy), Mem. Soc. Geol. Ital., vol. 34, pp. 5–44.

Brown, J. S.. 1943 Suggested use of the word microfacies, Economic Geology, 38, p. 325.

Brönnimann, P. and Zaninetti, L. 1972. On the occurrence of the serpulid *Spirorbis* Daudin, 1800 (Annelida, Polychaetia, Sedentarida) in thin sections of Triassic rocks of Europe and Iran. Rivista Italiana di Paleontologica e Stratigrafia, 78(1), 67-90.

Brönnimann, P., Whittaker, J.E. and Zaninetti L. 1975. Triassic foraminiferal biostratigraphy of the Kyaukme- Longtawkno area, northern Shan States, Burma. Rivista Italiana di Paleontologica e Stratigrafia, 81(1), 1-30.

Brönnimann, P., Zaninetti, L., and Bozorgnia, F. 1972a. Triassic (Scythian) smaller Foraminifera from the Elika Formation of the central Albourz, northern Iran, and from the Siusi Formation of the Dolomites, Northern Italy, Mitt. Ges. Geol. Bergbaustud., 1972a, vol. 21, pp. 861–884.

Canuti, P., Marcucci, M. and Pirini Radrizzani, C. 1970. Microfacies e microfaune nelle formazioni paleozoiche dell'anticlinale di Hazro (Anatolia sud-orientale, Turchia). Bolletino Societá Geologica Italiana, 89: 21-40.

Catuneanu, O., 2006. Principles of Sequence Stratigraphy. Elsevier, Amsterdam, 375 p.

Cherdyntsev, W. 1914. Foraminiferal fauna of the Permian deposits of the esatern belt of European Russia. Kazan, Trudy Obshchestva Estestvoispytateley pri Imperatorskomy Kazanskomy Universitety, 46, 3-88. (In Russian)

Chernysheva, N.E. 1941. Novyi rod foraminifer iz turneiskikh otlozhenii Urala (New genus of Foraminifera from the Tournaisian deposits of the Urals). Doklady Akademiya Nauk SSSR, 32 (1), 69-70 (in Russian).

Cirilli, S., Pirini Radrizzani, C., Ponton, M., Radrizzani, S. 1998. Stratigraphical and paleoenvironmental analysis of the Permian-Triassic transition in the Badia Valley (southern Alps, Italy). Palaeogeography, Palaeoclimatology, Palaeoecology, 138(1-4), 85-113.

Colani, M. 1924. Nouvelle contribution à l'étude des fusulinidés de l'Extrême-Orient. Mémoires du Service géologique de l'Indochine, 11 (1), 9–199.

Colchen, M., Bassoullet, J.P., Marcoux, J. and Mascle, G. 1980. La biozon a *Colaniella parva* du permien superieur et sa microfaune dans le bloc calcaire exotique de Lamayuru, Himalaya du Ladakh. Revue De Micropaleontologie, 23(2), 76-108.

Cushman J.A. and Waters J.A. 1928. Some Foraminifera from the Pennsylvanian and Permian of Texas. Contributions from the Cushman Laboratory for Foraminiferal Research 4 (2): 31-55.

Cushman, J. A., 1928. Foraminifera, Their Classification and Economic Use, Cushman Lab. for Foram. Research, Spec. Publ. No. 1, Sharon, Mass.

Cushman, J.A. and Waters, J.A. 1930. Foraminifera of the Cisco Group. Bulletin University of Texas, 3019: 22-81.

Çatal, E. and Dağer, Z. 1974. Description of new *Colaniella* species from the Permien of Taurus Region. Bulletin of the Geological Society of Turkey, 17(1), 187-191.

Daudin, F. M. 1800. Recueil de memories et de notes sur les especes peu connues de Mollusques, Vers et Zoopytes. Paris.

Davydov, I.V., Belasky, P. and Karavayeva I.N. 1996. Permian fusulinids from Koryak Terrane, Northeastern Russia, and their paleobiogeographic affinity. Journal of Foraminiferal Research, 26(3), 213-243.

Demirtaşlı, E., 1984. Stratigraphy and tectonic of the area between Silifke and Anamur, Central Taurus Mountains: In.Tekeli O. and Göncüoğlu M. C. (eds), Geology of the Taurus Belt. Mineral Research and Exploration Institute of Turkey Publication, 101-123.

Deprat, J. 1915. Les Fusulinides des Calcaires Carboniferiens e Permiens du Tonkin, du Laos et du Nord-Annam. Mem. Serv. Geol. de VIndochine, 4, Fasc. I, Etude des Fusulinides de Chine et d'Indochine et classification des calcaires a fusulines IV. Mem.: 1-30, pis. 1-3.

Dessauvagie, T.F.J. and Dağer, Z. 1963. Anadolu'da Lasiodiscidae zuhuratı. Maden Tetkik Arama Enstitüsü Dergisi, 60, 75-82.

Dinç, A. T. 2009. Micropaleontological Analysis and Sequence Stratigraphy Through The Upper Tournaisian Substage In Aladağ Unit (Central Taurides, Turkey). M.Sc. Thesis, Middle East Technical University, Ankara, Turkey, 121p. (unpublished).

Dumont, P.J.F. 1976. Etudes géologiques dans les Taurides Occidentals: Les formations paléozoiques et mésozoiques de la coupole de Karacahisar (Province d'Isparta, Turquie). These, l'Universite De Paris-Sud Centre D'Orsay, 213p.

Dunbar, C. O., and Skinner, J. W. 1937. Permian Fusulinidae of Texas. University of Texas Bulletin, 3 (2), N 3701, 517-825.

Dunham, R.J. 1962. Classification of carbonate rocks according to depositional texture. In: Ham, W.E. (eds.): Classification of carbonate rocks. A symposium. Amer. Ass. Petrol. Geol. Mem., 1, 108-171.

Efimova, N.A. 1974. Triasovye foraminifery severo-zapadnogo Kavkaza i Predkavkazya (Triassic foraminifers from northwestern Caucasus and Precaucasus). Voprosy Mikropaleontologii, 17: 54–83 (in Russian)

Ehrenberg, C.G. 1838. Über dem blossen Auge unsichtbare Kalkthierchen und Kieselthierchen als Hauptbestandtheile der Kreidgebirge. Bericht über die zu Bekanntmachung geeigneten Verhandlungen der königlischen preussischen Akademie der Wissenschaften zu Berlin, 1838 (3): 192-200.

Eiland, M. and Gudmundsson, G. 2004. Taxonomy of recent nodosariinae (foraminifera) from the North Atlantic, with notes on wall laminitaion. Micropaleontology, 50(2), 195-210.

Einsele, G., Ricken W. and Seilacher, A. 1991. Cycles and Events in Stratigraphy - basic concepts and terms. In: W. R. G. Einsele, W. Ricken & A. Seilacher (eds.), Cycles and Events in Stratigraphy, Berlin, Heidelberg, New York, Springer Verlag, 1-19.

Epshtein, O.G., Terekhova, G.P. and Solov'eva, M.N. 1985. The Paleozoic of the Koriyak upland (foraminiferal fauna, biostratigraphy). Akademiya Nauk SSSR, Vopsory Mikropaleontologii, 27, 47-77. (In Russian with English summary)

Erk, A.S. 1941. Sur la présence du genre *Codonofusiella* Dunb. et Skin. Dans le Permien de Bursa (Turquie). Eclogae geologicae Helvetiae, 34(2), 243-253.

Erwin, D. H. 1994. The Permo-Triassic extinction. Nature, 367 (20), 231-236.

Ezaki, Y., Liu, J. and Adachi, N., 2003. Earliest Triassic Microbialite Micro- to Megastructures in the Huaying Area of Sichuan Province Province, South China: Implications for the Nature of the Oceanic Conditions after the End-Permian Extinction. Palaios, 18, 388-402.

Flügel, E., 2004. Microfacies of carbonate rocks: analysis, interpretation and application. Springer, 976 p.

Folk, R.L. 1962. Spectral subdivision of limestone types. In: Ham, W.E. (ed.): Classification of carbonate rocks. A symposium. Amer. Ass. Petrol. Geol. Mem., 1,62-84

Fontaine, H., Bin Amnan, I., Khoo, H.P., Nguyen Duc Tien and Vachard, D. 1994. The *Neoschwagerina* and *Yabeina-Lepidolina* zones in Peninsular Malaysia, and Dzhulfian and Dorashamian in Peninsula Malaysia, the transition to the Triassic. Geological Survey of Malaysia, Geological Papers, 4: 1-175.

Gaillot, D., Vachard, T., Galfetti, R. Martini. 2009. New latest Permian foraminifers from Laren (Guangxi Province, South China). Palaeobiogeographic implications, Geobios, volume 42(2), 141-168.

Gaillot, J. and Vachard, D. 2007. The Khuff Formation (Middle East) and time-equivalents in Turkey and South China: biostratigraphy from Capitanian to Changhsingian times (Permian), new foraminiferal taxa, and palaeogeographical implications. Coloquios de Paleontología, 57: 37-223.

Gaziulusoy, Z. E. 1999. A sequence stratigraphical approach from microfacies analysis to the Aptian-Albian peritidal carbonates of Polat Limestone (Seydişehir), Western Taurides, Turkey. M.Sc. Thesis, M.E.T.U., Ankara, Turkey, 97 p. (unpublished).

Geinitz, H.B. and Gutbier, A. 1848. Die Versteinerungen des Zechsteingebirges und Rothliegenden. 26 pp. (Heft 1), Arnold, Dresden.

Goldhammer, R. K., Dunn, P. A. and Hardie, L. A. 1987. High frequency glacio-eustatic sea-level oscillations with Milankovitch characteristics recorded in Middle Triassic platform carbonates in northern Italy. Am. J. Sci., 287, 853-892.

Groves J. R., Rettori R., Boyce M. D., Altiner D. 2007. End-Permian mass extinction of lagenide foraminifers in the southern Alps (Northern Italy). Journal of Paleontology, 81, 3, 415-434.

Groves, J. R., Altiner, D. 2005. Survival and recorvery of calcareous foraminifera pursuant to the end- Permian mass extinction. C.R. Palevol, 4, pp. 487-500.

Groves, J. R., Altiner, D. and Rettori, R. 2003. Origin and early evolutionary radiation of the order Lagenida (foraminifera). J. Paleont., 77(5), pp. 831-843.

Groves, J.R. and Boardman, J.R. 1999. Calcareous smaller foraminifers from the lower Permian Council Grove Group near Hooser, Kansas. Journal of Foraminiferal Research, 29(3), 243-262.

Groves, J.R. and Wahlman, G.P. 1997. Biostratigraphy and evolution of late Carboniferous and early Permian smaller foraminifers from the Barents Sea (offshore Arctic Norway). Journal of Paleontology, 71 (5), 758-779.

Groves, J.R., Altıner, D. and Rettori, R. 2005. Extinction, survival, and recovery of lagenide foraminifers in the Permian-Triassic boundary interval, Central Taurides,Turkey. Journal of paleontology, 79, 1-38.

Groves, J.R., Rettori, R. and Altıner, D. 2004. Wall structures in selected Paleozoic lagenide foraminifera. J. Paleont., 78(2), 245-256.

Groves, J.R.2000. Suborder Lagenina and other smaller foraminifers from Uppermost Pennsylvanian-Lower Permian rocks of Kansas and Oklahoma. Micropaleontology, 46(4), 285-326.

Gutnic, M., Monod, O., Poisson, A. and Dumont, J.F. 1979. Géologie des Taurides occidentales (Turquie). Memories De La Société Géologique de France (Nouvelle Série), Mémoire No: 137, 109p.

Haas, J., Goczan, F., Oravecz-Scheffer, A., Barabasstuhl, A, Majoros, GY. and Berczi-makk, A. 1986. The Permian-Triassic Boundary in Hungary. Memorie della Società Geologica Italiana, 34, 21-241.

Haq, B.U., and Schutter, S.R., 2008. A chronology of Paleozoic sea-level changes. Science, 322: 64-68.

Hase, A. and Aiba, M. 1977. Stratigraphy of the Permian Karita Formation in the environs of Hiroshima, Japan. Journal of Science of the Hiroshima University, series C, 7, 203-216.

Hase, A., Hamanaka, K. And Okimura, Y. 1981. Paleozoic rocks in the eastern part of the Kamigori Belt near Tatsuno. Hyogo. Res. Mesoz. Tectonics in Japan, 3, 191-197.

Ho Y. 1959. Triassic Foraminifera from the Chialingkiang Limestone of South Szeczuan. - Acta Palaeont, Sinica, 7,(5), 387-418.

Hongfu, Y., Jinnan, T. 1998. Multidisciplinary high-resolution correlation of the Permian-Triassic boundary. Palaeogeography, Palaeoclimatology, Palaeoecology, 143, pp. 199-212.

Howchin W. 1895. Carboniferous foraminifera of Western Australia, with descriptions of new species. Transactions and Proceedings of the Royal Society of South Australia 19: 194-198.

Insalaco, E., Virgone, A., Courme, B., Gaillot, J., Kamali, M., Moallemi, A., Loftpour, M. and Monibi, S. 2006. Upper Dalan Member and Kangan Formation between the Zagros Mountains and Offshore Fars, Iran: depositional system, biostratigraphy and stratigraphic architecture. GeoArabia, 11 (2): 75-176.

Ishii, K.I., Okimura, Y. and Nakazawa, K. 1975. On the genus *Colaniella* and its biostratigraphic significance. Journal Geosciences, Osaka City University, 19 (6): 107-129.

Isozaki, BG.Y., Yao, J., Matsuda,T., Sakai, HY., Ji, Z., Shimizu, N., Kobayashi, N., Kawahata, H., Nishi, H., Takano, M. and Tomomi Kubo. 2004. Stratigraphy of the Middle-Upper Permian and Lowermost Triassic at Chaotian, Sichuan, China. Proc. Japan. Acad, 80, pp. 10-16.

Isozaki, Y., Ota, A. 2007. Reply to comment by Ali, J.R. and Wignall, P. on Ota, A. and Isozaki, Y., 2006. Fusuline biotic turnover across the Guadalupian-Lopingian (Middle-Upper Permian) boundary in mid-oceanic carbonate buildups: Biostratigraphy of accreted limestone, Japan. Journal of Asian Earth Sciences, 26, 353-368.

Işık, A. 1983. An example for the determination of the Permian-Triassic transition by the foraminifera population for current range zones (Aladağlar region, eastern Taurus Mountains). TMMOB Jeoloji Mühendisleri Odası Yayın Organı, 17, 63-68.

Jenny-Deshusses, C. 1985. *Rectostipulina* n. gen. (= *Stipulina* LYS, 1978), un organisme incertae sedis du Permien supérieur de la Téthys moyen-orientale: description morphologique et remarques stratigraphiques. Revue de Paléobiologie, 4 (1): 153–158.

Jenny-Deshusses, C.1991 The Permian-Triassic Boundary in the Carnic Alps of Austria (Gartnerkofel Region). Abh. Geol. B.-A., 99-108

Jin Yu-gan, Glenister B. F., Kotlyar G. V. and Sheng Jin-zhang.1994. An Operational Scheme of Permian Chronostratigraphy. Paleoworld, Number 4, 1-13.

Johnston G. (1865). A catalogue of the British non-parasitic worms in the collection of the British museum, London.

Karavaeva, N. and Nestell, G. P. 2007. Permian foraminifers of the Omolon Massif northeastern Siberia, Russia. Micropaleontology, 53(3), pp. 161-211.

Knoll, A.H., Bambach, R. K., Jonathan L. Payne, Sara Prussand Woodward W. Fischer 2007. Paleophysiology and end-Permian mass extinction. Earth And Planetary Science Letters , 256(3-4), 295-313.

Kobayashi, F. 1975. *Palaeofusulina-Reichelina* fauna contained in the pebbles of intraformational conglomerate distributed in the Okutama District, West Tokyo. Trans. Proc. Paleont. Soc. Japan, N.S., 100, 220-229.

Kobayashi, F. 1986. Middle Permian foraminifers of the Gozenyema Formations, southern Kwanto Mountains, Japan. Bull. Natn. Sci. Mus., Tokyo, Ser. C, 12(4), 131-163.

Kobayashi, F. 1988. Middle Permian foraminifers of the Omi Limestones, Central Japan. Bull. Natn. Sci. Mus., Tokyo, Ser. C, 14(1), 1-35.

Kobayashi, F. 1997. Upper Permian foraminifers from the Iwai-Kanyo area, west Tokyo, Japan. Journal of Foraminiferal Research, 27(3), 186-195.

Kobayashi, F. 1999. Tethyan uppermost Permian (Dzhulfia and Dorashamian) foraminiferal faunas and their paleogeographic and tectonic implications. Palaeogeography, Palaeoclimatology, Palaeoecology, 150, pp. 279-307.

Kobayashi, F. 2004. Late Permian foraminifers from the limestone block in the southern Chichibu Terrane of west Shikoku, SW Japan. J. Paleont., 78(1), pp. 62-70.

Kobayashi, F. 2005. Permian foraminifers from the Itsukaichi-Ome area, west Tokyo, Japan. J. Paleont., 79 (3), pp. 413-432.

Kobayashi, F. 2006. Early Late Permian (Wuchiapingian) foraminifers in the Tatsuno area, Hyogo-Late Paleozoic and Early Mesozoic foraminifers of Hyogo, Japan, Part 4-.Nature and Human Activites, 10, 25-33.

Kobayashi, F., Altıner, D. 2008a. Fusulinoidean faunas from the Upper Carboniferous and Lower Permian platfrom limestone in the Hadim area, Central Taurides, Turkey. Rivista Italiana di Paleontologia e Stratigrafia, 114, 191-232.

Kobayashi, F., Altiner D. 2008b. Late Carbonifeorus and Early Permian fusulinoideans in the Central Taurides, Turkey: biostratigraphy, and faunal composition and comparison. Journal of Foraminiferal Research, 38(1), 59-73.

Kobayashi, F., Martini, R., , L. 2005. Foraminiferes Anisiens dans les calcaires allochtones de la formation de Tanoura (Terrane de Kurosegawa, Ouest Kyushu, Japon). J. Geobios. 38, pp. 751-763.

Kotlyar, G. V., Zakharov, Y. D. and Polubotko, I.V. 2004. Late Changhsingian fauna of the northwestern Caucasus mountains, Russia. J. Paleont., 78 (3), pp. 513-527.

Kotlyar, G.V., Zakharov, YU.D., Kropacheva, G.S., Pronina, G.P., Chediya, I.O. and Burago, V.I. 1989. ozdnepermskii etap evolyutsii organicheskogo mira, Midinskii yarus SSSR (Evolution of the latest Permian biota, Midian regional stage of the USSR). 177 pp. (in Russian). Leningrad “Nauka”, Leningradskoe Otdelennie. Leningrad.

Kozur, H. W. 1998. Some aspects of the Permian-Triassic boundary (PTB) and of the possible causes for the biotic crisis around this boundary. Palaeogeography, Palaeoclimatology, Palaeoecology, 143, pp. 227-272.

Köylüoğlu, M., Altıner, D. 1989. Micropaleontologie (Foraminiferes) et biostratigraphie du Permien su-perieur de la region d’Hakkari (SE Turquie). Revue de Paleobiologie, 8(2), pp.467-503.

Krainer, K., Vachard, D. 2009. The lower Triassic Werfen formation of the Karawanken Mountains (Southern Austria) and its disaster survivor microfossils, with emphasis on *Postcladella* n. gen. (Foraminifera, Miliolata, Cornuspirida). Revue De Micropaleontologie, 173, 1-27.

Labkovsky, O. O. 2004. Permian fusulinids (foraminifera) of the subsurface of Israel: Taxonomy and biostratigraphy. Revista Espanola de Micropaleontologia, 36(3), pp. 389-406.

Lamarck, J. B. P. A. de, 1818. Histoire naturelle des animaux sans vertèbres. Paris. 5: 1-612.

Lamarck, J.B. 1812. Extrait du cours de Zoologie du Muséum d’Histoire Naturelle sur les animaux invertébrés. 127 pp. D’Hautel Publisher, Paris.

Lange, E. 1925. Eine mittelpermische Fauna von Guguk Bulat (Padanger Oberland, Sumatra). Verhandelingen van het Geologisch-Mijnbouwkunding Genootschap voor Nederland en Kolonien, geologisch serie, **7**: 213-295.

Leven, E. 1998. Permian fusulinids assemblages and stratigraphy of the Trancaucasia. Rivista Italiana di Paleontologia e Stratigrafia, 104 (3), 299-328.

Leven, E., and A. I. Okay. 1996. Foraminifera from the exotic Permo-Carboniferous limestone blocks in the Karakaya Complex, Northwestern Turkey. Rivista Italiana di Paleontologica e Stratigrafia, 102:139-174.

Li, W. Z., Shen, S.Z. 2008. Lopingian (late Permian) brachiopods around the Wuchiapingian-Changhsingian boundary at the Meishan Section C and D. Changxing, South China. Geobios, 41, pp. 307-320.

Likharev, B.K. (ed.) 1939. Atlas of leading forms of the fossil fauna of the USSR. Tsentralnyi Nauchno-Issledovatel’skii Geologo-Razvedochnyi Institut, Leningrad, 6, Permskaya Sistema, 268. (In Russian)

Likharev, B.K. (ed.) 1939. Atlas rukovodyashchikh form iskopaemykh fauna SSSR (Atlas of the leading forms of the fossil fauna of the U.S.S.R). 268 pp. (in Russian). Tsentralnyi Nauchno-issledovatelskii Geologo-razvedochnyi Institut, 6 (Permskaya sistema), Leningrad.

Likharev, B.K. 1926. *Palaeofusulina nana* sp. nov. des depots anthracolithiques du Caucase septentrional. Comm. Geol. Leningard, Bull., 45, 59-66.

Lin, J. 1987. Foraminifera, p. 149-157. In Meng Fassong and Zang Zhenlai (eds.), Biostratigraphy of the Yangtze Gorgr area (4) – Triassic and Jurassic. Geological Publishing House, Beijing. (In Chinese with English summary)

Lin, J., Li, J. and Quanying, S. 1990. Late Paleozoic foraminifera in South China. Science Publishing House, Beijing, 297 p. (In Chinese with English summary)

Lin, J.X. 1978. Carboniferous and Permian Foraminiferida. In: Paleontological Atlas of Central South China (micropaleontological volume). Hubei Institute of Geological Science and others Eds. pp. 10-43 (in Chinese). Geological Publishing House, Beijing.

Lin, J.X. 1984. Biostratigraphy of the Yangtze Gorge area, (3) Late Paleozoic era. pp. 110-117 (in Chinese), pp. 323-364 (in English). Museum Changzhou, Changzhou City, Jiangsu Province. Geological Publishing House, Beijing.

Lin, J.X., Li, L.X. and Sun Q.Y. 1990. Late Paleozoic foraminifers in South China. (in Chinese). Science Publication House, Beijing, 269 pp.

Linné, C. von. 1758. Systema Naturae, 1, 10th edition, Holmiae, L. Salvii, Stockholm.

Loeblich, A.R. and Tappan, H. 1984. Suprageneric classification of the Foraminiferida (Protozoa). Micropaleontology, 30 (1): 1-70.

Loeblich, A.R., Jr., and H. Tappan. 1964. Foraminiferal Classification and Evolution. Journal of the Geological Society of India 5:5-39.

Loriga, C.V. 1960. Foraminiferi del Permiano superiore dele Dolomiti (Val Gardena, Val Badia, Val Marebbe). Bollettino della Società Paleontologica Italiana, 1 (1): 33–73.

Lys, M. and Marcoux, J. 1978. Les niveaux du Permien superieur des Nappes d’Antalya (Taurides occidentales, Turquie). Comptes Rendus Academie Sciences Paris, 286, serie D, 1417–1420.

Lys, M., Colchen, M., Bassoullet, J.P., Marcoux, J. & Mascle, G. 1980. La biozone à *Colaniella parva* du Permien supérieur et sa microfaune dans le bloc calcaire exotique de Lamayuru, Himalaya du Ladakh. Revue de Micropaléontologie, 23 (2), 76-108.

Lys, M., Stampfli, G. and Jenny, J. 1978. Biostratigraphie du Carbonifère et du Permien de l’Elbourz oriental (Iran du NE). Notes Laboratoire Paléontologie Université Genève, 2: 63–99.

Mamet, B. and Pinard, S. 1992. Note sur la taxonomie des petits foraminifères du Paléozoïque supérieur. Bulletin de la Société belge de Géologie, 99 (imprinted 1990): 373-398.

Mamet, B. and Pinard, S. 1996. *Nodosinelloides potievskayae*, nomen novum (foraminifère). Revue de Micropaléontologie, 39: 223.

Marquez, L. 2005. Foraminiferal fauna recovered after the Late Permian extinctions in Iberia and the westernmost Tethys area. Palaeogeography, Palaeoclimatology, Palaeoecology, 229, pp. 137-157.

Martini, R. and Zaninetti, L. 1988. Structure et paleobiologie du foraminifere *Lasiodiscus* Reichel, 1946: etüde d'apres le materiel-type de permien superieur de Grece. Revue de Paleobiologie, 7(2), 289-300.

Miklukho- Maklay, K.V. 1954. Foraminifers from the Upper Permian deposits of the northertn Caucasus. Trudy Vsesoyuznogo Nauchno-Issledovatel'skogo Geologichekogo İnstuta (VSEGEI), Ministerstva Geologii i Okhrani Nedr, 163 (In Russian).

Miklukho-Maklay, A.D. 1953. K sistematike semeitsva Archaediscidae (On the systematics of the family Archaediscidae). Ezhegodnik Vsesoyuznogo Paleontologischeskogo Obshchestva (1948-1953), 14: 127-131 (in Russian).

Mithchum, R. M., Vail, P. R. and Thomson, S. 1977. Seismic stratigraphy and global changes of sea level, part 2: The depositional sequences as a basic unit of for stratigraphic analysis. Applications to Hydrocarbon Exploration: Association of Petroleum Geologist Memoir, 26, 53-62.

Mohtat-Aghai, P. and Vachard, D. 2003. *Dagmarita shahrezaensis* n. sp. Globivalvulinid foraminifer (Wuchiapingian, Late Permian, Central Iran). Rivista Italiana di Paleontologica e Stratigrafia, 109(1), 37-44.

Mohtat-Aghai, P., Vachard, D. 2005. Late Permian foraminiferal assemblages from the Hambast Region (Central Iran) and their extinctions. Revista Espanola de Micropaleontologia, 37(2), pp.205-227.

Monod, O. 1967. Presence d'une faune Ordovicienne dans les schistes de Seydişehir ala base des calcaries du Taurus occidental. MTA Bul., 69, 79-89.

Monod, O. 1977. Recherches géologiques dans le Taurus occidental au Sud de Beysehir (Turquie). These, Université de Paris-Sud, Centre d'Orsay, 442.

Nestell, G. P. and Nestell, M. K.. 2006 Late Capitanian foraminifers from Dark Canyon, Guadalupe Mountains, New Mexico. Micropaleontology, v. 52, p. 1-50.

Nestell, M.K. and Pronina, G.P. 1997. The distribution and age of the genus *Hemigordiopsis*. In: Late Paleozoic Foraminifera; their biostratigraphy, evolution, and paleoecology; and the Mid-Carboniferous boundary. Ross, C.A., Ross, J.R.P. and Brenckle, P.L. Eds., Cushman Foundation for Foraminiferal Research Special Publication, 36 (3), Washington, 105– 110

Neumayr, M., 1887. Über Trias und Kohlenkalkversteinerungen aus dem westlichen Kleinasien Anz. Kais. Akad. Wiss. v. 24, pp. 241-243

Noé, S. 1988. Foraminiferal ecology and biostratigraphy of the marine Upper Permian and of the Permian–Triassic boundary in the southern Alps (Bellerophon Formation, Tesero Horizon). Revue de Paléobiologie, Benthos '86, Spécial Volume 2:75–88.

Noé, S.U. 1987. Facies and paleogeography of the marine Upper Permian and of the Permian-Triassic boundary the southern Alps (Bellerophon Formation, Tesero Horizon). Facies, 16: 89-142.

Okimura, Y. 1988 Primitive colaniellid foraminiferal assemblage from the upper permian Wargal Formation of the Salt Range, Pakistan. J. Paleont., 62(5), 715-723.

Okimura, Y., Ishii K. 1981. Upper Permian and Lower Triassic foraminifera from Guryul Ravine and the spur three kilometers North of Barus. In K. Nakazawa and H.M. Kapoor (eds.), The Upper Permian and Lower Triassic Faunas of Kashmir. Memoirs of the Geological Survey of India, Paleontologia Indica, n. s., 46., p. 25-29.

Okimura, Y., Ishii K., K. Nakazawa, 1975. *Abadehella*, a new genus of tetrataxid foraminifera from the Late Permian. Memoirs of the Faculty of Science, Kyoto University, series of Geology and Mineralogy, 41:35-48.

Okuyucu, C. 1999. A new *Multidiscus* ? species (Foraminifera) from a Fusulinacean-rich succession encompassing the Carboniferous – Permian boundary in the Hadim Nappe (Central Taurus, Turkey) . Rivista Italiana di Paleontologia e Stratigrafia, 105(3), 439 -444.

Oravecz-Scheffer A. 1987. Triassic Foraminifers of the Transdanubian Central Range. Geologica Hungarica Paleontol., 50, 3-134.

Orlov-Labkovsky, O. 2004. Permian fusulinids (foraminifera) of the subsurface of Israel: taxonomy and biostratigraphy. Revista Española de Micropaleontología, 36(3), 389-406.

Ota, A., Isozaki, Y. 2006. Fusuline biotic turnover across the Guadalupian-Lopingian (Middle-Upper Permian) boundary in mid-oceanic carbonate buildups: Biostratigraphy of accreted limestone in Japan. Journal of Asian Earth Sciences, 26, pp. 353-368.

Özgül, N. 1971. Orta Torosların kuzey kesiminin yapısal gelişiminde blok hareketlerinin önemi. Türkiye Jeol. Kur. Bült., 14, 75-87.

Özgül, N. 1976. Some geological aspects of the Taurus oragenic belt (Turkey). Bulletin of the Geological Society of Turkey, 19, 65-78.

Özgül, N. 1984. Stratigraphy and tectonic evolution of the Central Taurides. In. Tekeli O. and Göncüoğlu M. C. (eds), Geology of the Taurus Belt. Mineral Research and Exploration Institute of Turkey Publication, 77-90.

Özgül, N. 1997. Stratigraphy of the tectono-stratigraphic units in the region Bozkır Hadim-Taşkent (northern central Taurides). Mineral Research and Exploration Institute of Turkey (MTA) Bulletin, 119, 113-174.

Özgül, N. ve Gedik, İ. 1973. Orta Toroslar'da Alt Paleozoyik yaşta Çaltepe Kireçtaşı ve Seydişehir Formasyonu'nun stratigrafisi ve konodont faunası hakkında yeni bilgiler. Türkiye Jeoloji Kurumu Bülteni, 16, 39-52.

Pantić, S. 1969: Litostratigrafske i mikropaleontološke karakteristike srednjeg i gornjeg perma zapadne Srbije (Caracteréstiques lithostratigraphiques et micropaléontologiques du Permian moyen et supérieur de la Serbie occidentale). — Vesnik zavod za geološka i geofizička istraživanja Seria A 27,. 201-211.

Payne, J.L., Lehrmann, D.J., Follett, D., Seibel, M., Kump, L.R., Riccardi, A., Altiner, D., Sano, H., and Wei, J. 2007. Erosional truncation of uppermost Permian shallow-marine carbonates and implications for Permian-Triassic boundary events: Geological Society of America Bulletin, v. 119, p. 771– 784.

Poisson, A. 1977. Recherches Geologiques dans les Taurides occidentales (Turquie). Ph.D. Thesis L'Universite de Paris-Sud (centre D'orsay). 394p.

Posamentier, H.W., Vail, P.R. 1988. Eustatic controls on clastic deposition. II. Sequence and systems tract models. In: Wilgus, C.K., Hastings, B.S., Kendall, C.G.St.C., Posamentier, H.W., Ross, C.A., Van Wagoner, J.C. (Eds.), Sea Level Changes An Integrated Approach, vol. 42. SEPM Special Publication, pp. 125– 154.

Pronina, G.P. 1988. The Late Permian smaller foraminifers of Transcaucasus. Revue de Paléobiologie, Benthos'86 spécial volume, 2, 89-96.

Pronina, G.P. 1989. Foraminifers from the *Paratirolites kittli* Zone, Dorashamian stage of the Late Permian, Transcaucasia. Ezhegodnik Vsesoyuznogo Paleontologicheskogo Obshchestva, 32: 30-42 (In Russian).

Pronina-Nestell, G.P., Nestell, M.K. 2001. Late Changhsingian foraminifers of the northwestern Caucasus. Micropaleontology, 47(3), 205-234.

Pütürgeli, E. 2002. Meter-scale shallowing upward cycles in the Midian (Upper Permian) strata (Central Taurides, Turkey). M.Sc. Thesis, Middle East Technical University, Ankara, Turkey, 103 p. (unpublished).

Ramovs, A. 1986. Marine development of the Upper Permian in the type of Karavanke Mountains and the Scythian. In: Permian and Permian-Triassic boundary in the South Alpine segment of the western Tethys. Editors Italian IGCP 203 Group Members, Excursion Guidebook, 43-53.

Rampino, M. R., Adler, A.C. 1998. Evidence for abrupt latest Permian mass extinction of foraminifera: Result of tests for the Signor- Lipps effect. Geology, 26(5), 415-418.

Rauzer-Chernousova, at all.. 1996. Spravochnik po sistematike foraminifer Paleozoya; Endothyroidy, Fuzulinoidy (Reference-book on the systematics of Paleozoic foraminifers; Endothyroida and Fusulinoida). 207 pp. (in Russian). Rossiiskaya Akademiya Nauk, Geologicheskii Institut, Moskva “Nauka”.

Rauzer-Chernousova, D.M., Bensh, F.R., Vdovenko, M.V., Gıbshman, N.B., Leven, E.YA., Lipina, O.A., Reitlinger, E.A., Solovieva, M.N. & Chediya, I.O. 1996. Spravochnik po sistematike foraminifer Paleozoya Endothyroidy, Fuzulinoidy (Reference-book on the systematics of Paleozoic foraminifers; Endothyroida and Fusulinoida). (in Russian). Rossiiskaya Akademiya Nauk, Geologicheskii Institut, Moskva “Nauka”. 207 pp.

Reichel, M. 1945. Sur un Miliolidé nouveau du Permien de l’île de Chypre. Verhandlungen der Naturforschenden Gesellschaft in Basel, 56 (2): 521-530.

Reichel, M. 1946. Sur quelques foraminiferés nouveaux du Permien méditerranéen. Eclogae Geologicae Helvetiae, 38 (2), 524-560.

Reitlinger, E. A. 1959. Atlas of microscopic fossils and problematics of ancient strata of Siberia. Izd. Akad. Nauk. SSSR Moscow, 25: 1-63 (In Russian).

Reitlinger, E. A. 1965. Evolution of foraminifers in the latest Permian and earliest Triassic epochs of the Transcaucasus. Akademiya Nauk SSSR, Otdelenie Nauk o Zemle, Geologicheskii Institut, Sistematika i Filogeniya Foraminifer i Ostrakod, Voprosy Mikropaleontologii, 9, 45-70. (In Russian)

Rettori, R. (1995). Foraminiferi del Trias inferiore e medio della Tetide: Revisione tassonomica, stratigrafia ed interpretazione filogenetica. Université de Genéve, Publications du Département de Géologie et Paléontologie, 18, 147 p.

Rettori, R. 1994. Replacement name *Hoyenella* gen. n. (Triassic Foraminiferida, Miliolina) for *Glomospira sinensis* Ho, 1959. Bolletino Societá Paleontologica Italiana, 33 (3): 341-343.

Revets, A. S. 2005. A key to unilocular hyaline foraminifera. Journal of Micropaleontology, 24, 145-158.

Sakagami, S. and A. Hatta. 1982. On the Upper Permian *Palaeofusulina-Colaniella* fauna from Khao Doi Pha Phlung, North Thailand. Geology and Paleontology of Southeast Asia, 24: 1-14.

Sarg, J. F., 1988. Carbonate sequence stratigraphy. In: Sea-level Changes: An integrated approach. Wilgus, C. K., Hastings, B. S. et al. (eds.), The Society of Economic Paleontologist and Mineralogist, Special Publication, 42, 155-181.

Schellwien, E. 1898. Upper Pennsylvanian Faunas in the Carnic Alps: Paleontographica 44: 237-282.

Schubert R.J. 1908. Zur Geologie des Osterreichischen Velebit. Jahrbuch der Geologischen Reichsanstalt 58: 345-386.

Schubert, R.J. 1921. Palaeontologische Daten zur Stammesgeschichte der Protozoen. Palaeontologische Zeitschrift, 3 (1920) (2): 129–188.

Sellier De Civrieux, J.M. and Dessauvagie, T.F.J. (1965). Reclassification de quelques Nodosariidae, particulièrement du Permien au Lias. Maden Tetkik ve Arama Enstitüsü Yayinlarindan (M.T.A.), 124, 1-178.

Sheng, J. C. 1963. Permian fusulinids of Khangsi, Kueichow and Szechhuan. Paleontologica Cínica, N.S.B., 149 (10), 11-247.

Sheng, J.C. and Chang, L.X. 1958. Fusulinids from the type locality of the Changhsing Limestone. Acta Paleontologica Sinica, 6 (2): 205-214.

Sheng, J.C., 1955., Some fusulinids from Changhsing Limestone. Acta Palaeontologica Sinica, 3, no:4, 305.

Sloss, L. L. 1963. Sequences in the cratonic interior of North America. Geological Society of America Bull. 74, 93-114.

Song, H. J., Tong, J. , Chen, Z. Q.,Yang, H. and Wang, Y. 2009. End-Permian mass extinction of foraminifers in the Nanpanjiang Basin, south China. J. Paleont., 83(5), 718-738.

Song, H. J., Tong, J. N., Zhang, K. X., Wang, Q. X.,Chen, Z. Q. 2007. Foraminiferal survivors from the Permian-Triassic mass extinction in the Meishan section, South China. Palaeoworld, 16, pp. 105-119.

Songzhu, G., Qinglai, F., Weihong, He. 2007. The last Permian deep-water fauna: Latest Changhsingian small foraminifers from southwestern Guangxi, South China. Micropaleontology, 53(4), 311-330.

Stanley, S.M. and Yang, X.N. 1994. A double mass extinction at the end of the Paleozoic Era. Science 266: 1340–1344.

Strasser, A. 1988. Shallowing-upward sequence in Purbeckian peritidal carbonates (Lowermost Createaceous, Swiss and French Jura mountains). Sedimentology, 35, 369-383.

Strasser, A., Pittet, B., Hillgärtner, H., Pasquier, J.B. 1999. Depositional sequences in shallow carbonate-dominated sedimentary systems: concepts for a high-resolution analysis. Sediment Geol., 128, 201-221.

Şen, A., 2002, Meter-scale subtidal cycles in the Middle Carboniferous of Central Taurides, Southern Turkey and response of fusulinacean foraminifers to sedimentary cyclicity, M.Sc. Thesis, Middle East Technical University, Ankara, Turkey, 121 p.

Şenel, M. 1999. Stratigraphic and tectonic features of the tecnostratigraphic units in the Taurus Belt, and the redefinition of these units. Proceeding of the 52nd Geological Congress of Turkey, 376-378.

Thompson, M.L. and Foster, C.L. 1937. Middle Permian fusulinids from Szechuan, China. Journal of Paleontology, 11 (2): 126-144.

Trifonova, E. 1993. Taxonomy of Bulgarian Triassic Foraminifera. III. Families Endothyridae to Oberhauserellidae. Geol. Balc. 24 (2), 21-70.

Ueno, K. 1992. Permian foraminifers from the Takakuruyama Group of the southern Abakuma Mountains, Northeast Japan. Trans. Proc. Paleont. Soc. Japan, 168, 1265-1295.

Ünal, E. 2002. Cyclic sedimentation across the Permian-Triassic boundary (Central Taurides, Turkey). M.Sc. Thesis, Middle East Technical University, Ankara, Turkey, 139p. (unpublished).

Ünal, E., Altıner, D., Yılmaz, İ. Ö., and Özkan-Altıner, S. 2003. Cyclic sedimentation across the Permian-Triassic boundary (Central Taurides, Turkey). Rivista Italiana di Paleontologia e Stratigrafia, 109, N. 2, 359-376.

Vachard, D. and Colinn, J.P. 1994. Etude micropaleontologique et palynologique du “Muschelkalk” de Minorque (Trias, Iles Baléares, Espagne, et precision sur la systematique des involutinides (foraminifères). Revue de Paléobiologie, 13, 235-257.

Vachard, D. and Ferriere, J. 1991. An assemblage with *Yabeina* (fusulinid foraminifer) from the Midian (Upper Permian) of Whangaroa area (Orua Bay, New Zealand). Revue de Micropaleontologie, 31(3), 201-230.

Vachard, D. and Montenat, C. 1981. Biostratigraphie, micropaléontologie et paléogéographie du Permien de la région de Tezak (Montagnes Centrales d’Afghanistan). Palaeontographica B, 178 (1-3): 1-8.

Vachard, D., Gaillot, J., Pıile, L. & Blazejowski, B. 2006. Problems on Biseriamminoidea, Mississippian-Permian biserially coiled Foraminifera, a reappraisal with proposals. Revista Española de Micropaleontología, 38 (2-3), 453-492.

Vachard, D., Rettori, R., Angiolini, L. and Checconi, A. 2008. *Glomomidiella* gen. n. (foraminifera, miliolata, neodiscidae): A new genus the Late Guadalupian-Lopingian of Hydra Island (Greece). Rivista Italiana di Paleontologica e Stratigrafia, 114(3), 349-361.

Vachard, D., Zambetakis-Lekkas, A., Skourtsos, E., Martini, R., Zaninetti, L. 2003. Foraminifera, Algae and carbonate microproblematica from the late Wuchiapingian/Dzhulfian (Late Permian) of Peloponnesus (Greece). Rivista Italiana di Paleontologia e Stragrafia, 109, pp. 339-358.

Vail, P. R. 1975. Eustatic cycles from seismic data for global stratigraphic analysis (abstract). American Association of Petroleum Geologists Bulletin, 59, 2198-2199.

Vail, P. R., Mitchum, R. M. and Thompson, S. 1977. Seismic stratigraphy and global changes of sea level, Part 4: Global cycles of relative changes of the sea level, in Payton, C. E., eds., seismic stratigraphy. Application to Hydrocarbon Exploration. Am. Association of Petroleum Geologist Memoir, 26, 83-97.

Van Wagoner, J.C., Posamentier, H.W., Mitchum, R.M., Vail, P.R., Sarg, J.F., Loutit, T.S., Hardenbol, J., 1988. An overview of sequence stratigraphy and key definitions. In: Wilgus, C.K., Hastings, B.S., Kendall, C.G.St.C., Posamentier, H.W., Ross, C.A., Van Wagoner, J.C. (Eds.), Sea Level Changes-An Integrated Approach, vol. 42. SEPM Special Publication, 39-45.

Vuks, G.P. and Chediya, I.O. 1986. Foraminifery lyudyanzinskoi svity bukhty neizvestnaya (Yuznnoe Primorye) [Foraminifers from the Lyudyansk Suite (southern Primoye)]. In: Korrelyatsiya Permo-Triasovykh otlozhenii Vostoka SSSR (Correlations of Permian-Triassic deposits of Eastern USSR). Academy of Sciences

USSR, Far-Eastern Scientific Centre, Institute of Biology and Pedology, Project IGCP no. 203: 82-88 (in Russian).

Wang, K. 1986. Lower Permian foraminiferal fauna from Xainza of Xizang, Bulletin of the Nanjing Institute of Geology and Palaeontology, Academia Sinica, 10, 123-140. (In Chinese with English summary)

Wang, Y. and Ueno, K. 2009. A new fusulinoidean genus *Dilatofusulina* from the Lopingian (Upper Permian) of southern Tibet, China. Journal of Foraminiferal Research, 39(1), 56-65.

Wang, Y., Ueno, K., Zhang, Y. and Cao, C. Q. 2010. The Changhsingian foraminiferal fauna of a Neotethyan seamount: the Gyanyima limestone along the Yarlung-Zangbo Suture in southern Tibet, China. Geological Journal, 45, pp. 308-318.

Warthin, A.S. 1930. Micropaleontology of the Wetumka, Wewoka, and Holdenville formations. Oklahoma Geological Survey Bulletin, 53: 32-34.

Warthin, A.S. 1930. Micropaleontology of the Wetumka, Wewoka, and Holdenville formations. Oklahoma Geological Survey Bulletin, 53: 32-34.

Whittaker, J.E., Zaninetti, L. and Altıner, D. 1979. Further remarks on the micropaleontology of the late Permian of Eastern Burma. Notes du Laboratoire de Paleontologie de L'Universite de Geneve, 5, 11-21.

Wignall, P.B. and Hallam, A. 1996. Facies change and the end-Permian mass extinction in S.E. Sichuan, China. Palaios, 11, 587-596.

Wignall, P.B., Hallam, A. 1999. Mass extinctions and sea-level changes. Earth-Science Reviews, 48, pp. 217-250.

Wilson, J. L. 1975. Carbonate facies in geologic history. Springer- Verlag, New York, 469.

Wolanska, H., 1959. *Agathammina pusilla* (Geinitz) z dolnego Cechztynu Sudetow i Gor Swietokrzyskich. Acta Palaeontologica Polonica, 4(1):27-59. (in Polish.)

Yılmaz, 2002. Applications of cyclostratigraphy and sequence stratigraphy in determination of the hierarchy in peritidal and pelagic successions (NW, SW and WNW of Turkey) by using sedimentology and sedimentary geochemistry Ph.D. Thesis M.E.T.U., Ankara, Turkey, 248 p., (unpublished).

Yılmaz, İ. Ö. 1997. Sequence stratigraphy and dasyclad algal taxonomy in the Upper Jurrasic (Kimmeridgian) – Upper Cretaceous (Cenomanian) peritidal carbonates of the Fele area, Western Taurides, Turkey. M.Sc. Thesis, M.E.T.U., Ankara, Turkey, 223 p. (unpublished).

Yılmaz, İ. Ö. and Altıner D. 2001. Use of sedimentary structures in the recognition of sequence boundaries in the Upper Jurassic (Kimmeridgian) - Upper Cretaceous (Cenomanian) peritidal carbonates of the Fele (Yassıbel) area (Western Taurides, Turkey). International Geological Review, 43, 8, 736-753.

Yin H., Wu, S., Din M., Zhang, K., Tong, J. and Yang F. 1994. The Meishan section and point (GSSP) of the Permian-Triassic Boundary (PTB). Albertina, 14, 15-31.

Yin H., Yang F., Zhang K. and Yang W. 1986. A proposal to the biostratigraphic criterion of Permian/Triassic boundary. Memorie della Societa Geologica Italiana, 34, 329–344.

Yin, H. and Tong, J. 1998. Multidisciplinary high-resolution correlation of the Permian-Triassic boundary. Palaeogeography, Palaeoclimatology, Palaeoecology, 143(4), 199-212.

Yin, H., Feng, Q., Lai, X., Baud, A., Tong, J. 2007. The protracted Permo-Triassic crisis and multi-episode extinction around the Permian-Triassic boundary. Global and Planetary Change, 55, pp. 1-20.

Yin, H., Zhang, K., Tong, J., Yang, Z., Wu, S. 2001. The global stratotype section and point (GSSP) of the Permian-Triassic boundary. Episodes, 24(2), 102-114.

Yue, W. Shuzhong, S., Changqun, C., Wei, W., Herderson, C., Yugan, J. 2006. The Wuchiapingian-Changhsingian boundary (UpperPermian) at Meishan of Changxing County, South China. Journal of Asian Earth Sciences, 26, pp. 575-583.

Zaninetti, L. and Altıner, D. 1981. Les biseriamminidae (Foraminiferes) dans le Permien supérieur mésogéen: évolution et biostratigraphie. Notes du Laboratoire de Paleontologie de L'Universite de Geneve, 7/2, 39-47.

Zaninetti, L., Altıner, D. and Çatal, E. 1981. Foraminiféres et biostratigraphie dans le Permien supérieur du Taurus oriental, Turquie. Notes du Laboratoire de Paleontologie de L'Universite de Geneve, 7, 1-37.

Zaninetti, L., Brönnimann, P., Huber, H. and Moshtaghian, A. 1978. Microfaciès et microfaunes du Permien au Jurassique au Kuh-e Gahkum, Sud-Zagros, Iran. Rivista Italiana di Paleontologia, 84 (4): 865-896.

Zhao et Al. 1981. The Changhsingian and Permian-Triassic boundary of South-China. Bulletin Nanjing Institute Geology and Paleontology, Academia Sinica, 2 (4), 58-69 (in Chinese with English abstract).

Zolotova, V.P., Baryshnikov, V.V., 1980. Foraminifers from the stra- totype area of the Kungurian Stage. Akademiya Nauk SSSR, Ural'skii Nauchnyi Tsentr, pp. 72-105.

APPENDIX

EXPLANATION OF PLATES

PLATE I

Figure 1: *Nodosinelloides sagitta*, sample no: AH-44, X4

Figure 2: *Nodosinelloides sagitta*, sample no: AH-59, X10

Figure 3: *Nodosinelloides sagitta*, sample no: AH-44, X10

Figure 4: *Nodosinelloides sagitta*, sample no: AH-61, X20

Figure 5: *Nodosinelloides sagitta*, sample no: AH-59, X10

Figure 6: *Nodosinelloides sagitta*, sample no: AH-72, X10

PLATE I

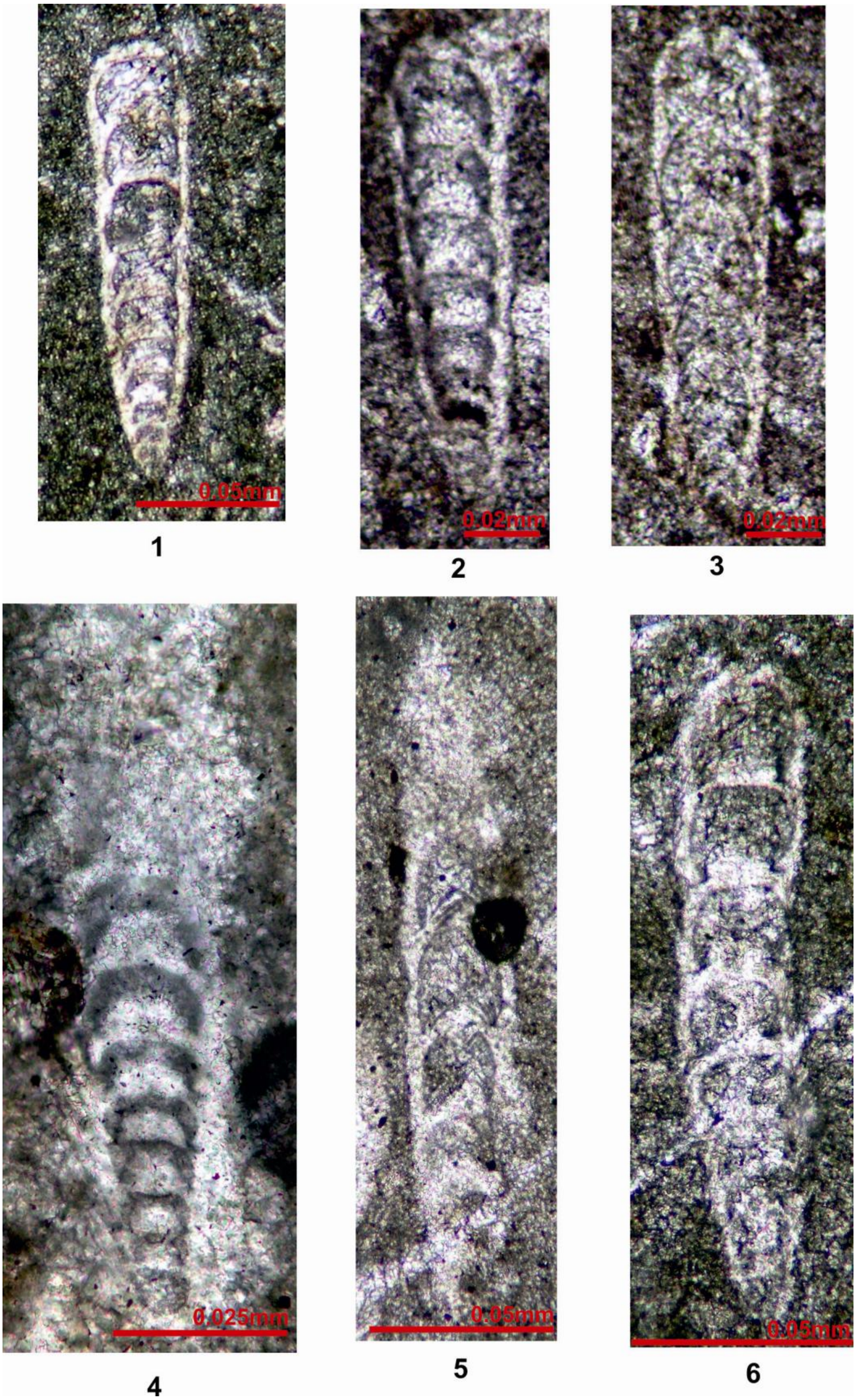

PLATE II

Figure 1: *Nodosinelloides sagitta*, sample no: AH-67, X10

Figure 2: *Nodosinelloides sagitta*, sample no: AH-72, X4

Figure 3 *Nodosinelloides sagitta*, sample no: AH-33, X4

Figure 4: *Nodosinelloides sagitta*, sample no: AH-58, X10

Figure 5 *Nodosinelloides sagitta*, sample no: AH-59, X10

Figure 6: *Nodosinelloides sagitta*, sample no: AH-29, X10

Figure 7: *Nodosinelloides sagitta*, sample no: AH-30, X10

Figure 8: *Nodosinelloides sagitta*, sample no: AH-53, X10

Figure 9: *Nodosinelloides sagitta*, sample no: AH-30, X4

Figure 10: *Nodosinelloides sagitta*, sample no: AH-62, X10

Figure 11: *Nodosinelloides sagitta*, sample no: AH-25, X10

Figure 12: *Nodosinelloides sagitta*, sample no: AH-58, X10

Figure 13: *Nodosinelloides sagitta*, sample no: AH-54, X10

Figure 14: *Nodosinelloides sagitta*, sample no: AH-33, X10

PLATE II

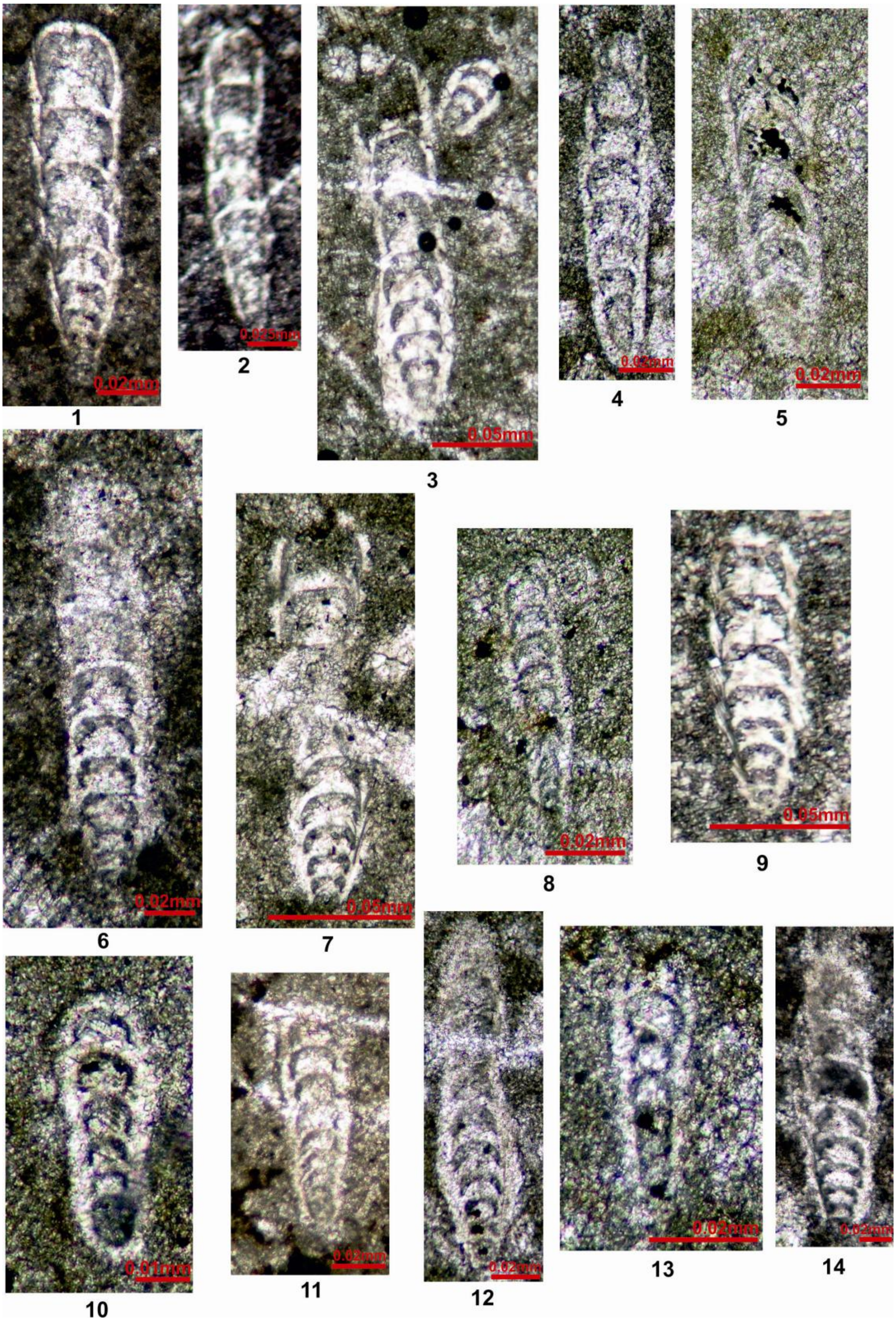

PLATE III

Figure 1: *Nodosinelloides camerata*, sample no: AH-34, X10

Figure 2: *Nodosinelloides camerata*, sample no: AH-34, X20

Figure 3: *Nodosinelloides camerata*, sample no: AH-34, X10

Figure 4: *Nodosinelloides camerata*, sample no: AH-34, X10

Figure 5: *Nodosinelloides camerata*, sample no: AH-34, X10

Figure 6: *Nodosinelloides camerata*, sample no: AH-34, X20

Figure 7: *Nodosinelloides camerata*, sample no: AH-28, X10

Figure 8: *Nodosinelloides camerata*, sample no: AH-28, X10

Figure 9: *Nodosinelloides camerata*, sample no: AH-93, X10

Figure 10: *Nodosinelloides camerata*, sample no: AH-93, X10

Figure 11: *Nodosinelloides camerata*, sample no: AH-93, X10

Figure 12: *Nodosinelloides camerata*, sample no: AH-93, X10

PLATE III

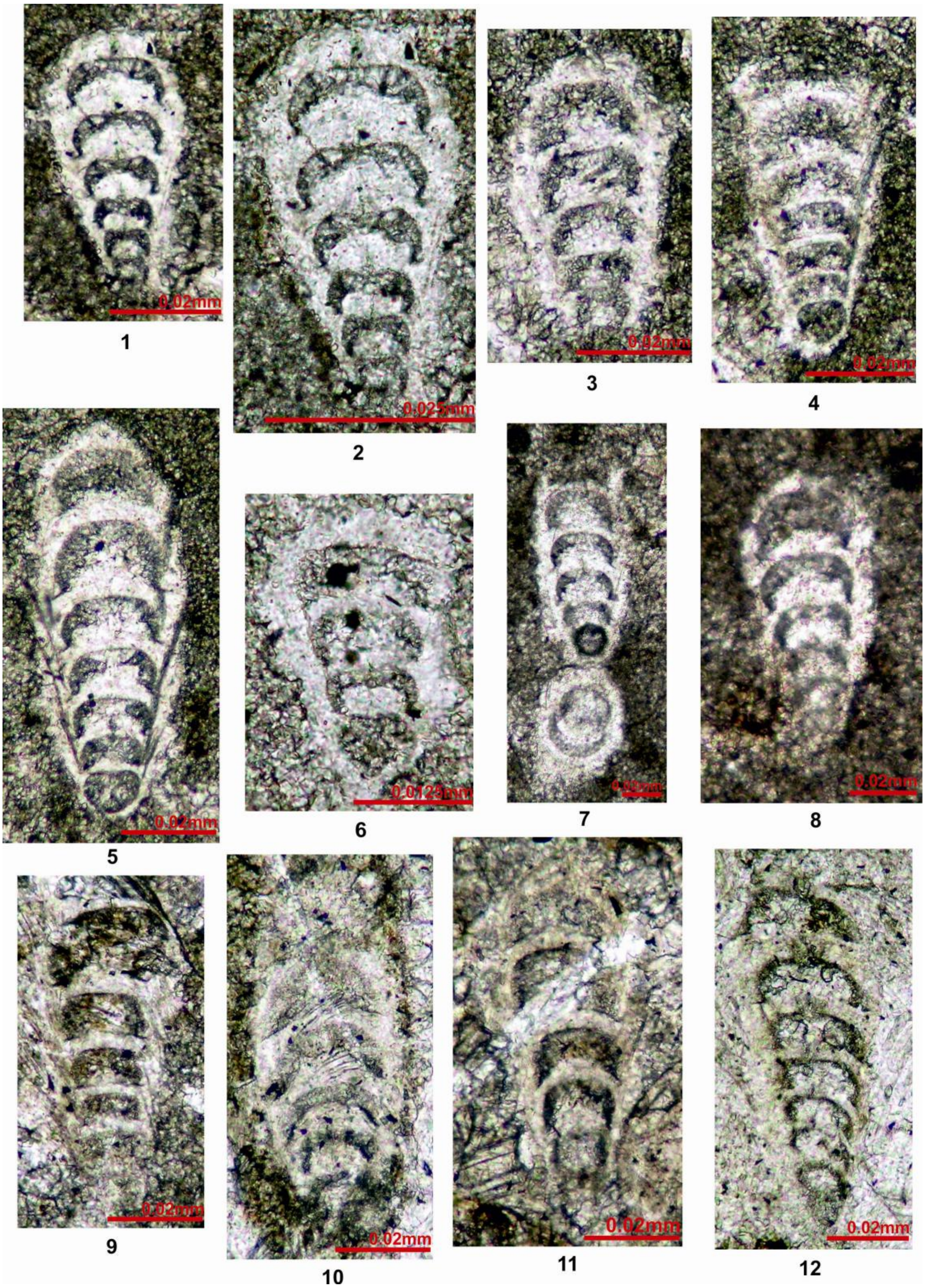

0.02mm
1
0.025mm
2
0.02mm
3
0.02mm
4
0.02mm
5
0.0125mm
6
0.02mm
7
0.02mm
8
0.02mm
9
0.02mm
10
0.02mm
11
0.02mm
12

PLATE IV

Figure 1: *Pachyphloia schwageri*, sample no: AH-32, X10

Figure 2: *Pachyphloia ovata,* sample no: AH-9, X10

Figure 3: *Pachyphloia ovata,* sample no: AH-63, X10

Figure 4: *Pachyphloia ovata,* sample no: AH-9, X10

Figure 5: *Pachyphloia ovata,* sample no: AH-9, X10

Figure 6: *Pachyphloia ovata,* sample no: AH-9, X10

Figure 7: *Pachyphloia ovata,* sample no: AH-9, X10

Figure 8 *Pachyphloia* sp.*,* sample no: AH-93, X10

Figure 9: *Pachyphloia ovata,* sample no: AH-93, X10

Figure 10: *Pachyphloia* sp.*,* sample no: AH-34, X4

Figure 11: *Geinitzina araxensis,* sample no: AH-25, X10

PLATE IV

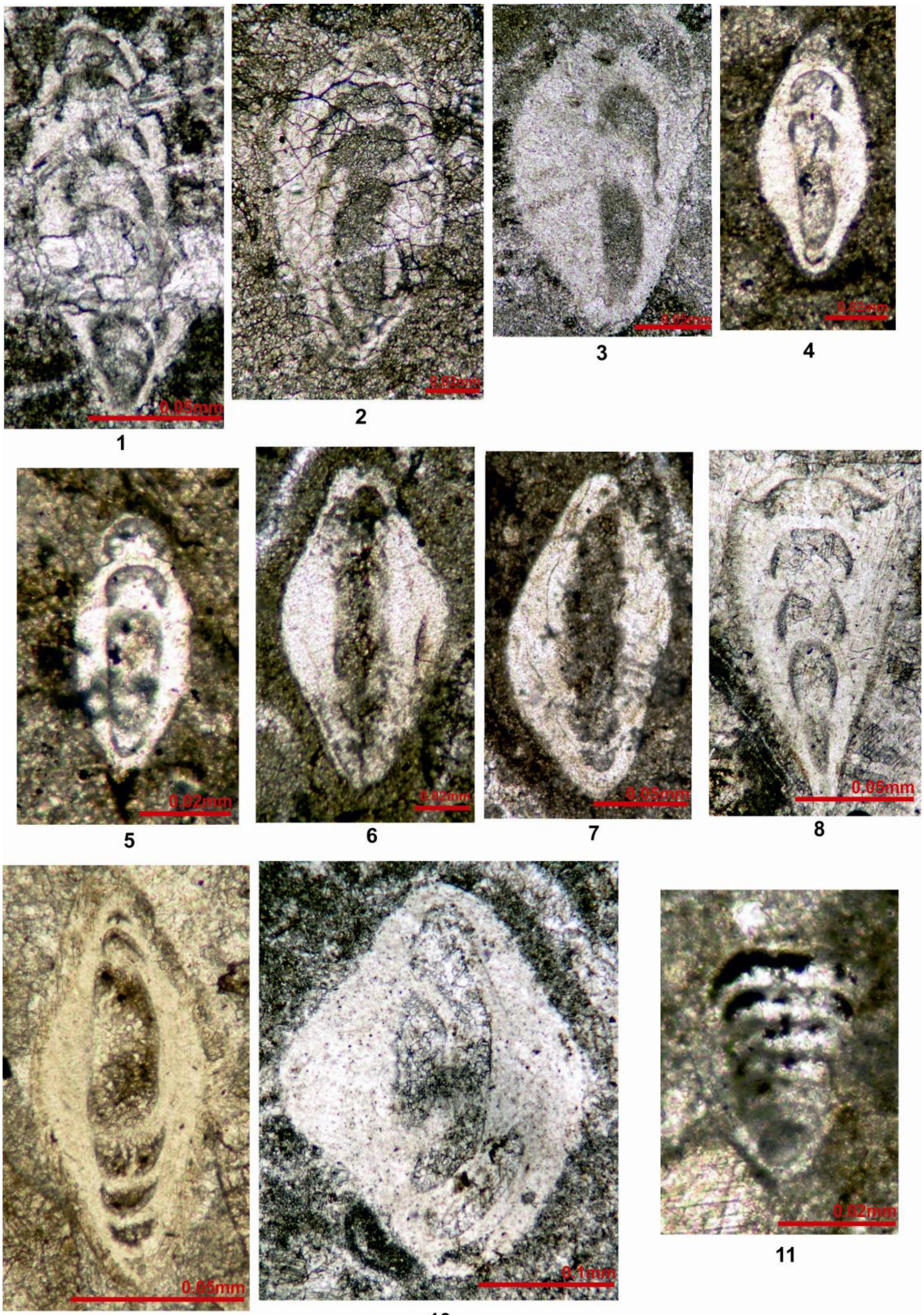
0.05mm
1
0.02mm
2
0.05mm
3
0.02mm
4
0.02mm
5
0.02mm
6
0.05mm
7
0.05mm
8
0.05mm
9
0.1mm
10
0.02mm
11

PLATE V

Figure 1: *Geinitzina araxensis*, sample no: AH-2, X10

Figure 2: *Geinitzina araxensis* sample no: AH-44, X10

Figure 3: *Geinitzina araxensis*, sample no: AH-44, X10

Figure 4: *Geinitzina araxensis*, sample no: AH-93, X10

Figure 5: *Frondina permica*, sample no: AH-2, X10

Figure 6: *Frondina permica*, sample no: AH-25, X10

Figure 7: *Frondina permica*, sample no: AH-61, X20

Figure 8: *Frondina permica*, sample no: AH-43, X10

Figure 9: *Frondina permica*, sample no: AH-20, X10

Figure 10: *Frondina permica*, sample no: AH-29, X10

Figure 11: *Pseudolangella* sp., sample no: AH-2, X10

Figure 12: *Langella* ? sp., sample no: AH-34, X10

Figure 13: *Langella perforata*, sample no: AH-34, X4

Figure 14: *Cryptomorphina limonitica*, sample no: AH-32, X4

Figure 15: *Cryptomorphina limonitica*, sample no: AH-46, X4

Figure 16: *Calvezina ottomana*, sample no: AH-46, X4

PLATE V

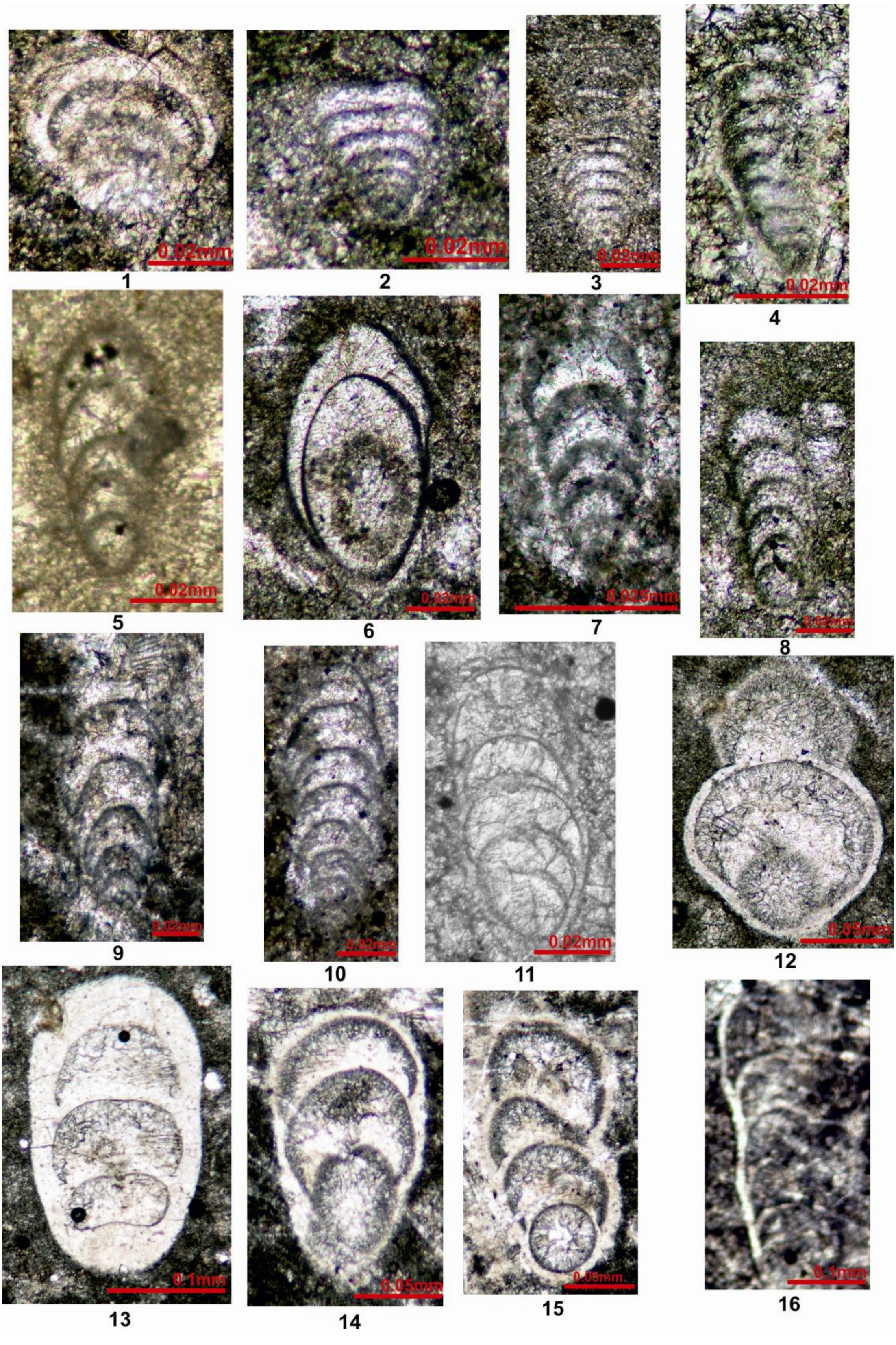

0.02mm
1
0.02mm
2
0.02mm
3
0.02mm
4
0.02mm
5
0.02mm
6
0.025mm
7
0.02mm
8
0.02mm
9
0.02mm
10
0.02mm
11
0.05mm
12
0.1mm
13
0.05mm
14
0.05mm
15
0.1mm
16

PLATE VI

Figure 1: *Calvezina ottomana*, sample no: AH-80, X10

Figure 2"*Nodosaria*" *elabugae*, sample no: AH-17, X10

Figure 3: "*Nodosaria*" *elabugae*, sample no: AH-38, X20

Figure 4: "*Nodosaria*" *elabugae*, sample no: AH-29, X10

Figure 5: "*Nodosaria*" *elabugae*, sample no: AH-53, X10

Figure 6: "*Nodosaria*" *elabugae*, sample no: AH-46, X20

Figure 7:"*Nodosaria*" *skyphica*, sample no: AH-2, X10

Figure 8: **"***Nodosaria*" sp. A, sample no: AH-59, X10

Figure 9: **"***Nodosaria*" sp. A, sample no: AH-32, X10

Figure 10: **"***Nodosaria*" sp. A, sample no: AH-57, X10

Figure 11: **"***Nodosaria*" sp. A, sample no: AH-33, X4

Figure 12: *Nodosinelloides* sp. A, sample no: AH-2, X10

Figure 13: *Nodosinelloides* sp. A, sample no: AH-17, X10

Figure 14: *Nodosinelloides* spp., sample no: AH-46, X10

PLATE VI

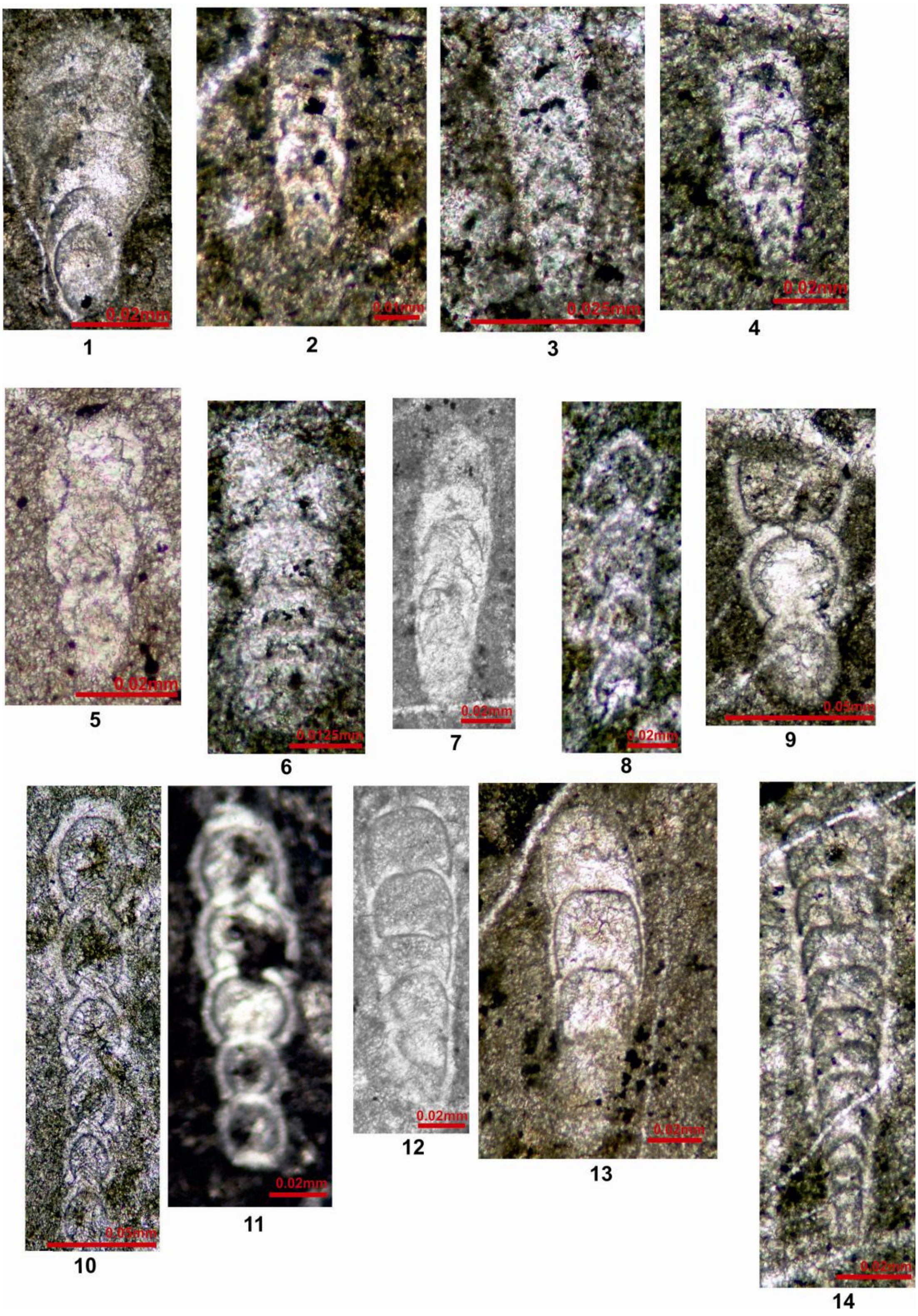

PLATE VII

Figure 1: *Nestellorella dorashamensis*, sample no: AH-29, X10

Figure 2: *Nestellorella dorashamensis*, sample no: AH-30, X10

Figure 3: *Nestellorella dorashamensis*, sample no: AH-30, X10

Figure 4: *Nestellorella dorashamensis*, sample no: AH-32, X20

Figure 5: *Nestellorella dorashamensis*, sample no: AH-33, X10

Figure 6: *Nestellorella dorashamensis*, sample no: AH-37, X10

Figure 7: *Nestellorella dorashamensis*, sample no: AH-32, X10

Figure 8: *Nestellorella dorashamensis*, sample no: AH-37, X20

Figure 9: *Nestellorella dorashamensis*, sample no: AH-25, X10

Figure 10: *Nestellorella dorashamensis*, sample no: AH-23, X10

Figure 11: *Nestellorella dorashamensis*, sample no: AH-16, X10

Figure 12: *Nestellorella dorashamensis*, sample no: AH-21, X10

Figure 13: *Nestellorella dorashamensis*, sample no: AH-25, X10

Figure 14: *Nestellorella dorashamensis*, sample no: AH-25, X10

Figure 15: *Nestellorella dorashamensis*, sample no: AH-29, X10

Figure 16: *Nestellorella dorashamensis*, sample no: AH-28, X10

PLATE VII

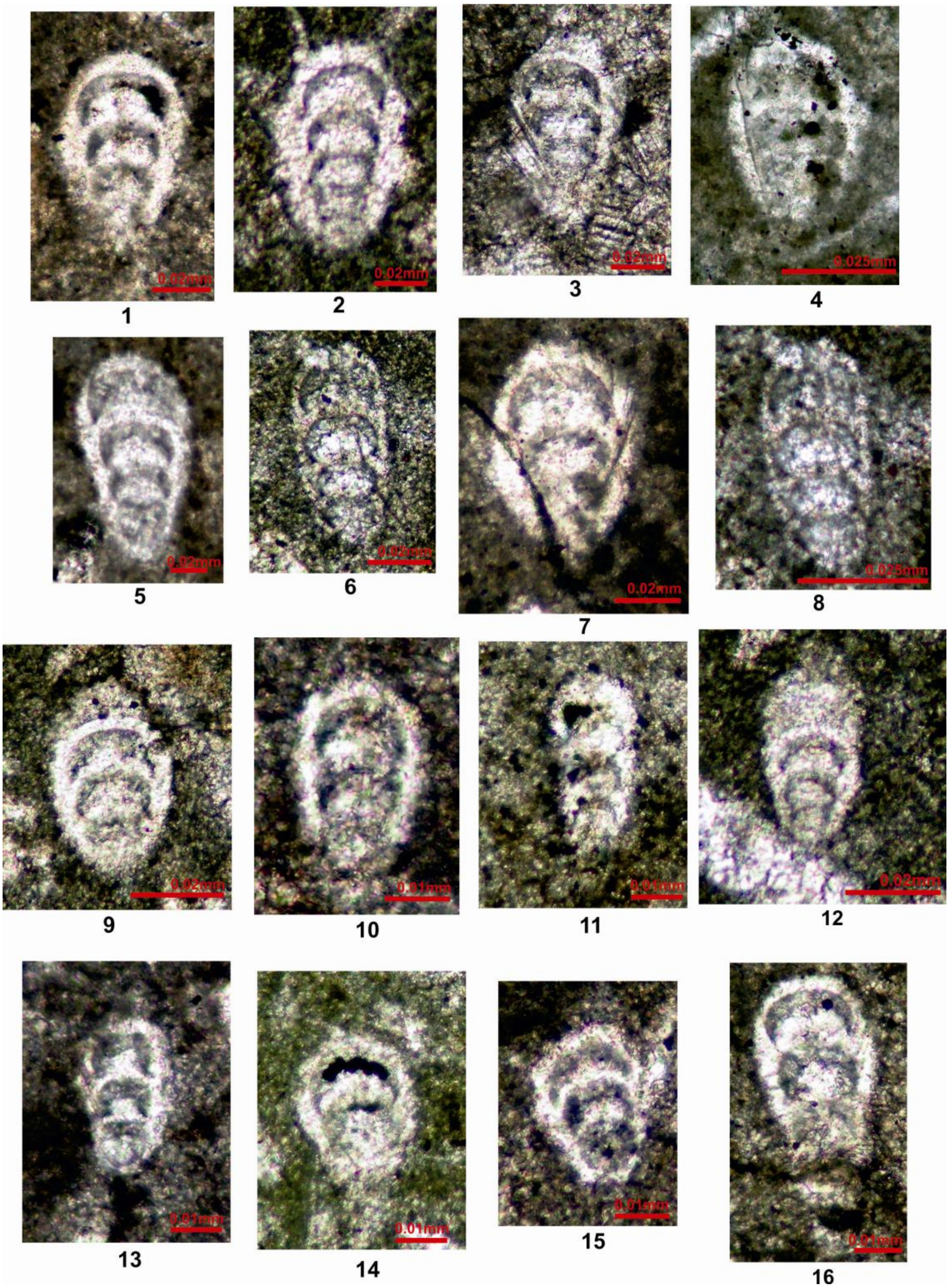

PLATE VIII

Figure 1: *Rectostipulina quadrata,* sample no: AH-9, X10

Figure 2: *Rectostipulina quadrata,* sample no: AH-39, X10

Figure 3: *Rectostipulina pentamerata,* sample no: AH-9, X10

Figure 4: *Rectostipulina pentamerata,* sample no: AH-9, X10

Figure 5: *Rectostipulina pentamerata,* sample no: AH-93, X10

Figure 6: *Globivalvulina vonderschmitti,* sample no: AH-9, X10

Figure 7: *Globivalvulina vonderschmitti,* sample no: AH-9, X10

Figure 8: *Globivalvulina vonderschmitti,* sample no: AH-32, X10

Figure 9: *Globivalvulina vonderschmitti,* sample no: AH-32, X10

Figure 10: *Globivalvulina vonderschmitti,* sample no: AH-33, X10

Figure 11: *Retroseptellina decrouezae,* sample no: AH-2, X4

Figure 12: *Retroseptellina decrouezae,* sample no: AH-43, X10

Figure 13: *Retroseptellina decrouezae,* sample no: AH-54, X10

PLATE VIII

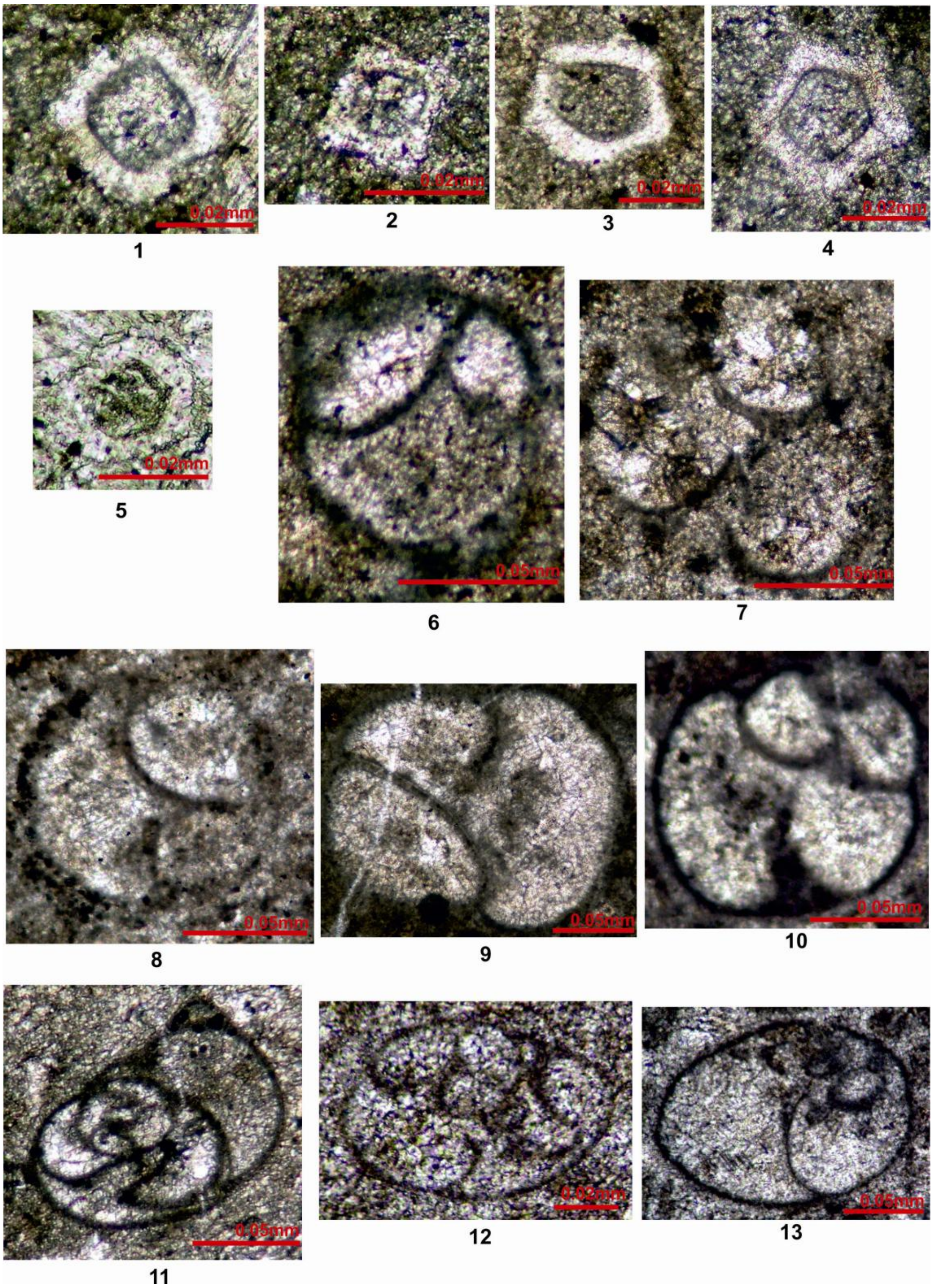
0.02mm
0.02mm
0.02mm
0.02mm
0.02mm
0.05mm
0.05mm
0.05mm
0.05mm
0.05mm
0.05mm
0.02mm
0.05mm
1
2
3
4
5
6
7
8
9
10
11
12
13

PLATE IX

Figure 1: *Globivalvulina* ex gr. *cyprica*, sample no: AH-34, X10

Figure 2: *Globivalvulina* ex gr. *cyprica*, sample no: AH-34, X10

Figure 3: *Globivalvulina* ex gr. *cyprica*, sample no: AH-1, X10

Figure 4: *Septoglobivalvulina gracilis*, sample no: AH-93, X10

Figure 5: *Septoglobivalvulina gracilis*, sample no: AH-70, X10

Figure 6: *Septoglobivalvulina gracilis*, sample no: AH-3, X10

Figure 7: *Paraglobivalvulina mira*, sample no: AH-28, X4

Figure 8: *Paraglobivalvulina mira*, sample no: AH-32, X10

Figure 9: *Dagmarita chanakchiensis*, sample no: AH-5, X10

Figure 10: *Dagmarita chanakchiensis*, sample no: AH-45, X10

Figure 11: "*Dagmarita*"*shahrezaensis*, sample no: AH-28, X10

Figure 12: "*Dagmarita*"*shahrezaensis*, sample no: AH-30, X10

Figure 13: *Paradagmarita monodi* ?, sample no: AH-37, X10

PLATE IX

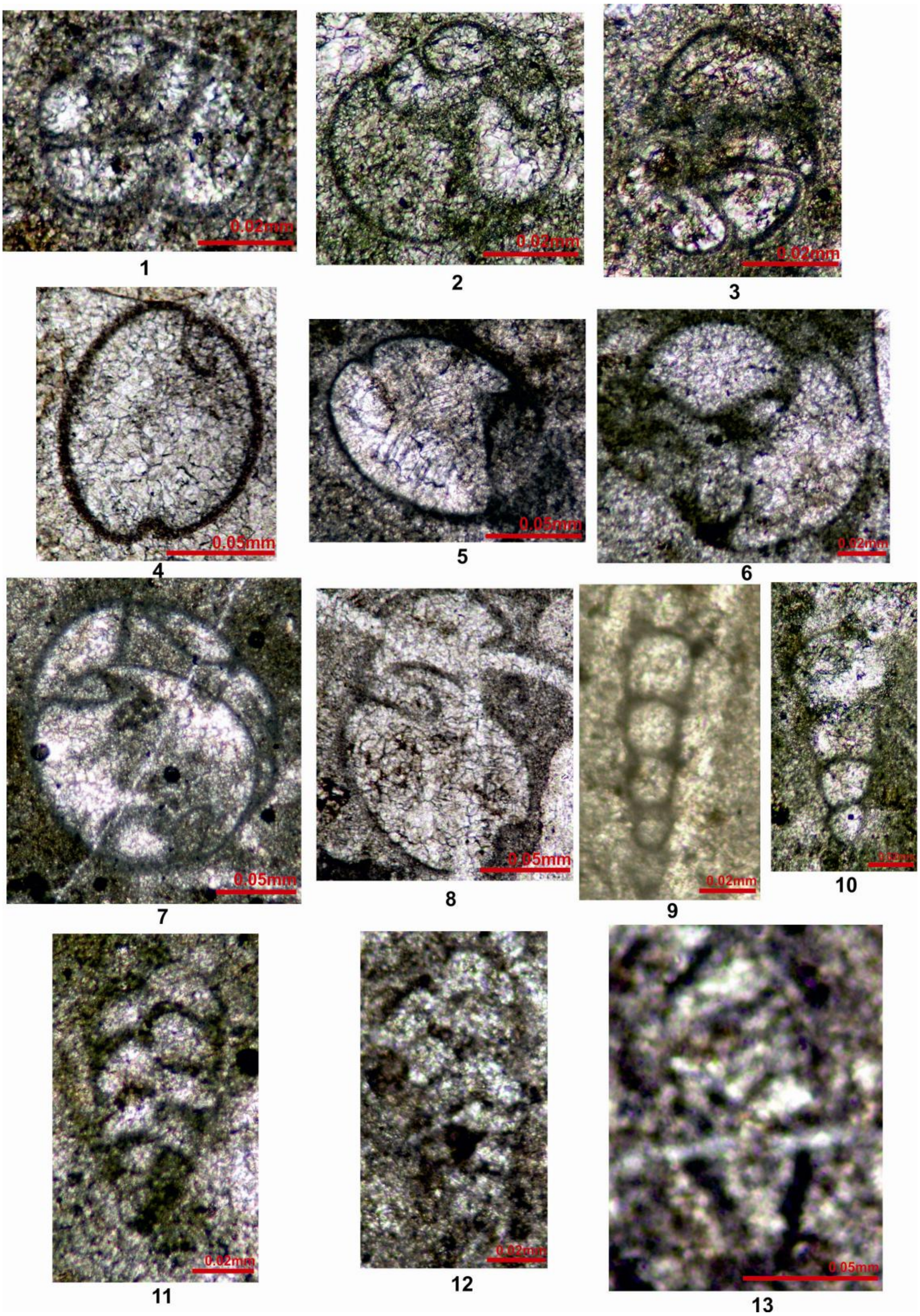

PLATE X

Figure 1: *Paradagmarita monodi* ?, sample no: AH-32, X10

Figure 2: *Charliella altıneri*, sample no: AH-36, X10

Figure 3: *Charliella altıneri*, sample no: AH-46, X10

Figure 4: *Charliella altıneri*, sample no: AH-33, X10

Figure 5: *Reichelina changhsingensis*, sample no: AH-93, X4

Figure 6: *Reichelina changhsingensis*, sample no: AH-93, X10

Figure 7: *Reichelina changhsingensis*, sample no: AH-88, X10

Figure 8: *Reichelina changhsingensis*, sample no: AH-93, X4

PLATE X

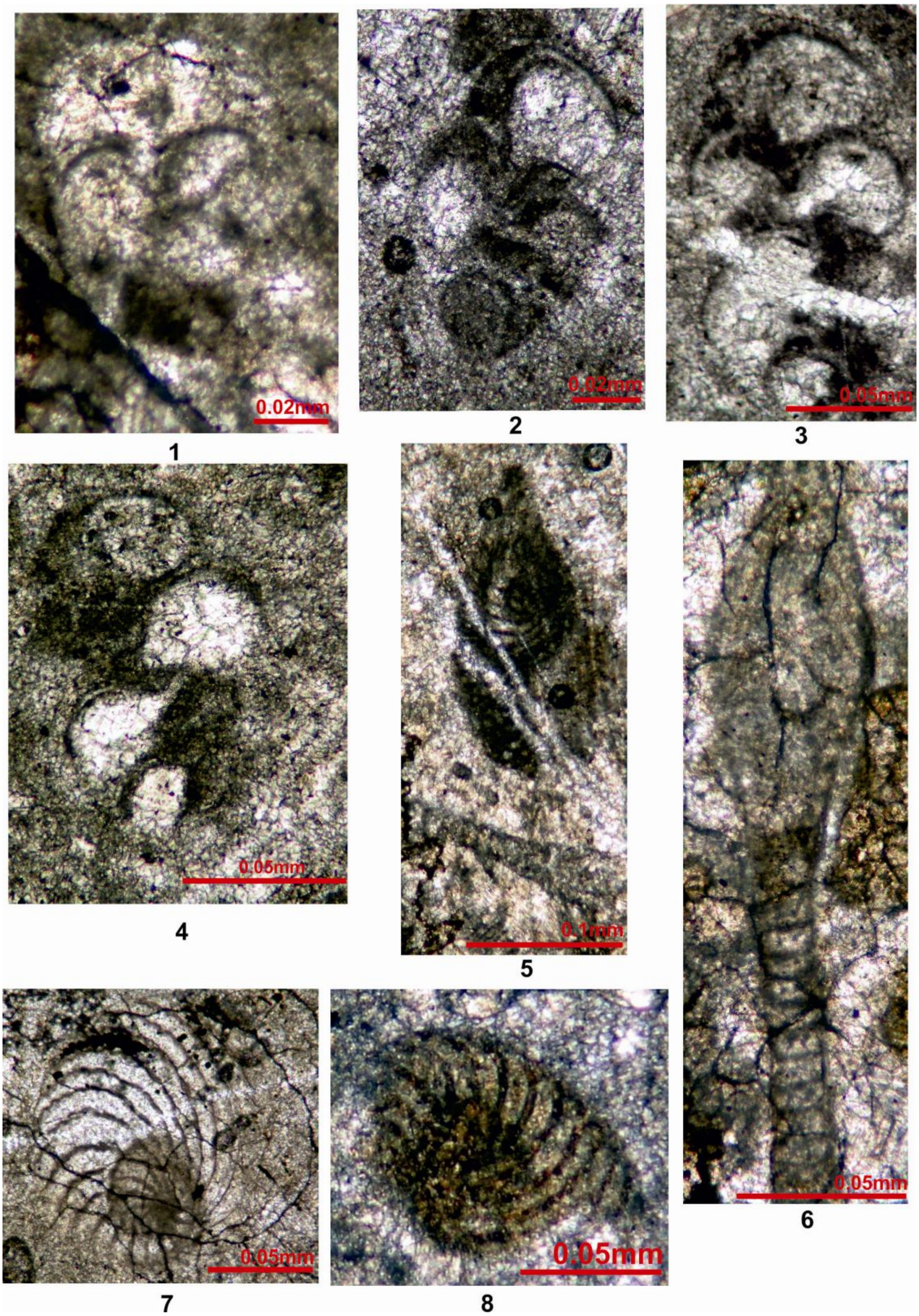

PLATE XI

Figure 1: *Floritheca variata*, sample no: AH-2, X4

Figure 2: *Floritheca variata*, sample no: AH-32, X10

Figure 3: *Colaniella parva*, sample no: AH-93, X10

Figure 4: *Colaniella parva*, sample no: AH-93, X10

Figure 5: *Neoendotyra* sp., sample no: AH-88, X20

Figure 6: *Nankinella* sp., sample no: AH-9, X4

Figure 7: *Agathammina pusilla*, sample no: AH-93, X10

Figure 8: *Agathammina pusilla*, sample no: AH-51, X4

Figure 9: *Agathammina* ex gr. *pusilla*, sample no: AH-9, X10

Figure 10: *Crassispirella hughesi*, sample no: AH-46, X10

Figure 11: *Crassispirella* sp., sample no: AH-32, X10

Figure 12: *Hemigordius* sp., sample no: AH-93, X10

Figure 13: *Hemigordius* sp., sample no: AH-93, X10

Figure 14: *Hemigordius* sp., sample no: AH-93, X10

Figure 15: *Hemigordius* sp., sample no: AH-47, X4

Figure 16: *Hemigordius* sp., sample no: AH-93, X10

Figure 17: *Hemigordius* sp., sample no: AH-93, X10

Figure 18: *Hemigordius* sp., sample no: AH-93, X10

PLATE XI

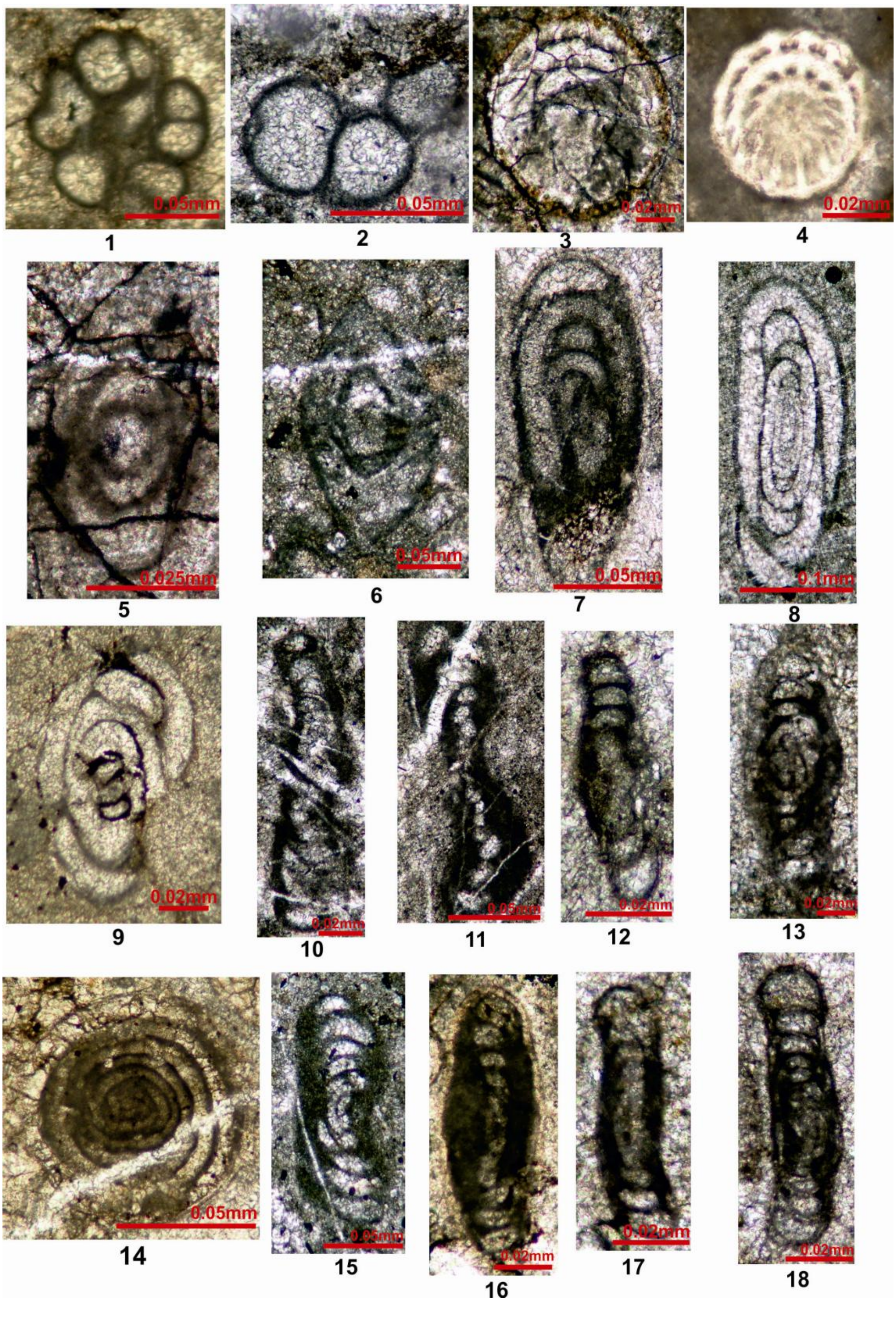
1
0.05mm
2
0.05mm
3
0.02mm
4
0.02mm
5
0.025mm
6
0.05mm
7
0.05mm
8
0.1mm
9
0.02mm
10
0.02mm
11
12
0.02mm
13
14
0.05mm
15
16
0.02mm
17
0.02mm
18
0.02mm

PLATE XII

Figure 1: *Hemigordius* sp., sample no: AH-93, X10

Figure 2: *Hemigordius guvenci*, sample no: AH-93, X20

Figure 3: *Midiella zaninettiae* ?, sample no: AH-51, X10

Figure 4: *Midiella bronnimanni*, sample no: AH-93, X10

Figure 5: *Midiella* sp., sample no: AH-93, X10

Figure 6: *Multidiscus* sp., sample no: AH-10, X10

Figure 7: *Multidiscus* sp. A, sample no: AH-93, X4

Figure 8: *Multidiscus* sp. B, sample no: AH-93, X10

Figure 9: *Multidiscus* sp. B, sample no: AH-93, X10

Figure 10: *Hemigordiellina* sp., sample no: AH-33, X10

Figure 11: *Neodiscopsis* sp., sample no: AH-5, X10

Figure 12: *Neodiscopsis* ? sp., sample no: AH-5, X10

Figure 13: *Neodiscopsis* sp., sample no: AH-9, X10

Figure 14: *Neodiscopsis* sp., sample no: AH-5, X10

Figure 15: *Neodiscopsis* sp., sample no: AH-5, X10

Figure 16: *Neodiscopsis* sp., sample no: AH-5, X10

Figure 17: *Neodiscopsis* sp., sample no: AH-9, X10

PLATE XII

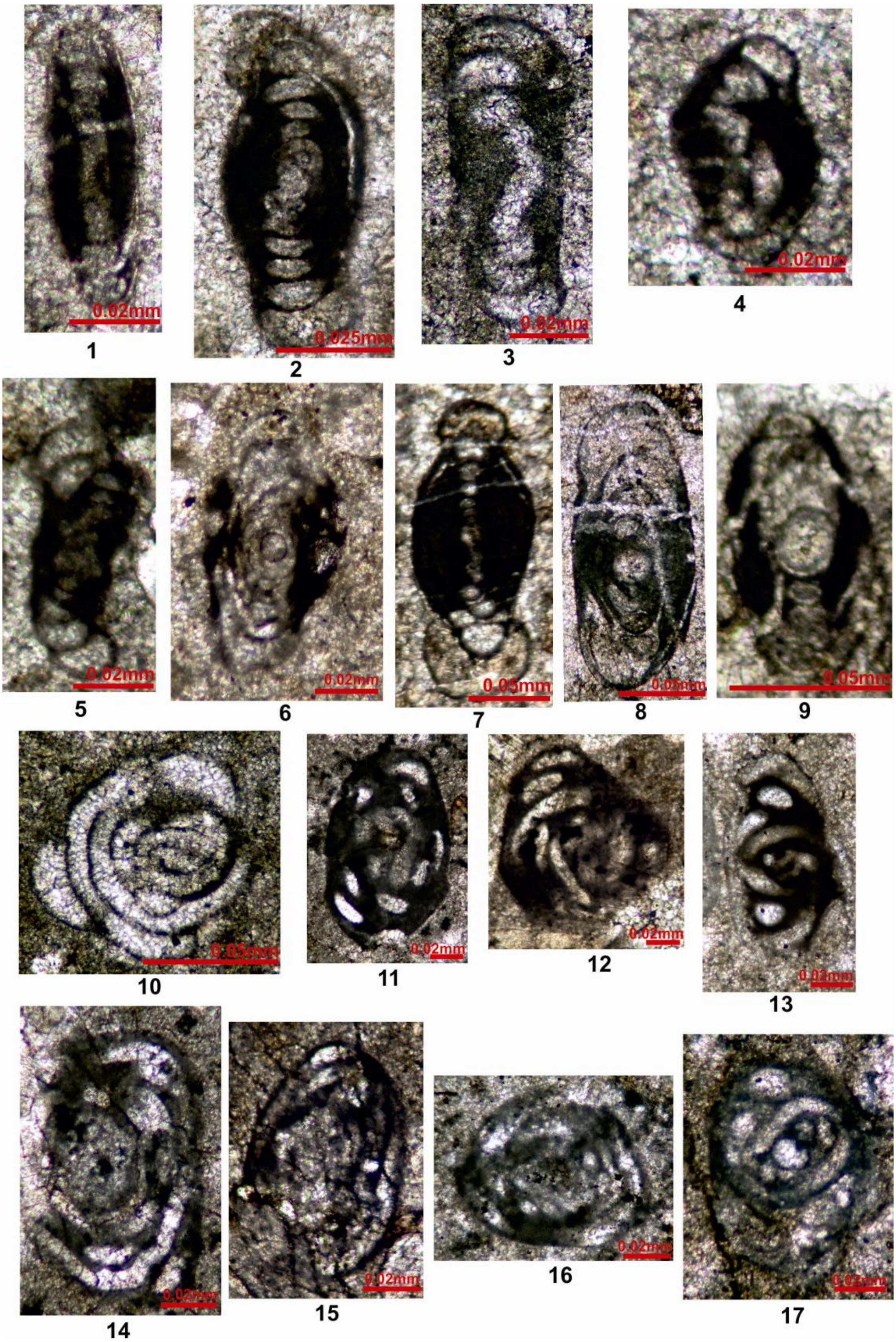
0.02mm
0.025mm
0.02mm
0.02mm
1
2
3
4
0.02mm
0.02mm
0.05mm
0.05mm
0.05mm
5
6
7
8
9
0.05mm
0.02mm
0.02mm
0.02mm
10
11
12
13
0.02mm
0.02mm
0.02mm
0.02mm
14
15
16
17

PLATE XIII

Figure 1: *Neodiscopsis* sp., sample no: AH-6, X10

Figure 2: *Neodiscopsis* sp., sample no: AH-34, X10

Figure 3: *Neodiscopsis* sp., sample no: AH-93, X4

Figure 4: *Neodiscopsis* sp., sample no: AH-33, X10

Figure 5: *Neodiscopsis graecodisciformis*, sample no: AH-2, X10

Figure 6: *Neodiscopsis graecodisciformis*, sample no: AH-9, X10

Figure 7: *Neodiscopsis graecodisciformis*, sample no: AH-9, X10

Figure 8: *Neodiscopsis graecodisciformis*, sample no: AH-10, X10

Figure 9: "*Hoyanella*" sp., sample no: AH-9, X10

Figure 10: "*Hoyanella*" sp., sample no: AH-37, X10

Figure 11: *Glomomidiella* sp., sample no: AH-4, X10

Figure 12: *Glomomidiella* sp., sample no: AH-4, X10

Figure 13: *Glomomidiella* sp., sample no: AH-4, X10

Figure 14: *Glomomidiella* sp., sample no: AH-5, X10

Figure 15: *Glomomidiella* sp., sample no: AH-35, X10

Figure 16: *Glomomidiella* sp., sample no: AH-48, X10

Figure 17: *Glomomidiella* sp., sample no: AH-31, X10

PLATE XIII

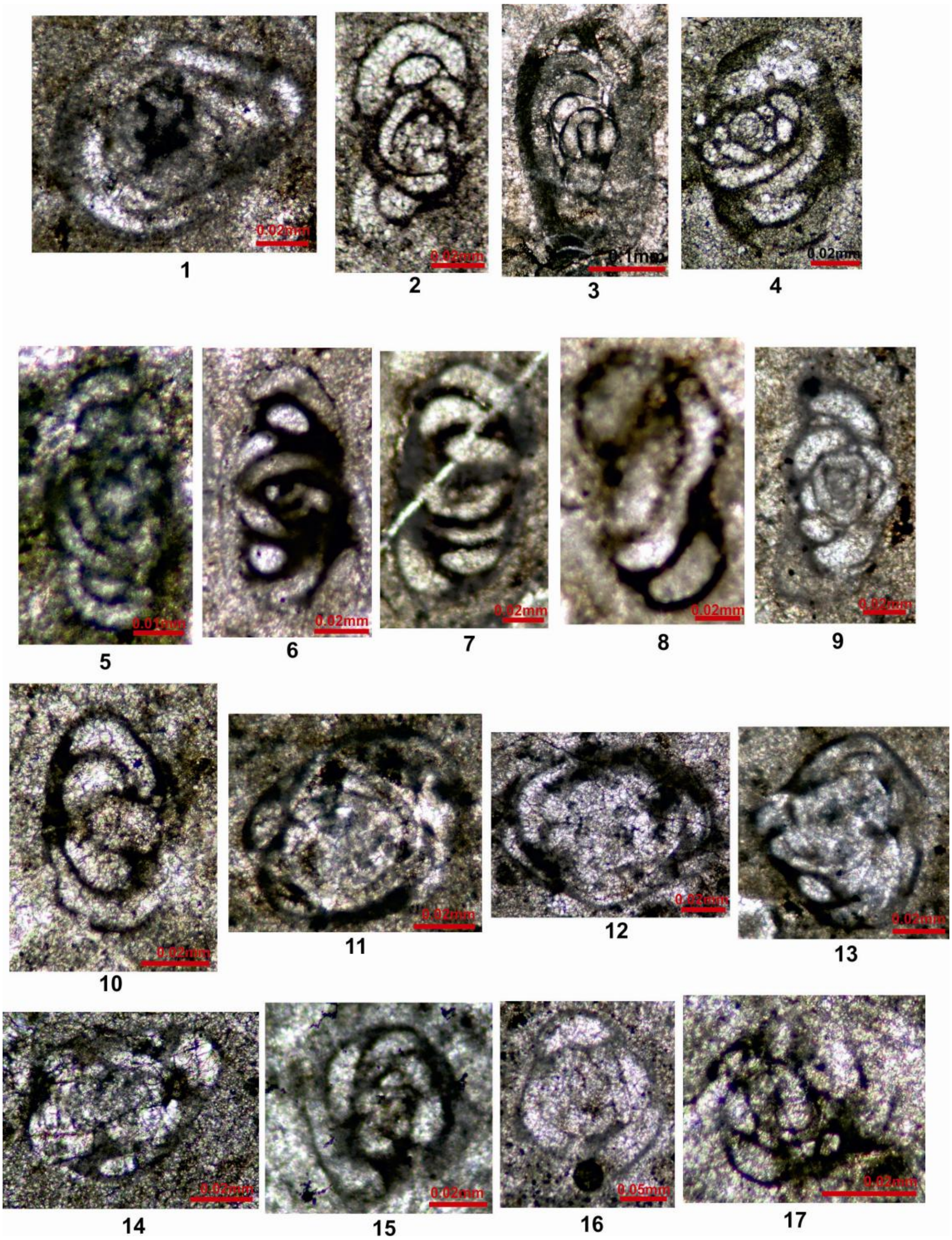
0.02mm
1
0.02mm
2
0.1mm
3
0.02mm
4
0.01mm
5
0.02mm
6
0.02mm
7
0.02mm
8
0.02mm
9
0.02mm
10
0.02mm
11
0.02mm
12
0.02mm
13
0.02mm
14
0.02mm
15
0.05mm
16
0.02mm
17

PLATE XIV

Figure 1: *Glomomidiella* sp., sample no: AH-31, X10

Figure 2: *Glomomidiella* sp., sample no: AH-37, X10

Figure 3: *Glomomidiella* sp., sample no: AH-37, X10

Figure 4: *Glomomidiella* sp., sample no: AH-57, X10

Figure 5: *Crassiglomella* sp., sample no: AH-3, X10

Figure 6: *Crassiglomella* sp., sample no: AH-38, X10

Figure 7: *Crassiglomella* sp., sample no: AH-88, X10

Figure 8: *Crassiglomella* sp., sample no: AH-88, X10

Figure 9: *Crassiglomella* sp., sample no: AH-88, 10

Figure 10: *Crassiglomella* sp., sample no: AH-88, X10

Figure 11: *Ammovertella* sp., sample no: AH-61, X20

Figure 12: *Ammovertella* sp., sample no: AH-61, X20

Figure 13: *Dunbarula* ? sp., sample no: AH-31, X10

Figure 14: *Codonofusiella* cf. *kwangsiana*, sample no: AH-30, X10

Figure 15: *Codonofusiella* cf. *kwangsiana*, sample no: AH-46, X10

PLATE XIV

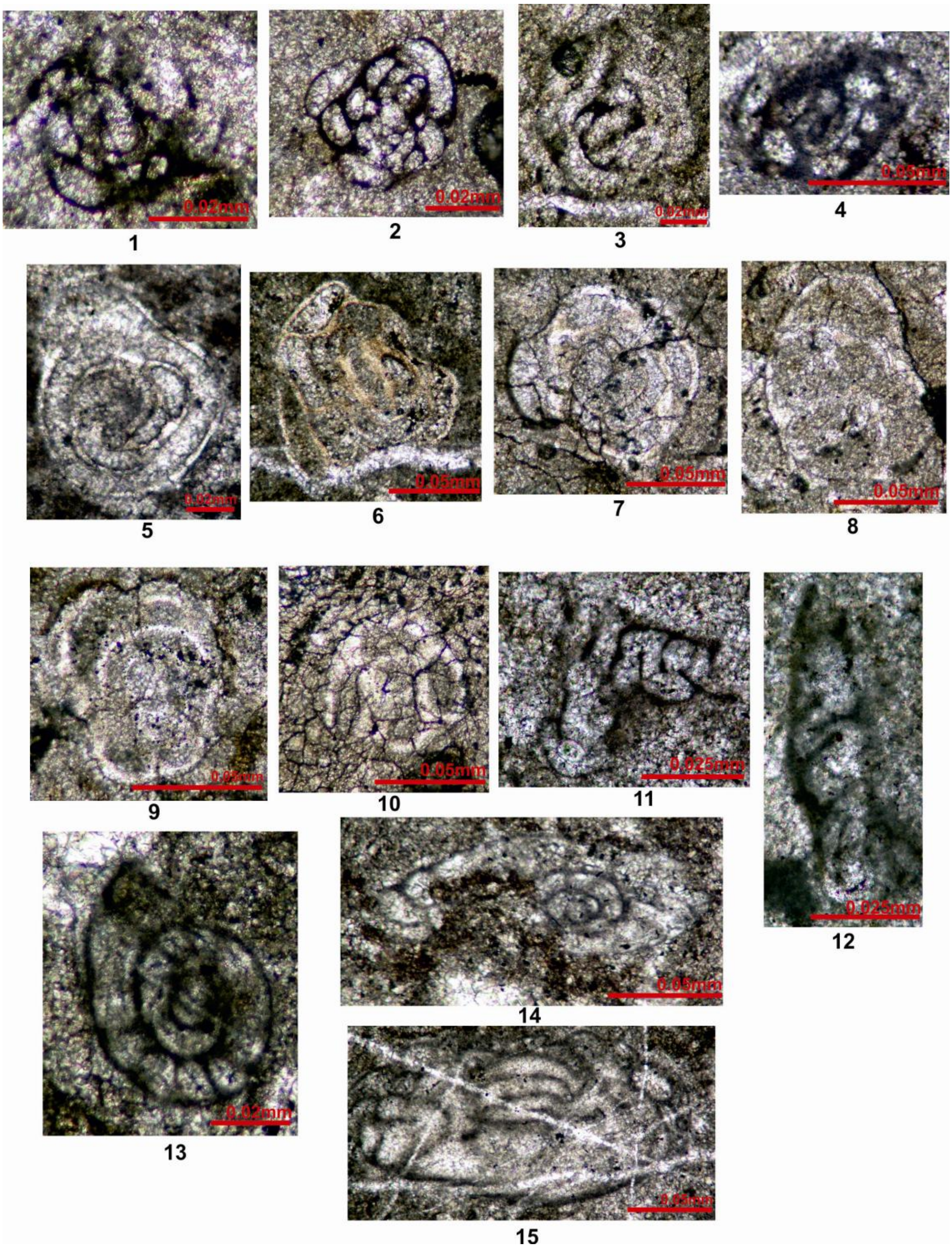

0.02mm
1
0.02mm
2
0.02mm
3
0.05mm
4
0.02mm
5
0.05mm
6
0.05mm
7
0.05mm
8
9
0.05mm
10
0.025mm
11
0.025mm
12
0.02mm
13
0.05mm
14
15

PLATE XV

Figure 1: *Codonofusiella* cf. *kwangsiana*, sample no: AH-32, X10

Figure 2: *Codonofusiella* cf. *kwangsiana*, sample no: AH-33, X10

Figure 3: *Codonofusiella* cf. *kwangsiana*, sample no: AH-34, X10

Figure 4: *Codonofusiella* cf. *kwangsiana*, sample no: AH-34, X10

Figure 5: *Codonofusiella* cf. *kwangsiana*, sample no: AH-33, X10,

Figure 6: *Codonofusiella* cf. *kwangsiana*, sample no: AH-47, X4

Figure 7: *Codonofusiella* cf. *kwangsiana*, sample no: AH-47, X4

Figure 8: *Codonofusiella* cf. *kwangsiana*, sample no: AH-30, X10

Figure 9: *Codonofusiella* cf. *kwangsiana*, sample no: AH-33, X10

Figure 10: *Codonofusiella* cf. *kwangsiana*, sample no: AH-32, X10

Figure 11: *Codonofusiella* cf. *kwangsiana*, sample no: AH-34, X10

Figure 12: *Codonofusiella* cf. *kwangsiana*, sample no: AH-34, X10

PLATE XV

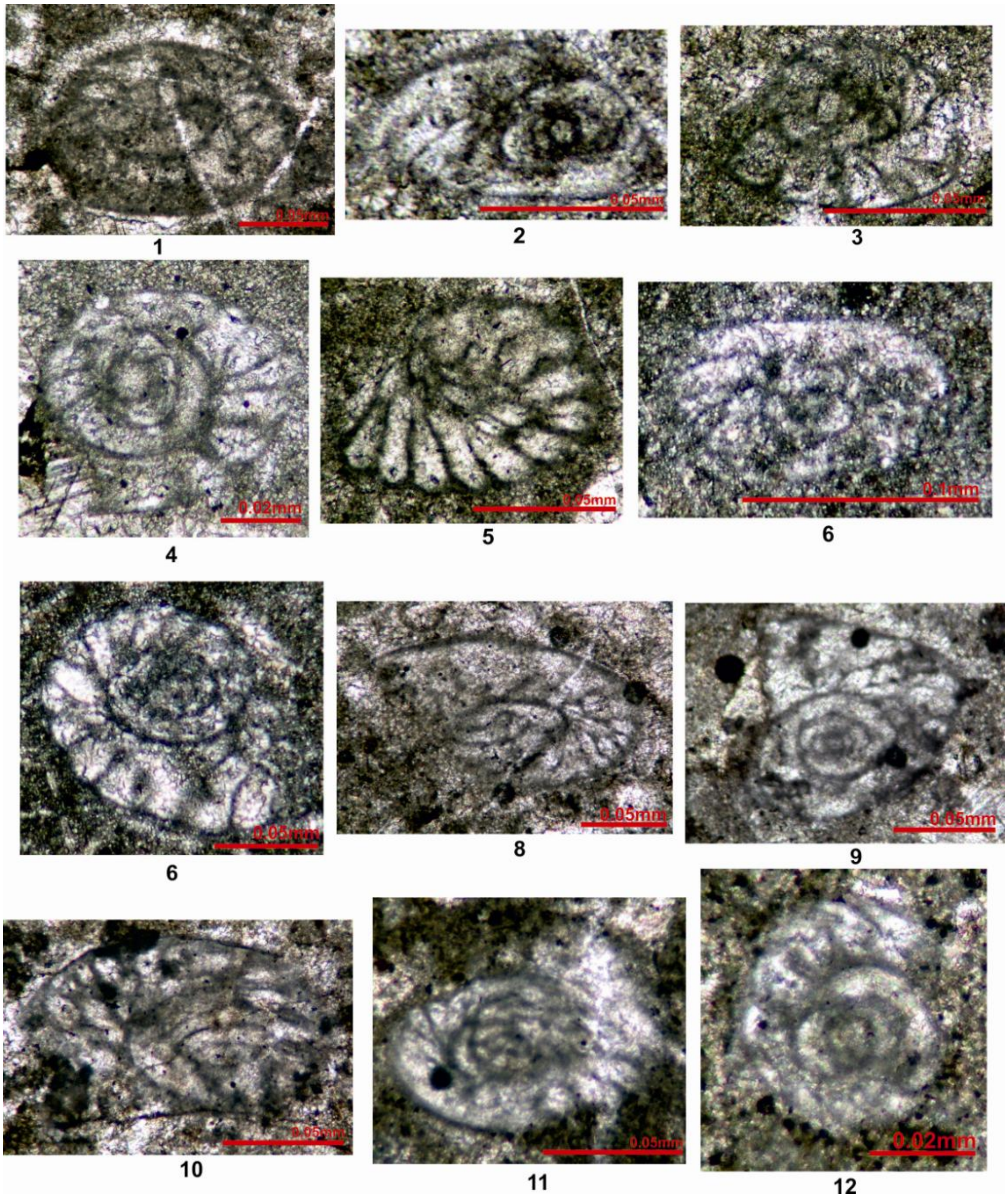

PLATE XVI

Figure 1: *Codonofusiella* cf. *kwangsiana*, sample no: AH-34, X10

Figure 2: *Codonofusiella* cf. *kwangsiana*, sample no: AH-34, X10

Figure 3: *Codonofusiella* cf. *kwangsiana*, sample no: AH-33, X10

Figure 4: *Codonofusiella* cf. *kwangsiana*, sample no: AH-46, X10

Figure 5: *Codonofusiella* cf. *schubertelloides*, sample no: AH-30, X10

Figure 6: *Codonofusiella* sp., sample no: AH-47, X10

Figure 7: *Codonofusiella* ? sp., sample no: AH-97, X10

Figure 8: *Palaeofusulina* cf. *nana,* sample no: AH-76, X4

Figure 9: *Palaeofusulina* cf. *nana*, sample no: AH-76, X10

PLATE XVI

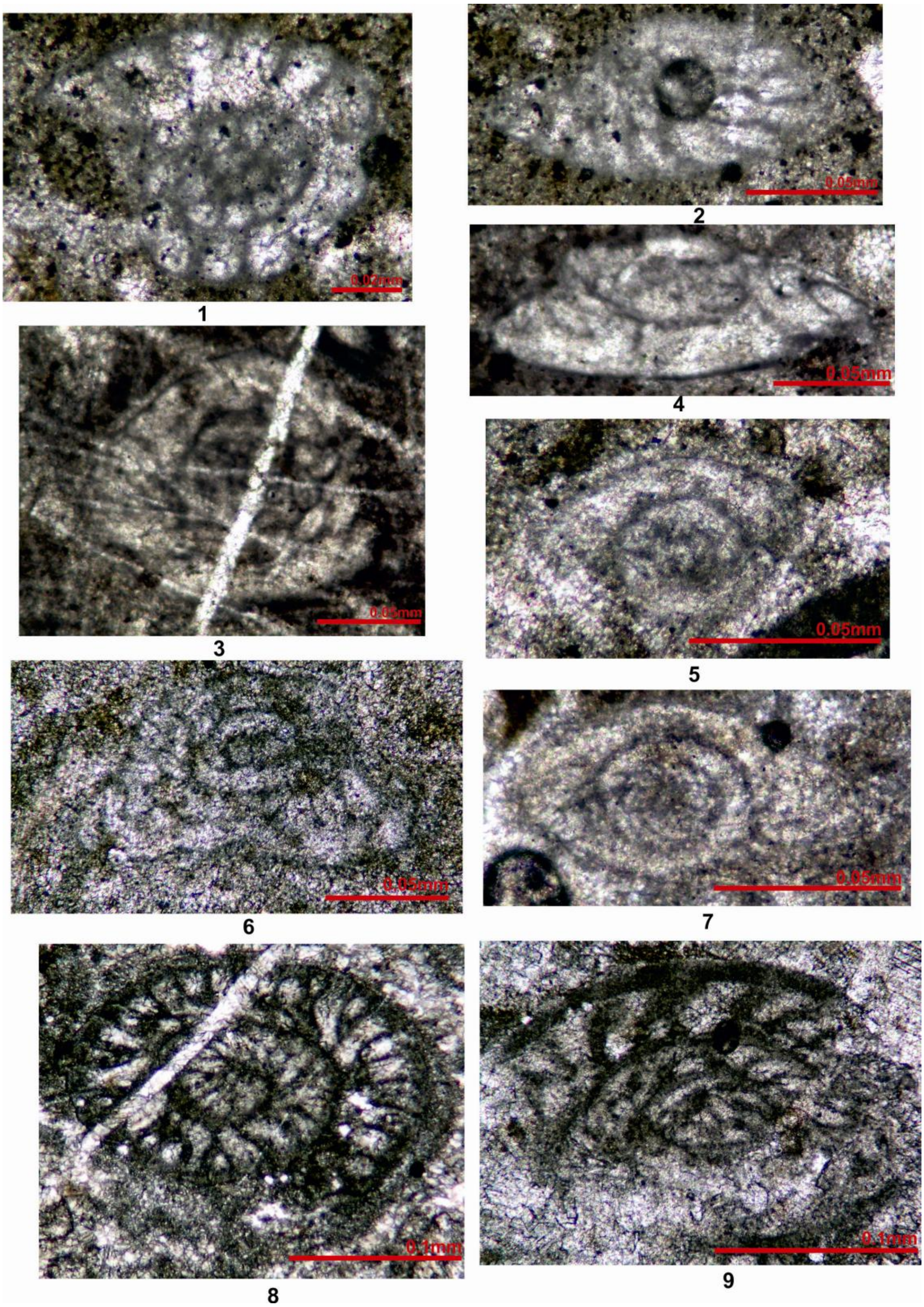
0.02mm
1
0.05mm
2
0.05mm
3
0.05mm
4
0.05mm
5
0.05mm
6
0.05mm
7
0.1mm
8
0.1mm
9

PLATE XVII

Figure 1: *Rectocornuspira kalhori*, sample no: AH-111, X20

Figure 2: *Rectocornuspira kalhori*, sample no: AH-113, X20

Figure 3: *Rectocornuspira kalhori*, sample no: AH-113, X10

Figure 4: *Rectocornuspira kalhori*, sample no: AH-113, X10

Figure 5: *Rectocornuspira kalhori*, sample no: AH-113, X20

Figure 6: *Rectocornuspira kalhori*, sample no: AH-113, X20

Figure 7: *Rectocornuspira kalhori*, sample no: AH-114, X20

Figure 8: *Spirorbis phlyctaena*, sample no: AH-115, X10

Figure 9: *Spirorbis phlyctaena*, sample no: AH-104, X4

Figure 10: *Spirorbis phlyctaena*, sample no: AH-105, X10

Figure 11: *Spirorbis phlyctaena*, sample no: AH-105, X10

PLATE XVII

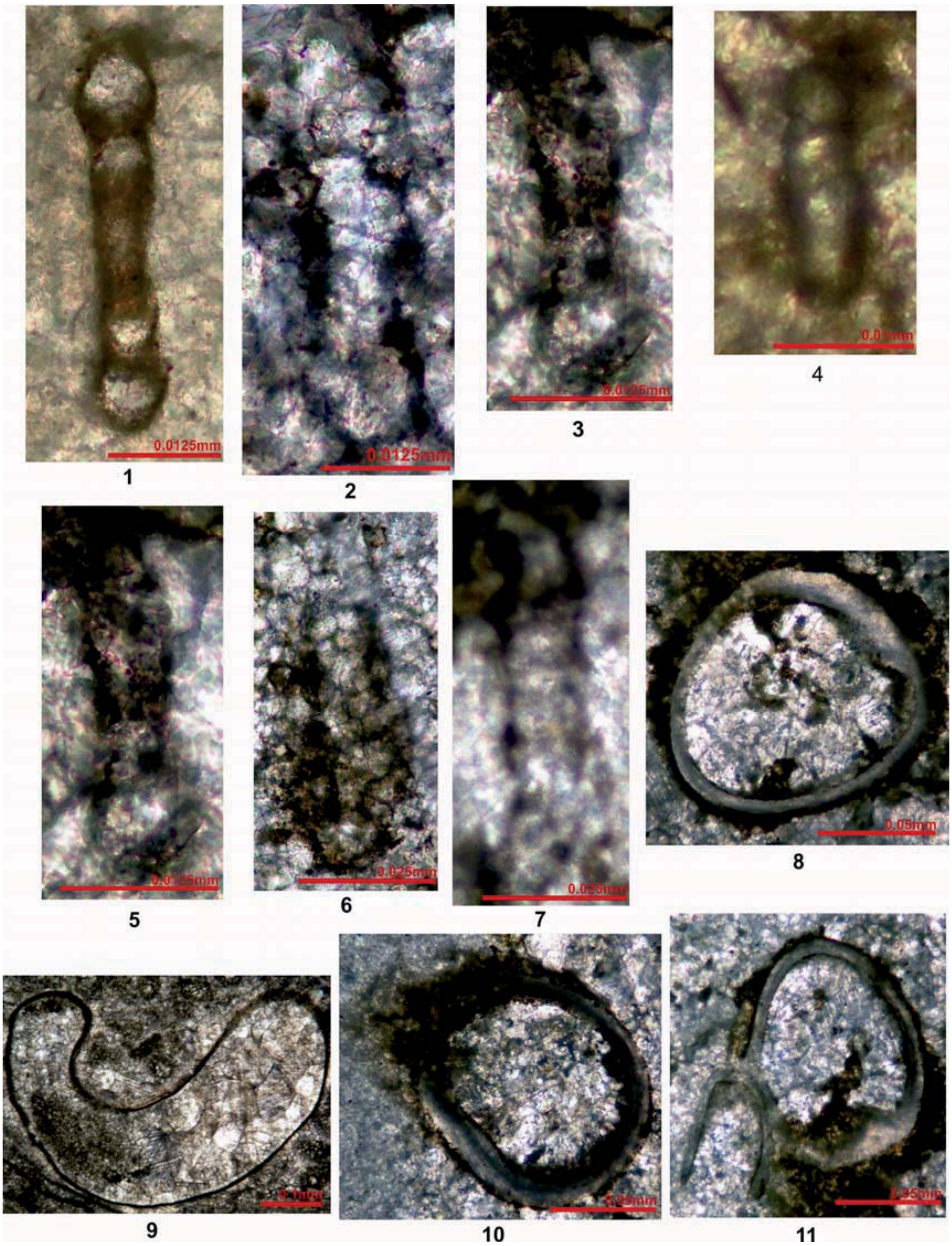

PLATE XVIII

Figure 1: *Spirorbis phlyctaena*, sample no: AH-105, X4

Figure 2: *Spirorbis phlyctaena*, sample no: AH-105, X4

Figure 3: *Spirorbis phlyctaena*, sample no: AH-105, X10

Figure 4: *Spirorbis phlyctaena*, sample no: AH-105, X10

Figure 5: *Spirorbis phlyctaena*, sample no: AH-105, X10

Figure 6: *Spirorbis phlyctaena*, sample no: AH-105, X10

Figure 7: *Spirorbis phlyctaena*, sample no: AH-106, X10

Figure 8: *Spirorbis phlyctaena*, sample no: AH-106, X4

Figure 9: *Spirorbis phlyctaena*, sample no: AH-106, X4

Figure 10: *Spirorbis phlyctaena*, sample no: AH-106, X10

Figure 11: *Spirorbis phlyctaena*, sample no: AH-107, X10

Figure 12: *Spirorbis phlyctaena*, sample no: AH-107-2, X4

Figure 13: *Spirorbis phlyctaena*, sample no: AH-107, X4

Figure 14: *Spirorbis phlyctaena*, sample no: AH-107, X4

Figure 15: *Spirorbis phlyctaena*, sample no: AH-107-2, X4

Figure 16: *Spirorbis phlyctaena*, sample no: AH-107-2, X4

Figure 17: *Spirorbis phlyctaena*, sample no: AH-115, X10

Figure 18: *Spirorbis phlyctaena*, sample no: AH-113, X10

PLATE XVIII